

**Newcastle**  
University

---

The Role of Telomere Damage in  
Cardiomyocyte Ageing

---

Rhys Kyle Anderson

Doctor of Philosophy

Institute of Cell and Molecular Biology  
Newcastle University Institute for Ageing  
Faculty of Medicine  
Newcastle University  
UK

June 2016



## Abstract

Cellular senescence is often defined as an irreversible cell cycle arrest of mitotic cells, however post-mitotic cells, including adipocytes and neurons, have also been shown to display senescent-like characteristics, such as elevated SA- $\beta$ -Gal activity and increased production of pro-inflammatory cytokines, in response to persistent DNA damage. Our group have shown that a persistent DDR can occur at telomeres independently of length. We investigated the possibility of telomere dysfunction being associated with senescence in a non-rapidly dividing cell type, which is not subject to repeated end-replication problem-associated telomere shortening.

We show that telomere damage can be induced in cardiomyocyte cell lines with X-irradiation or oxidative stress in the absence of cell division, with live-cell imaging revealing the presence of persistent DNA damage foci. Endonuclease-mediated telomere-specific double-strand DNA breaks trigger a senescent-like phenotype in cardiomyocytes *in vitro*, including elevated SA- $\beta$ -Gal activity, p21 expression, hypertrophy and decrease of proliferation marker Ki-67.

We observed an age-dependent increase in telomere dysfunction in both murine and human cardiomyocytes, occurring independently of telomere length. Furthermore, murine cardiomyocytes *in vivo* are associated with numerous markers of senescence, such as p15, p16 and p21 elevation, along with increased TGF- $\beta$  expression and increased prevalence of senescence-associated distension of satellites.

Increased oxidative stress via MnSOD- $\pm$ , Catalase- $\pm$ , or MAO-A overexpression (resulting in excess H<sub>2</sub>O<sub>2</sub> production), can drive telomere dysfunction in murine cardiomyocytes *in vivo*, which correlates with a decrease in heart function, both of which can be rescued with anti-oxidant supplementation. Finally, we show that rapamycin, a drug shown to increase lifespan and delay age-related diseases in numerous organisms, can attenuate the accumulation of TAF in murine cardiomyocytes *in vivo*, and is associated with a decrease in senescence markers.

Our data provide evidence that telomere dysfunction occurs independently of length in cardiomyocytes, and is associated with a senescent-like phenotype.

## **Dedication**

I dedicate this thesis to my parents, Ian and Freda Anderson – thank you for everything, you are amazing.

## Acknowledgements

I would like to thank my supervisor João Passos for providing me the opportunity to research in his laboratory and for the generous time committed and unfaltering support throughout my PhD. I would like to also thank Majlinda Lako for agreeing to co-supervise my PhD.

I would like to thank all members of Passos lab, past and present, for their help throughout this project, especially Clara Correia-Melo for sharing her tissue expertise, Jodie Birch for IHC, Anthony Lagnardo for live-cell imaging analysis, Graeme Hewitt for NAC *in vitro* experiments, and Mikolaj Ogrodnik for SADS. Thank you also to Gavin Richardson and Andrew Owens for sharing their cardiac know-how and providing human tissues, to Jordan Miller for providing catalase<sup>-/-</sup> and MnSOD<sup>-/+</sup> tissues, as well as Damien Maggiorani and Jeanne Mialet-Perez for providing the MAO-A tissues and valuable experimental contributions, including cardiomyocyte isolations to provide material for gene expression analysis and producing conditioned medium. Thanks also go to Thomas von Zglinicki for kindly providing me with tissue samples, Glyn Nelson for being my microscopy agony aunt, to Jelena Mann for ChIP experiments, and to Gabriele Saretzki for teaching me the TRAP assay and, along with Viktor Korolchuk, for being my internal assessors throughout my PhD.

To Berni, Graeme, Baby Len (and Prang) - my surrogate family, it's been a blast!

To Michael and Clara - my surrogate parents, thanks for being great friends and a particular thank you for providing me shelter from the northern elements when I was destitute and hungry.

To all my IAH friends and to Rafal, James, Chico and Antho for making these years especially interesting, and who I'm only convinced aren't merely figments of my imagination due to the inconceivable level of imagination one would require to dream you up.

To David Bowie and the Beatles for keeping me company during the many hours (perhaps weeks, or even months) spent looking down microscopes.

Finally, to Katie who is never far from my thoughts, and to my loving family: Mum & Dad, my brothers Ryan, Tim and Noel, and grandparents - for their keen interest and support in whatever I do, I love you all x.

“I am a scientist and I know what constitutes proof. But the reason I call myself by my childhood name is to remind myself that a scientist must also be absolutely like a child. If he sees a thing, he must say that he sees it, whether it was what he thought he was going to see or not. See first, think later, then test. But always see first. Otherwise you will only see what you were expecting. Most scientists forget that.”

Wonko the Sane (Douglas Adams): So Long and Thanks for all the Fish.

## Awards and Publications

### Awards

- Newcastle University Travel Award: Molecular Basis of Ageing and Disease. Suzhou, China. 2015.
- Conference Travel Award: International Cell Senescence Association Conference. Santiago de Compostela, Spain. 2015.
- Newcastle University Public Insights Lecture Prize. 2015.
- People's Choice Winner of the UK 3 Minute Thesis Competition 2014.
- Travel award: Coimbra Healthy Ageing Symposium 2014.
- Best Oral Presentation: Newcastle University Faculty of Medical Sciences Inter-Institution Research Day 2014.
- Travel Award: Groningen University Spring School for Healthy Ageing 2013.

### Publications

**Telomere Dysfunction and Senescence-associated Pathways in Bronchiectasis.** Jodie Birch, Stella Victorelli, Dina Rahmatika, Rhys K Anderson, Kasim Jiwa, Elizabeth Moisey, Chris Ward, Andrew J Fisher, Anthony de Soyza, Joao Passos. *American Journal of Respiratory and Critical Care Medicine*. 2016.

**JNK/SAPK Signalling is Essential for Efficient Reprogramming of Human Fibroblasts to Induced Pluripotent Stem Cells. Senescence.** Irina Neganova, Evgenija Shmeleva, Jennifer Munkley, Valeria Chicagova, George Anyfantis, Rhys K Anderson, Joao Passos, David J Elliot, Lyle Armstrong and Majlinda Lako. *Stem Cells*. 2016.

**Mitochondrial Hypertrophy Drives and Sustains a DNA Damage Response During Senescence.** Clara Correia-Melo, Francisco Marques, Rhys K Anderson, Graeme Hewitt, Alina Merz, Michael Rushton, Bernadette Carroll, Michelle Charles

, Diana Jurk , Stephen Tait , Thanet Sornda , Glyn Nelson , James Wordsworth , Laura Greaves , Satomi Miwa , Antje Thien , Kathrin Thedieck , Fiona Oakley , Rafal Czapiewski , Antonio Vidal-Puig , Sergio Rodriguez-Cuenca , Derek Mann , Gabriele Saretzki , Thomas von Zglinicki , Viktor Korolchuk, Mohammad Bohlooly-Y, Joao Passos. *EMBO*. 2016.

**DNA Damage Response at Telomeres Contributes to Lung Ageing and Chronic Obstructive Pulmonary Disease.** Jodie Birch, Rhys Anderson, Clara-Correia Melo, Diana Jurk, Graeme Hewitt, Francisco Marques, Nicola Green, Elizabeth Moisey, Mark Birrell, Maria Belvisi, Fiona Black, John Taylor, Andrew Fisher, Anthony de Souza and Joao Passos. *American Journal of Physiology - Lung Cellular and Molecular Physiology*. 2015.

**Chronic Inflammation Induces Telomere Dysfunction, Limits Regenerative Capacity, and Accelerates Ageing in Mice.** Diana Jurk, Caroline Wilson, Joao Passos, Fiona Oakley, Clara Correia-Melo, Laura Greaves, Gabriele Saretzki, Chris Fox, Conor Lawless, Rhys Anderson, Graeme Hewitt, Silvia Pender, Nicola Fullard, Glyn Nelson, Jelena Mann, Bart van de Sluis, Derek Mann, Thomas von Zglinicki. *Nature Communications*, 2014.

**Telomeres are Favoured Targets of a Persistent DNA Damage Response in Ageing and Stress-Induced Senescence.** Graeme Hewitt, Diana Jurk, Francisco D.M. Marques, Clara Correia-Melo, Timothy Hardy, Agata Gackowska, Rhys Anderson, Morgan Taschuk, Jelena Mann & Joao Passos. *Nature Communications*, 2012.

## Abbreviations

4-HNE	4-Hydroxynonenal
8-oxo-dG	8-Oxo-2'-deoxyguanosine
53BP1	Tumour Suppressor p53-Binding Protein 1
ADP	Adenosine Diphosphate
ALT	Alternate Lengthening of Telomeres
ATP	Adenosine Triphosphate
ATM	Ataxia Telangiectasia Mutated
AMPK	AMP-Activated Protein Kinase
ATR	ATM and Rad3 Related
$\beta$ -Gal	Beta-Galactosidase
CCL2	Chemokine (C-C Motif) Ligand 2
CDC25	Cell Division Cycle 25 Phosphatases
CDK1	Cyclin-Dependent Kinase 1
CDKI	Cyclin-Dependent Kinase Inhibitor Protein
CDKN1A	Cyclin-Dependent Kinase Inhibitor 1A
DAPI	4',6-Diamidino-2-Phenylindole
DBD	DNA-Binding Domain
DDF	DNA Damage Foci
DDR	DNA Damage Response
DHE	Dihydroethidium
DMSO	Dimethyl sulfoxide

DNA-PKcs	DNA-Dependent Protein Kinase Catalytic Subunit
DSB	Double-Strand Break
ECM	Extracellular Matrix
EMT	Epithelial-Mesenchymal Transition
FISH	Fluorescence <i>in situ</i> Hybridisation
H2A	Histone H2A
H2AX	Histone 2AX
γH2AX	Gamma-Histone 2AX
H <sub>2</sub> O <sub>2</sub>	Hydrogen Peroxide
HSC	Haematopoetic Stem Cell
ICC	Immunocytochemistry
IHC	Immunohistochemistry
IPF	Idiopathic Pulmonary Fibrosis
MAPK	Mitogen-Activated Protein Kinase
MIP	Macrophage Inflammatory Protein
MCP	Monocyte Chemo-attractant Protein
MDC1	Mediator of DNA Damage Checkpoint Protein 1
MDM2	Mouse Double Minute Homolog 2
MEF	Mouse Embryonic Fibroblast
MMP	Mitochondrial Membrane Potential
MRN	MRE11–RAD50–NBS1
mtDNA	Mitochondrial DNA
mRNA	Messenger Ribonucleic Acid

mTOR	Mechanistic Target of Rapamycin
NAC	<i>N</i> -Acetylcysteine
NAO	Nonyl Acridine Orange
NF- $\kappa$ B	Nuclear Factor Kappa-Light-Chain-Enhancer of Activated B Cells
NHEJ	Non-Homologous End Joining
NK	Natural Killer
OIS	Oncogene-Induced Senescence
OXPPOS	Oxidative Phosphorylation
p21	Cyclin-Dependent Kinase Inhibitor 1
p38MAPK	p38 Mitogen-Activated Protein Kinase
PBS	Phosphate-Buffered Saline
PCM1	Pericentriolar Material 1
PCNA	Proliferating Cell Nuclear Antigen
PCR	Polymerase Chain Reaction
PD	Population Doubling
PIKK	Phosphatidylinositol 3-Kinase-Related Kinase
PIN	Intraepithelial Neoplasia
PML	Promyelocytic Leukaemia
PNA	Peptide Nucleic Acid
POT1	Protection of Telomeres Protein 1
pRb	Retinoblastoma Protein
RFP	Red Fluorescent Protein

RNA	Ribonucleic Acid
ROS	Reactive Oxygen Species
RT-PCR	Reverse Transcription Polymerase Chain Reaction
SSB	Single-Strand Break
SSC	Saline Sodium Citrate
SDS	Sodium Dodecyl Sulfate
SASP	Senescence-Associated Secretory Phenotype
SA- $\beta$ -Gal	Senescence-Associated Beta-Galactosidase
siRNA	Small Interfering Ribonucleic Acid
SOC	Super Optimal Broth with Catabolite Repression
SOD	Superoxide Dismutase
TAF	Telomere-Associated Foci
TGF- $\beta$	Transforming Growth Factor Beta
TIF	Telomere-Induced Foci
TIN2	TERF1-Interacting Nuclear Factor 2
TNF- $\alpha$	Tumour Necrosis Factor Alpha
TPP1	Tripeptidyl Peptidase 1
TRF1	Telomeric Repeat-Binding Factor 1
TRF2	Telomeric Repeat-Binding Factor 2
TUNEL	Terminal Deoxynucleotidyl Transferase dUTP Nick End Labelling
UV	Ultraviolet
VEGF	Vascular Endothelial Growth Factor

# Table of Contents

Abstract.....	i
Dedication.....	ii
Acknowledgments.....	iii
Awards and Publications.....	v
Abbreviations.....	vii
1 Introduction.....	7
1.1 Introduction to Senescence .....	7
1.2 Senescence Causes .....	8
1.2.1 DNA Damage .....	8
1.2.2 Telomeres and Replicative Senescence.....	11
1.2.3 Telomere-Associated DNA Damage Foci.....	16
1.2.4 Oncogene-Induced Senescence.....	18
1.3 Senescence Control Pathways .....	19
1.3.1 P53-P21 .....	20
1.3.2 P16-pRb .....	21
1.3.3 Role of ROS in Senescence .....	23
1.3.4 mTOR Signalling.....	26
1.4 Senescence Phenotype.....	28
1.4.1 Growth Arrest .....	28
1.4.2 Apoptosis Resistance .....	28
1.4.3 Altered Gene Expression .....	29
1.4.4 Senescence Markers .....	30
1.5 Physiological Role of Senescence.....	32
1.5.1 Anti-tumour mechanism.....	32
1.5.2 Development .....	34
1.5.3 Wound Healing.....	36
1.5.4 Immune Clearance .....	37
1.6 Senescence and Ageing.....	38
1.6.1 Pro-tumourigenic properties.....	38
1.6.2 Disease .....	40
1.7 Post-Mitotic Senescence.....	44

1.8	Aims .....	48
2	Chapter 2 - Materials and Methods.....	49
2.1	Chemicals and Reagents.....	49
2.2	Buffers and Solutions .....	49
2.3	Cell Culture .....	50
2.3.1	Cell lines .....	50
2.3.2	Primary Embryonic Mouse Cardiomyocytes.....	51
2.3.3	Primary Adult Mouse Cardiomyocytes .....	52
2.3.4	Cryogenic Storage .....	53
2.3.5	Resuscitation of Frozen Cells .....	53
2.3.6	Calculating Cell Density and Population Doublings .....	53
2.4	Live Cell Imaging .....	54
2.4.1	Foci Dynamic Quantification .....	54
2.5	T-Loop Detection via STORM.....	55
2.5.1	Nuclei Isolation .....	55
2.5.2	DNA Crosslinking.....	55
2.5.3	Chromatin Spread.....	56
2.5.4	FISH.....	56
2.5.5	STORM Imaging .....	56
2.6	Plasmid Expansion and Purification.....	57
2.7	Transfection .....	59
2.8	Conditioned Medium .....	60
2.9	EdU Incorporation.....	60
2.10	Genotoxic Stress.....	61
2.10.1	X-Ray Irradiation .....	61
2.10.2	Chemical-induced .....	61
2.11	Treatment with Pathway Inhibitors.....	61
2.11.1	Inhibition of mTORC1 .....	61
2.12	Knock down by small Interfering RNA .....	61
2.13	Flow Cytometry .....	62
2.13.1	Mitochondrial Mass.....	62
2.13.2	Reactive Oxygen Species .....	62
2.14	Mice.....	62
2.14.1	Mice Groups and Treatments .....	62
2.14.2	Animal Housing .....	63

2.14.3	Mice Tissue Collection and Preparation .....	64
2.15	Human Tissue Collection, Preparation and Ethics.....	64
2.16	Immunocytochemistry .....	64
2.16.1	ICC on fixed cells.....	64
2.16.2	Telomere-FISH on Fixed Cells following ICC.....	66
2.16.3	ICC on Paraffin Embedded Mouse and Human Tissue .....	67
2.16.4	Telomere-FISH on Mouse and Human Tissues following ICC.....	69
2.17	Q-FISH .....	69
2.18	Immunohistochemistry .....	69
2.18.1	IHC on paraffin embedded tissue.....	69
2.19	CHIP-PCR .....	71
2.19.1	Crosslinked ChIP Assay .....	71
2.19.2	Real-time PCR .....	71
2.20	Senescence Associated $\beta$ Galactosidase Activity Assay.....	71
2.20.1	SA- $\beta$ -Gal on Fixed Cells.....	71
2.21	Telomeric Repeat Amplification Protocol (TRAP) Assay .....	72
2.22	Protein Expression Analysis .....	72
2.22.1	Protein Extraction .....	72
2.22.2	Protein Quantification.....	73
2.22.3	Western Blot.....	73
2.23	Gene Expression Analysis .....	75
2.23.1	RNA Extraction.....	76
2.23.2	cDNA Synthesis .....	76
2.23.3	Real Time Polymerase Chain Reaction (RT-PCR) .....	76
3	External Stress Induces Persistent DNA Damage at Telomeres in Cardiomyocytes.....	78
3.1	TAF are Persistent in Mouse Embryonic Fibroblasts following X- Irradiation .....	79
3.2	TAF are Persistent in H9C2 Cardiomyocytes following X-Irradiation.....	81
3.3	TAF are Induced Independently of DNA Replication .....	84
3.4	TAF Induce Senescence <i>in vitro</i> .....	87
3.5	Does Genomic Stress Induce Telomere Uncapping?.....	92
3.6	Discussion .....	95
4	Effect of Ageing on Telomere Dysfunction in Cardiomyocytes <i>in vivo</i> .....	102
4.1	X-irradiation Induces TAF in Mouse Cardiomyocytes <i>in vivo</i> .....	103
4.2	TAF Increase in Mice Cardiomyocytes with Age Independently of Telomere Length .....	104

4.3	TAF Accumulate in Human Cardiomyocytes Independently of Telomere Length..	109
4.4	Cardiomyocytes are Associated with Senescent Markers. ....	112
4.5	An Age Dependent Bystander Effect from Mouse Cardiomyocytes .....	116
4.6	An Age-Dependent Increase in Quad Myocytes TAF .....	117
4.7	Discussion.....	118
5	Effects of Oxidative Stress/Rapamycin on Cardiomyocyte Telomere Dysfunction .....	125
5.1	MAO-A Overexpression Drives TAF <i>in vivo</i> .....	126
5.2	A Reduction in MnSOD or Catalase Activity can Drive TAF Generation <i>in vivo</i> .....	130
5.3	mTOR Inhibition Impacts on ROS and Senescence in Human Fibroblasts .....	132
5.4	mTOR Inhibition Impacts on DDR During Senescence in Human Fibroblasts .....	137
5.5	mTOR Inhibition Impacts on TAF and ROS in Cardiomyocytes.....	141
5.6	Discussion.....	144
6	Conclusions .....	153
7	References.....	158

## List of Tables

Table 1. Buffers and Solutions.....	50
Table 2. Transfection Reagents. ....	60
Table 3. Primary Antibodies for ICC on Cells.....	66
Table 4. Secondary Antibodies for ICC on Cells.....	66
Table 5. Primary Antibodies for ICC on Mouse and Human Tissues .....	68
Table 6. Secondary Antibodies for ICC on Mouse and Human Tissue .....	68
Table 7. Primary Antibodies for IHC on Tissues .....	70
Table 8. Secondary Antibodies for IHC on Tissues.....	71
Table 9. Telomere Sequence for RT-PCR for Telomeric Repeats .....	71
Table 10. Acrylamide gel recipe for western blot .....	74
Table 11. Primary Antibodies for Western Blot.....	75
Table 12. Secondary Antibodies for Western Blot.....	75
Table 13. Primer Sequences for RT-PCR on Isolated Mouse Cardiomyocytes .....	77

## List of Tables

Figure 1-1. Scheme for DDR-Induced Signalling Pathway (Kastan, 2008).....	9
Figure 1-2. Schematic of Telomere-Associated Foci (TAF).....	18
Figure 1-3. A Stochastic Feedback Loop Model Predicts the Kinetics of DDR Growth Arrest at the Single Cell Level.....	26
Figure 1-4. Mechanisms of Tissue and Organ Deterioration by Cellular Senescence (van Deursen, 2014).....	44
Figure 3-1. X-Ray Irradiation induces Persistent TAF in Mouse Embryonic Cardiomyocytes....	81
Figure 3-2. X-Ray Irradiation induces Persistent TAF in H9C2 Cardiomyocytes.....	82
Figure 3-3. Live-cell Time-lapse Microscopy reveals Persistent IR-induced DDR foci in H9C2 cells.....	84
Figure 3-4. TAF are induced Independently of DNA Replication in X-irradiated H9C2 cells.....	85
Figure 3-5. TAF are induced Independently of DNA Replication in H <sub>2</sub> O <sub>2</sub> H9C2 cells.....	87
Figure 3-6. X-Irradiation induces Senescence in H9C2 Cardiomyocytes.....	88
Figure 3-7. TRF1-FokI Fusion Protein induces Telomere-specific Double Strand Breaks.....	90
Figure 3-8. Double Strand Telomeric Breaks Drive Cellular Senescence in H9C2 Cardiomyocytes.....	90
Figure 3-9. STORM Microscopy enhances Resolution of MEF Telomeres compared to Conventional Confocal Microscopy.....	93
Figure 3-10. 10Gy X-Irradiation does not alter the Percentage of t-loops in Chromatin Spreads of MEF Nuclei.....	94
Figure 4-1. Whole body X-irradiation induced TAF in Mouse Cardiomyocytes.....	104
Figure 4-2. TAF Accumulate with Age in Mouse Cardiomyocytes.....	107
Figure 4-3. TAF Accumulate in Mouse Cardiomyocytes Independently of Telomere Length...	108
Figure 4-4. TAF Accumulate with Age in Human Cardiomyocytes.....	110
Figure 4-5. TAF occur Independently of TRF2 Abundance in Human Cardiomyocytes.....	112
Figure 4-6. Senescence-associated Genes are Upregulated with Age in Mouse Cardiomyocytes.....	113
Figure 4-7. Senescence Makers Increase with Age in Mouse Cardiomyocytes.....	116
Figure 4-8. Conditioned Medium from Old Mouse cardiomyocytes reduces Proliferation of Fibroblasts.....	117
Figure 4-9. TAF Accumulate with Age in Mouse Quad Muscle Myocytes.....	118
Figure 5-1. An Age-Dependent Increase in MAO-A Expression in Mouse Cardiomyocytes.....	127
Figure 5-2. MAO-A Overexpression drives TAF generation in Mouse Cardiomyocytes <i>in vivo</i> .....	130
Figure 5-3. Catalase <sup>-/-</sup> and MnSOD <sup>-/+</sup> Models of Elevated Oxidative Stress also Drive TAF in Cardiomyocytes <i>in vivo</i> .....	131
Figure 5-4. Mitochondrial Mass increases with X-Irradiation and is associated with Cellular Senescence.....	132
Figure 5-5. X-Irradiation-induced increases in Mitochondrial Mass can be attenuated with Rapamycin Treatment .....	135
Figure 5-6. mTOR Inhibition attenuates Genotoxic Stress-induced Senescence.....	137
Figure 5-7. mTOR Inhibition reduces Replenishment of Short-lived Foci following X-irradiation via ROS attenuation.....	140
Figure 5-8. An Epistatic Association between mTOR and ATM Inhibition in attenuating the Development of X-Irradiation-induced Senescence.....	141
Figure 5-9. Rapamycin-supplemented Diet reduces Age-associated TAF Accumulation, Oxidative Stress and Senescence Markers.....	143

# 1 Introduction

## 1.1 Introduction to Senescence

Once upon a time, it was believed that human cells had the capability of proliferating indefinitely *in vitro*, given suitable culture conditions, however, this paradigm was revised when in 1961 Hayflick and Moorhead showed that human fibroblast cells grown *in vitro* have a limited proliferative capacity (Hayflick and Moorhead, 1961; Hayflick, 1965). This was demonstrated by co-culturing young and old fibroblasts and observing that the older ones entered an irreversible cell cycle arrest sooner than the younger ones, thus showing that proliferation cessation is, contrary to previous criticism, not merely an artefact of poor cell culture conditions (Hayflick and Moorhead 1961; Hayflick 1965). This observed proliferative cessation is now referred to as cellular senescence, however, a universal and concise definition for cellular senescence is a much-debated subject, as initially senescence was regarded as a state of irreversible growth arrest in somatic cells, however research has emerged which argues that even post-mitotic cells can elicit a senescent-like phenotype (Minamino *et al.*, 2009; Jurk *et al.*, 2012). Moreover, in addition to cell cycle arrest, senescent cells also display various other phenotypic changes, which will be discussed in greater detail throughout.

Physiologically, senescence is thought to act as a tumour suppressor mechanism by inhibiting the division of pre-cancerous cells (Serrano *et al.*, 1997; Ramsey and Sharpless, 2006), and evidence is emerging which implicates roles for senescent cells in various other biological processes, such as wound healing (Jun and Lau, 2010) and embryonic development (Rajagopalan and Long, 2012; Muñoz-Espín *et al.*, 2013a; Storer *et al.*, 2013). In contrast to this, senescent cells have also been linked to contributing to a severe decline in tissue homeostasis (Campisi and d'Adda di Fagagna, 2007), driving age-related diseases (Baker *et al.*, 2011), inducing paracrine senescence (Hubackova *et al.*, 2012a; Nelson *et al.*, 2012; Acosta *et al.*, 2013), and even promoting a pro-tumourigenic microenvironment (Alspach *et al.*, 2013). Senescence can therefore be considered antagonistically pleiotropic; as a mechanism causative of both beneficial and detrimental effects (George, 1957).

## 1.2 Senescence Causes

Senescence can be induced by different factors, which vary dependent on cell and tissue type. In this section, I will explain different mechanisms which have been implicated in driving cellular senescence.

### 1.2.1 DNA Damage

DNA damage, in particular double-strand breaks (DSBs), has been shown to trigger cellular senescence in various cell lines (Di Leonardo *et al.*, 1994). In response to DNA damage, several members of the phosphoinositide-3-kinase-related protein kinase (PIKK) family can be activated and subsequently amplify the DNA damage signal, allowing downstream effector proteins to take the necessary action in relation to halting the cell cycle, the restructuring of chromatin and repairing the DNA damage (Rouse, 2002). Furthermore, Ataxia-telangiectasia Mutated (ATM) and DNA-dependent protein kinase (DNA-PK) mainly respond to double strand breaks, whereas Ataxia-telangiectasia and Rad3-related (ATR) is activated by stalled DNA replication forks and single-stranded breaks (SSBs) (Falck *et al.*, 2005). The binding of these proteins to sites of damage is aided by other proteins, for example, ATR binding is mediated by ATRIP (Zou, 2003), whereas DNA-PK recruitment is facilitated by the Ku70-Ku80 heterodimer (Tanya and Stephen, 1993).

Upon a DSB, autophosphorylation occurs on Ser<sup>1981</sup> of the ATM dimer, resulting in dimer dissociation, which consequently frees the kinase domain of monomeric ATM, thus allowing the phosphorylation of downstream substrates containing the ATM consensus target sequence (Bakkenist and Kastan, 2003). ATM phosphorylates histone H2AX, known as gamma-H2AX ( $\gamma$ H2AX), which in turn recruits additional ATM to the lesion, thus initiating a positive feedback loop which amplifies the DDR signal, which is capable of spreading up to several hundreds of kilobases from the break (Rogakou *et al.*, 1999; Meier *et al.*, 2007; Iacovoni *et al.*, 2010). This process is facilitated by DDR mediators p53-binding protein 1 (53BP1) and mediator of DNA damage checkpoint (MDC1), which facilitate the interaction between ATM and  $\gamma$ H2AX (Bekker-Jensen *et al.*, 2005; Lou *et al.*, 2006). Independently of ATM activation, multiple proteins get recruited to the site of damage, including 53BP1,

BRCA1 and the MRN complex (Kastan, 2008). ATM recruitment to double strand breaks has been shown to be facilitated by the NBS1 protein of the evolutionary conserved Mre11-Rad50-Nbs1 (MRN) complex (Carson *et al.*, 2003). Moreover, activated ATM kinase can then phosphorylate substrates such as BRCA1, 53BP1, NBS1 and histone H2AX, which can all play a role in the DDR (Fig 1.1) (Kastan, 2008).

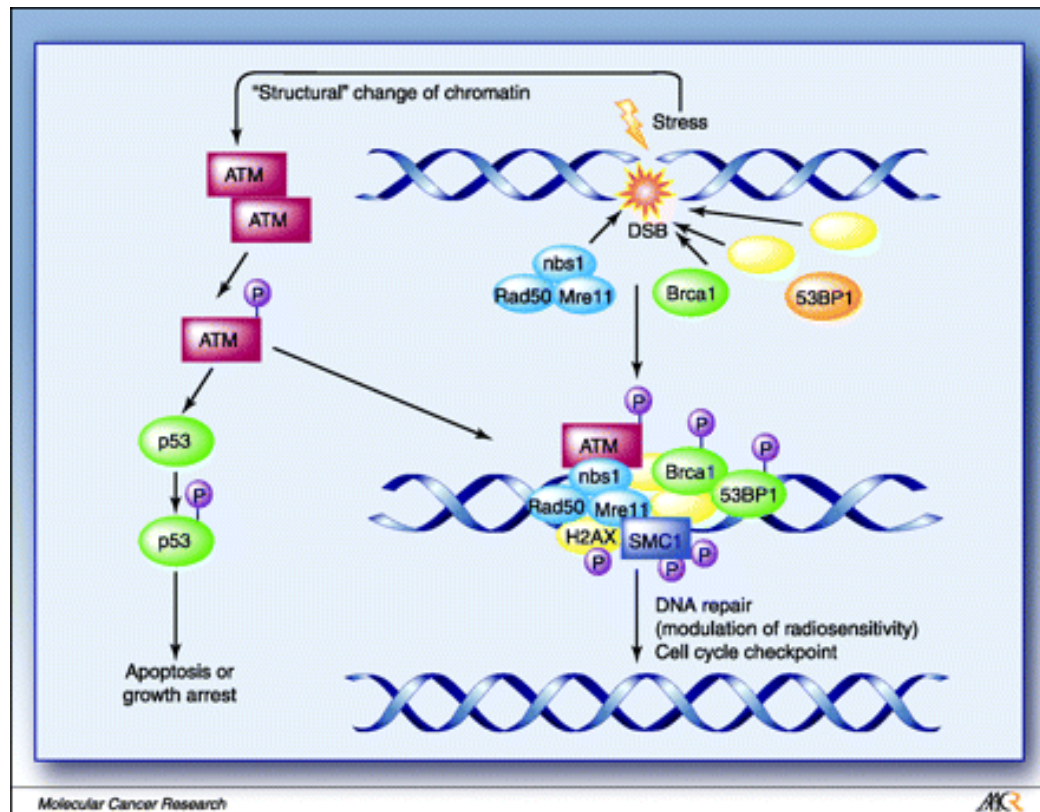


**Figure 1-1 Scheme for DDR-induced Signalling Pathway (Kastan, 2008).** Following a stress-induced DSB, numerous DDR proteins, including 53BP1, BRCA1 and the MRN-complex (NBS1, Rad50 and Mre11) are recruited to the site of damage. ATM becomes phosphorylated and can activate p53 to signal for apoptosis of growth arrest, unless the lesion is repaired, and the cell can re-enter the cell cycle.

SSBs elicit binding of the single-stranded DNA-binding protein replication protein (RPA), which acts to recruit ATR (Cortez *et al.*, 2001). However, during DSB repair, processing of the DSB leads to exposed single-stranded DNA which recruits RPA, and thus both ATR and ATM can be present at the same lesion in an ATM-dependent manner (Jazayeri *et al.*, 2006). Persistence of ATR and ATM above a certain threshold can lead to CHK2 phosphorylation by ATM, which can activate key cell cycle determinants such as the cell-division cycle 25 (CDC25) phosphatases and the tumour suppressor protein p53. Moreover, CDC25 phosphatases are required for

progression from G1 to S phase during cell replication, and thus the cell cycle is rapidly arrested upon their DDR-induced inactivation (Mailand *et al.*, 2000). This cell cycle arrest can be bypassed by overexpression of the cell cycle regulator cyclin-dependent kinase 1 (CDK1), however this leads to increased DNA damage and decreased cell survival following genotoxic stress (Mailand *et al.*, 2000). Activated CHK2, and ATM, can phosphorylate p53 at Ser-15 and Ser-20 respectively, which dissociates p53 from its negative regulator MDM2, leading to p53 stabilisation and transcription of downstream proteins such as the cyclin dependent cell cycle inhibitor p21. Subsequently, p21 leads to a stable cell cycle arrest (Di Leonardo *et al.*, 1994; Deng *et al.*, 1995; d'Adda di Fagagna *et al.*, 2003; Herbig *et al.*, 2004). In addition, in a large number of cell lines, the cyclin-dependent kinase inhibitor p16 is also expressed in response to a persistent DDR and thus provides an extra enforcer of cell cycle inhibition (Stein *et al.*, 1999; Beauséjour *et al.*, 2003; Jacobs and de Lange, 2004). However, there is still doubt about the factors responsible for p16 activation, since data indicates that p16 is induced during senescence independently from a DDR (Herbig *et al.*, 2004). Moreover, the p53-p21 and p16-Rb pathways will be discussed in greater depth later on.

DNA damage occurs frequently from both endogenous and exogenous sources, with estimates from mouse and human fibroblasts suggesting that thousands of SSBs and around 10 DSBs are generated per cell every day (Lieber, 2010). SSBs are thought to be less threatening to genomic integrity *per se*, however they can form DSBs if encountered by the DNA replication machinery during S phase (Kuzminov, 1999). DSBs arising during S phase are usually repaired via homologous recombination (HR), by using the homologous sister chromatid DNA as a template for efficient repair (Saleh-Gohari *et al.*, 2005). DSBs can also occur stochastically due to aberrant nuclear enzyme activity, ionising radiation and reactive oxygen species (ROS), and are often repaired by non-homologous end joining (NHEJ), a mechanism which ligates broken strands in the absence of sister chromatid DNA (Riballo *et al.*, 2004).

Upon eliciting a DDR, cell-cycle progression is temporary halted until the DNA damage has been resolved (Jackson and Bartek, 2009). However, if the DNA damage is not resolved or exceeds a certain threshold, cells may initiate senescence or apoptosis. Furthermore, due to a basal rate of DNA damage being constantly induced and repaired, it is difficult to ascertain the exact thresholds, both numerically and temporally, for when the cellular decision is made to enter senescence or

undergo apoptosis. Research into DNA damage uses a number of different genotoxic agents, for example, neocarzinostatin is a protein-chromophore complex which is a very-potent DNA damaging agent and known for its anti-tumour activity, and etoposide is a cytotoxic agent which causes DNA damage by inhibiting topoisomerase II from re-ligating DNA strands, both of which have been shown to increase SA- $\beta$ -Gal activity in human fibroblasts following exposure (Hewitt *et al.*, 2012). In addition, less specific DNA damaging agents are used such as ionising radiation or hydrogen peroxide ( $H_2O_2$ ), which is a strong oxidiser that can cause both single and double strand breaks in the DNA, and following  $H_2O_2$  exposure, human fibroblasts have been shown to enter a G1 cell cycle arrest and display elevated SA- $\beta$ -Gal activity (Duan *et al.*, 2005). Understanding the threshold for DNA damage-induced senescence is also made more difficult due to the varying forms of DNA damage induced. For example, etoposide-induced DNA damage results in a bimodal repair kinetic, with 90% of foci having half-lives of around 2 hours, whereas 10% of the foci have half-lives of around 12 hours (Shibata *et al.*, 2011). These observations compliment the two-lesion kinetic (TLK) model of DSB, which proposes there are simple DSBs which are rapidly repaired, and complex DSBs, which may contain additional damage such as base deletions, or strand breaks, and thus take significantly longer to repair (Stewart, 2001; Ma *et al.*, 2005).

### 1.2.2 Telomeres and Replicative Senescence

Genomic DNA in eukaryotic organisms is packaged into chromosomes, which due to their linearity have physical ends. However, eukaryotes have evolved complex DNA repair machinery which recognise exposed ends of DNA, and elicit a DNA Damage Response (DDR) in attempt to repair them, however, early observations revealed that the ends of chromosomes were resistant to a DDR and subsequent fusion reactions, which would otherwise occur in other broken and exposed regions of the genome (McClintock, 1938; McClintock, 1941). Interestingly, it was shown that introduction of linear plasmids into eukaryotic cells were unstable and prone to recombination with the genome, however, this could be stabilised with the addition of G-rich repeats from yeast chromosome ends (Orr-Weaver *et al.*, 1981; Szostak and Blackburn, 1982; Shampay *et al.*, 1984). These ends of chromosomes were shown to be distinct from genomic DNA in that they consist of a 5'-3' genetic repeat of code, consisting of the

hexamer 5'-TTAGGG-3' in mammalian species and other variations across most, if not all, eukaryotes from yeast to vertebrates (Blackburn, 1991). These repeat sequences were coined 'telomeres' and were also shown to end with a G-rich 3' single-stranded overhang (Klobutcher *et al.*, 1981; Henderson and Blackburn, 1989). In addition, telomeres were also shown to be unique from the rest of the genome by associating with a 6-subunit protein complex: TRF1, TRF2, POT1, RAP1, TIN2 and POT1 (de Lange, 2005). Both TRF1 and TRF2 contain SANT/Myb-type DNA-binding domains (DBD) in their carboxy terminus which recognise and bind to the sequence 5'-YTAGGGTTR-3' in double-stranded DNA, and can form homodimers as well as high order oligomers, thus providing numerous DBDs for the protein complex to bind to large sequences of telomeric DNA (Bianchi *et al.*, 1999; Court *et al.*, 2005; Hanaoka *et al.*, 2005). In addition, POT1 also has a DBD with a high affinity for the single stranded 5'(T)TAGGGTTAG-3' sequence found on the 3' G-rich overhangs on telomeres (Lei *et al.*, 2004; Ye *et al.*, 2004). Rap1 associates with TRF2, and both TRF1 and TRF2 bind to TIN2, which interacts with the TPP1/POT1 heterodimer, thus creating a stable telomere-binding complex, with multiple telomeric DNA binding sites, thus allowing the 6-subunit protein complex high specificity and affinity for telomeric repeats. Electron microscopy images showed that purified telomeric restriction fragments were able to form a lariat-like structure *in vitro*, thought to be a consequence of the invasion and subsequent binding of the 3' overhang into the downstream duplex telomeric DNA (Griffith *et al.*, 1999). The formation of the lariat-like structure, coined the 't-loop' was shown to be dependent on the telomere-associated protein TRF2 (Griffith *et al.*, 1999). Moreover, the formation of the t-loop provides an elegant mechanism which physically "shelters" the end of the chromosome from DDR proteins, and thus the name shelterin was given to the 6-protein complex which associates with telomeres and facilitates this process (de Lange, 2005). However, TRF2 inhibition in both mouse and humans has been shown to activate ATM kinase at telomeres (Karlseder *et al.*, 1999; Celli and de Lange, 2005), which in turn leads to the accumulation of DDR proteins such as MDC1, 53BP1 and  $\gamma$ H2AX at telomeres, resulting in p53 upregulation and a p21-mediated G1/S cell cycle arrest (Karlseder *et al.*, 1999; d'Adda di Fagagna *et al.*, 2003; Takai *et al.*, 2003). Furthermore, TRF2 inhibition also leads to NHEJ-mediated and end-to-end chromosome fusions (van Steensel *et al.*, 1998; Smogorzewska *et al.*, 2002; Celli and de Lange, 2005). The mechanism for this NHEJ suppression, results from TRF2 and its binding partner RAP1 having an inhibitory effect on DNA-PK and

ligase-IV-mediated NHEJ (Bae and Baumann, 2007). Whilst TRF2 inhibition leads to an ATM-dependent DDR at telomeres, POT1 deletion results in ATR-dependent DDR and phosphorylation of Chk1 (Hockemeyer *et al.*, 2006; Guo *et al.*, 2007), highlighting that telomeres are associated with two proteins which independently repress the two major DDR pathways, thus differentiating telomeres from internal DSBs. Interestingly, dysfunctional telomeres elicit an ATM-dependent DDR in which CHK2 is not phosphorylated, which is distinct from ATM-dependent genomic DSBs (Cesare *et al.*, 2013). In addition, telomere dysfunction, unlike genomic DSBs, does not activate a G2/M checkpoint, but allows mitosis to complete before arresting cells in p53-dependent G1 cell cycle arrest (Cesare *et al.*, 2013).

Telomere dysfunction can also arise as a consequence of telomere attrition, resulting from an inability of the telomere sequence to be fully replicated during DNA replication. DNA polymerase can only synthesise DNA in the 5'-3' direction, thus resulting in a leading and lagging strand of DNA. The lagging strand requires the binding of RNA primers to enable DNA polymerase to bind to and replicate DNA, followed by the degradation of the RNA primer and replacement with DNA. However, the final attached RNA primer does not have a DNA template behind it, and eventually succumbs to degradation, thus resulting in telomere shortening; a phenomenon coined the 'end replication problem' (Olovnikov, 1971; Watson, 1972). It is thought that telomere shortening and associated dysfunction is responsible for triggering replicative senescence, and it has been observed that different cell types have a reproducible number of times they can divide before entering senescence, known as their 'Hayflick limit'. Moreover, it has been proposed that telomeres reflect a cell's replication history, thus acting as a molecular clock (Harley *et al.*, 1990; Harley *et al.*, 1992). However, the end replication problem is only predicted to result in a loss of around 20 base pairs per cell division, whereas evidence suggests that around 50-200 base pairs of telomere DNA are lost each cell division. Interestingly, it has been shown that telomere attrition is accelerated by oxidative stress (von Zglinicki *et al.*, 1995; von Zglinicki *et al.*, 2000), and thus telomeres appear not to represent merely a tally counter for replication history, but a proxy for their history of cellular stress as well.

Once telomeres reach a critical length, it is thought that steric constraints on the t-loop structure cause the 3' overhang to dissociate from its complementary DNA strand, thus linearising the telomere, or 'uncapping', therefore exposing the physical

end of the telomere to the nucleoplasm where it can be recognised as DNA damage and lead to p53-dependent cell cycle arrest (Herbig *et al.*, 2004). Moreover, dysfunctional telomeres accumulate DDR proteins such as  $\gamma$ H2AX, 53BP1, MRE11, which subsequently signal through ATM, to p53, which upregulates p21, leading to G1 cell cycle arrest (Herbig *et al.*, 2004). Inhibition of ATM results in cells re-entering the cell cycle, suggesting that a persistent DDR signal is required for cell cycle arrest (Herbig *et al.*, 2004). An on-going DNA damage response at telomeres has been shown to contribute to the development of the senescence phenotype (d'Adda di Fagagna *et al.*, 2003; Passos *et al.*, 2010). It has been proposed that a threshold of 5 telomeric DNA damage foci can predict the onset of senescence in human fibroblasts (Kaul *et al.*, 2012). Interestingly, if senescence pathways are bypassed, for example by p53 inactivation with SV40 transformation, cells can continue to proliferate with extremely short telomeres, until the level of telomere erosion causes complete telomere de-protection and cells enter a state of crisis, as defined by chromosomal fusions and eventually cell death (Counter *et al.*, 1992).

Germline immortality is dependent upon a telomere maintenance mechanism to prevent replicative senescence or crisis occurring as a result of telomere shortening. Moreover, eukaryotes evolved a solution to the end-replication-problem, which is dependent upon the ribonucleoprotein telomerase. Telomerase is a reverse transcriptase, which consists of a catalytic domain, known as Telomerase Reverse transcriptase (TERT), which recognises the 3'-OH group at the end of the G-rich overhang and elongates the telomeric DNA (Blasco, 2005). Moreover, this elongation is made possible by the Telomerase RNA Component (TERC), which also binds to the 3' overhang and creates a template for TERT to add complementary nucleotides (Elizabeth, 2001). Telomerase activity is essential for telomere length maintenance in human germ and stem cells, and defective telomerase can lead to disease pathologies, for example dyskeratosis, in which patients have severely shortened telomeres (Mitchell *et al.*, 1999). Telomerase activity is either absent or negligible in other somatic cells, therefore resulting in proliferation-associated telomere shortening (Wright *et al.*, 1996; Yui *et al.*, 1998), however, replicative senescence in somatic cells can be avoided via ectopic expression of telomerase, which replenishes the telomeric DNA and thus maintains the telomeres from reaching a critical length (Bodnar *et al.*, 1998b). This was first shown by transfection of both retinal pigment epithelial cells and foreskin fibroblasts with the telomerase catalytic subunit; it was

observed that the cells were still proliferating when the data was published, having already exceeded their Hayflick limit by 20 population doublings. Moreover, they showed decreased SA- $\beta$ -Gal activity and had significantly elongated telomeres (Bodnar *et al.*, 1998a). However, upregulated telomerase activity cannot prevent genotoxic stress-induced senescence, for example hTERT overexpressing human fibroblasts still enter cellular senescence following exposure to high doses of X-irradiation (Hewitt *et al.*, 2012), and H<sub>2</sub>O<sub>2</sub> treatment has also been shown to induce senescence in human fibroblasts independently of telomere length (Chen *et al.*, 2001).

Telomere length maintenance in the germline and stem cell populations is essential for the persistent proliferative potential by ensuring telomere lengths are substantial enough to prevent uncapping and subsequent cell cycle arrest. However, telomere maintenance mechanisms are also hijacked by cancer cells to assist immortality, with around 85% of human cancers presenting an upregulation of telomerase activity (Shay and Bacchetti, 1997). Almost all other cancer types maintain telomere length with a telomerase-independent mechanism known as Alternate Lengthening of Telomeres (ALT) (Heaphy *et al.*, 2011). Furthermore, ALT has been shown to rely on a recombination event (Dunham *et al.*, 2000), however the exact mechanism for telomere elongation requires further research.

Contrary to the regulation of telomere attrition, mechanisms have also evolved which limit telomerase-mediated elongation of telomeres, for example, telomere length in many immortalised human cell lines is stable, despite persistent telomerase upregulation (van Steensel and de Lange, 1997). Furthermore, different species are associated with different telomere lengths (Kipling and Cooke, 1990), which are kept constant throughout numerous generations (Wright *et al.*, 1996), suggesting the process of telomere elongation is controlled in the germline. Various shelterin proteins are involved in telomere elongation regulation; overexpression of TRF1 in the HT1080 tumour cell line leads to gradual telomere shortening, and conversely, expression of a dominant-negative TRF1 resulted in telomere elongation (van Steensel and de Lange, 1997), suggesting that TRF1 acts as a negative regulator of telomere elongation. TRF2 has also shown to be a negative regulator of telomere elongation, as TRF2 overexpression accelerates telomere shortening, however neither TRF1 nor TRF2 overexpression have any effect on telomerase expression levels (Smogorzewska and van, 2000). Moreover telomere elongation can be

induced by introducing a mutant POT1 with deficient TRF2 binding, however the mechanism of this effect is yet to be understood (Kendellen *et al.*, 2009).

### 1.2.3 Telomere-Associated DNA Damage Foci

Telomere shortening and dysfunction, leading to a persistent DDR and cell cycle arrest is well documented *in vitro* (as discussed above). However, it is not fully understood if telomere shortening *per se* has a pathological effect *in vivo*. The study of telomere dysfunction in mice has largely involved producing telomerase-null mice, which lack either functional TERT or TERC activity, and therefore cannot elongate telomeres, including the germline, and thus with each successive generation, progeny are born with shorter telomeres (Lee *et al.*, 1998; Hande *et al.*, 1999; Karl Lenhard *et al.*, 1999). However, the physiological relevance of this is questionable, considering that the level of telomere shortening in these models is far greater than what would be expected in wild-type mice. Telomerase-null mice lose around 4-5 kilobases of telomere per generation (Blasco *et al.*, 1997; Rudolph *et al.*, 1999), and wild-type mice lose around 15 kilobases of telomeric DNA throughout their lifetime (Vera *et al.*, 2012). No significant alterations in lifespan were observed after comparing G3 TERC<sup>-/-</sup> mice to wild-type mice (Rudolph *et al.*, 1999). Considering that G3 mice are born with telomere lengths comparable to those found in severely aged mice, and G3 mice continue to show telomere shortening throughout their life, this would suggest that telomere shortening is not having an effect on lifespan. G6 TERC<sup>-/-</sup> mice do display significantly shortened lifespans, but this level of telomere shortening cannot be considered physiological (Rudolph *et al.*, 1999), and is more akin to a telomerase-defective disease such as dyskeratosis congenita (Mitchell *et al.*, 1999).

Our group observed an age-dependent increase in telomeres co-localising with a DDR in murine hepatocytes and enterocytes, however, interestingly, Q-FISH analysis revealed that this was occurring independently of telomere length, which contradicted the hypothesis that telomere dysfunction is driven purely by attrition and subsequent uncapping (Hewitt *et al.*, 2012). Our group and another showed *in vitro* that SA- $\beta$ -Gal activity could be increased upon treatment with genotoxic stresses, such as X-irradiation, H<sub>2</sub>O<sub>2</sub> or neocarzinostatin, all of which are known to cause DSBs, and we

observed a DDR detectable by  $\gamma$ H2AX occurring in both genomic and telomeric DNA (Fumagalli *et al.*, 2012; Hewitt *et al.*, 2012). However, with time genomic DDR foci are resolved, whereas telomeric DDR remained persistent (Fumagalli *et al.*, 2012; Hewitt *et al.*, 2012). Several models were proposed to explain this phenomenon. It has been observed that oxidative damage disrupts the recognition of telomeres by TRF1 and TRF2 (Opresko *et al.*, 2005), and thus the observed DDR foci at telomeres could occur due to telomere uncapping, however telomeres devoid of TRF2 are known to undergo end-to-end fusions (van Steensel *et al.*, 1998), which we did not observe (Hewitt *et al.*, 2012). Another group observed spontaneous DDR foci at telomeres in human cancer cells, which retained an abundance of TRF2, yet a DDR was present (Cesare *et al.*, 2009). Considering this, another possibility could be that genotoxic stress leads to t-loop uncapping, whilst retaining enough TRF2 to inhibit NHEJ, without affecting initiation of a DDR. Finally, we proposed that similar to genomic DNA, genotoxic stress could lead to physical DSBs within the telomeric region which remain persistent due to presence of TRF2 inhibiting a DDR. Moreover, an endonuclease-induced DSB next to ectopically expressed TRF2 remained persistent, thus suggesting that the inhibitory effect of TRF2 on DNA repair is independent of telomeric location and t-loop (Fumagalli *et al.*, 2012).

To differentiate stress-induced telomere dysfunction from telomere-shortening induced dysfunction, we shall herein refer to the varying proposed mechanisms of telomere dysfunction as either Telomere-Associated Foci (TAF) or Telomere-Induced Foci (TIF) respectively. Furthermore, TIF are thought mainly to arise due to uncapping, either as a result of steric constraints on critically short telomeres, or due to inhibition of shelterin proteins, whereas TAF have been proposed to arise due to physical DSBs within telomeric regions (Hewitt *et al.*, 2012), although further research is required to determine DDR signalling varies between TIF and TAF.

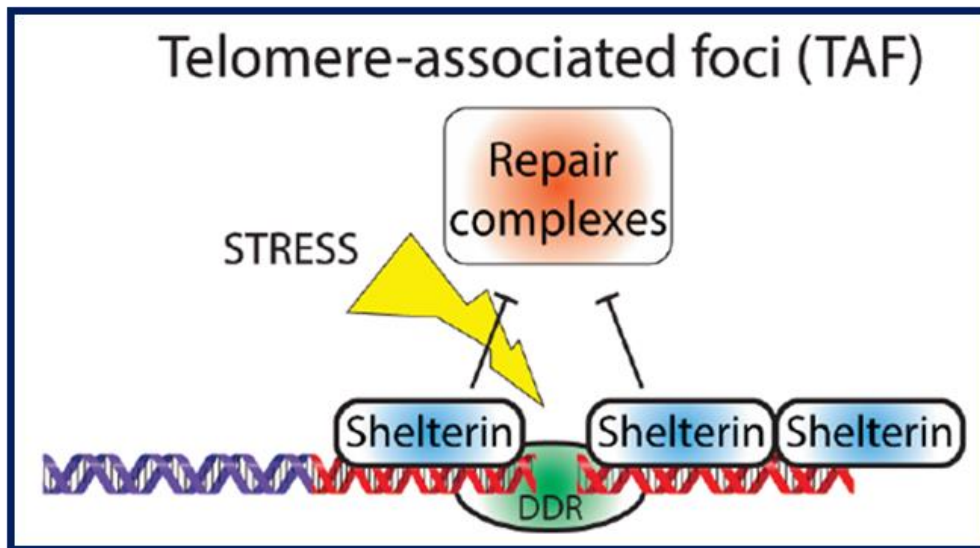


**Figure 1-2. Schematic of Telomere-Associated Foci (TAF).** It has been proposed that DSBs occurring within telomeres are irreparable due to the inhibitory action of the shelterin complex on DNA repair proteins (Hewitt *et al.*, 2012).

To conclude, it would appear that the inhibitory effect of TRF2 on DNA-PK and ligase IV prevents healthy telomeres from undergoing NHEJ-mediated end-to-end fusions (Smogorzewska *et al.*, 2002; Bae and Baumann, 2007), however, in the context of telomere dysfunction independently of length, TRF2 serves to inhibit DNA repair. In this context, telomeres can be considered both a molecular clock for telomere shortening, as well as a molecular diary for past genotoxic stress due to their irreparability.

#### 1.2.4 Oncogene-Induced Senescence

Oncogenes are genes that when are over-expressed or mutated, have the potential to turn a normal cell into a cancer cell. Before the concept of oncogene-induced senescence (OIS) had arisen, *Ras* was identified as an oncogene, capable of transforming immortalised rat cells once activated (Der *et al.*, 1982; Parada *et al.*, 1982). However, RAS activation alone was shown not to be capable of transforming normal primary embryonic cells, and required additional mutations, such as p53 inhibition by large T antigen, for transformation to occur (Land *et al.*, 1983). OIS was first characterised, when an activated allele of the mitogenic signal transducer RAS (H-*ras* V12), was introduced into human fibroblasts (Serrano *et al.*, 1997). At first, the

cells displayed hyper-proliferation however soon displayed an accumulation of p16 and p53 accompanied with a G1 cell cycle arrest, which could be bypassed by inhibition of either of the aforementioned tumour suppressor proteins (Serrano *et al.*, 1997). These observations show that initiation of cellular senescence is not simply a consequence of the number of cell divisions, as oncogenic stimuli can induce senescence prematurely. Many cell types have now been shown to acquire a senescent phenotype after the aberrant function of various oncogenes, including MEK, MOS, RAF and BRAF (Serrano *et al.*, 1997; Zhu *et al.*, 1998; Michaloglou *et al.*, 2005).

There are many proposed models for the mechanism which drives OIS, such as hyper-proliferation leading to replication errors and subsequent DDR activation (Di Micco *et al.*, 2006), or by altering intra-cellular levels of ROS production which could also lead to genotoxic stress (Lee *et al.*, 1999a). Interestingly, OIS can be bypassed in mouse cells grown under hypoxic conditions (Lee *et al.*, 1999a). Other research has shown that Rb-mediated formation of heterochromatin, leads to suppression of E2F target genes and subsequent cellular senescence (Narita *et al.*, 2003). These models of OIS induction are not mutually exclusive and it will be important to ascertain the relationship between these different mechanisms.

OIS has recently been observed to occur *in vivo* in both mice and humans, for example, as a barrier to t-cell lymphoma development (Braig *et al.*, 2005), and ras positive senescent cells have been shown to exist in pre-malignant tumours, but not in malignant, and interestingly inactivation of PTEN specifically in mouse prostate leads to invasive prostate cancer (Collado *et al.*, 2005). Therefore OIS appears to have a physiological role in tumour suppression *in vivo*, and is not simply an artefact of cell culture, as once thought.

### 1.3 Senescence Control Pathways

Senescence is often induced and maintained by either the p53 or p16-Rb tumour suppressor pathways. These signal transduction cascades can react with one another, although they can each stop cell-cycle progression independently. Which of these pathways induces senescence appears to be both species-specific and cell-

specific, although examples exist of senescence induction via alternative pathways (Olsen *et al.*, 2002; Michaloglou *et al.*, 2005).

### 1.3.1 P53-P21

P53 is transcription factor, encoded by the *TP53* gene, which is activated in response to various stresses, including the overexpression of oncogenes, and DNA damage, and is responsible for the regulation of the expression of numerous genes involved in processes such as DNA repair, apoptosis and senescence (Harms *et al.*, 2004; Green and Chipuk, 2006). P53 has therefore been bestowed with monikers such as the 'guardian of the genome' (el-Deiry *et al.*, 1993) and the 'cellular gatekeeper' (Levine, 1997). Classically, the activation of p53 can be described in 3 steps: stabilisation of p53 via ATR/ATM-mediated phosphorylation, DNA binding, and the activation of target genes by interaction with the transcriptional machinery (Kruse and Gu, 2009).

First discovered in mice, one of the main regulators of p53 is mouse double minute 2 homolog (MDM2), or HDM2 in humans, an E3 ubiquitin-protein ligase which acts to regulate both the activity and expression of p53 in several ways. MDM2 can facilitate the nuclear export of p53, thus inhibiting any transcriptional activity (Tao and Levine, 1999), as well as ubiquitinating p53 for proteosomal degradation (Haupt *et al.*, 1997; Kubbutat *et al.*, 1997). MDM2 can also inhibit p53-mediated transactivation by binding to and inhibiting the transactivation domain of p53 (Momand *et al.*, 1992). MDM2 is itself inhibited by the alternative-reading-frame (ARF) protein (Sherr and McCormick, 2002), thus highlighting various regulation points in the p53 pathway. Interestingly, the *MDM2* gene is a transcriptional target of p53, therefore instigating a negative feedback loop which acts to maintain p53 homeostasis (Wu and Levine, 1997). One mechanism of p53 stabilisation involves in the inhibition of the mdm2-p53 interaction through N-terminal phosphorylation of Ser15 and Ser20 or Ser18 and Ser23, in humans and mice respectively (Kruse and Gu, 2009). These phosphorylation reactions are performed by DDR protein kinases such as ATR, ATM, DNA-PK, Chk1 and Chk2, in response to cellular stressors such as DNA damage (Shieh *et al.*, 1997; Shieh *et al.*, 2000; Appella and Anderson, 2001).

Cellular senescence can be triggered in response to stimuli such as telomere dysfunction or DNA damage, which lead to an activated DDR, and the subsequent up-regulation of the p53 transcriptional target gene *CDKN1A*, which encodes cyclin-dependent kinase inhibitor 1 (p21) (Brown *et al.*, 1997). P21 contains a PCNA binding domain, which allows p21 to compete with PCNA for binding to DNA-polymerase- $\delta$ , therefore physically inhibiting DNA synthesis (Moldovan *et al.*, 2007). Another mechanism for p21-mediated cell cycle inhibition is through its CDK-cyclin inhibitory domain, which can inhibit various cyclin-dependent kinases (CDKs), in particular CDK2, which is responsible for the phosphorylation of retinoblastoma protein (pRb), which in turn releases and activates E2F, which is responsible for the transcription of numerous cell cycle regulators such as cyclin A, cyclin D1, cyclin E, Cdc2 and Cdc25A (Dyson, 1998). However, p21 is not a stalwart maker of irreversible cell cycle arrest, as p21 expression is elevated in response to transient cell cycle arrest in response to acute DNA damage, however, the exact threshold of DNA damage required to trigger the decision to enter cellular senescence remains elusive (Barnouin *et al.*, 2002). Interestingly, both telomere dysfunction-induced senescence and DNA damage-induced senescence can be evaded through the down-regulation or inhibition of either p53 or p21, and likewise, with the inhibition of upstream DDR proteins such as CHK2 or ATM (Brown *et al.*, 1997; Gire *et al.*, 2004).

The p53 pathway acts to halt cell-cycle progression in cells which have endured serious DNA damage, thus helping to prevent the possibility of the dissemination of potentially oncogenic mutations (Bartkova *et al.*, 2005; Gorgoulis *et al.*, 2005). In fact, compromised p53 function, due to mutation of the *TP53* gene, is found in around 50% of all human cancers, and the significant majority of the remaining cancers display aberrant function of p53 regulators, for example, the *MDM2* gene is amplified in at least 7% of *TP53* wild-type cancers (Momand *et al.*, 1998; Vousden and Lu, 2002). In the case of cells which lack or have aberrant p53 function, mitotic catastrophe often occurs, therefore acting as another anti-tumour mechanism, however a subset of cancer cells overcome this and succeed in surviving through the activation of telomerase, or ALT, to stabilise telomere length (Hanahan and Weinberg, 2000; Shay and Wright, 2005; Heaphy *et al.*, 2011).

### 1.3.2 P16-pRb

Another important pathway in the induction of senescence is the p16-pRb pathway, which can be activated following p53-p21 pathway induction, however, it can also be activated independently of p53 (Jacobs and de Lange, 2004). P16 is a tumour suppressor protein which inhibits cell cycle progression from G1 to S phase (Agarwal *et al.*, 2013). The mechanism of action involves p16 inhibiting the interaction between CDK4/6 and cyclin D1, therefore preventing pRb phosphorylation, and inhibiting the dissociation and subsequent activation of E2F (Vidal and Koff, 2000). p16 has emerged as a good marker for senescence, as it has been observed to accumulate in a wide variety of cell lines under multiple senescence-inducing stimuli (Lowe and Sherr, 2003; Campisi, 2005). However, elucidating the exact nature of the p16-pRb pathway activation will be difficult, as there are not only cell-specific differences, but also species-specific differences. Moreover, in response to telomeric disruption, mouse fibroblasts will only engage the p53 pathway, whereas human cells will engage both the p53 pathway and the p16-pRb pathway (Smogorzewska and de Lange, 2002). Interestingly, p53 inhibition can reverse senescent arrest in a variety of cell types; however, the phenotype cannot be reversed in cells which have engaged the p16-pRb pathway (Beauséjour *et al.*, 2003). Moreover, this irreversible proliferation arrest is thought to occur through the generation of SAHFs, which can modify the chromatin to repress a number of genes, including E2F target genes (Narita *et al.*, 2003). Once a SAHF is developed, the condensed chromatin can be maintained in the absence of p16-pRb pathway proteins (Narita *et al.*, 2003), and thus may help to explain the irreversibility of p16-pRb-induced senescence.

Exactly how p16 is expressed in response to senescence-inducing stimuli remains unclear, but it has been suggested to be causative of the observed repression of Polycomb INK4a repressors such as CBX7 or BMI1, coinciding with p16-pRb induced senescence (Gil *et al.*, 2004; Bracken *et al.*, 2007). What is more, in both mice and human fibroblasts, replicative lifespan has been increased via the overexpression of CBX7 or BMI1, thus strengthening the idea of the involvement of Polycomb INK4a repressors in cellular senescence (Itahana *et al.*, 2003; Gil *et al.*, 2004). Interestingly, a reduction of p16-pRb signalling results in the stabilisation of p53 due to the activation of E2F, which is a transcription factor for ARF which inhibits MDM2 and thus prevents the degradation of p53 (Zhang *et al.*, 2006).

### 1.3.3 Role of ROS in Senescence

Atoms or molecules which have unpaired valence electrons are known as free radicals, and are highly reactive. Reactive Oxygen Species (ROS) in particular, are oxygen-containing chemically reactive molecules, which include free radicals such as hydroxyl radical and superoxide anion, as well other oxidisers, for example hydrogen peroxide ( $\text{H}_2\text{O}_2$ ). ROS play important physiological roles, for example, as signalling molecules in several pathways (D'Autréaux and Toledano, 2007), as well as being produced by macrophages and neutrophils to combat microbial pathogens (Dupre-Crochet *et al.*, 2013). However, molecules and cellular structures can be damaged via oxidative stress caused by unregulated ROS levels, which can act in a chain-reaction caused by a ROS molecule ionising another molecule to stabilise its own electron configuration, consequently turning the target into a ROS molecule (Cui *et al.*, 2012). In the 1950s, Denham Harman proposed the 'free radical theory of ageing', which hypothesised that an accumulation of free radical damage over time could be driving organismal ageing (Harman, 1956). In eukaryotic cells, the majority of intra-cellular ROS are generated as a by-product of mitochondrial oxidative phosphorylation, due to leakage of electrons from the electron transport chain (ETC), and subsequent reduction of oxygen to form superoxide anion (Quinlan *et al.*, 2013). Superoxide anion is not a strong oxidant *per se*, however it can undergo further redox reactions with other molecules to form stronger oxidants such as hydroxyl radicals and  $\text{H}_2\text{O}_2$ . Considering the role of mitochondria in ROS production, Denham Harman updated the 'free radical theory of ageing', to implicate mitochondria as the main drivers of ROS-driven ageing (Harman, 1972). It has subsequently been postulated that ROS, produced as a consequence of oxidative phosphorylation, can cause mtDNA mutations which lead to deficient oxidative phosphorylation activity, which in turn leads to further electron leakage and increased ROS production, therefore instigating a positive feedback, or 'vicious cycle' (Alexeyev *et al.*, 2004). To counteract ROS damage, cells have evolved a number of antioxidant enzymes, for example superoxide dismutases (SODs) are a family of metalloenzymes which convert superoxide anion into  $\text{H}_2\text{O}_2$ , which can then be broken down into water and oxygen by either catalase or glutathione peroxidases (Fridovich, 1995). To combat superoxide anion generated either on the inner side of the inner mitochondrial membrane, or in the mitochondrial matrix, a specific form of SOD is expressed in the

mitochondrial matrix which contains manganese in the active site (MnSOD) (Fridovich, 1995).

In addition to oxidative phosphorylation, other intra-cellular sources of ROS generation include NADPH oxidases (NOX), xanthine oxidase, nitric oxide synthase and mono-amine oxidase (MAO-A) (Holmstrom and Finkel, 2014). MAO-A localises to the outer mitochondrial membrane and is involved in catalysing the oxidative deamination of monoamines, which produces H<sub>2</sub>O<sub>2</sub> as a by-product (Youdim *et al.*, 2006). ROS can also be generated by extra-cellular sources, for example ionising radiation from both X- and  $\gamma$ -rays, originating from either outer-space or decay of terrestrial radioactive elements, constantly pass through our body, which generate free radicals, usually as a consequence of the ionising particles reacting with cellular water (Lieber, 2010). Other sources of ROS include herbicides, pesticides and cigarette smoke (Valavanidis *et al.*, 2009).

Elevated ROS levels have been linked with oncogene-induced- and stress-induced senescence and replicative senescence (Saretzki *et al.*, 2003; Ramsey and Sharpless, 2006; Passos *et al.*, 2007). Treatment of cells with sub-lethal doses of hydrogen peroxide has been shown to induce senescence in human fibroblasts via the p53 pathway (Chen *et al.*, 1998). ROS can directly damage DNA, resulting in a DDR which may lead to senescence (Chen *et al.*, 1995; Lu and Finkel, 2008a). von Zglinicki *et al.*, 1995, first showed that mild oxidative stress leads to accelerated telomere shortening (von Zglinicki *et al.*, 1995) suggesting that ROS-driven single strand breaks at telomeres could accelerate telomere shortening (von Zglinicki, 2002). It was later shown that mitochondrial superoxide levels increase with replicative age and can also lead to accelerated telomere shortening (Passos *et al.*, 2007). Interestingly, mitochondrial superoxide levels can be decreased by the overexpression of TERT, independent of telomere length, in human fibroblasts exposed to oxidative stress (Ahmed *et al.*, 2008). This suggests that telomerase can have functions in mitochondria independent of its role in the nucleus, however, the mechanisms have not yet been elucidated. Furthermore, recent research has shown that mitochondrial telomerase leads to less DNA damage in the nucleus, possibly due to reduced ROS (Singhapol *et al.*, 2013).

A comprehensive causal relationship between senescence and ROS remains elusive as it has been shown that ROS production can be induced by downstream effectors

of the DDR/senescence checkpoint (Polyak *et al.*, 1997; Macip *et al.*, 2002; Macip *et al.*, 2003). The DDR protein ATM exists as an inactive dimer, which, in response to irradiation, undergoes autophosphorylation resulting in dimer dissociation and the initiation of its cellular kinase activity (Bakkenist and Kastan, 2003). However, hydrogen peroxide has recently been shown to activate dimeric ATM in the absence of DNA damage and suggests that cells have developed an intrinsic mechanism to sense ROS (Guo *et al.*, 2010; Perry and Tainer, 2011). ROS levels have been shown to increase with replicative senescence and OIS (Furumoto *et al.*, 1998; Lee *et al.*, 1999b), with the majority being produced from dysfunctional mitochondria (Lu and Finkel, 2008a; Moiseeva *et al.*, 2009). It has previously been shown that a positive feedback loop involving sustained activation of the checkpoint gene CDKN1A (p21) results in both the induction of mitochondrial dysfunction and increased production of reactive oxygen species (ROS) via a signalling cascade through GADD45-MAPK14(p38MAPK)-GRB2-TGFBR2-TGF $\beta$  (Passos *et al.*, 2010)(Figure 1-3).

OIS via expression of V12Ras, has been shown to increase production of mitochondrial ROS, and interestingly, human diploid fibroblasts grown in 1% oxygen, were unable to undergo Ras-induced OIS (Lee *et al.*, 1999a). Similarly, MEFs were shown to accumulate more DNA damage when cultured in 20% compared to 3% oxygen, and were resistant to stress-induced senescence when cultured in a hypoxic environment (Parrinello *et al.*, 2003). HDFs have been shown to undergo more population doublings before entering senescence when cultured in 3% compared to 20% oxygen (Chen *et al.*, 1995).

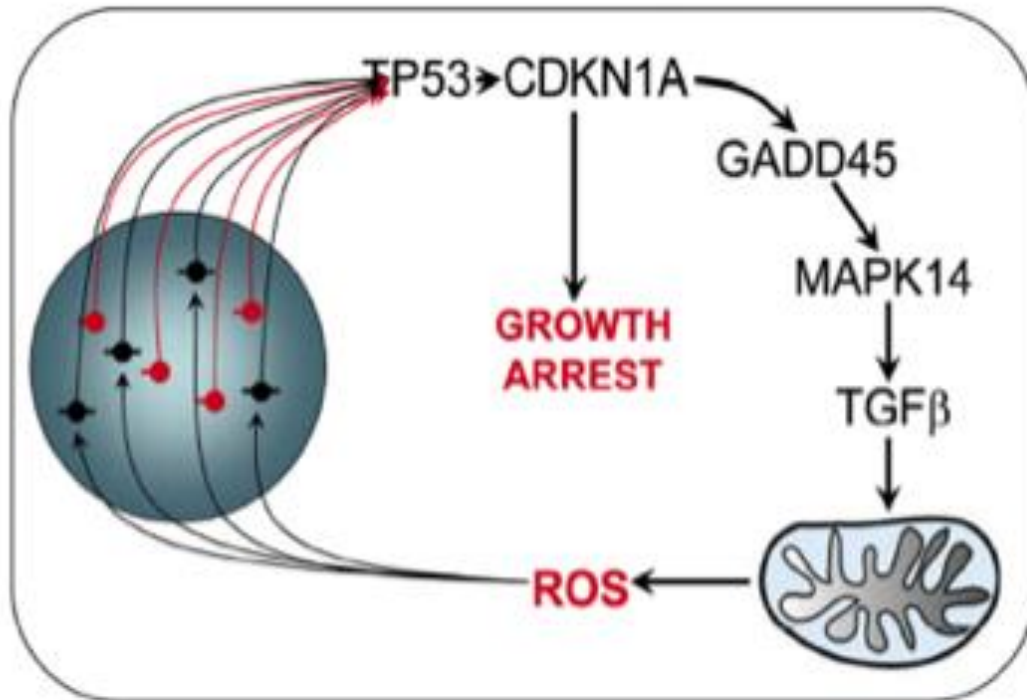


**Figure 1-3. A Stochastic feedback loop model predicts the kinetics of DDR growth arrest at the single cell level (Passos *et al.*, 2010).** Red and black circles represent telomeric and non-telomeric DSBs respectively, which signal to TP53 and CDKN1A, resulting in growth arrest. The signalling cascade continues through GADD45-MAPK14-TGFβ, resulting in mitochondrial dysfunction and elevated ROS production, which in turn causes further DSBs, thus instigating a feedback loop which sustains cellular senescence.

#### 1.3.4 mTOR Signalling

All eukaryotic organisms express the target of rapamycin (TOR) signalling pathway (known as mTOR in mammalian organisms). Moreover, this pathway is responsible for sensing both nutrient and energy abundance to coordinate cellular responses such as growth, proliferation, autophagy, protein synthesis and many others (Zoncu *et al.*, 2011). The mTOR protein belongs to PIKK family and acts as the catalytic subunit in two well described complexes known as mTOR complex 1 (mTORC1) and mTORC2, which have a variety of shared and non-shared proteins, for example the mTORC1 and mTORC2 complexes can be distinguished by the binding of the accessory proteins raptor and rictor respectively (Hara *et al.*, 2002; Sarbassov *et al.*, 2004).

Interestingly, the intervention of dietary restriction, by experimentally reducing the amount of food an organism has access to, yet without causing malnutrition, has been shown to increase the lifespan of in many organisms from yeast to mammals (Mair *et al.*, 2003). Moreover, it would appear that DR acts mainly through the inhibition of mTORC1 and experiments have shown that manipulation of nutrient sensing pathways has led to a similar increased lifespan in a range of different organisms (Zoncu *et al.*, 2011). In fact, experiments performed in yeast and flies, involving the genetic down-regulation of mTORC1 pathway components, coupled with DR, provided no additive effect on lifespan, thus strengthening this hypothesis (Kaeberlein *et al.*, 2005; Bjedov *et al.*, 2010).

In response to growth stimuli, activated mTORC1 signals to promote protein translation and growth and proliferation (Fingar and Blenis, 2004). Rapamycin is a drug which inhibits mTORC1 signalling, however does not appear to affect mTORC2 signalling, a mechanism proposed to act via dissociating raptor from the mTORC1 complex (Yip *et al.*, 2010). Feeding rapamycin to aged mice has been shown to significantly extend lifespan (Harrison *et al.*, 2009). Beneficial effects of mTORC1 inhibition on cellular ageing may be attributable to a number of factors. Moreover, mTORC1 inhibition results in a decrease in protein translation and therefore exerts less stress on protein folding systems, thus reducing the number of mis-folded protein aggregates (Zoncu *et al.*, 2011). Consequently, research has shown that a sustained rapamycin diet in a mouse model for Huntingdon's disease resulted in the reduction of toxic huntingtin aggregates (Brinda *et al.*, 2004). Activated mTORC1 signalling inhibits autophagy, however rapamycin treatment can counteract this and upregulate autophagy, which complements data showing that lifespan extension is dependent on autophagy in drosophila and nematodes (Hansen *et al.*, 2008; Bjedov *et al.*, 2010). mTOR inhibition has been shown to impact on cellular senescence. Recently, it has been shown that rapamycin suppresses replicative senescence in rodent embryonic cells (Pospelova *et al.*, 2012) and in oncogene-induced senescence (Kolesnichenko *et al.*, 2012). Furthermore, mTORC1 inhibition has been shown to suppress the secretion of numerous pro-inflammatory cytokines in senescent fibroblasts (Laberge *et al.*, 2015). Moreover, this secretory phenotype is a hallmark of senescent cells and has been shown to have detrimental effects on surrounding cells (Coppé *et al.*, 2010a), a phenomenon which will be discussed in further detail throughout.

## 1.4 Senescence Phenotype

The term senescence traditionally referred to somatic mitotic cells which had permanently lost the ability to divide, as opposed to cells that are simply in a quiescent state, i.e. those which have the potential to divide, but are currently residing in the G0 phase of the cell cycle. More recently, evidence has arisen which shows that cellular senescence is induced by very specific signalling programs, and besides cell cycle arrest, is associated with other phenotypes such as apoptosis resistance, altered gene expression, a specific secretory phenotype and elevated ROS (Campisi and d'Adda di Fagagna, 2007; Coppé *et al.*, 2008). Furthermore, these characteristics have also been observed in post-mitotic neurons and adipocytes (Minamino *et al.*, 2009; Jurk *et al.*, 2012), suggesting that senescence is more multi-faceted than just permanent cell cycle arrest, and that a redefinition of senescence may be required. In the following section, I will describe in more details characteristics of the senescent phenotype.

### 1.4.1 Growth Arrest

The quintessential senescent phenotype is the inability of a cell to advance through the cell cycle. Despite this arrest, cells still continue to be metabolically active but tend to stay locked in the G1 phase of the cell cycle (Di Leonardo *et al.*, 1994; Herbig *et al.*, 2004). Moreover, observations have shown cells to arrest in alternate stages of the cell cycle, for example G2/M (Wada *et al.*, 2004). The reasons for cells arresting at particular phases of the cell cycle are attributable to activation of different cell cycle inhibitors, such as p16 and p21 (Herbig *et al.*, 2004).

### 1.4.2 Apoptosis Resistance

Apoptosis is a mechanism for programmed cell death, followed by the removal and degradation of the resultant cellular debris by cells such as phagocytes (Ellis *et al.*, 1991). Apoptosis plays vital roles in organism development, however, like

senescence, it can also act as a mechanism to suppress tumourigenesis in times of severe cellular stress (Green and Evan, 2002). Under a particular stress condition, one cell type might preferentially senesce, whereas another may apoptose, although this decision can be altered by proteins which are involved in apoptotic signalling, for example, caspase inhibition has been shown to switch doxorubicin-induced apoptosis to senescence in a neuroblastoma cell line (Rebbaa *et al.*, 2003). Exactly how senescent cells manage to evade apoptosis remains unknown, however, both the apoptosis and senescence pathways are influenced by the p53 tumour suppressor protein and thus the cell's response to the p53 pathway may be what influences the subsequent cell fate (Seluanov *et al.*, 2001).

### 1.4.3 Altered Gene Expression

Gene expression in senescent cells varies significantly compared to their corresponding quiescent and dividing cells, for example, activators and inhibitors of the cell cycle are often differentially expressed in senescent cells (Mason *et al.*, 2004; Jackson and Pereira-Smith, 2006). Senescent cells commonly express the cyclin-dependent kinase inhibitors (CDKI) p16 and p21, which are downstream of the retinoblastoma (pRb) and p53 proteins respectively (Campisi, 2001; Braig and Schmitt, 2006). Moreover, both pRb and p53 are crucial transcriptional regulators in two of the major tumour suppressor pathways often perturbed in cancer (Sherr and McCormick, 2002). In addition, senescent cells have also been shown to down-regulate the expression of proteins that are involved in cell cycle progression (e.g. cyclin A, cyclin B, c-FOS, replication dependent histones and PCNA (Seshadri and Campisi, 1990; Stein *et al.*, 1991; Pang and Chen, 1994; Narita *et al.*, 2003)). Many of the above mentioned genes are not expressed due to their transcription factor E2F being silenced by pRb, which is kept in a hypophosphorylated state by p16 and p21. Moreover, pRb also has the ability to remodel the chromatin structure into punctate structures coined Senescence-Associated Heterochromatin Foci (SAHF), which can physically block the transcription machinery from accessing certain E2F target genes (Narita *et al.*, 2003). The mechanism for chromatin reorganisation is thought to act through the ability of Rb-family members to recruit histone deacetylases (HDACs) to E2F-dependent promoters, which consequently results in the deacetylation of neighbouring histones. Moreover, this increases the positive charge of the histones,

therefore allowing the histone to bind more strongly to the negatively charged DNA, thus creating heterochromatin which represses gene expression (Narita *et al.*, 2003).

In addition, senescent cells also display differentially expressed genes with functions other than proliferative arrest. Moreover, research has shown senescent cells to up-regulate proteins which can be secreted, such as extracellular matrix components, growth factors and inflammation factors (Shelton *et al.*, 1999; Yoon *et al.*, 2004; Trougakos *et al.*, 2006). Antibody array experiments first showed the upregulation of these secretory cytokines in senescent cells and this senescence associated secretome is referred to as the Senescence-Associated Secretory Phenotype (SASP) and is associated with both stress, replicative and oncogene senescence (Coppé *et al.*, 2008). The SASP has been suggested to have beneficial effects via the signalling of warning signals to cells in the surrounding microenvironment (Kuilman and Peeper, 2009). In addition, another possibility is that the SASP is a mechanism to recruit immune cells to clear senescent cells from the tissue (Chien *et al.*, 2011), which will be discussed further later on. However, the SASP has also been implicated in the transformation of pre-malignant epithelial cells, for example, SASPs have been shown to promote invasiveness and induce an epithelial-mesenchymal transition via a paracrine mechanism that relies heavily upon the SASP factors IL-6 and IL-8 (Coppé *et al.*, 2008).

#### 1.4.4 Senescence Markers

For decades, scientists have been trying to find specific markers for senescent cells, which would allow for their specific detection both *in vitro* and *in vivo*. Hitherto, the search for a truly specific senescence marker has remained elusive, and although markers have been found, none are solely capable of identifying the senescent state alone (Lawless *et al.*, 2010). By definition, senescent cells do not replicate and therefore proliferation markers can be used to identify cells which are not senescent, although this still would show false negatives for cells that are in a quiescent state or post-mitotic. Currently used proliferation markers include labelled synthetic nucleoside analogues which get incorporated into the DNA, for example <sup>3</sup>H-thymidine or 5-bromodeoxyuridine. Antibodies for replication specific proteins can also be used such as Ki-67 and PCNA (Lawless *et al.*, 2010).

Senescence-Associated Beta-Galactosidase (SA- $\beta$ -Gal) was the first marker used to specifically detect the difference between a senescent mitotic cell compared to a cell that is quiescent or post-mitotic (Dimri *et al.*, 1995). However, SA- $\beta$ -Gal has been shown to be limited by the fact it can be detected in cells which have been cultured at confluence for prolonged periods of time (Severino *et al.*, 2000) and thus not fully specific to the senescent state. Research has also shown that there is no difference in SA- $\beta$ -Gal activity in either fibroblast cells or skin tissues sections taken from donors of different ages, therefore questioning SA- $\beta$ -Gal as a marker for cellular ageing *in vivo* (Severino *et al.*, 2000). In addition, why senescent cells have increased beta-galactosidase activity at pH6 is unknown, however it is believed that senescent cells display elevated levels of lysosomal biogenesis and it has been shown that cells with defective lysosomal beta-galactosidase do not express SA- $\beta$ -Gal even at late passages when the cells have gone through replicative senescence (Lee *et al.*, 2006).

In recent years, p16 has become a commonly used marker of senescence as it has been shown to be a principal mediator of senescence (Krishnamurthy *et al.*, 2004), however, despite being upregulated in a large number of cell lines undergoing senescence, there are examples of p16 being expressed in pre-senescent cells, for example WI-38 fibroblasts, and therefore it cannot be considered a universal senescence marker (Beauséjour *et al.*, 2003; Itahana *et al.*, 2003). In addition p16 levels have been shown to increase with age in almost all examined organs in a variety of mice and rats, however, an increase was also observed in post-mitotic tissues in the brain and heart, suggesting that p16 as a senescence marker may lack specificity (Melk *et al.*, 2003; Krishnamurthy *et al.*, 2004).

Other markers of senescence, include the presence of Senescence-Associated Heterochromatin Foci (SAHF) (Narita *et al.*, 2003), which appear in some but not all cell lines, and Senescence-Associated DNA Damage Foci (SDF) (d'Adda di Fagagna *et al.*, 2003; Takai *et al.*, 2003). It has recently been observed that both mouse and human fibroblasts display an unravelling of centromeric DNA, which has been coined senescent-associated distension of satellites (SADs) (Swanson *et al.*, 2013). SADs are particularly interesting as a marker for cellular senescence, as they are also found in cells from Hutchinson Gilford Progeria patients (Swanson *et al.*, 2013), moreover, it will be interesting to see if SADs are present in other senescent cell types. Phosphorylated p38MAPK is a novel DDR-independent regulator of the SASP

which has been detected in response to various senescence-inducing stimuli in human fibroblasts, however p38MAPK can also phosphorylate independently of senescence (Freund *et al.*, 2011).

To conclude, hitherto there is not a marker solely specific to senescent cells, and perhaps due to the multifarious phenotype of senescent cells, the identification of a single marker may prove difficult, and thus when analysing senescence, it is advisable to use a combination of markers.

## 1.5 Physiological Role of Senescence

Senescence has been traditionally thought of as a mechanism to suppress uncontrolled proliferation, thus acting as an important barrier to suppress tumourigenesis (Serrano *et al.*, 1997). However, research is emerging which shows that senescent cells are involved in a multifarious array of other organismal processes such as tissue repair (Krizhanovsky *et al.*, 2008), wound healing (Jun and Lau, 2010), and embryonic development (Rajagopalan and Long, 2012; Muñoz-Espín *et al.*, 2013b; Storer *et al.*, 2013).

### 1.5.1 Anti-tumour mechanism

We have previously described some of the causes of cellular senescence, including DNA damage, telomere dysfunction and OIS, all of which provide proficient mechanisms for preventing uncontrollable proliferation *in vitro*; herein we will discuss the evidence for these mechanisms providing a barrier to tumourigenesis *in vivo*.

Human nevi are extremely common, and their monoclonality dictates they should be considered as pre-malignant lesions, however they are able to stay in a state of cell-cycle arrest for many decades and rarely undergo tumourigenesis (Robinson *et al.*, 1998). Interestingly, the vast majority of nevi present oncogenic mutations, most commonly BRAF<sup>V600E</sup>, which would seem contradictory to their quiescent nature, if it were not for our understanding of OIS (Pollock *et al.*, 2003). Moreover BRAF is a downstream effector of RAS, the first oncogene shown to induce OIS *in vitro*

(Serrano *et al.*, 1997). Furthermore, constitutive activation of BRAF<sup>V600E</sup> can induce cell cycle arrest and increase expression of p16<sup>INK4a</sup> and SA-β-Gal activity in melanocytes *in vitro* (Michaloglou *et al.*, 2005). Nevi were subsequently analysed for detection of senescent markers *in vivo*, and were shown to display both p16<sup>INK4a</sup> and SA-β-Gal activity in the absence of telomere shortening, thus suggesting that OIS can driving cell cycle arrest *in vivo* (Michaloglou *et al.*, 2005). Contrary to this, another study attempted to categorise the difference between benign nevus cells and transformed melanocytes in terms of senescence, and found no variation between many markers, including γH2AX, p53, p16<sup>INK4a</sup>, SA-β-Gal, PML bodies, heterochromatin foci (DAPI, H3K9Me) and nuclear size (Tran *et al.*, 2012). Considering that around 25% of melanomas are either associated with, or arise from a pre-existing nevus (Marks *et al.*, 1990; Bevona *et al.*, 2003; Tsao *et al.*, 2003), and senescence is considered to be a state of permanent cell cycle arrest, this means either not all of the cells present in the nevi are senescent, or OIS-induced nevi cells are not permanently arrested, thus questioning if these cells are truly senescent.

Ras activity has been implicated in driving OIS in other human tumour settings, for example senescent cells have been shown to accumulate in neurofibromatosis type 1 lesions (Courtois-Cox *et al.*, 2006). Neurofibromatosis type 1 is a familial cancer syndrome which is prevalent in patients who have a loss-of-function mutation in the tumour suppressor neurofibromin 1 (NF1) (Courtois-Cox *et al.*, 2006). Moreover, NF1 is a negative regulator of Ras activity, and thus a loss-of-function mutation leads to hyperactive Ras, resulting in the formation of neurofibromas, a type of neoplastic lesion, which are associated with numerous senescence markers (Courtois-Cox *et al.*, 2006). Senescent cells have also been observed in other pre-malignant lesions, for example biopsies of pre-malignant intraepithelial neoplasia (PIN) and pre-malignant human colon adenomas, have shown to be associated with senescence cells, and it is thought that further mutations are required in order for these benign lesions to transform into malignant tumours (Chen *et al.*, 2005; Bartkova *et al.*, 2006; Kuilman *et al.*, 2008; Fujita *et al.*, 2009).

Although senescent cells have been shown to be associated with pre-malignant lesions, this correlation does not imply causality in suppression of malignancy. However, in many mouse tumour models, for example HRAS<sup>G12V</sup>-induced mammary tumours (Sarkisian *et al.*, 2007), BRAF<sup>V600E</sup>-induced melanomas (Goel *et al.*, 2009), BRAF<sup>V600E</sup>-induced lung tumours (Dankort *et al.*, 2007), genetic deletion of TP53 or

CDKN2A, resulted in an attenuation of senescence and development of malignancy, therefore providing evidence for a causal link between senescence induction and tumour suppression (Dankort *et al.*, 2007; Sarkisian *et al.*, 2007; Goel *et al.*, 2009).

Unfortunately, patients do succumb to malignant carcinomas, and thus senescence is not an infallible natural response, however, some malignant tumour cells are still able to be stimulated to enter cellular senescence *in vivo* (Shay and Roninson, 2004), and thus the efficacy of many anti-cancer treatments exploit this by targeting DNA damage signalling pathways which can induce either senescence or apoptosis, thus inhibiting tumour progression (Schmitt *et al.*, 2002; Coppé *et al.*, 2010b). Moreover, restoration of p53 function has been shown to result in tumour regression *in vivo* (Ventura *et al.*, 2007; Xue *et al.*, 2007).

Whilst activation of senescence in pre-malignant and even malignant cells appears to be a viable method of intervention for inducing cell cycle arrest in individual cells, research suggests that the persistence of senescent cells could be contributing to pathological ageing (Baker *et al.*, 2008; Baker *et al.*, 2011) and even driving tumourigenesis in neighbouring cells (Pribluda *et al.*, 2013); an issue I will discuss in further depth later on.

### 1.5.2 Development

Cellular senescence and apoptosis are the main cellular responses to damage, and can both be activated by common triggers such as oncogenic stress or DNA damage, as reviewed in (Campisi and d'Adda di Fagagna, 2007). However, apoptosis has long been shown to play important roles in embryogenesis, and in this context is referred to as 'programmed cell death'; a well-known example being the death of interdigital webs in the formation of digits in higher vertebrates (Lindsten *et al.*, 2000). Research is now emerging which suggests that senescence also plays important roles in embryogenesis development (Muñoz-Espín *et al.*, 2013a; Storer *et al.*, 2013). Transient accumulation of senescent natural killer (NK) cells have been observed during uterine neovascularisation, a key developmental stage which involves vascular remodelling to provide a maternal blood supply to embryo (Rajagopalan and Long, 2012). In addition, embryonic trophoblast cells were observed to secrete HLA-G, which triggers a senescence-like response in nearby NK

cells by activating the CD158d receptor, which initiates signalling through DNA-PK, Akt and NF- $\kappa$ B, leading to p21 activity, and ultimately resulting in a SASP which increases vascular permeability and promotes angiogenesis (Rajagopalan and Long, 2012). Further studies have shown that mouse embryogenesis appears to rely on senescent cells for the remodelling of numerous other tissues, such as the endolymphatic sac of the inner ear, the mesonephros (Muñoz-Espín *et al.*, 2013a). Moreover, an accumulation of senescent cells has also been shown to be present during embryogenesis at the apical ectodermal ridge (AER) and the neural roof plate (Storer *et al.*, 2013). Interestingly, p21<sup>-/-</sup> mice failed to accumulate senescent cells at the AER, and showed severe patterning defects in the limbs (Storer *et al.*, 2013). These cells shared some similar characteristics to OIS cells, including expression of p15, p21 and mediators of the SASP, however varied in that they were not associated with a DDR or p16 (Storer *et al.*, 2013). Furthermore, developmental-associated senescent cells were not associated with IL-6 or IL-8, which have been implicated as mediators of senescence reinforcement (Acosta *et al.*, 2008). Interestingly, senescent cells in the AER were shown to be cleared by an apoptosis and macrophage-mediated phagocytosis, however it remains unknown whether these cells underwent apoptosis prior to clearance or if the macrophages induce apoptosis (Storer *et al.*, 2013).

In adults, senescence has also been associated with the natural maturation of placental syncytiotrophoblasts (Chuprin *et al.*, 2013) and megakaryocytes (Besancenot *et al.*, 2010). Megakaryocyte senescence shares a similar phenotype to developmental senescence, in that it is p21-dependent, but devoid of p16 or p53 upregulation (Besancenot *et al.*, 2010).

Senescence during development has now been observed across numerous species, including quail (Nacher *et al.*, 2006), chicken (Storer *et al.*, 2013), mouse (Muñoz-Espín *et al.*, 2013a; Storer *et al.*, 2013) and human (Muñoz-Espín *et al.*, 2013a) embryos. These observations suggest that developmental senescence could be an evolutionary conserved mechanism in embryogenesis across multiple species. However, due to a lack of a universal marker for senescence, there is an ongoing debate on what actually constitutes senescence, and thus caution has to be taken in defining observed phenotypes. Moreover, SA- $\beta$ -Gal activity has been observed in proliferating cells of the visceral endoderm layer of the yolk sack (Huang and Rivera-Pérez, 2014), thus questioning the specificity of the marker in this context, or

highlighting the potential for developmental senescence to be a separate phenomenon to, for example OIS thus requiring a distinction in definition.

### 1.5.3 Wound Healing

Wound healing is a highly co-ordinated process which involves haemostasis, inflammation, proliferation and remodelling. Moreover, each of these phases is associated with a number of soluble factors, a number of which have been shown to associate with the SASP (Tomasek *et al.*, 2002; Midwood *et al.*, 2004). Senescent cells have been shown to accumulate at sites of subcutaneous wounding, and it was observed that the matricellular protein CCN1, which is highly expressed at sites of wound repair, could trigger fibroblast senescence, by inducing a DDR and activating p53 (Jun and Lau, 2010). In addition, CCN1 also activates the ROS generating RAC1-NOX1 complex, which induces ROS-dependent p16 activation. Senescent cells were shown to be associated with the secretion of anti-fibrotic genes, and a knock-in CCN1 mutant showed a lack of senescence accumulation and increased fibrosis at sites of wounding. Moreover, fibrosis could be attenuated with topical application of CCN1 (Jun and Lau, 2010). To specifically target senescent cells in wound healing, the Campisi group developed a p16-3MR transgenic mouse, in which the p16<sup>INK4a</sup> promoter drives the expression of 3MR, a fusion protein consisting of the herpes simplex virus-1 thymidine kinase, which induces apoptosis upon ganciclovir treatment, conjugated to a red fluorescence protein (RFP) reporter. After wounding with a dermal skin punch, an accumulation of RFP positive cells and p16 mRNA, was observed, peaking at 6 days and returning to basal levels at 9. In ganciclovir treated p16-3MR mice, there was no increase in p16 following wounding, and interestingly, the wound took significantly longer to heal (Demaria *et al.*, 2014). These observations suggest that senescent cells facilitate the speed of wound healing, however are not essential. Several SASP components are shown to be upregulated following dermal skin wounding, including CCL5, PAI-1, VEGF and PDGF-A. Furthermore, PDGF-A from senescent cells was shown to facilitate wound healing by driving myofibroblast differentiation, promoting optimal granulation tissue formation (Demaria *et al.*, 2014).

#### 1.5.4 Immune Clearance

During embryonic development, senescent cells in the AER and mesonephros become surrounded by macrophages at days E13.5-E14.5 (Muñoz-Espín *et al.*, 2013a; Storer *et al.*, 2013). However, in *Cdkn1a*<sup>-/-</sup> mice, this recruitment of macrophages to senescent cells does not occur, therefore suggesting a causal role for senescent cells driving macrophage recruitment during development (Storer *et al.*, 2013).

It is thought that the SASP factors secreted from DNA-damage-induced senescent cells can attract phagocytic cells (Xue *et al.*, 2007; Kuilman and Peeper, 2009; Campisi, 2013). In the liver, there is evidence for an immune surveillance of senescent cells which is mediated by CD4<sup>+</sup> T cells (Kang *et al.*, 2011). Moreover, transduction of hepatocytes with oncogene *Nras* (*Nras*<sup>G12V</sup>) lead to cellular senescence, shown by increased p16, p21 and ERK phosphorylation, in all *Nras* expressing cells, which was associated with immune cell clustering around the senescent hepatocytes (Kang *et al.*, 2011). All *Nras* positive senescent hepatocytes were subsequently cleared over the course of 2 months, whereas cell numbers of *Nras*<sup>G12V/D38A</sup> cells, lacking downstream pathway signalling (Khwaja *et al.*, 1997), remained constant. Furthermore, Terminal deoxynucleotidyl transferase dUTP nick end labelling (TUNEL) assay revealed that the senescent hepatocytes were not being removed by apoptosis (Kang *et al.*, 2011). These data suggest a causal role for the immune system in removing senescent cells, further strengthened by the observation that among patients with a hepatitis C infection, those with HIV were shown to have a greater accumulation of p-16 positive senescent hepatocytes compared to immune-competent patients (Kang *et al.*, 2011).

Despite evidence showing that there is an immune system-mediated clearance of senescent cells, an age-dependent increase in senescent cells has been observed in numerous tissues across several mammalian species (Dimri *et al.*, 1995; Paradis *et al.*, 2001; Melk *et al.*, 2003; Erusalimsky and Kurz, 2005; Jeyapalan *et al.*, 2007). There is therefore an age-dependent imbalance between the rate of senescence generation and clearance of senescent cells. Evidence has emerged which shows that the immune system does mount a response to remove cells which have undergone damage-induced senescence, however this mechanism is thought to decline with age (Xue *et al.*, 2007; Kang *et al.*, 2011; Hoenicke and Zender, 2012).

Furthermore, it has been observed that there is an age-dependent decrease in the ability of haematopoietic stem cells (HSCs) to undergo lymphoid differentiation (Wang *et al.*, 2011), therefore leading to a decrease T cells, which have been shown to drive senescence clearance (Kang *et al.*, 2011). It is therefore tempting to speculate that an age-dependent decline in the immune system could allow for senescent cells to accumulate as a result of attenuated clearance capabilities, however further is required before such hypotheses can be conclusively proven.

## 1.6 Senescence and Ageing

Contrary to the above described beneficial roles, senescent cells have also been implicated in having pathological effects (Baker *et al.*, 2008; Baker *et al.*, 2011). In the context of wound healing and embryonic development, the presence of senescent cells is only transient (Jun and Lau, 2010; Demaria *et al.*, 2014), however persistent senescent cells are thought to accumulate in aged organisms (Dimri *et al.*, 1995; Paradis *et al.*, 2001; Melk *et al.*, 2003; Erusalimsky and Kurz, 2005; Jeyapalan *et al.*, 2007). Moreover, evidence is emerging that chronic persistence of senescent cells may contribute to a decline in tissue homeostasis, promote age-related diseases, and even contribute to a pro-tumourigenic micro-environment (Alspach *et al.*, 2013).

### 1.6.1 Pro-tumourigenic properties

Senescence has been shown to act as a barrier to uncontrolled proliferation in response to various stimuli (Serrano *et al.*, 1997; d'Adda di Fagagna *et al.*, 2003), therefore it would seem paradoxical that the same mechanism could act to promote tumourigenesis. However, besides cell cycle arrest, one of the fundamental senescence traits is the SASP (Coppé *et al.*, 2008), and whilst this may have a beneficial role in wound healing (Jun and Lau, 2010; Demaria *et al.*, 2014), where the SASP is only acute and transient, it appears that chronic SASP can have detrimental effects. Moreover, both senescent mesothelial and fibroblast cells secrete Vascular Endothelial Growth Factor (VEGF), which can stimulate endothelial cell migration and

invasion (Coppé *et al.*, 2006; Ksiazek *et al.*, 2008). Pre-malignant epithelial cells can be stimulated to undergo an epithelial-mesenchymal transition (EMT), leading to an invasion of the basement membrane, by prolonged exposure to IL-6 and IL-8, both of which are highly upregulated in numerous senescent cell types, (Coppé *et al.*, 2008). Invasiveness of tumour cells has been shown to be increased by matrix metalloproteinases (MMPs), which are secreted by both senescent keratinocytes and fibroblasts (Millis *et al.*, 1992; Kang *et al.*, 2003; Coppé *et al.*, 2010b).

*In vivo*, co-injection of keratinocytes with senescent fibroblasts into nude mice, leads to a significantly increased rate of tumour formation when compared to co-injection of keratinocytes with pre-senescent fibroblasts (Krtolica *et al.*, 2001). In addition, tumour formation rate has been shown to be significantly accelerated when senescent cells are injected into already malignant cancer cells (Krtolica *et al.*, 2001; Liu and Hornsby, 2007; Bhatia *et al.*, 2008; Bartholomew *et al.*, 2009). Evidence therefore implicates senescent cells in promoting tumourigenesis in an experimental setting, however further research is required to determine if tumourigenesis is promoted by naturally occurring senescent cells *in vivo*. In contrast to the observed pro-tumourigenic effects, the anti-angiogenic factor maspin has been observed to be secreted by senescent keratinocytes (Nickoloff *et al.*, 2004). To add further complication, IL-6 and IL-8 have been associated with tumour suppression in human colon adenomas, yet implicated in driving tumourigenesis in carcinogen-induced skin tumours (Ancrile *et al.*, 2007), therefore implying that there isn't a universal effect of the SASP on the tumourigenic environment, and has varying effects dependent on cell and tissue type.

Interestingly, patients on immunosuppressive therapy, or sufferers from HIV, are known to have increased rates of hepatocellular carcinoma, and as discussed previously, senescent cells are known to accumulate in the liver of these patients, and thus it is interesting to speculate if persistent senescence could be contributing to the observed increase in tumourigenesis in this context (Hensel *et al.*, 2011).

The role of senescent cells in tumourigenesis appears to be multi-faceted, and considering cancer is pre-dominantly an age-associated disease, and thus often presents past a fertile age, there is little selective pressure to remove deleterious effects of senescent cells in aged organisms. This may help to resolve the apparent paradox of senescent cells having both anti- and pro-tumourigenic properties, a

phenomenon which is consistent with the evolutionary theory of antagonistic pleiotropy, which proposes that a biological process may have either detrimental or beneficial outcomes depending upon the setting in which the trait is activated (George, 1957; Rauser *et al.*, 2006).

### 1.6.2 Disease

In addition to tumour promotion, senescent cells have been implicated in driving other pathological effects, for example, an accumulation of senescent cells has been observed in multiple diseases (Martin and Buckwalter, 2003; Erusalimsky and Kurz, 2005) (Noureddine *et al.*, 2011).

Ageing is commonly associated with sarcopenia, and evidence is mounting that a decline in proliferative potential of muscle stem cells could be driving this age-associated loss of muscle mass. Moreover, data shows that activated p38 kinase leads to an accumulation p16 and increased SA- $\beta$ -gal activity in muscle stem cells in both mice and humans, and inhibition of p38 can attenuate this increase in senescence, resulting in improved muscle regeneration after injury (Bernet *et al.*, 2014; Cosgrove *et al.*, 2014; Sousa-Victor *et al.*, 2014).

An upregulation of both p16 and p21, as well as an increase in SA- $\beta$ -Gal activity has been observed in various cell types involved in idiopathic pulmonary fibrosis (IPF) (Aoshiba *et al.*, 2003; Aoshiba *et al.*, 2013; Hecker *et al.*, 2014). Treatment of mice with the DNA-damaging agent bleomycin induces many features of IPF, however, this effect can be attenuated when mice are treated with a chemical inhibitor for NOX4, a NADPH-dependent oxidase which generates excessive ROS, as well as with the anti-inflammatory rupatadine (Lv *et al.*, 2013; Hecker *et al.*, 2014). Furthermore, elevated ROS and inflammation are associated with cellular senescence, and inhibition of these attenuates the bleomycin-induced increase in p16, p21 as well as subsequent fibrotic damage, thus implying that senescence could be involved in driving the pathological IPF (Lv *et al.*, 2013; Hecker *et al.*, 2014).

If lipid accumulation exceeds a certain threshold in adipocyte tissue, an inflammatory response, involving the recruitment of macrophages, occurs which is associated with various pathologies such as insulin resistance and liver steatosis (Gregor and

Hotamisligil, 2011). It has been observed in adipose tissue of both mice and humans, that obesity and the subsequent immune response is associated with an upregulation of both p21 and p53, as well as an increase in SA- $\beta$ -gal activity and SASP activation (Minamino *et al.*, 2009; Tchkonja *et al.*, 2010; Markowski *et al.*, 2013). Interestingly, adipose-specific deletion of p53 in mice protects against high fat diet-induced insulin resistance, reduces the expression of pro-inflammatory cytokines, and ameliorates senescent-like changes (Minamino *et al.*, 2009). To compensate for obesity-induced insulin resistance, pancreatic  $\beta$ -cells undergo increased proliferation to produce excess insulin, however this proliferative response to chronic insulin tolerance cannot be sustained, eventually leading to an exhaustion of proliferation, and a decline in  $\beta$ -cell mass (Sharpless and DePinho, 2007; Donath *et al.*, 2013). Moreover, mice on a high fat diet show increased  $\beta$ -cell proliferation compared to control diet mice at 4 months, however at 12 months, the proliferation rates are actually lower in the mice on a high fat diet, which is associated with an increase in SA- $\beta$ -Gal activity in the  $\beta$ -cell islets (Sone and Kagawa, 2005).

Multiple models of how senescent cells might cause age-related tissue decline have been proposed (Figure 1-4). In the absence of a compensatory mechanism, if a stem cell, or even a non-terminally differentiated cell, were to undergo senescence, this would prevent daughter cells being produced and thus hinder the generation of proper tissue formation and regeneration leading to a decline in tissue homeostasis (Figure 1-4). Cell cycle arrest is a cell-autonomous consequence of senescence, however compelling evidence is arising that senescent cells can also elicit a non-cell autonomous, or paracrine effect, on neighbouring cells. Interestingly, senescent fibroblasts, when cultured next to young fibroblasts, elicit a 'bystander effect' which causes an increase in DNA damage, and drives cellular senescence in young cells (Nelson *et al.*, 2012). It is thought that this effect is driven by ROS mediated by gap junction cell to cell contact (Nelson *et al.*, 2012). Other groups have also observed a bystander effect, thought to be driven by SASP factors. Moreover, conditioned medium taken from either, drug-induced, OIS, or replicative senescence cells was able to drive a ROS-generated DDR in bystander cells (Hubackova *et al.*, 2012a). Both SASP factors IL-1 and TGF $\beta$  were upregulated in senescent cells, and inhibition of either the IL1/NF $\kappa$ B or TGF $\beta$ /SMAD pathway resulted in an attenuation of both a DDR and ROS production in bystander cells (Hubackova *et al.*, 2012a; Acosta *et al.*, 2013).

If the senescent cell bystander effect occurs *in vivo*, this could potentially drive a chain-reaction of senescence-induced-senescence in neighbouring cells, thus accelerating the rate of senescent cell generation (Figure 1-4). If immune clearance was not able to keep up with increased rate, this could complement observations that senescent cells accumulate with age (Dimri *et al.*, 1995; Paradis *et al.*, 2001; Melk *et al.*, 2003; Erusalimsky and Kurz, 2005; Jeyapalan *et al.*, 2007). These hypotheses are however speculative, and although clustering of 4-HNE positive cells has been observed in the hepatocytes, further research is required to elucidate if the bystander effect occurs *in vivo* (Nelson *et al.*, 2012).

Senescent cells have also been implicated in causing a decline in tissue architecture through both extracellular matrix degradation and tissue fibrosis (Figure 1-4). Furthermore, the SASP includes several proteases, which have the potential to cleave ECM proteins, signalling ligands and membrane-bound receptors, thus leading to an aberrant microenvironment (Parrinello *et al.*, 2005; Jean-Philippe *et al.*, 2008). Senescent cells have also been implicated in driving an EMT in epithelial cells, thought to act through secretion of IL-6 and IL-8 SASP factors, which may lead to increased tissue fibrosis (Laberge *et al.*, 2012).

Pathological ageing is associated with chronic inflammation, a process which is categorised by lymphocyte and macrophage infiltration, fibrosis and cell death; which is thought to drive a number of age-related diseases, such as osteoarthritis, atherosclerosis and cancer (Freund *et al.*, 2010). Senescent cells have been shown to be present at sites of inflammation in numerous age-related pathologies, which has led to speculation that the perhaps the SASP is responsible for inducing chronic inflammation via persistent secretion of chemokines, cytokines and pro-inflammatory growth factors, known to attract immune cells, such as monocyte chemo-attractant proteins (MCPs), macrophage inflammatory proteins (MIPs), as well as IL-1, IL-6, IL-8 and GRO $\alpha$  (Coppé *et al.*, 2008). However, further research is required to ascertain whether senescent cells are causative in inducing age-associated chronic inflammation.

Due to the difficulty of creating mouse models devoid of cellular senescence, it is hard to distinguish correlation from causality when trying to elucidate the role of senescence in disease. Moreover, p16<sup>Ink4a</sup> and p53 are key effectors in the induction of senescence in response to various stresses, however disruption of these genes in

mice results in premature death from cancer (Sherr, 2000). Furthermore, p53 is also a key mediator of apoptosis, making it challenging to discern the effects of senescence specifically (Coppé *et al.*, 2010a; Campisi, 2011; Rodier and Campisi, 2011). To address this issue, the van Deursen group generated a transgenic mouse with a novel transgene, coined INK-ATTACK, in which p16<sup>Ink4a</sup> expressing cells could be eliminated via apoptosis upon drug treatment (Baker *et al.*, 2011). The transgene was expressed in the BubR1<sup>H/H</sup> progeroid mouse background, and it was observed that both late-life and life-long clearance of p16<sup>Ink4a</sup> expressing cells could delay several age-related pathologies (Baker *et al.*, 2011). These data provide a causal role for senescence promoting age-related diseases, at least in the BubR1 model. BubR1<sup>H/H</sup> mice, develop aneuploidy as a result of levels of the mitotic checkpoint protein BubR1, are associated with early onset of several age-related diseases and have a short life span (Baker *et al.*, 2004; Hartman *et al.*, 2007; Matsumoto *et al.*, 2007); it will therefore be important to study the effect of senescent cell clearance in the development of age-related pathologies in wild-type mice, to ensure that the effects aren't simply an artefact specific to this model.

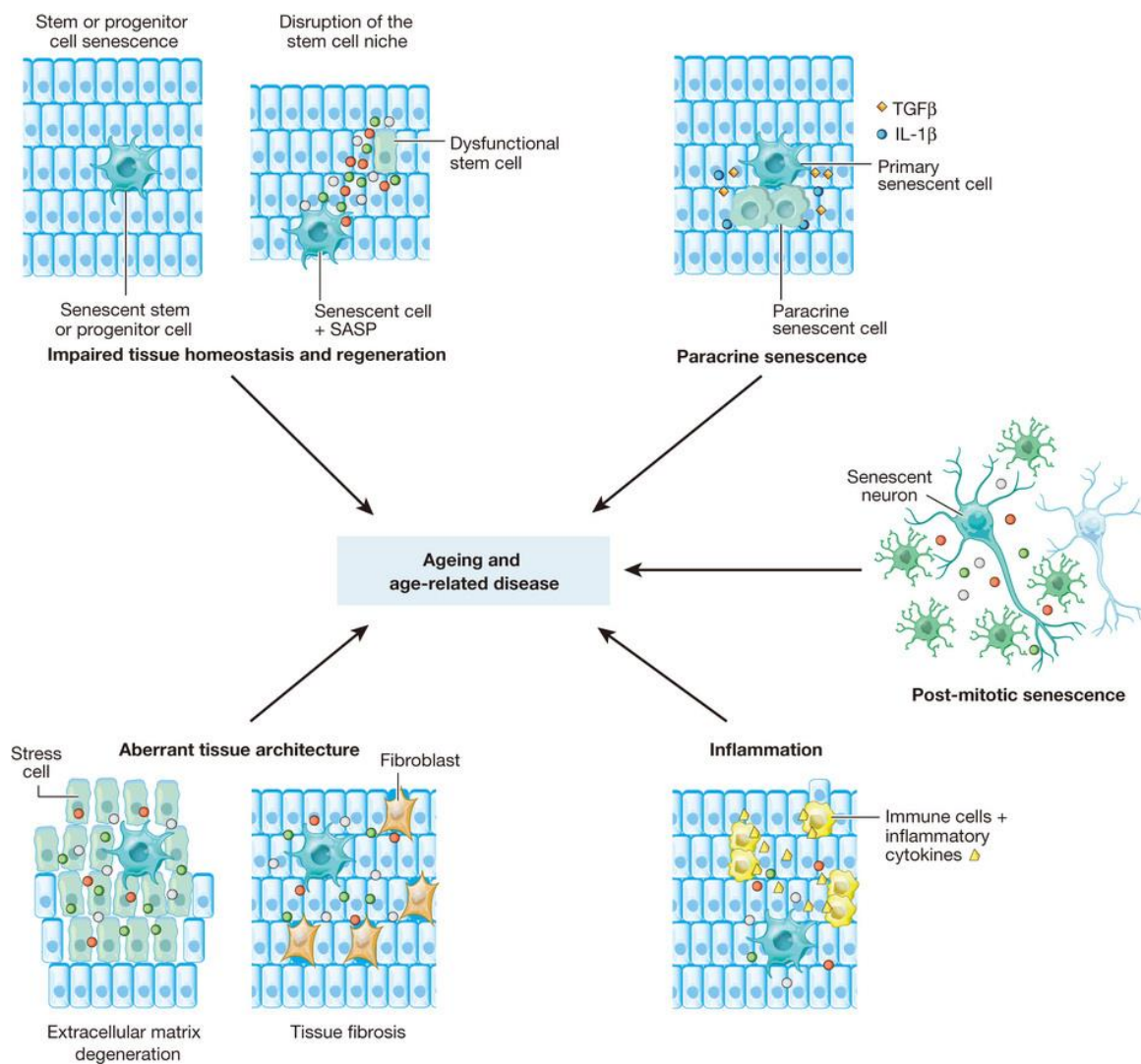


**Figure 1-4. Mechanisms of Tissue and Organ Deterioration by Cellular Senescence (van Deursen, 2014).** Senescent cells have been implicated in leading to impaired tissue homeostasis and regeneration, causing paracrine senescence through the secretion of TGF $\beta$  and IL-1 $\beta$ , and recruiting immune cells, therefore leading to inflammation. Aberrant tissue architecture can develop through senescent cells causing ECM degradation. Post-mitotic neurones have also been observed to display a senescent-like phenotype.

## 1.7 Post-Mitotic Senescence

A senescent phenotype has now been observed in scenarios in which the required function of senescence is not cell cycle arrest, for example in wound healing and embryonic development (Jun and Lau, 2010; Muñoz-Espín *et al.*, 2013a; Storer *et al.*, 2013; Demaria *et al.*, 2014). It is therefore interesting to consider if post-mitotic cells can also develop a senescent-like phenotype, and what the physiological relevance of this would be. Interestingly, both adipocytes and neurones have been shown to

elicit a senescent-like phenotype *in vivo* (Minamino *et al.*, 2009; Jurk *et al.*, 2012). An age-dependent increase in various senescent markers has been observed in both murine purkinje cells and cortical neurones, including  $\gamma$ H2AX, activated p38 MAPK, 4-HNE, IL-6, macro-H2A, auto-fluorescence and SA- $\beta$ -Gal, with individual cells displaying multiple markers (Jurk *et al.*, 2012). Mitotic cells have been shown to senesce in response to a sustained DDR (d'Adda di Fagagna *et al.*, 2003; Fumagalli *et al.*, 2012; Hewitt *et al.*, 2012), and purkinje cells and cortical neurones also showed increased IL-6 production, 4-HNE, and activated p38MAPK, in G4TERC<sup>-/-</sup> mice, which have severe telomere dysfunction, and hence a persistent DDR (Karl Lenhard *et al.*, 1999). Interestingly, in G4TERC<sup>-/-</sup>CDKN1A<sup>-/-</sup> mice, these senescent markers were completely rescued in both purkinje cells and cortical neurones, suggesting that the development of a senescent phenotype in these cells is dependent upon p21 (Jurk *et al.*, 2012). Adipocytes from both mice fed on a high calorie diet and G4TERC<sup>-/-</sup> mice, have also been shown to have an increased production of pro-inflammatory cytokines, including tumour necrosis factor- $\alpha$  (TNF- $\alpha$ ) and chemokine (C-C motif) ligand-2 (CCL2), as well as increased p53 expression, and increased SA- $\beta$ -Gal activity (Minamino *et al.*, 2009). These markers of senescence were shown to be rescued in *Trp53*<sup>+/-</sup> mice, therefore showing that the activated p53-p21 pathway can induce a senescence-like phenotype in both murine neurones and adipocytes (Minamino *et al.*, 2009; Jurk *et al.*, 2012). An upregulation of inflammatory cytokines, an increase in SA- $\beta$ -gal activity and increased p53 was also observed in adipocytes from human patients, providing evidence that post-mitotic senescence is not only a phenomenon unique to murine cells (Minamino *et al.*, 2009).

Hitherto, a substantial categorisation of post-mitotic senescence *in vivo* has not extended beyond adipocytes and neurones (Minamino *et al.*, 2009; Jurk *et al.*, 2012).

Senescence has been observed in cardiomyocytes *in vitro*, for example H9C2 rat cardiomyocytes, which still retain proliferative potential, have been shown to cease proliferation and have increased SA- $\beta$ -Gal activity, or undergo apoptosis, when exposed to low or high doses of oxidative or genotoxic stress respectively (Spallarossa *et al.*, 2009; Dong *et al.*, 2013). Induced telomere dysfunction, via siRNA-mediated downregulation of TRF2, has also been shown to trigger either senescence or apoptosis in a dose-dependent manner in H9C2 cardiomyocytes (Spallarossa *et al.*, 2009). It will be important to investigate if cardiomyocyte

senescence also occurs *in vivo*, and what the physiological relevance of this maybe. Moreover, the significance of permanent cell cycle exit of a non-dividing cell type would seem to be inconsequential with regard to tissue homeostasis, however, evidence is emerging that cardiomyocytes are not entirely post-mitotic. Moreover, during development, cardiomyocytes proliferate rapidly, then after birth, heart enlargement relies mainly on cell growth, and it was previously thought that all the cardiomyocytes a human would ever have are present at birth (Li *et al.*, 1997). However, nuclear bomb testing during the Cold War generated an abundance of carbon-14, which was subsequently incorporated into living organisms, and patient analysis of carbon-14 in DNA from cardiomyocytes, revealed cardiomyocyte DNA containing carbon-14, suggesting that new cardiomyocytes had been generated (Bergmann *et al.*, 2009). Subsequent research has confirmed these findings, and identified that cardiomyocytes themselves are capable of replication, as opposed to a stem cell population (Malliaras *et al.*, 2013; Senyo *et al.*, 2013). Despite this evidence for cardiomyocyte proliferation, the role of cell cycle arrest is still questionable, as adult human cardiomyocyte division is still a relative rare event, with turnover rates around 1% per year in 25 year olds, which gradually decreases to around 0.45% per year in 75 year olds (Bergmann *et al.*, 2009). Furthermore, evidence suggests that a 50 year old human is likely to have around 60% of the same cardiomyocytes present at birth (Bergmann *et al.*, 2009). However, cardiomyocyte replication is significantly increased at sites adjacent to myocardial stress (Malliaras *et al.*, 2013; Senyo *et al.*, 2013), and thus one could hypothesise that cardiomyocyte senescence could alter regenerative ability following myocardial injury. Among patients who have undergone radiotherapy treatment for breast cancer, those which were treated for left breast cancer have an increased incidence of cardiac disease compared to those treated for right breast cancer (Darby *et al.*, 2003; Taylor *et al.*, 2008; Taylor *et al.*, 2009). Moreover, the mechanism for this is not understood, however, X-irradiation is known to cause senescence in numerous cell types, and it will therefore be important to investigate if senescence is occurring and contributing to disease progression.

As previously described, cell cycle arrest is not the only phenotype of senescence, and it will be will be important to understand the physiological relevance of senescence even in post-mitotic / non-rapidly dividing cells, such as neurones, adipocytes and cardiomyocytes, to determine if they are associated with a SASP, and if this is detrimental to surrounding cells. Another important factor will be to

understand what drives cellular senescence in cell types which are not affected by significant proliferation-associated telomere shortening and thus should not undergo canonical replicative senescence. Hitherto, little research has focused on telomere damage in post-mitotic cells, perhaps due to the perceived lack of telomere dysfunction.

## 1.8 Aims

Telomere dysfunction is a major hallmark of cellular senescence, and DDR foci at telomeres have been observed to occur independently of telomere length in murine enterocytes and hepatocytes *in vivo* (Hewitt *et al.*, 2012). A senescent-like phenotype has also been observed to occur in post-mitotic adipocytes and neurones *in vivo* (Minamino *et al.*, 2009; Jurk *et al.*, 2012). We aimed to ascertain if telomere dysfunction occurred in cardiomyocytes, and if this was associated with cellular senescence. The main aims were:

- Can cardiomyocytes elicit persistent telomere dysfunction *in vitro*, and if so, can this drive cellular senescence?
- Is there an age-associated increase in telomere dysfunction in cardiomyocytes *in vivo* which is associated with a senescent-like phenotype?
- Can we modulate telomere dysfunction in cardiomyocytes?

## 2 Chapter 2 - Materials and Methods

### 2.1 Chemicals and Reagents

Unless stated otherwise, all chemicals were obtained from Sigma-Aldrich Company Ltd (Poole, Dorset, UK).

### 2.2 Buffers and Solutions

All solutions dissolved in deionised water unless otherwise stated.

<b>Solution</b>	<b>Components</b>
PGB-Triton	0.5% Bovine Serum Albumin, 0.25% Gelatin from cold water fish skin (SIGMA, G7765) and 0.5% Triton™ X-100 in PBS.
TBS-Triton	10mM Tris, 150mM NaCl and 0.25% Triton™ X-100. Adjusted to pH7.0 with HCl.
Cardiomyocyte Buffered Salt Buffer	116mM NaCl, 20mM HEPES, 1mM NaH <sub>2</sub> PO <sub>4</sub> , 5.365mM KCl and 831nM MgSO <sub>4</sub> .
Cardiomyocyte Enzyme Solution	5mM Glucose, 80U mL <sup>-1</sup> Collagenase Type 2 (Worthington, LS004174), 0.25mg mL <sup>-1</sup> in CBSB.
Fibroblast Lysis Buffer	12.5mM Tris pH7.4, 5mM KCl, 0.1mM Spermine, 0.25mM Spermidine, 175mM Sucrose and 1 protease inhibitor tablet (Roche).
Chromatin Spreading Buffer	10mM Tris pH7.4, 10mM EDTA, 0.05% SDS and 1M NaCl.
Nuclei Wash Buffer	10mM Tris pH7.4, 15mM NaCl, 60mM KCl, 5mM EDTA and 300mM Sucrose.
2 X SSC	300mM NaCl and 30mM sodium citrate. Adjusted to pH7.0 with HCl.
PNA Wash A	10mM Tris pH7.5 and 70% formamide.

PNA Wash B	50mM Tris pH7.5, 150mM NaCl and 0.08% Tween-20.
Citrate Buffer	10mM Sodium Citrate, Dihydrate. Adjusted to pH6.0 with HCl.
Hybridisation buffer for FISH	70% deionised formamide, 25mM MgCl <sub>2</sub> , 10mM Tris pH7.2, 5% blocking reagent (Roche, Welwyn), 4ng $\mu\text{L}^{-1}$ TelC-Cy3/Cy5 PNA probe (C <sub>3</sub> TA <sub>2</sub> ) <sub>3</sub> (Panagene, F1002-5/F1003-5) in dH <sub>2</sub> O.
Haematoxylin	5g Haematoxylin, 50g Aluminium potassium sulphate, 0.5g Sodium iodate, 300mL Glycerin, 40mL glacial acetic acid, in 700mL dH <sub>2</sub> O.
RIPA	150mM NaCl, 1% Triton™ X-100, 0.5% sodium deoxycholate, 0.1% SDS and 50mM Tris pH8.0.
STORM Imaging Buffer	50mM Tris-HCl pH8.0, 10mM NaCl, 100mM MEA, 5 unit ml <sup>-1</sup> glucose oxidase and 50 unit mL <sup>-1</sup> catalase.
Krebs solution	130mM NaCl, 5.4mM KCl, 1.4mM MgCl <sub>2</sub> , 0.4mM NaH <sub>2</sub> PO <sub>4</sub> , 4.2mM HEPES, 10mM glucose, 20mM taurine, 10mM creatine monohydrate.

**Table 1. Buffers and Solutions**

## 2.3 Cell Culture

### 2.3.1 Cell lines

#### Human Cell Lines

Human embryonic lung MRC5 fibroblasts (ECACC, Salisbury, UK) were cultured in Dulbecco's Modified Eagle's Medium (DMEM), supplemented with 10% heat inactivated foetal bovine serum (FBS) (Biosera, Ringmer, UK), 100 $\mu\text{g ml}^{-1}$  streptomycin, 100 units  $\text{ml}^{-1}$  penicillin and 2mM l-glutamine, incubated in a humidified atmosphere at 37°C with 95% air and 5% CO<sub>2</sub>.

#### Mouse Cell Lines

Mouse Embryonic Fibroblasts (MEFs), isolated from C57BL/6 mice, were cultured in Dulbecco's Modified Eagle's Medium (DMEM), supplemented with 10% heat

inactivated foetal bovine serum (FBS) (Biosera, Ringmer, UK), 100 $\mu$ g ml<sup>-1</sup> streptomycin, 100 units ml<sup>-1</sup> penicillin and 2mM l-glutamine, incubated in a humidified atmosphere at 37°C with 3% O<sub>2</sub> and 5% CO<sub>2</sub>.

H9C2 rat cardiac-derived myoblasts were a kind gift from Jeanne Mialet-Perez and were cultured in Dulbecco's Modified Eagle's Medium (DMEM), supplemented with 10% heat inactivated foetal bovine serum (FBS) (Biosera, Ringmer, UK), 100 $\mu$ g ml<sup>-1</sup> streptomycin, 100 units ml<sup>-1</sup> penicillin and 2mM l-glutamine, incubated in a humidified atmosphere at 37°C with 95% air and 5% CO<sub>2</sub>.

### 2.3.2 Primary Embryonic Mouse Cardiomyocytes

17.5 day old mouse embryos were dissected from pregnant C57/BL6 mice, and all embryos were subsequently used without consideration for gender. Under a dissecting microscope, the middle of each embryo's sternum was cut with scissors to open the ribcage, and then the hearts were removed with scissors, and placed into ice-cold Cardiomyocyte Balanced Salt Buffer (CBSB) (Table 1) in a 15mL centrifuge tube. After all hearts were removed, they were transferred onto a 250 $\mu$ L droplet of CBSB on a petri dish in class 2 laminar flow cabinet, and were cut into multiple fragments each. Heart fragments were then transferred to Cardiomyocyte Enzyme Solution (CES) (Table 1), without trypsin, (1mL per embryo) and incubated at 37°C for 5 minutes. During incubation, trypsin was added to the remaining CES, to a final concentration of 0.25mg mL<sup>-1</sup>. After incubation\*, the tissue fragments were allowed to settle, and then the supernatant was transferred to a 15mL centrifuge tube and centrifuged at 700g for 5 minutes. The remaining tissue fragments were re-suspended in CES, with trypsin, (1mL per embryo), and incubated at 37°C for 30 minutes, whilst gently shaking the tube each 5-10 minutes. The supernatant from the centrifuged tube was then aspirated, and the pellet was re-suspended in 1mL of FBS and stored at 4°C. After the 30 minute incubation period, the steps from the asterisk were repeated 5-6 times, or until the tissue fragments were totally disintegrated. The enzyme solution from each step was added to the same 15mL centrifuge tube, with fresh FBS added after each centrifugation, with the collection tube stored at 4°C throughout. After the final centrifugation, cells were re-suspended in 5mL Cardiomyocyte Growth Medium and transferred to a collagen-coated T25 flask and

incubated in a humidified atmosphere at 37°C with 95% air and 5% CO<sub>2</sub> for 2 hours. After incubation, the growth medium was collected from the pre-plating flask and transferred to a 15mL centrifuge tube, and topped up with Cardiomyocyte Growth Medium, to a total volume of 10mL. Cells were re-suspended and a sample taken for counting on a haemocytometer. The cell suspension was then centrifuged at 700g for 5 minutes at room temperature, the supernatant was aspirated, and then cells were re-suspended in Cardiomyocyte Growth Medium to desired concentration, and seeded onto collagen-coated culture vessels. Cells were then incubated in a humidified atmosphere at 37°C with 95% air and 5% CO<sub>2</sub> for 2-3 days to allow cardiomyocytes to settle. Growth medium was then aspirated, and cells were washed 2-3 times with PBS at 37°C before fresh Cardiomyocyte Growth Medium was added.

Mouse Embryonic Cardiomyocytes were cultured in Dulbecco's Modified Eagle's Medium (DMEM), supplemented with 17% Medium 199, 5% heat inactivated foetal bovine serum (FBS) (Biosera, Ringmer, UK), 10% Horse serum (SIGMA, H0146), 100µg ml<sup>-1</sup> streptomycin, 100 units ml<sup>-1</sup> penicillin and 2mM l-glutamine, incubated in a humidified atmosphere at 37°C with 95% air and 5% CO<sub>2</sub>.

### **2.3.3 Primary Adult Mouse Cardiomyocytes**

Male mice of either 3 or 20 months of age were anaesthetised with 150µL pentobarbital and treated with 500 units of heparine. The hearts were then removed and assembled with a canula through the aorta for the Langendorff heart assay. The hearts were then washed with Krebs solution (Table 1) for 5 minutes, and then incubated in digestion solution for 8 minutes. The hearts were then minced into small pieces with a pair of surgical scissors, and the fragments were filtered through a 200µM filter. Liberase activity was then inhibited by adding Krebs solution plus 12.5µM calcium chloride to the suspension. The cell suspension was then incubated for 10 minutes to allow separation of cell types. The supernatant was then discarded, and calcium reintroduction was performed by incubating the cells in increasing concentrations of calcium chloride (12.5µM, 62µM, 112µM, 212µM, 500µM, 1mM) in Krebs solution, and with each increment, the cells were mixed thoroughly and incubated at room temperature for 4 minutes. After cell sedimentation, the

supernatant was then aspirated. Cardiomyocytes were then seeded onto a laminin-coated substratum and cultured in M199 culture medium, supplemented with 5% heat inactivated foetal bovine serum (FBS) (Biosera, Ringmer, UK), 100µg ml<sup>-1</sup> streptomycin, 100 units ml<sup>-1</sup> penicillin, 2µM L-carthinine, 5µM creatine and 5µM taurine, incubated in a humidified atmosphere at 37°C with 95% air and 5% CO<sub>2</sub>. Growth medium was then aspirated and replenished after the first 2 hours, and every 24 hours thereafter.

#### **2.3.4 Cryogenic Storage**

Growth medium was aspirated from exponentially growing adherent cells, followed by washing with 37°C PBS and then incubated with 37°C trypsin for 3 minutes. The trypsin activity was neutralised with the addition of full growth medium to the suspension and then cell numbers were counted. The desired number of cells were then centrifuged at 150g for 5 minutes. Supernatant was then aspirated, and cells were re-suspended in 10% DMSO in foetal calf serum at a concentration of 1 X 10<sup>6</sup> cells ml<sup>-1</sup>. Aliquots of 1mL were then pipetted into cryovials and each transferred to a Nalgene™ Cryo freezing container filled with isopropanol. To ensure a slow and consistent freezing process, the freezing container was placed at -80°C for 24 hours before cryovials were removed and frozen in liquid nitrogen for long-term storage.

#### **2.3.5 Resuscitation of Frozen Cells**

Cryovials were removed from liquid nitrogen, and then immediately incubated at 37°C for 2 minutes. The cells were then transferred to a 75cm<sup>2</sup> culture flask containing 20mL of 37°C growth medium. After 24 hours, growth medium was replenished to remove DMSO and cell debris.

#### **2.3.6 Calculating Cell Density and Population Doublings**

To calculate the number of cells within a suspension, 20µL of suspended cell solution was transferred to a Fuchs Rosenthal haemocytometer (VWR, International UK).

Using an optical microscope (DMIL, Leica Microsystems, UK), the number of cells within 8 adjacent squares was then determined, and repeated at 3 random locations on the haemocytometer. For each square, only cells within the boundaries, and those touching the left or top boundary were counted. The mean number of cells, for every 8 random squares, was then calculated and multiplied by  $1 \times 10^4$ , to give the density of cells per millilitre.

To calculate the total number of cells in a given suspension, the density of cells (cells  $\text{ml}^{-1}$ ) was multiplied by the total volume of suspension (mL).

To calculate the Population Doubling (PD), both the number of cells seeded, and the number of cells harvested is required. The following formula is then applied:  $\text{PD} = X + (\ln(N1 / N2)) / \ln 2$

PD = Population Doubling

X = Previous PD

N1 = Number of cells seeded

N2 = Number of cells harvested

## 2.4 Live Cell Imaging

For live-cell time-lapse microscopy, cells were plated on glass coverslip bottomed dishes (Mattek), and incubated for 24 hours to adhere to the glass substratum. Images were taken every 10 minutes for the duration of each time-course. Using a 63X objective (NA=1.4). Z-stacks over  $7\mu\text{m}$  were obtained, using a Zeiss Spinning Disk confocal microscope. Cells were incubated at  $37^\circ\text{C}$  in a humidified environment with air plus 5%  $\text{CO}_2$ .

### 2.4.1 Foci Dynamic Quantification

DNA damage foci (DDF) from live-cell time-lapse microscopy were tracked using the Imaris module 'ImarisCell'.

## 2.5 T-Loop Detection via STORM

The below protocol is optimised for  $>1 \times 10^7$  MEFs grown on a 175 cm<sup>2</sup> culture flask.

### 2.5.1 Nuclei Isolation

MEFs were washed twice in PBS at 37°C and then incubated in trypsin at 37°C for 3 minutes. The trypsin was neutralised in MEF growth medium, cell number was determined using a haemocytometer, and then cells were centrifuged at 700g for 5 minutes. The supernatant was aspirated and cells were washed once in PBS at 4°C. Cells were then re-suspended in 4°C Fibroblast Lysis Buffer (Table 1) at a concentration of  $8 \times 10^6$  mL<sup>-1</sup> and incubated on ice for 10 minutes. 10% NP-40 was added to the cell suspension to a final concentration of 0.2% and gently vortexed. The tube was then inverted 3 times and incubated for a further 5 minutes on ice. The cell suspension was then centrifuged at 1,000g for 5 minutes at 4°C, the cytoplasmic fraction-containing supernatant was discarded, and the remaining nuclei pellet was washed once with 4°C Nucleic Wash Buffer (Table 1).

### 2.5.2 DNA Crosslinking

Nuclei were then re-suspended in 100µg mL<sup>-1</sup> trioxsalen in nucleic wash buffer, and incubated in a 3cm diameter petri dish placed on ice, in the dark, stirring on an orbital shaker at 60RPM, for 5 minutes. The petri dish containing nuclei suspension was then exposed to 365nm UV light at 3cm from the light source for 30 minutes whilst still placed on ice, and stirring on an orbital shaker at 60RPM. During cross-linking, microscope slides, with a glass coverslip fixed on top, were assembled into the cytospin apparatus (a glass microscope slide is too thick for STORM imaging, and thus cells are centrifuged onto a glass coverslip). After cross-linking, the nuclei suspension was pipetted numerous times to remove clumping. The nuclei suspension was then centrifuged at 1,000g for 5 minutes at 4°C. The supernatant was then aspirated and pellet was washed with 4°C nucleic wash buffer. Nuclei were

then counted using a haemocytometer and re-suspended in nucleic wash buffer to a final concentration of  $10 \times 10^6 \text{ mL}^{-1}$ .

### 2.5.3 Chromatin Spread

Nuclei were diluted 1:10 in 37°C spreading buffer (Table 1), and 100µL of suspension was added to each cyto-centrifuge tube and centrifuged at 600RPM for 1 minute. The glass coverslip was separated from the microscope slide and were then incubated in methanol at -20°C for 10 minutes, followed by incubation in acetone at -20°C for 1 minute. Coverslips were then washed in PBS and dehydrated through a graded ethanol series (70, 95 and 100%), for 3 minutes each. At this point, chromatin spreads can be stored in the dark at room temperature for several months.

### 2.5.4 FISH

Chromatin spreads were rehydrated in PBS for 15 minutes. After rehydration, chromatin spreads were dehydrated through a graded ethanol series (70, 95 and 100%), for 3 minutes each. 10µL FISH hybridisation mix (Table 1) with TelC-Cy5 PNA probe was added to a glass microscope slide and then the glass coverslip-bound chromatin spreads were placed on top and incubated at 80°C for 10 minutes. After incubation, the chromatin spreads were incubated in a humidified chamber at room temperature overnight. The chromatin spreads were then washed in PNA wash A (Table 1) (2 X 15 minutes), followed by washes in PNA wash B (Table 1) (3 X 5 minutes). Chromatin spreads were then rinsed several times in dH<sub>2</sub>O, dehydrated through a graded ethanol series (70, 95 and 100%), for 3 minutes each and left to air dry in the dark.

### 2.5.5 STORM Imaging

Using conventional silicone grease, a hollow Perspex cylinder of 0.5cm in both height and diameter was adhered to the glass coverslip so that the perimeter of the cylinder was surrounding the chromatin spread. STORM Imaging buffer (Table 1) was then

pipetted onto the chromatin spreads, until the level reached the brim of the cylinder, and a glass coverslip was placed on top to create an airtight environment.

Imaging was performed on a Nikon N-STORM imaging system comprising of a NikonTi, Andor iXon 887 camera and Nikon Elements acquisition software. dSTORM images were captured at a rate of 50 frames per second with a 647nm laser with an excitation intensity of 200mW

## 2.6 Plasmid Expansion and Purification

### Plasmid Elution

Plasmids were received precipitated on filter paper. To elute the plasmid DNA, a small section of filter paper was cut out using sterile scissors and then placed into a 1.5mL micro-centrifuge tube with 20 $\mu$ L of nuclease-free H<sub>2</sub>O. A sterile pipette tip was used to mix the filter paper with the H<sub>2</sub>O, and then left to rest at room temperature for 2 minutes.

### High Efficiency Transformation Protocol

10 $\mu$ L of NEB Stable Competent E.coli cells (from stock) were thawed on ice in a 1.5mL microcentrifuge tube for 10 minutes. 1-2 $\mu$ L of eluted plasmid DNA (containing 100pg – 100ng of plasmid DNA) was added to NEB Stable Competent E.coli cells, and then gently flicked 5 times to mix cells and DNA (note: do not vortex). The mixture was then placed on ice for 30 minutes. After this, the cells were heat shocked at 42°C for 30 seconds, followed by being placed on ice for 5 minutes. 500 $\mu$ L of room temperature SOC medium was added to the mixture, and then incubated on an orbital shaker at 250RPM at 30°C for 60 minutes. Agar selection plates, with the necessary antibiotic drug, were warmed at 30°C. After incubation, the cells were mixed thoroughly, by flicking and inverting the tube. 50-100 $\mu$ L of cell suspension was then streaked onto an agar selection plate, followed by incubation at 30°C for 24 hours.

(Alternatively, for previously transformed NEB Stable Competent E.coli cells stored in glycerol at -80°C: a sterile pipette was used to transfer cell stocks to 50-100 $\mu$ L of

SOC medium. Cell suspension was then was then streaked onto an agar selection plate, and incubated at 30°C for 24 hours).

### Plasmid Expansion

Using a sterile pipette tip, a single NEB Stable Competent E.coli colony was picked and placed in 5mL of LB and then incubated shaking horizontally at 30°C for 6 hours. The suspension was then transferred to a vented conical flask containing 100mL LB plus antibiotic (50ng mL<sup>-1</sup> Ampicillin) and incubated on an orbital shaker at 180RPM at 30°C for 24 hours.

### Bacterial Glycerol Stock

2mL of bacterial cell suspension, from previous 'Plasmid Expansion' step, was transferred to a 15mL centrifuge tube and then centrifuge at 5000g for 10 minutes at room temperature. The supernatant was aspirated and the cell pellet was re-suspended in 1mL of 30% glycerol: 70% LB (v/v) in a cryovial and placed at -80°C for long-term storage.

### Plasmid Isolation

Plasmids were purified from NEB Stable Competent E.coli cells, following plasmid expansion, using the PureYield™ Plasmid Midiprep System (Promega). Briefly, 100mL of LB and NEB Stable Competent E.coli suspension was transferred into two 50mL centrifuge tubes and centrifuged at 5000g for 10 minutes at room temperature (all steps carried out at room temperature). The two pellets were re-suspended in 3mL of Cell Suspension Solution and pooled together. 3mL of Cell Lysis Solution was added, and the mixture was inverted 5 times and incubated for 3 minutes. 5mL of neutralisation was added to the mixture and inverted 10 times. The lysate was then centrifuged at 15,000g for 15 minutes. A column stack consisting of a blue PureYield™ Clearing Column placed on top of a white PureYield™ binding column was assembled onto a vacuum pump. The liquid was poured transferred into the column stack and a vacuum applied, until all of the liquid had passed through. 5mL of Endotoxin Removal Wash was added to the binding column, and a vacuum applied until all the solution had been pulled through. 20mL of Column Wash Solution was added to the binding column, and a vacuum applied until all the solution had been pulled through. A vacuum was applied for 60 seconds to try the binding column, followed by removal and placement onto a paper towel to remove excess ethanol.

To elute the DNA, the binding column was first placed into a new 50mL centrifuge tube. 600µL of nuclease-free water was added to the binding column, and incubated for 1 minute. The binding column was then centrifuged at 2,000g for 5 minutes in a swinging bucket rotor centrifuge, followed by collection of the filtrate into a new 1.5mL microcentrifuge tube.

#### Assessment of Nucleic Acid Purity and Quantification

Using the NanoDrop 2000 software, the DNA - Nucleic Acid option was selected. 1µL of nuclease-free water was added to the spectrophotometer (Nanodrop 2000, Thermo Scientific), and the 'blank' option selected to assess background fluorescence. 1µL of plasmid DNA solution was added to the spectrophotometer and quantified. A 260/280 ratio of near 1.8 was considered to have a satisfactory level of DNA purity.

#### Isolated Plasmid Storage

Isolated plasmid solutions were aliquoted into 1.5mL microcentrifuge tubes and stored at -20°C.

## 2.7 Transfection

All reagent amounts for transfection are stipulated in Table 2. H9C2 cells were seeded onto glass coverslips 24 hours prior to transfection.

Equal volumes of Opti-MEM® were added to two 1.5mL microcentrifuge tubes. Purified plasmid DNA was then added to one of the microcentrifuge tubes, gently vortexed and left to stand at room temperature for 5 minutes. Lipofectamine® 2000 was then added to the other microcentrifuge tube and gently vortexed. The contents of both microcentrifuge tubes were added together, gently vortexed, and left to stand at room temperature for 20 minutes. The mixture was then added dropwise to the growth medium, whilst gently moving the culture plate in a figure-of-8 motion. Cells were then incubated for 24 hours before replenishing the growth medium.

Vessel	Optimem (µL)	DNA (µg)	Lipofectamine (µL)
24-well	12.5	0.25	0.75

12-well	25	0.5	1.5
6-well	50	1	3

**Table 2. Transfection Reagents.**

## 2.8 Conditioned Medium

$5 \times 10^4$  adult cardiomyocytes were seeded onto laminin-coated 6 well plates and incubated in 2mL of M199 culture medium, supplemented with 5% heat inactivated foetal bovine serum (FBS) (Biosera, Ringmer, UK),  $100\mu\text{g ml}^{-1}$  streptomycin, 100 units  $\text{ml}^{-1}$  penicillin,  $2\mu\text{M}$  L-carthine,  $5\mu\text{M}$  creatine and  $5\mu\text{M}$  taurine. After two hours, the growth medium was aspirated, the cells were washed with 1 X PBS, and cells were cultured in the above culture medium minus the foetal bovine serum. After 48 hours, the conditioned growth medium was collected, and passed through a sterile syringe filter with a  $0.22\mu\text{m}$  pore size. The conditioned medium from isolated mouse cardiomyocytes was mixed with normal MAF medium at a ratio of 1:1. MAFs were then incubated in this conditioned medium, which was replenished every 48 hours, for experimentally defined amounts of time.

## 2.9 EdU Incorporation

For EdU incorporation assays, 50% of growth medium was aspirated from cell cultures, and an equal volume replaced with fresh growth medium containing  $20\mu\text{M}$  EdU, to ensure a final  $10\mu\text{M}$  EdU concentration. Cells were then cultured in the presence of EdU for desired experimental time period, followed by PBS washes (2 X 5 minutes) at  $37^\circ\text{C}$ , then fixation with 2% PFA for 10 minutes (at this point, cells can be stored in PBS at  $4^\circ\text{C}$  for several months). Cells were then washed twice 3% BSA in PBS (2 X 5 minutes) whilst gently stirring on an orbital shaker at 60RPM. The wash solution was removed, and cells were permeabilised with 0.5% Triton® X-100 for 20 minutes at room temperature, gently stirring on an orbital shaker.

The subsequent EdU detection steps were carried out according to manufacturer's instructions: Click-iT EdU Alexa Fluor Imaging Kit (ThermoFisher Scientific).

## 2.10 Genotoxic Stress

### 2.10.1 X-Ray Irradiation

MRC5 fibroblasts were seeded onto 6/12/24 well plates (Corning) and incubated to grow overnight. Cells were then exposed to varying levels of irradiation ranging from 1-50Gy using an X-Ray Irradiator (X-Rad 225, Precision X-Ray INC, N-BRANFORD, CT USA). Growth medium was replenished immediately after irradiation.

### 2.10.2 Chemical-induced

- Neocarzinostatin (SIGMA, N9162): Cells were treated with 80 ng ml<sup>-1</sup> neocarzinostatin for 1 hour, followed by 2 X PBS washes at 37°C, then re-incubated in full growth medium.
- Hydrogen peroxide (H<sub>2</sub>O<sub>2</sub>) (SIGMA, H1009): Cells were treated with 400µM H<sub>2</sub>O<sub>2</sub> for 1 hour in serum free medium, followed by PBS washes (2 X 5 minutes) at 37°C, then re-incubated in full growth medium.
- Etoposide (SIGMA, E1383): Cells were grown for 10 days in the presence of 50µM Etoposide with fresh medium and etoposide being added every 3 days.

## 2.11 Treatment with Pathway Inhibitors

### 2.11.1 Inhibition of mTORC1

Cells were treated with 100nM rapamycin in DMSO for varying amounts of time depending on experimental design. As a negative control, cells were treated with an equal volume of DMSO.

## 2.12 Knock down by small Interfering RNA

MRC5 cells (PD<25) were seeded onto glass coverslips in 24-well plates, and incubated with 500µL growth medium, 24 hours prior to siRNA treatment. 75ng of siRNA was diluted in 100µL serum-free medium and briefly mixed by vortexing. 3µL HiPerFect Transfection Reagent was added to the mixture and then vortexed for 10 seconds, followed by incubation at room temperature for 10 minutes. The mixture

was then added dropwise to the growth medium, whilst gently moving the culture plate in a figure-of-8 motion (this gives a final siRNA concentration of 10nM).

Knock-down efficiency was performed by western blotting.

## 2.13 Flow Cytometry

Flow cytometry was carried out using Partec PAS equipment. For calibration purposes, fluorescent microspheres were used. For each measurement,  $1 \times 10^4$  cells were analysed.

### 2.13.1 Mitochondrial Mass

Mitochondrial mass was determined by re-suspending and incubating  $\sim 2 \times 10^5$  live cells with 10 $\mu$ M 10-n-nonyl-acridine orange (NAO) in serum-free DMEM for 10 minutes at 37°C in darkness. Cells were then centrifuged at 1600 RPM for 2 minutes and the supernatant was discarded. Cells were then re-suspended in 3mL serum-free DMEM and levels of fluorescence were determined via flow cytometry using the green fluorescence (FL1) channel.

### 2.13.2 Reactive Oxygen Species

Mitochondrial superoxide levels were determined using the same protocol as for mitochondrial mass, however incubating the live cells in 10 $\mu$ M dihydroethidium (ThermoFisher, D-1168) for 30 minutes and then using the red fluorescence (FL3) channel for flow cytometry.

## 2.14 Mice

### 2.14.1 Mice Groups and Treatments

#### Ageing Colony

A long established colony of inbred C57/BL6 mice (n=10/group) were fed *ad libidum*, with constant access to water, and culled at 3, 15 or 30 months of age, as described in (Wang *et al.*, 2009; Cameron *et al.*, 2011).

#### Rapamycin Colony

C57/BL6 mice were age-matched and randomly split into groups (n=10/group). For each group, mice were fed *ad libidum* on either a control or rapamycin diet from 3 months of age. A control and rapamycin group were then culled at 6.5 months and 15 months of age. Mouse feed was purchased from TestDiet:

- Control diet: 5LG6/122 PPM EUDRAGIT 3/8 #1814831 (5AS0).
- Encapsulated Rapamycin diet: 5LG6/122 PPM ENCAP RAP 3/8 #1814830 (5ARZ).

All mice were monitored weekly.

#### MAO-A Colony

Transgenic p $\alpha$ MHC-MAO-A C57/BL6J mice were generated as described in (Villeneuve *et al.*, 2013). Mice were culled at 3 or 5 months of age.

Formalin-fixed paraffin-embedded mouse heart tissues were provided as a kind gift from Dr. Jeanne Mialet-Perez, Claudius Regaud Institute, University Paul Sabatier, Toulouse, France.

#### Catalase<sup>-/-</sup> and MnSOD<sup>+/-</sup> Colonies

Cryo-frozen mouse heart tissues from Catalase<sup>-/-</sup> and MnSOD<sup>+/-</sup> genotype male mice between the ages of 17 and 27 months were provided as a kind gift from Dr. Jordan Miller, Mayo Clinic, Rochester, US.

### 2.14.2 Animal Housing

All animal husbandry and experimental procedures were performed in compliance with the Animals (Scientific Procedures) Act 1986 (ASPA). Mice were housed in a temperature-regulated environment (20±2°C) with a 12 hour light/dark cycle, with lights turned on at 7 am.

### 2.14.3 Mice Tissue Collection and Preparation

All tissues were placed in 10% neutral buffered formalin (VWR, 9713.9010) immediately after dissection. After fixation, tissues were dehydrated through a series of graded ethanol baths, before being treated with xylene, followed by paraffin embedding.

## 2.15 Human Tissue Collection, Preparation and Ethics

Human heart tissue was obtained from patients undergoing open heart surgery for aortic stenosis, with a section of the right atrial appendage being placed in 10% neutral buffered formalin (VWR, 9713.9010) immediately after dissection. Subsequent processing steps for paraffin embedding were the same as for mouse tissue (as described above). Heart surgery was performed by Andrew Owens.

All tissue samples were obtained under the clause in the Human Tissue act that enables anonymised samples to be taken without consent in the context of an ethically approved study.

This study: “The isolation and characterisation of cell lines, including adult stem cells, from tissue discarded following cardiothoracic surgery”, was approved by the Research Ethics Committee UK, REC reference number: 10/H0908/56.

## 2.16 Immunocytochemistry

### 2.16.1 ICC on fixed cells

N.B. All wash steps were carried out stirring on an orbital shaker at 80RPM and all antibody incubations steps carried out in an opaque humidifier chamber, unless otherwise stated.

#### Fixation

Cells were grown on sterile coverslips until 50-80% confluency, washed in PBS (2 X 5 minutes) and then fixed in 2% PFA for 10 minutes at room temperature. Following fixation, cells were washed with PBS (2 X 5 minutes).

At this point, fixed cells can be stored in PBS at 4°C for several months, or at -80°C for longer term storage.

### Permeabilisation

Fixed cells were incubated in PBG-T (Table 1) for 45 minutes, whilst stirring on an orbital shaker at 80 RPM.

### Immunofluorescent Staining

Cells were then incubated with a primary antibody (Table 3) diluted in PBG-T in a humidifier chamber overnight at 4°C. After washing in PBG-T (3 X 5 minutes), cells were then incubated with a secondary antibody (Table 4) for 1 hour at room temperature in the dark. Darkness was achieved by wrapping the culture plates in aluminium foil. Cells were then washed in PBS (3 X 5 minutes), and cells were mounted on to glass microscope slides with ProLong® Gold Antifade Mountant (ThermoFisher, P36930).

Primary Antibodies:

Target	Host Species	Supplier, Cat#	Dilution
PCM-1	Rabbit Polyclonal	SIGMA, HPA023374	1:300
Troponin-C	Goat	Abcam, ab30807	1:200
γH2AX (Ser139)	Rabbit Monoclonal	Cell Signalling, #9718	1:200
γH2AX (Ser139)	Mouse Monoclonal	Millipore, 05-636	1:2000
53BP1	Rabbit Polyclonal	Cell Signalling, #4937	1:200
Ki-67	Rabbit	Abcam, 15580	1:250

	Polyclonal		
FLAG	Mouse Monoclonal	SIGMA, F1804	1:1000

**Table 3. Primary Antibodies for ICC on Cells**

Secondary Antibodies:

Target	Host	Supplier, Cat#	Dilution
anti-Mouse IgG (H+L), Alexa Fluor® 488	Goat Polyclonal	Invitrogen, A-1101	1:4000
anti-Mouse IgG (H+L), Alexa Fluor® 594	Goat Polyclonal	Invitrogen, A-11005	1:4000
anti-Mouse IgG (H+L), Alexa Fluor® 647	Goat Polyclonal	Invitrogen, A-21235	1:4000
anti-Rabbit IgG (H+L), Alexa Fluor® 488	Goat Polyclonal	Invitrogen, A-11008	1:4000
anti-Rabbit IgG (H+L), Alexa Fluor® 594	Goat Polyclonal	Invitrogen, A-11012	1:4000
anti-Goat IgG (H+L), Alexa Fluor® 647	Donkey Polyclonal	Invitrogen, A-21447	1:2000

**Table 4. Secondary Antibodies for ICC on Cells**

N.B. All antibodies were dissolved in PBG-T.

### 2.16.2 Telomere-FISH on Fixed Cells following ICC

After immunocytochemistry (described above), cells were washed in PBS (2 X 5 minutes). A fixative of methanol: acetic acid (3:1 respectively) was added for 30 minutes. Sections were then dehydrated using a cold ethanol gradient of 70%, 90% and 100% for 2 minutes each. After air drying, the samples were then incubated in PBS at 37°C for 5 minutes, followed by incubation in 4% PFA for 2 minutes. Samples were then washed in PBS and dehydrated through an ethanol gradient once more (as described previously). Coverslips were then placed onto a glass slide containing 10µL of hybridisation mix (Table 1) and incubated at 80°C for 10 minutes. Samples were then placed into a humidifier chamber and incubated at room temperature for 2

hours. Coverslips were then transferred back into the 12 well plate and washed in wash buffer (3 X 10 minutes). Cells were then washed in TBS-Tween (0.05%) (Table 1) (3 X 5 minutes). Samples were then taken through a final ethanol dehydration, air dried and then cells were mounted on to glass microscope slides with ProLong® Gold Antifade Mountant (ThermoFisher, P36930).

### 2.16.3 ICC on Paraffin Embedded Mouse and Human Tissue

3µM tissue sections were cut on a microtome, adhered to 4% APES coated slides and incubated at 37°C overnight.

Sections were de-paraffinised by incubating in histoclear (2 X 5 minutes), followed by hydration through an ethanol gradient of 100% (2 X 5 minutes), 90% (5 minutes), 70% (5 minutes) ethanol and then incubated in dH<sub>2</sub>O (2 X 5 minutes).

For antigen retrieval, sections were submerged in 0.01M citrate buffer pH6.0 (Table 1) and then heated with microwaves (800W) until solution was boiling, and then the power was reduced (400W) and the solution was simmered for 10 minutes. Sections were then left to rest until the citrate buffer reached room temperature, and then they were washed twice in distilled water for 5 minutes each.

- For anti-mouse primary antibodies used on mouse tissue: Sections were incubated in M.O.M.™ IgG blocking (Vector Laboratories, MKB-2213) reagent diluted 1:25 in TBS-Triton for 1 hour at room temperature. Sections were then washed in PBS (2 X 5 minutes) and then incubated in primary antibody (Table 5), diluted in M.O.M diluents diluted 1:12 in TBS-Triton at 4°C overnight.
- For all other primary antibodies used on either mouse or human tissue: Sections were then incubated in blocking reagent, consisting of normal goat serum (NGS) diluted 1:60 in 0.1% BSA in PBS for 30 minutes at room temperature. Blocking solution was then tipped off, and sections were incubated in primary antibody (Table 5), diluted in blocking reagent, at 4°C overnight.

Sections were then washed in PBS (3 X 5 minutes).

- For anti- $\gamma$ H2AX primary antibody: sections were incubated in biotinylated secondary antibody (1:200 in blocking serum) (Table 6) for 30 minutes at room temperature. Sections were then washed in PBS (3 X 5 minutes) and then incubated in avidin DCS (1:500 in PBS) (Table 6) for 30 minutes.
- For all other primary antibodies: sections were incubated in an Alexa Fluor conjugated secondary antibody (1:2000 in blocking serum or M.O.M diluents) (Table 6) for 1 hour.

Sections were then washed in PBS (3 X 5 minutes) and glass coverslips were mounted onto the sections with ProLong® Gold Antifade Mountant (ThermoFisher, P36930).

#### Primary Antibodies:

Target	Host Species	Supplier, Cat#	Dilution
$\alpha$ -Actinin	Mouse Monoclonal	SIGMA, A7811	1:200
$\gamma$ H2AX	Rabbit Monoclonal	Cell Signalling, #9718	1:200
PCM-1	Mouse Monoclonal	Abcam, ab154142	1:200
TRF2	Mouse Monoclonal	Millipore, 05-521	1:200

**Table 5. Primary Antibodies for ICC on Mouse and Human Tissues**

#### Secondary Antibodies:

Target	Host	Supplier, Cat#	Dilution
Anti-Mouse IgG (H+L), Alexa Fluor® 647	Goat Polyclonal	Invitrogen, A-21235	1:2000
Biotinylated anti-Rabbit IgG (H+L)	Goat	Vector Laboratories, BA-1000	1:200
Fluorescein-labelled Avidin DCS	N/A	Vector Laboratories, A-2011	1:500

**Table 6. Secondary Antibodies for ICC on Mouse and Human Tissue**

#### **2.16.4 Telomere-FISH on Mouse and Human Tissues following ICC**

If required and prior to mounting, FISH was coupled with ICC-stained mouse or human tissues.

Sections were incubated in 4% paraformaldehyde in PBS for 20 minutes at room temperature, followed by PBS washes (3 X 5 minutes). Sections were then dehydrated through an graded ethanol series (70, 90 and 100%), for 3 minutes each at -20°C. Sections were allowed to air dry, then 10µL of telomere-FISH hybridisation mix (Table 1) was added to the section and a glass coverslip was placed on top. Sections were then placed at 80°C for 10 minutes to denature the DNA. Following this, sections were incubated in an opaque humidifier chamber at room temperature for 2 hours to allow the probe to hybridise. Following incubation, sections were washed in 70% formamide in 2 X SSC (1 X 10 minute), 2 X SSC (1 X 10 minute), and PBS (3 X 10 minutes). Glass coverslips were then mounted on to the sections with ProLong® Gold Antifade Mountant (ThermoFisher, P36930).

#### **2.17 Q-FISH**

For Q-FISH analysis of telomere-FISH performed on either fixed cells or tissue sections: spinning disk confocal microscopy was used to image Z-stacks through the entire nucleus of each cell with Z-depths of 0.1µM with 100X objective (NA=1.4). ImageJ software was used to create maximum intensity Z projections, and then the oval tool was used to create a circle to measure the integrated density of individual telomere signals.

#### **2.18 Immunohistochemistry**

##### **2.18.1 IHC on paraffin embedded tissue**

Tissue sectioning, deparaffinisation, antigen retrieval, blocking and primary antibody incubation were carried out as described above for ICC on tissue sections, except for

the addition of an endogenous biotin blocking step. Moreover, prior to incubation with primary antibody, sections were incubated in avidin (SP-2001, Vector Laboratories) for 15 minutes at room temperature, followed by a PBS wash (1 X 5 minutes), then incubated in biotin (SP-2001, Vector Laboratories) for 15 minutes at room temperature, followed by a further PBS wash (1 X 5 minutes).

Following overnight primary antibody (Table 7) incubation at 4°C, sections were washed with TBS-T (2 X 5 minutes) and then incubated in biotinylated secondary antibody (1:200 in blocking solution) (Table 8) for 30 minutes. Sections were then washed in TBS-T (2 X 5 minutes), and then endogenous peroxidase activity was blocked by incubating sections in 0.9% H<sub>2</sub>O<sub>2</sub> in dH<sub>2</sub>O for 30 minutes at room temperature. Following PBS washes (2 X 5 minutes), sections were incubated in VECTASTAIN® ABC Reagent (PK-6100, Vector Laboratories) according to manufacturer's instructions. Sections were then washed in PBS (3 X 5 minutes), followed by visual detection of peroxidase activity by treating slides with VECTOR NovaRED Peroxidase (HRP) substrate according to manufacturer's instructions.

Sections were then washed with dH<sub>2</sub>O (1 X 5 minutes), counterstained with haematoxylin for 1-2 minutes, washed with dH<sub>2</sub>O (2 X 1 minute), incubated in 1% acid alcohol for 5 seconds, washed in dH<sub>2</sub>O (1 X 1 minute), incubated in ammonia water for 20 seconds and washed in dH<sub>2</sub>O (1 X 1 minute). Sections were then dehydrated through an ethanol gradient of 90% ethanol (2 X 30 seconds), 100% ethanol (2 X 30 seconds) and then incubated in histo-clear (2 X 5 minutes). Glass coverslips were then mounted on top of the sections with DPX.

Target	Host Species	Supplier, Cat#	Dilution
P21	Rabbit Polyclonal	Abcam, 7960	1:200
4-HNE	Mouse Monoclonal	JaICA, MHN	1:100
8-OHdG	Rabbit Polyclonal	JaICA, MOG	1:100

**Table 7. Primary Antibodies for IHC on Tissues**

Target	Host	Supplier, Cat#	Dilution
--------	------	----------------	----------

Biotinylated anti-Mouse IgG (H+L)	Horse	Vector Laboratories, BA-2000	1:200
Biotinylated anti-Rabbit IgG (H+L)	Goat	Vector Laboratories, BA-1000	1:200

**Table 8. Secondary Antibodies for IHC on Tissues.**

## 2.19 CHIP-PCR

### 2.19.1 Crosslinked ChIP Assay

Crosslinked ChIP assay was carried out using 25µg crosslinked chromatin prepared from 3 or 30 month ground mouse heart tissue as described in (Mann *et al.*, 2010), using anti-γH2AX (phospho S139) (Abcam, ab2893) and species and isotype matched control ChIP grade IgG (Abcam, ab46540).

### 2.19.2 Real-time PCR

Real-time PCR for telomeric repeats was performed as described previously (Cawthon, 2002), using primers targeted against mouse telomeres (Table 9).

Primer Direction	Primer Sequence 5' to 3'
Forward	CGGTTTGTGGTTGGGTTTGGGTTTGGGTTTGGGTTTGGGTT
Reverse	GGCTTGCCTTACCCTTACCCTTACCCTTACCCTTACCCT

**Table 9. Telomere Sequence for RT-PCR for Telomeric Repeats**

## 2.20 Senescence Associated β Galactosidase Activity Assay

### 2.20.1 SA-β-Gal on Fixed Cells

Cellular senescence was determined using the Senescence-Associated  $\beta$  Galactosidase assay, as described previously (Dimri *et al.*, 1995). Briefly, cells were fixed with 2% paraformaldehyde for 5 minutes at room temperature. Following PBS washes (2 X 5 minutes), cells were incubated in SA- $\beta$ -Gal staining solution (Table 1) at 37°C in the dark overnight. Cells were then washed in PBS (3 X 5 minutes) and then mounted on to glass microscope slides with ProLong® Gold Antifade Mountant (ThermoFisher, P36930).

Using a Leica DM5500B microscope and a Leica DFC420 camera, random fields (20X objective) were imaged and cells were scored either positive or negative for SA- $\beta$  Gal staining.

## 2.21 Telomeric Repeat Amplification Protocol (TRAP) Assay

Whole hearts, flash frozen in liquid nitrogen, were ground to a fine powder using a liquid nitrogen-chilled pestle and mortar and stored at -80°C.

To assess telomerase activity, the *TeloTAGGG* Telomerase PCR ELISA kit (Roche, 11854666910) was used according to manufacturer's instructions.

## 2.22 Protein Expression Analysis

### 2.22.1 Protein Extraction

Growth medium was aspirated, and then cells were washed once with 4°C PBS. Following aspiration of PBS, 80-100 $\mu$ L of 4°C RIPA buffer (Table 1) and 1X protease and phosphatase inhibitors (Thermo Scientific, 78442) were added to the cells, which were then scraped with a rubber policeman. Cell lysis solution was then transferred to a 1.5mL microcentrifuge tube, pre-chilled on ice, and then either used instantly for protein quantification, or placed at -80°C for long term storage.

### 2.22.2 Protein Quantification

Cell lysates were defrosted on ice and then centrifuged at 16,000g for 10 minutes at 4°C. Protein concentration was determined using the BioRad Protein Assay (Biorad; Reagent A, 500-0113; Reagent B, 500-0114; Reagent C, 500-0115) according to manufacturer's instructions. Protein absorbance was then quantified using a FLUOstar Omega microplate reader (BMG Labtech), and a regression line, for protein concentration estimates, calculated based on absorbance values from known BSA protein standards. Protein concentrations were then normalised by mixing protein lysates with loading buffer (2X Laemmli buffer (Biorad, 161-0737) and 2-mercaptoethanol (SIGMA, M6250) at a ratio of 19:1). Proteins were then denatured by incubating in a heating block at 100°C for 5 minutes, and then placed on ice temporarily before performing western blotting, or placed at -80°C for long term storage.

### 2.22.3 Western Blot

#### Gel Electrophoresis

Ammonium persulphate was diluted in dH<sub>2</sub>O to a concentration of 100mg mL<sup>-1</sup>. A 10mL resolving gel solution was prepared with the required percentage of acrylamide (Table 10), and then pipetted into an empty western blot cassette (Invitrogen, NC2010 or NC2015), with dH<sub>2</sub>O gently pipetted on top to level the acrylamide solution. Once polymerised, the dH<sub>2</sub>O was poured off, and 3mL of stacking gel solution (Table 10) was pipetted on top of the resolving gel and left to polymerise, with a western-blot comb inserted to create the desired number and volume of loading wells. Once the stacking gel polymerised, the cassette was loaded into a XCell SureLock™ Mini-Cell Electrophoresis System (Invitrogen, EI001) and running buffer (Table 1) was poured in until the cassettes were fully submerged. The western-blot combs were then removed and protein samples were pipetted into the wells, along with Precision Plus Protein™ Dual Colour Standards (Biorad, 1610374), for use as a protein molecular weight estimation ladder. Electrophoresis was then performed by applying 125V for 90 minutes.

<b>1 X Stacking Gel 5ml</b>	<b>5%</b>	<b>8%</b>	<b>10%</b>	<b>12%</b>	<b>15%</b>
Sterile H <sub>2</sub> O	3.4ml				
30% Acrylamide	850ul				
1.5M Tris <b>pH 6.8</b>	1.3ml				
10% SDS	50ul				
10% Ammonium Persulphate (w/v in H <sub>2</sub> O)	50ul				
TEMED	4ul				
<b>1 X Resolving Gel 10ml</b>					
<b>Protein Size (kDa)</b>	<b>&gt;250</b>	<b>250-120</b>	<b>120-40</b>	<b>40-15</b>	<b>&lt;20</b>
Sterile H <sub>2</sub> O	6.8ml	5.1ml	4ml	3.3ml	2.3ml
30% Acrylamide	1.7ml	2.6ml	3.3ml	4ml	5ml
1.5M Tris <b>pH 8.8</b>	2.5ml	2.5ml	2.5ml	2.5ml	2.5ml
10% SDS	100ul	100ul	100ul	100ul	100ul
10% Ammonium Persulphate (w/v in H <sub>2</sub> O)	100uL	100ul	100ul	100ul	100ul
TEMED	8ul	4ul	4ul	4ul	4ul

**Table 10. Acrylamide gel recipe for western blot**

### Protein Transfer to PVDF Membrane

Once electrophoresis had finished, a PVDF membrane (Millipore, IPVH00010) was incubated briefly in methanol and then submerged in transfer buffer (Table 1). The gel was then placed on top of the PVDF membrane and sandwiched between blotting pads (VWR, 732-0594), soaked in transfer buffer (Table 1) and loaded into a Trans-Blot® SD Semi-Dry Transfer Cell (Biorad) and transferred at 20V for 1 hour.

### Blocking and Antibody Incubation

Unless otherwise stated, all block and antibody incubations were performed on a laboratory rocker set to 12 RPM / ±8° tilt.

To block non-specific antibody binding, the membrane was incubated in 5% non-fat dry milk and 0.1% Tween® 20 in PBS (PBST-Milk) for 1 hour at room temperature. The PBST-Milk blocking solution was removed, and the membrane was incubated in primary antibody (Table 11) diluted in PBST-Milk overnight at 4°C. The membrane was then washed with dH<sub>2</sub>O (3 X 5 minutes), and then incubated in secondary antibody (Table 12) for 1 hour at room temperature. The membrane was then washed in PBS-T (3 X 5 minutes), followed by several rinses in dH<sub>2</sub>O.

Target	Host Species	Supplier, Cat#	Dilution
P21	Rabbit Monoclonal	Cell Signalling, #2947	1:1000
GAPDH	Rabbit Monoclonal	Cell Signalling, #5174	1:5000

Table 11. Primary Antibodies for Western Blot

Target	Host Species	Supplier, Cat#	Dilution
anti-rabbit IgG- Peroxidase	Goat	Sigma, A0545	1:5000

Table 12. Secondary Antibodies for Western Blot

### Chemiluminescent Detection

Chemiluminescent detection was performed using Clarity™ ECL Western Blot Substrate (Bio-rad, 170-5060) according to manufacturer's instructions, and visualised using a Fujifilm Las 1000 Intelligent Darkbox with Luminescent Image Reader Las-1000 Software.

Bands intensity was quantified using ImageJ software, with background subtraction and protein-of-interest normalised to a loading control protein.

## 2.23 Gene Expression Analysis

The following gene expression analysis was performed on freshly isolated adult mouse cardiomyocytes.

### 2.23.1 RNA Extraction

RNA extraction was performed using the RNeasy Mini Kit (QIAGEN), according to manufacturer's instructions.

### 2.23.2 cDNA Synthesis

cDNA was synthesised by reverse transcription of 0.5µg of RNA per reaction, using the High-Capacity cDNA Reverse Transcription Kit (ThermoFisher Scientific; 4368814), according to manufacturer's instructions.

### 2.23.3 Real Time Polymerase Chain Reaction (RT-PCR)

20µL Real time PCR reaction mix (10µL Taq polymerase, 2µL SYBR green, 300nM forward and reverse primer, 10ng cDNA and deionised H<sub>2</sub>O to total volume of 20µL) was added to each RT-PCR well. The thermocycler conditions were 95°C for 10 seconds, 65°C for 30 seconds for 45 cycles, followed by an incremental temperature increase for melt-curve analysis. Primer sequences are provided below

Target	Forward	Reverse
P15	AGATCCCAACGCCCTGAAC	CAGTTGGGTTCTGCTCCGT
P16	CCGAACTCTTTCGGTCGTACCC	CTGCTACGTGAACGTTGCCCA
TGFb	AGGGCTACCATGCCAACTTCT	CCGGGTTGTGTTGGTTGTAGA

MAO-A	GGAAGCCCGGGATAGAGTTG	TGGGTTGGTCCCACATAAGC
GAPDH	AGGTCGGTGTGAACGGATTTG	TGTAGACCATGTAGTTGAGGTCA

**Table 13. Primer Sequences for RT-PCR on Isolated Mouse Cardiomyocytes**

### 3 External Stress Induces Persistent DNA Damage at Telomeres in Cardiomyocytes

Previous studies have shown that telomeric damage in both human and murine fibroblasts is irreparable, resulting in a persistent DDR signal; a hallmark of DNA-damage induced cellular senescence (Fumagalli *et al.*, 2012; Hewitt *et al.*, 2012). Interestingly, Q-FISH analysis of telomere length in murine hepatocytes and enterocytes revealed an age-dependent increase in telomere damage occurring independently of telomere length (Hewitt *et al.*, 2012). These data contradict the hypothesis that telomere dysfunction occurs mainly as a result of progressive shortening of the telomeres, as a consequence of the end-replication problem; a process which is accelerated by oxidative stress-induced single strand breaks during replication (von Zglinicki *et al.*, 1995; von Zglinicki *et al.*, 2000), suggesting that an additional mechanism may also drive telomere dysfunction. Furthermore, this suggests a possibility for persistent telomere dysfunction to occur in post-mitotic and non-rapidly dividing cells types, which are not subject to proliferation-associated telomere shortening; a prospect of special interest, considering that research has shown that post-mitotic adipocytes and neurones can also elicit a senescent-like phenotype *in vivo* (Minamino *et al.*, 2009; Jurk *et al.*, 2012).

The t-loop structure forms an elegant mechanism for physically sheltering the ends of chromosomes from being recognised by the DDR machinery, thus preventing end-to-end fusions resulting from non-homologous end joining (NHEJ) (Griffith *et al.*, 1999). However, research has shown that NHEJ can be inhibited in the absence of t-loop formation, providing a RAP1/TRF2 complex is bound to as little as 12-telomeric repeats (Bae and Baumann, 2007). Interestingly, overexpression of TRF2 has been shown to attenuate single-strand break repair at telomeres (Richter *et al.*, 2007) and ectopic localisation of TRF2 next to a double-strand break (DSB) inhibits repair (Fumagalli *et al.*, 2012). Our group and another, therefore proposed a model in which if a physical double strand break were to occur in a telomeric region, this would be irreparable and lead to a persistent DDR (Fumagalli *et al.*, 2012; Hewitt *et al.*, 2012). Moreover, this would provide an explanation to our observations of telomere dysfunction occurring independently of telomere shortening *in vivo* (Hewitt *et al.*, 2012). However, another proposed mechanism for a persistent DDR at telomeres independently of telomere length, stipulates that partial TRF2 inhibition could lead to

telomere uncapping and a DDR, however still retaining enough TRF2 to inhibit end-to-end fusions via NHEJ (Cesare *et al.*, 2009).

Irrespective of the verisimilitude of either proposed theory, and one cannot reject the proposition that the two aren't mutually exclusive, we sought to investigate if post-mitotic/non-rapidly dividing cell types, which are not subject to proliferation-associated telomere shortening, could also be associated with persistent telomere dysfunction, and if so, does this drive a senescent-like phenotype. To investigate this, we used cardiomyocytes as our model, as proliferation is negligible in adult tissue, and there are two commonly used *in vitro* cardiomyocytes models we could utilise, namely: E17.5 embryonic mouse cardiomyocytes which retain the ability to contract when cultured *in vitro* and thus are a valuable tool for investigating cardiac diseases, and H9C2 rat-derived cardiomyocytes. Hitherto, and to our knowledge, telomere dysfunction in cardiomyocytes *per se* has been overlooked, perhaps because of the false assumption that telomere dysfunction is solely a consequence of telomere shortening, and thus of little interest in cardiomyocytes.

Secondly, we also aimed to investigate the nature of genotoxic-stress induced telomere damage, to ascertain whether it was a consequence of telomere-uncapping or a physical DSB within a telomeric region.

### **3.1 TAF are Persistent in Mouse Embryonic Fibroblasts following X-Irradiation**

Our group have previously published that stress-induced DNA damage, via X-irradiation (IR) or H<sub>2</sub>O<sub>2</sub> treatment in human fibroblasts, leads to both telomeric-associated DNA damage foci (TAF) and non-telomeric DNA damage foci (non-TAF), however, whilst non-TAF are largely repaired, TAF are irreparable (Hewitt *et al.*, 2012). To begin, we sought to ascertain if we could induce TAF in cardiomyocytes, and if so, was this persistent. We isolated E17.5 mouse embryonic cardiomyocytes, exposed them to 10Gy IR, and then performed telo-FISH coupled with ICC for  $\gamma$ H2AX (immuno-FISH) to analyse both TAF and non-TAF at 0, 3, 5 and 10 days following IR. The cardiomyocyte isolation procedure produces a heterogeneous population of cell types, also including endothelial cells and fibroblasts, so to ensure specificity of cardiomyocytes, only cells staining positive for Troponin I were

analysed. Our immuno-FISH analysis revealed a significant increase in both TAF and non-TAF at 3 days after IR, however, 5 days following IR, the mean number of non-TAF had significantly decreased compared to the value at 3 days, whereas the number of TAF did not significantly change (Figure 3-1A&D). Moreover, from 5 to 10 days, there was a non-significant ( $p=0.056$ ) trend towards a decrease in non-TAF, whereas the mean number of TAF remained insignificantly changed (Figure 3-1A&D). We observed a significant enrichment of the percentage of total DDR foci which were TAF from day 3 to 5 and day 5 to 10 following IR (Figure 3-1B&D). Finally, the percentage of cells positive for TAF remained insignificantly altered for each time point from day 3 to 10 following 10Gy IR (Figure 3-1C-D).

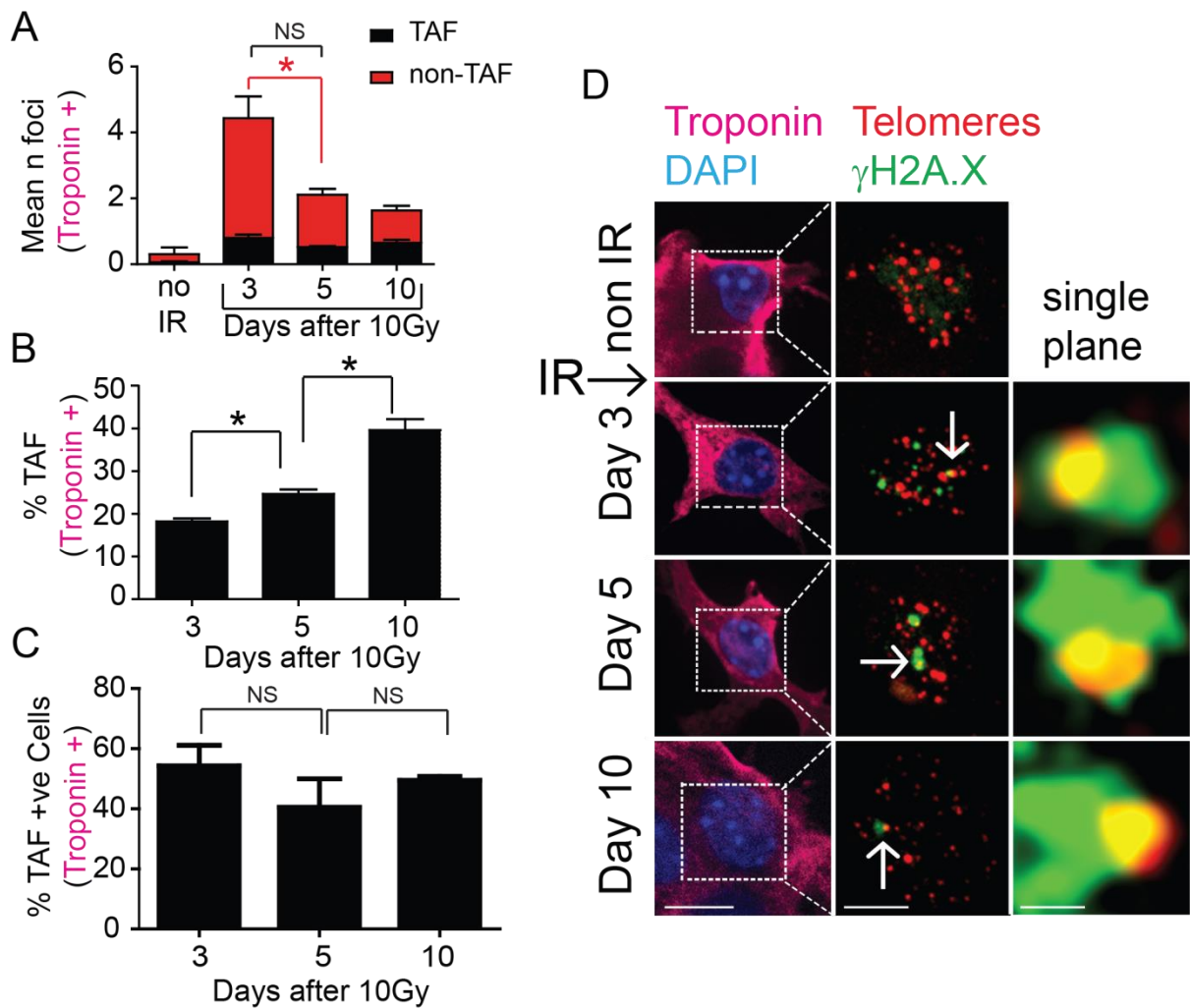


**Figure 3-1. X-Ray irradiation induces persistent TAF in Mouse Embryonic Cardiomyocytes.** (A) Mean number of both TAF and non-TAF-, (B) Mean percentage of DNA damage foci which are TAF-, (C) and percentage of TAF positive cells, in troponin-positive mouse embryonic cardiomyocytes at 3, 5 and 10 days following X-irradiation with 10Gy. Data are mean  $\pm$  SEM of  $n=3$ . (D) Representative images of embryonic cardiomyocytes at days 0, 3, 5 and 10 following X-irradiation with 10Gy. Left panel represents troponin-positive embryonic cardiomyocytes (troponin – magenta; DAPI - light blue). Middle panel white arrows indicate co-localisation between DDR, detected as  $\gamma$ H2AX foci (green), and telomeres, detected using a telomeric-PNA probe (red) in Z projections of  $0.1\mu\text{M}$  slices. Co-localising foci are amplified in the right-hand panel (amplified images represent a single Z-plane where co-localisation was observed). Scale bars: left panel -  $10\mu\text{M}$ ; middle panel  $5\mu\text{M}$ ; right panel  $0.5\mu\text{M}$ . Statistical analysis performed using One Way ANOVA or two tailed t test; \*  $P<0.05$ , NS (Non-Significant)  $P>0.05$ .

### 3.2 TAF are Persistent in H9C2 Cardiomyocytes following X-Irradiation

To confirm if persistent TAF could be induced in another cell model, we used H9C2 rat-derived cardiomyocytes. We treated H9C2 cells with 10Gy IR and then performed

immuno-FISH analysis for both TAF and non-TAF at 0, 3, and 5 days following IR. We observed a significant increase in both TAF and non-TAF at 3 days after IR, followed by a non-significant decrease in the number of non-TAF at day 5, however the number of TAF did not significantly change from 3 to 5 days (Figure 3-2A). We observed a non-significant trend towards an enrichment of the percentage of total DDR foci which are TAF from day 3 to 5 following IR (Figure 3-2B). Lastly, the percentage of cells positive for TAF remained insignificantly altered from day 3 to 5 following IR (Figure 3-2C).

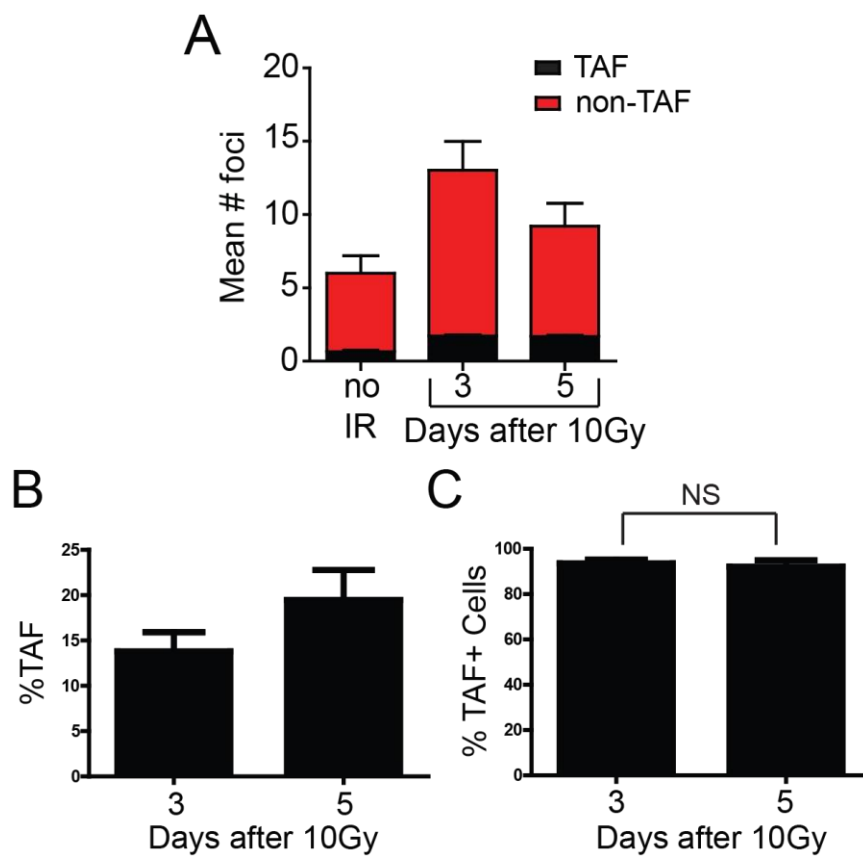


**Figure 3-2. X-Ray irradiation induces persistent TAF in H9C2 Cardiomyocytes.** (A) Mean number of both TAF and non-TAF-, (B) Mean percentage of DNA damage foci which are TAF-, (C) and percentage of TAF positive cells, in H9C2 cardiomyocytes at 3 and 5 days following X-irradiation with 10Gy. Data are mean ± SEM of  $n=3$ . Statistical analysis performed using One Way ANOVA or two tailed t test; \*  $P<0.05$ , NS (Non-Significant)  $P>0.05$ .

Previously, using a AcGFP-53BP1c fusion protein, coupled with microbead-mediated incorporation of the telomere-specific PNA probe, our group were able to track DNA Damage Response Foci (DDF) and telomeres simultaneously via live-cell time lapse

microscopy (Hewitt *et al.*, 2012). Interestingly, we discovered that all IR-induced DDF in Mouse Embryonic Fibroblasts (MEFs), which did not co-localise with telomeres were transient and therefore reparable, with a maximum lifespan of less than 3 hours, whereas around 50% of those DDF co-localising with telomeres survived for the entire course of the experiment (>6 hours) and are likely irreparable (Hewitt *et al.*, 2012). We therefore wanted to ascertain if persistent DDF could be induced in cardiomyocytes. In collaboration with Anthony Lagnardo in our laboratory, we transfected H9C2 cells with an AcGFP-53BP1c fusion protein, irradiated them with 10Gy, waited 72 hours and then performed live-cell time-lapse microscopy; imaging DDF every 10 minutes for 10 hours. Our data show that after 10Gy IR, the majority of DDF are resolved within 8 hours, however around 20% of DDF remain persistent, with no significant variations in foci dynamics after this time (Figure 3-3A-B). We also tracked DDF in untreated H9C2 cells, and observed that the starting number of DDF was significantly lower compared to IR-treated cells (data not shown), and the DDF foci present at the start were all resolved within 8 hours (Figure 3-3A-B).

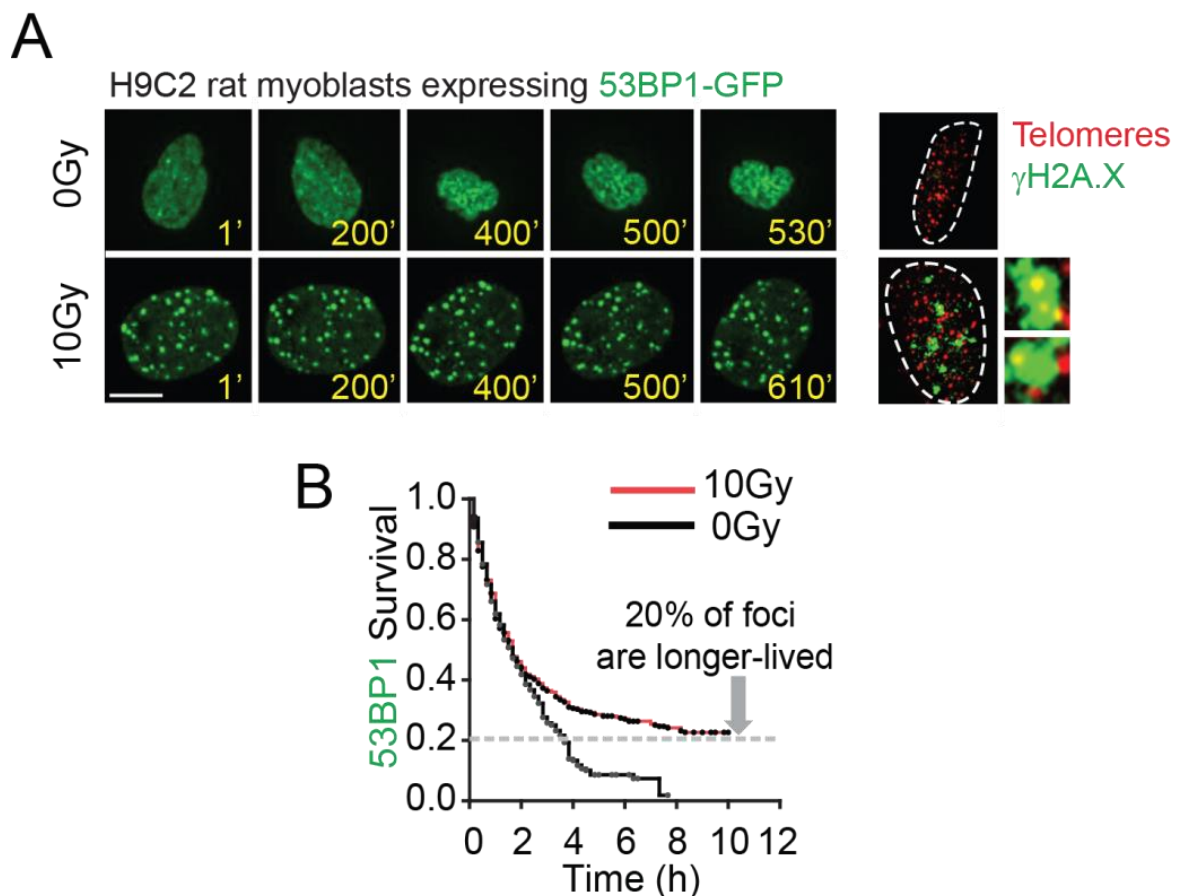


**Figure 3-3. Live-cell time-lapse microscopy reveals persistent IR-induced DDR foci in H9C2 Cells.** (A) Representative time-lapse images of H9C2 cells expressing AcGFP-53BP1 from 72 hours after 10Gy irradiation at the indicated times (mins). Images are maximum intensity projections with a 6.7 $\mu$ M focal depth. Scale bar: 5 $\mu$ M. (B) Kaplan-Meier survival curves for AcGFP-53BP1c DDR foci in H9C2 cells 2 days after 10Gy irradiation.

### 3.3 TAF are Induced Independently of DNA Replication

The H9C2 cardiomyocyte cell line still retain proliferative capability, therefore leaving the possibility that observed TAF could be induced as a result of DNA replication errors (Kuzminov, 1999). However, cardiomyocyte proliferation *in vivo* is negligible, with data suggesting that less than 1% of the cardiomyocyte population turn over annually in young adult humans (Bergmann *et al.*, 2009), and thus we sought to determine if TAF could arise independently of DNA replication.

We incubated H9C2 cells in the presence of a modified thymidine analogue (EdU), for 3 hours, followed by irradiation with 10Gy, and then cultured cells for a further 24 hours in the presence of EdU (Figure 3-4A-C). The prior EdU incubation period revealed that H9C2 cells had proliferation potential prior to X-irradiation, however the IR treatment significantly decreased the percentage of cells which underwent DNA replication during the time course of the experiment (Figure 3-4A-C). We then analysed the mean number of TAF in EdU negative cells, and found that the number of TAF are significantly increased 24 hours after IR with 10Gy (Figure 3-4D).

To determine if the length of telomeres affects susceptibility to IR-induced dysfunction, we performed Q-FISH analysis, and quantified the intensity of telomeres co-localising with a DDR, compared to telomeres not co-localising with a DDR. Our data show that, after 10Gy IR, the average length of telomeres co-localising with a DDR is significantly higher than telomeres not co-localising with a DDR (Figure 3-4E).

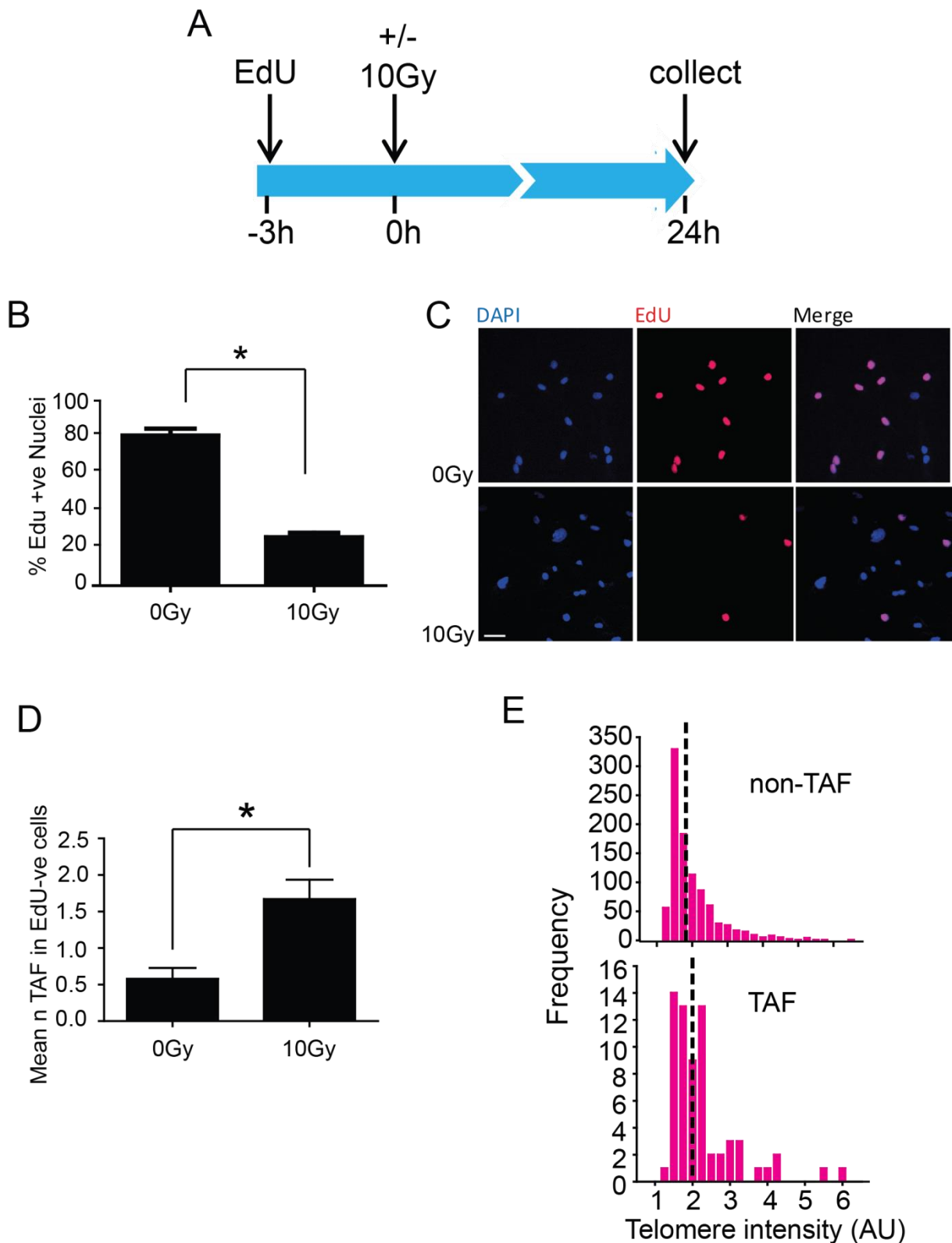


**Figure 3-4. TAF are Induced Independently of DNA Replication in X-irradiated H9C2 Cells.** **(A)** Schematic illustration showing H9C2 cells were incubated in 10µM EdU in normal growth medium for 3 hours, following X-irradiation with 10Gy and cultured for a further 24 hours in the presence of 10µM EdU in normal growth medium. **(B)** Mean percentage of EdU positive cells. Data are mean  $\pm$  SEM of  $n=3$ . **(C)** Representative images H9C2 cells 24 hours after X-irradiation with 10Gy (DAPI - light blue; EdU - pink). Scale bar: 30µM. **(D)** Mean number of TAF in EdU negative cells, 24 hours after 10Gy IR. Data are mean  $\pm$  SEM of  $n=3$ . **(E)** Histograms

displaying telomere intensity for telomeres co-localising (bottom) or not co-localising (top) with  $\gamma$ H2AX DDR foci in EdU negative cells (n=3). Red lines represent median intensity of > 65 telomeres per condition. Statistical analysis performed using two tailed t test; \*  $P < 0.05$ . Mann-Whitney tests show a significant increase in telomere intensity in TAF compared to non-TAF  $P < 0.05$ .

Hitherto, the irradiation model has been used as a proof-of-principle for the existence and persistence of TAF in both embryonic cardiomyocytes and H9C2 rat-derived cardiomyocytes. However, we wanted to ascertain if TAF could be induced, irrespective of DNA replication, with a more physiologically relevant model of oxidative stress i.e. via hydrogen peroxide exposure. Using the same experimental plan from above (Figure 3-4A), instead of X-irradiation, we cultured H9C2 cells in EdU for 3 hours, and then exposed them to 10 $\mu$ M H<sub>2</sub>O<sub>2</sub> for 2 hours, followed by a further culture in the presence of EdU for 24 hours. Similarly to exposure with 10Gy IR, we observed a significant decrease in the percentage of cells which underwent DNA replication following treatment with H<sub>2</sub>O<sub>2</sub> (Figure 3-5B). Moreover, the mean number of TAF is significantly increased in EdU negative H9C2 cells 24 hours after treatment with H<sub>2</sub>O<sub>2</sub> (Figure 3-5C).

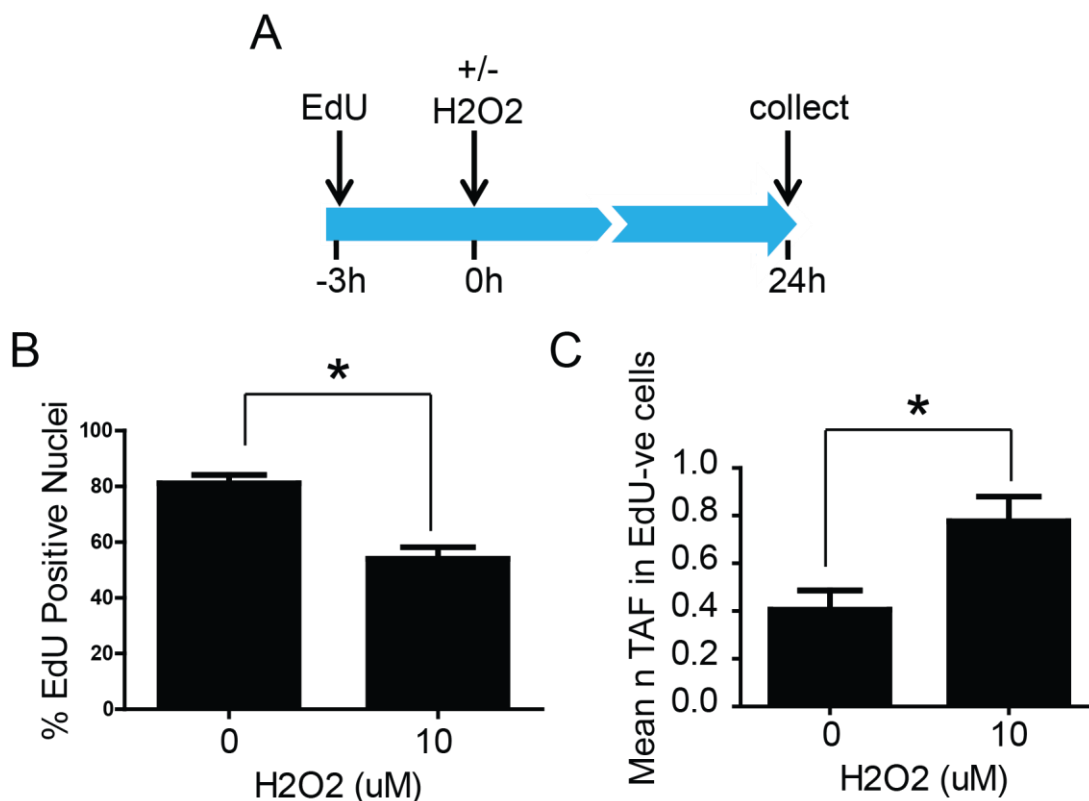


**Figure 3-5. TAF are Induced Independently of DNA Replication in H<sub>2</sub>O<sub>2</sub>-treated H9C2 Cells.** (A) Schematic illustration showing H9C2 cells were incubated in 10 $\mu$ M EdU in normal growth medium for 3 hours, followed by X-irradiation with 10Gy and cultured for a further 24 hours in the presence of 10 $\mu$ M EdU in normal growth medium. (B) Mean percentage of EdU positive cells. Data are mean  $\pm$  SEM of  $n=3$ . (C) Mean number of TAF in EdU negative cells, 24 hours after 10Gy IR. Data are mean  $\pm$  SEM of  $n=3$ . Statistical analysis performed using two tailed t test; \*  $P<0.05$ .

### 3.4 TAF Induce Senescence *in vitro*

Research has shown that SA- $\beta$ -Gal activity, an established marker of senescence, becomes elevated in H9C2 cardiomyocytes 3 days after exposure with either oxidative stress or genotoxic stress (Spallarossa *et al.*, 2009; Dong *et al.*, 2013). Our data show that SA- $\beta$ -Gal activity also becomes elevated in the majority of H9C2 cells, 3 days following exposure to 10Gy X-irradiation (Figure 3-6A-B). However, these interventions cause DNA damage in a non-specific manner, resulting in elevated levels of both TAF and non-TAF, both of which have been implicated in driving senescence (Nakamura *et al.*, 2008). We sought to determine if DSBs specifically at telomeres could induce senescence in cardiomyocytes. To achieve this, we acquired a FLAG-tagged expression plasmid (TRF1-FokI), encoding an endonuclease (FokI) conjugated to the shelterin component TRF1. FokI non-specifically cleaves DNA adjacent to its recognition site (Sugisaki and Kanazawa, 1981), and thus, when conjugated to TRF1, FokI can induce DSBs specifically in telomeric DNA. As a control, we used a point-mutated expression plasmid (TRF1-FokI-D450A), with a loss of function in endonuclease activity. We transfected H9C2 cells with either TRF1-FokI or TRF1-FokI-D450A, and cultured them for 4 days. Immuno-FISH analysis revealed an induction of both  $\gamma$ H2AX DDF and 53BP1 DDF in TRF1-FokI transfected cells, with the vast majority of DDF co-localising with telomeres (Figure 3-7A-B). We performed Q-FISH to analyse the length of telomeres co-localising with a DDF ( $\gamma$ H2AX+/53BP1+) compared to those that were not ( $\gamma$ H2AX-/53BP1-). Our analysis revealed that TRF1-FokI-induced double-strand cleavage of telomeres occurred independently of telomere length, as the distribution of telomere length was the same for DDF+ telomeres compared to DDF- telomeres, for both  $\gamma$ H2AX or 53BP1 DDF (Figure 3-7C).

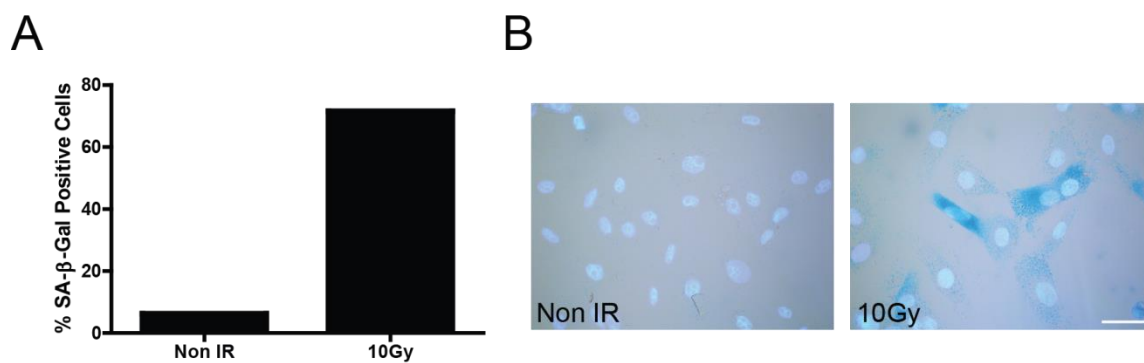


**Figure 3-6. X-Irradiation induces Senescence in H9C2 Cardiomyocytes. (A)** Percentage of SA-β-Gal positive cells in H9C2 cells at 3 days following 10Gy IR. Data are for a representative experiment. **(B)** Representative images of SA-β-Gal staining (light blue – DAPI; darker cytoplasmic blue - SA-β-Gal). Scale bar: 30μM.

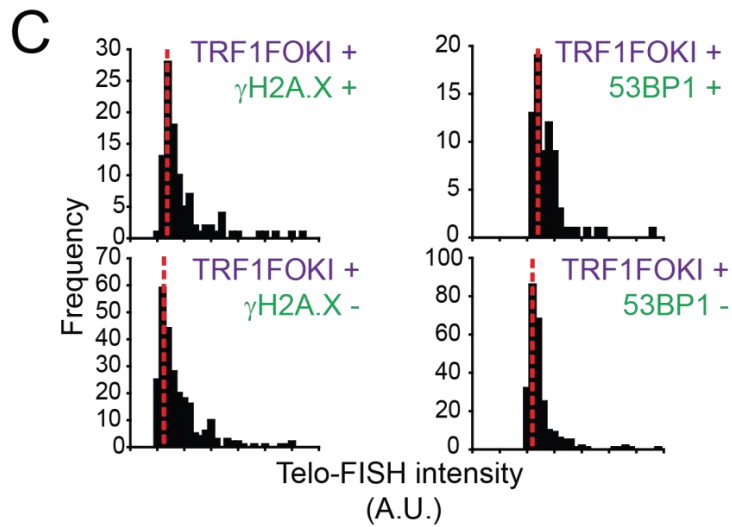
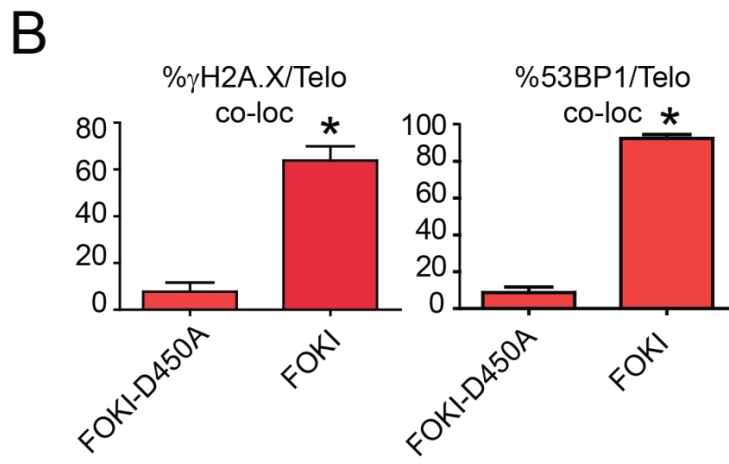
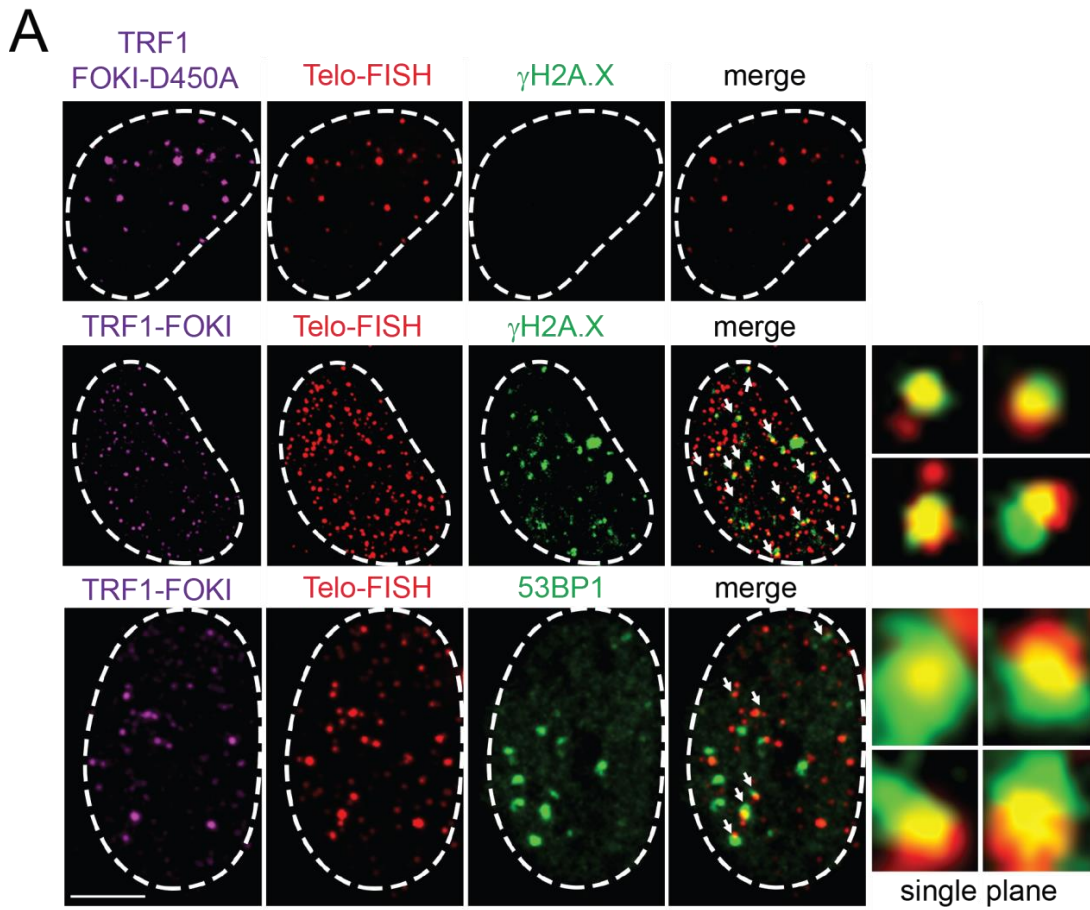


**Figure 3-7. TRF1-FokI Fusion Protein Induces Telomere Specific Double Strand Breaks.** **(A)** H9C2 cells 4 days following transfection with a FLAG-tagged TRF1-FokI-D450A (top row) or TRF1-FokI (middle and bottom row) fusion protein (purple – FLAG; red – telo-FISH; green –  $\gamma$ H2AX or 53BP1). Images are z projections of 0.1 $\mu$ M stacks taken with 100X objective. White arrows indicate co-localisation between telomeres and  $\gamma$ H2AX/53BP1, with co-localising foci amplified in the right panels (taken from single z planes where co-localisation was found). Scale bar: 5 $\mu$ M. **(B)** Graphs represent the percentage of  $\gamma$ H2AX (left) or 53BP1 (right) foci co-localising with telomeres 4 days following transfection with either a TRF1-FokI-D450A or TRF1-FokI fusion protein. Data are mean  $\pm$  SEM of  $n=3$ . **(C)** Histograms displaying telomere intensity for telomeres co-localising (bottom) or not co-localising (top) with  $\gamma$ H2AX (left) or 53BP1 (right) DDR foci for H9C2 cells 4 days following transfection with TRF1-FokI fusion protein. Red dotted lines represent median  $> 60$  telomeres per condition. Statistical analysis performed using two tailed t test; \*  $P<0.05$ . Mann-Whitney tests show no significant difference in telomere intensity between TAF and non-TAF, with either  $\gamma$ H2AX (left) or 53BP1 (right) DDR foci.

Previous research has shown that fibroblasts transfected with a dominant-negative TRF2 (TRF<sup>2 $\Delta$ B $\Delta$ M</sup>), elicit a DDR at telomeres and undergo cellular senescence (Takai *et al.*, 2003). This model provides insights into the effects of telomere uncapping, but hitherto, it is unknown whether DSBs specifically at telomeres can drive cellular senescence. Having shown the specificity of the TRF1-FokI fusion protein to induce telomere-specific DSBs (Figure 3-7A-B), we transfected H9C2 cells with either TRF1-FokI or TRF1-FokI-D450A, cultured them for 4 days, and then assessed various senescence markers. Our analysis revealed that H9C2 cells expressing the TRF1-FokI fusion protein had a significantly reduced percentage of cells positive for the proliferation marker Ki-67, an increased cell size, and a significant increase in the percentage of cells positive for both the cyclin-dependent kinase inhibitor p21, and SA- $\beta$ -Gal activity (Figure 3-8A-E).

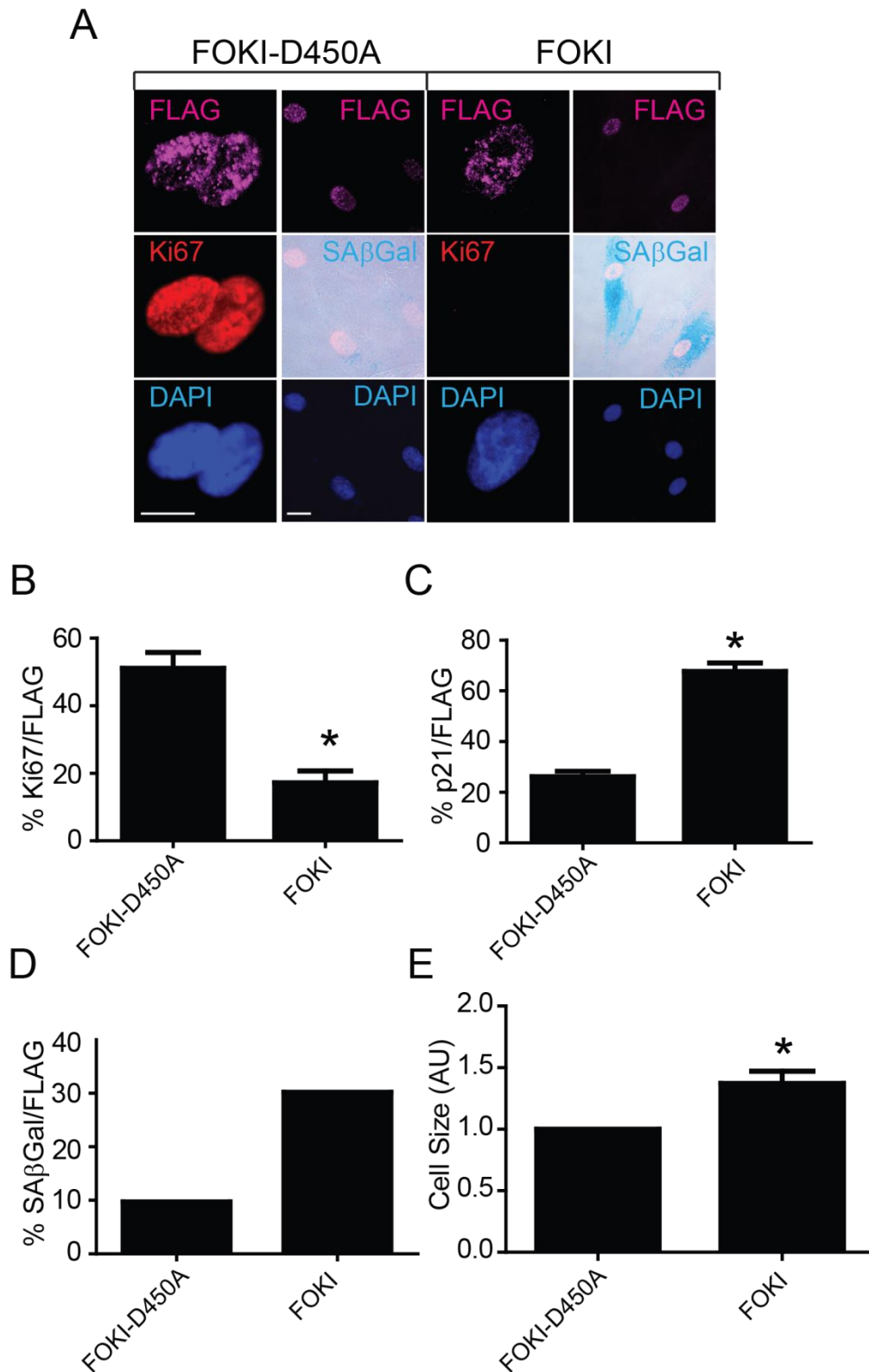


**Figure 3-8. Double Strand Telomeric Breaks Drive Cellular Senescence in H9C2 Cardiomyocytes.** **(A)** Representative images of senescent markers in H9C2 cells 4 days following transfection with either TRF1-FokI-D450A or TRF1-FokI fusion protein (purple – FLAG; red – Ki-67; light blue – DAPI; darker cytoplasmic blue – SA-β-Gal). Scale bars: left panel - 10μM; right panel 20μM. **(B)** Quantification of mean percentage of FLAG-positive cells stained positive for Ki-67. Data are mean ± SEM of  $n=3$ . **(C)** Quantification of mean percentage of FLAG-positive cells stained positive for p21. Data are mean ± SEM of  $n=3$ . **(D)** Quantification of mean percentage of

FLAG-positive cells stained positive for SA- $\beta$ -Gal activity. Data are mean  $\pm$ s.e.m of  $n=3$ . Data are presented as mean of  $>100$  cells representative of 1 experiment. Two independent experiments confirmed these findings (not shown). **(E)** Quantification of mean cell size of FLAG-positive cells. Data are mean  $\pm$  SEM of  $n=3$ . Statistical analysis performed using two tailed t test; \*  $P<0.05$

### 3.5 Does Genomic Stress Induce Telomere Uncapping?

Telomere dysfunction can be induced via a number of genotoxic stresses (Hewitt *et al.*, 2012), however the mechanism for the induction of a DDR at telomeres which are not critically short is not yet fully understood. The previous model of endonuclease-induced telomeric damage provides interesting insights into the effects of DSBs at telomeres, but cannot be considered a physiological representation of the induction of telomere dysfunction. As previously mentioned, there are two proposed theories for the generation of telomere dysfunction in non-critically short telomeres. Our group proposed that genomic stress leads to DSBs within telomeric regions, which are irreparable and lead to persistent telomere dysfunction (Hewitt *et al.*, 2012). Moreover, another group suggested that uncapping of telomeres, which still retain enough shelterin proteins to inhibit NHEJ, could elicit a persistent DDR at telomeres (Cesare, Kaul *et al.* 2009). To address this, we utilised the resolving power of super-resolution fluorescence imaging, specifically: stochastic optical reconstruction microscopy (STORM), to visualise t-loop structures after X-irradiation, a model which has shown to induce persistent DDR foci at telomeres (Hewitt *et al.*, 2012).

To optimise conditions for STORM imaging, we first visualised telomeres of proliferating untreated paraformaldehyde-fixed MEF cells. Telomeres were visualised using FISH with a telomere-specific PNA probe conjugated to a photo-switchable dye (TelC-Cy5). Merged images comparing conventional confocal microscopy against STORM imaging show an enhanced resolution of telomere signal with STORM imaging (Figure 3-9A).

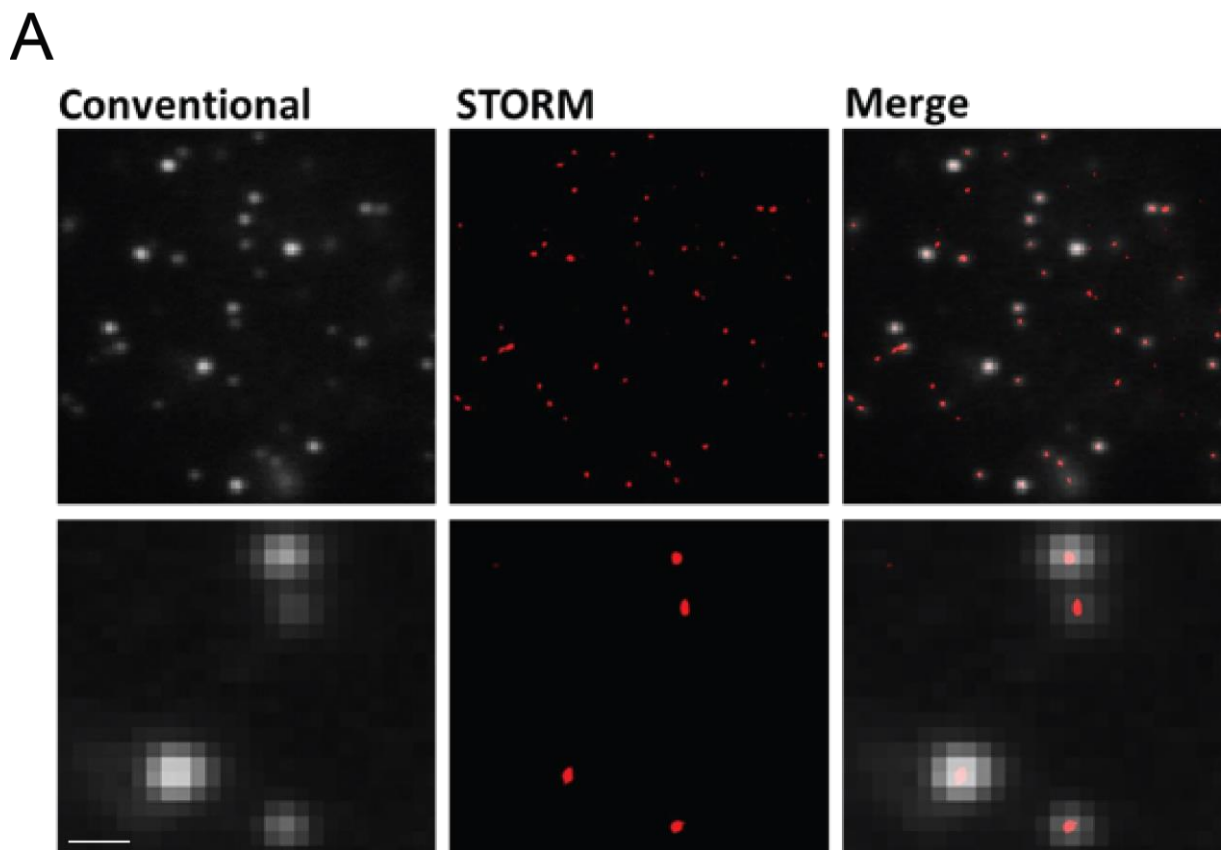


**Figure 3-9. STORM Microscopy Enhances Resolution of MEF Telomeres compared to Conventional Confocal Microscopy. (A)** Untreated MEFs were fixed on coverslips, and telomeres were detected using FISH with a telomere specific PNA probe conjugated to a photoswitchable dye (TelC-Cy5). Images represent MEF telomeres visualised with conventional confocal microscopy and STORM imaging at 100X objective. Lower panels display an amplification of an area of the above image. Scale bar: 0.5 $\mu$ M.

Having optimised experimental conditions for the utilisation of the TelC-CY5 PNA probe for use with STORM imaging, we next performed chromatin spreads to orientate telomeres in a way which the t-loop can be visualised by STORM imaging. We show that the t-loop structure can be visualised with STORM imaging, however not with conventional confocal microscopy (Figure 3-10A-B). Previous experimentation has shown that conventional confocal microscopy does not have the resolving power to visualise the t-loop structure (Doksani *et al.*, 2013).

We then quantified the percentage of t-loops in telomeres from MEFs which were untreated, compared to those which had been treated with 10Gy IR. In untreated MEFs, we observed that slightly under 25% of all telomeres presented a t-loop structure, and there was no significant difference in the percentage of telomeres with t-loops 3 days following X-irradiation with 10Gy (Figure 3-10C). These data would

suggest that telomere dysfunction is not dependent upon t-loop uncapping, although there are some experimental caveats which prevent the firm assumption of this conclusion, which will be discussed later on.

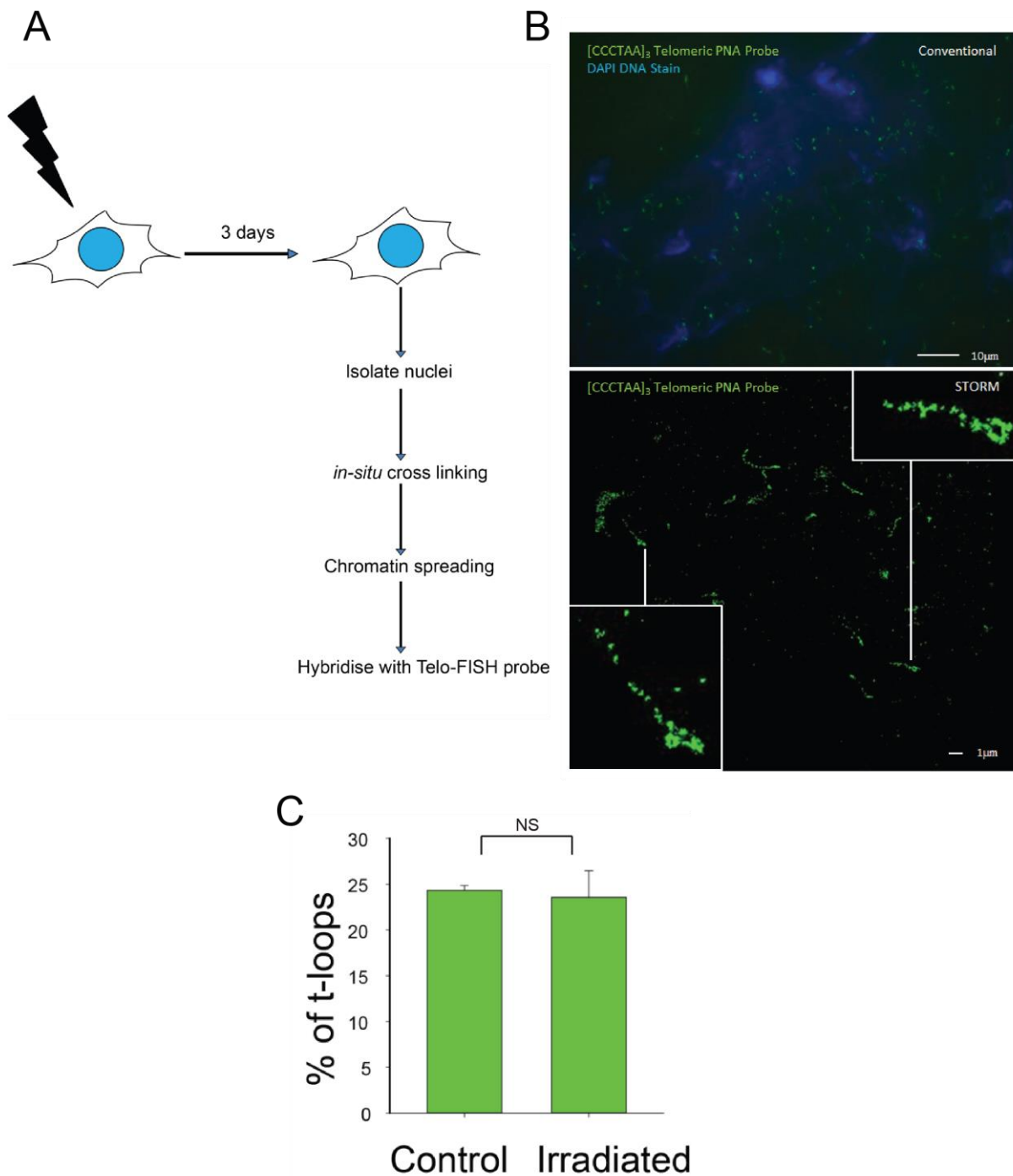


**Figure 3-10. 10Gy X-Irradiation does not alter the Percentage of t-loops in Chromatin Spreads of MEF Nuclei.** (A) MEFs were irradiated with 10Gy and incubated for 3 days. Nuclei were then isolated, followed by *in situ* cross-linking with psoralen, chromatin spreading, and telomeres were detected by FISH with a

telomere specific PNA probe conjugated to a photoswitchable dye (TelC-Cy5), before STORM imaging. **(B)** (Top Panel) Representation of chromatin-spread telomeres (green) and DAPI (blue) via conventional confocal microscopy with 100X objective. (Bottom Panel) Representation of chromatin-spread telomeres (green) via STORM imaging with 100X objective. **(D)** Percentage of t-loops in 10Gy irradiated MEF cells. Data are mean  $\pm$  SEM of  $n=3$ . Statistical analysis performed using two tailed t test; NS (Non-significant)  $P>0.05$ .

### 3.6 Discussion

For some time after the discovery of telomeres, an understanding of the mechanism which prevented telomeres from undergoing end-to-end fusion remained elusive. Research finally emerged which showed that fibroblasts transfected with a dominant-negative TRF2 became susceptible to end-to-end fusions (van Steensel *et al.*, 1998). Soon after, it was discovered that TRF2 could drive the formation of the t-loop structure in isolated telomere fragments *in vitro*, thus physically sheltering the ends of telomeres (Griffith *et al.*, 1999). Research then showed that NHEJ in de-protected telomeres was dependent on DNA ligase IV (Smogorzewska *et al.*, 2002). More recently, it was shown via STORM imaging that TRF2 was essential for the formation of t-loops in MEFs *in vitro* (Doksani *et al.*, 2013). The t-loop therefore provides an elegant mechanism to protect the ends of chromosomes from being recognised by the DDR machinery, however, evidence is emerging which suggests that the mechanisms which protect chromosome ends from being recognised as DNA damage, and inhibit end-to-end fusion, could be preventing telomeric DNA repair from stochastic DNA damage. Moreover, it was published that cells exposed to X-irradiation, or other genotoxic stresses such as hydrogen peroxide or neocarzinostatin were able to repair non-telomeric DNA damage, however telomere damage was irreparable, therefore resulting in a persistent DDR at telomeres (Hewitt *et al.*, 2012). Another striking observation was that Q-FISH analysis showed that telomere dysfunction in murine enterocytes and hepatocytes was occurring independently of telomere length *in vivo* (Hewitt *et al.*, 2012). A possible explanation for this phenomenon has been proposed by our group and another, which suggests that a persistent DDR could be elicited at telomeres due to the presence of a physical DSB, which remains irreparable due to the inhibitory effect of the shelterin complex on the DDR machinery (Fumagalli *et al.*, 2012; Hewitt *et al.*, 2012). This idea is supported by data showing that ectopic expression of the shelterin protein TRF2 next

to a DSB within non-telomeric DNA leads to an inhibition of repair and a prolonged DDR (Fumagalli *et al.*, 2012). However, another proposed models suggest that telomere uncapping could be induced in long telomeres due to inhibition of TRF2 (Cesare *et al.*, 2009), and interestingly, oxidative stress has been shown to disrupt the ability of both TRF1 and TRF2 to recognise telomeric DNA (Opresko *et al.*, 2005). Furthermore, TRF2 has also been shown to localise to genomic DSB following X-irradiation (Bradshaw *et al.*, 2005). Together, these data provide evidence that oxidative stress can result in a reduction of shelterin components at telomeres, thus adding credence to the idea that a DDR at long telomeres could be due to inhibition of TRF2 and subsequent uncapping, independently of a DSB. Whilst further research is required to fully ascertain the mechanism leading to telomere damage in non-critically short telomeres, these observations that telomere length-independent damage can occur, suggest that telomere dysfunction might also affect non-proliferative cell types. We sought to ascertain if the phenomenon of telomere irreparability was unique to proliferative cells such as fibroblasts, or whether non-rapidly dividing cells, could also be subject to persistent telomeric damage. To begin, we isolated mouse embryonic cardiomyocytes and exposed them to X-irradiation. Our data showed that there is an initial increase in both telomeric damage and genomic damage following IR, however with time, the majority of genomic damage is repaired, yet the telomeric damage remains unaltered, leading to an enrichment of the percentage of total damage co-localising with telomeres over time. Furthermore, there was no significant change in the percentage of cells positive for TAF over the time course of the experiment, suggesting that once a cell acquires a TAF, it is persistent. These data confirmed that mouse embryonic cardiomyocyte TAF are also persistent upon stress-induced damage, as previously shown in both mouse and human fibroblasts (Hewitt *et al.*, 2012). To validate our findings in another cell model, we used H9C2 rat-derived cardiomyocytes and performed the same experiment and analysis, which revealed similar results; persistent telomeric damage following IR. A persistent DDR has previously been shown to activate p21, which in turn causes mitochondrial dysfunction and aberrant ROS generation, which can lead to further DNA damage, thus initialising a feedback loop (Passos *et al.*, 2010). Therefore, it could be hypothesised that, although TAF persistence over the course of several days following IR would imply irreparability, TAF numbers could potentially be maintained by a feedback loop resulting in a balanced flux between induction an repair, however evidence suggests that only short-lived DDF are generated as a

result of senescence-associated ROS *in vitro* (Passos *et al.*, 2010). To test this in cardiomyocytes, live-cell time-lapse microscopy was used, and H9C2 cells were transfected with the fusion protein AcGFP-53BP1c, to allow foci dynamics to be tracked in real-time. Our group have previously published, using a AcGFP-53BP1c fusion protein, coupled with microbead-mediated incorporation of a fluorescent telomere specific PNA probe, that all persistent DDR foci over the course of several hours co-localise with telomeres, whereas those DDR foci not co-localising with telomeres are transient (Hewitt *et al.*, 2012). We had initially planned to emulate this experiment using microbead-mediated incorporation of a PNA probe, however sensitivity of the H9C2 cells to the microbeads resulted in considerable cell death. We therefore transfected H9C2 cells with AcGFP-53BP1c alone, and tracked DDR foci in H9C2 cells, 72 hours after 10Gy IR, every 10 minutes for 10 hours. We observed that the majority of DDR foci are resolved within 8 hours, however a repair plateau is reached at this point, with around 20% of the foci persistent throughout. Our data in fixed cells show that at the same time point of 3 days following 10Gy IR, around 15% of DDR foci co-localise with telomeres in H9C2 cells. Our observations in both fixed cells and live-cells complement one another to suggest that X-irradiation can induce irreparable TAF in H9C2 cardiomyocytes.

One mechanism for the induction of double strand breaks involves replication errors from the DNA replication machinery, when replication forks encounter single strand breaks in the genome (Kuzminov, 1999). However, the relevance of this in the context of cardiomyocytes *in vivo* is questionable, as the proliferation rates of cardiomyocytes is negligible, with estimates suggesting that 60% of cardiomyocytes present in humans at birth, still remain at 50 years of age (Bergmann *et al.*, 2009). Furthermore, evidence now suggests that mouse cardiomyocytes can undergo proliferation, however estimates suggest the rate to be less than around 4% per year in young adult mice, which decreases significantly with age (Malliaras *et al.*, 2013; Senyo *et al.*, 2013), therefore suggesting that replication-associated telomere shortening is not a major factor in both mouse and human cardiomyocytes. We therefore wanted to investigate if TAF could be induced in cardiomyocytes independently of DNA replication. Our data show that X-irradiation can induce TAF in cardiomyocytes that have not undergone DNA replication, as evident by an increase of TAF in cells which did not incorporate the thymidine analogue EdU following IR. X-irradiation is a useful tool for inducing double strand breaks within the genome,

however it cannot be considered a physiologically relevant model. To address this, we investigated if TAF could also be induced with H<sub>2</sub>O<sub>2</sub> exposure. One group have observed an age-dependent increase in cardiac mitochondrial H<sub>2</sub>O<sub>2</sub> production (Judge *et al.*, 2005), thus H<sub>2</sub>O<sub>2</sub> treatment more closely emulates physiological endogenous oxidative stress. Our data show, that similarly to IR, TAF can be induced independently of replication with H<sub>2</sub>O<sub>2</sub> treatment.

Telomere dysfunction has previously been shown to play a role in driving cellular senescence and apoptosis in H9C2 cardiomyocytes. Moreover, low level TRF2 down-regulation by siRNA induced cellular senescence, whereas high concentrations of TRF2 siRNA led to apoptosis (Spallarossa *et al.*, 2009). TRF2 is the quintessential shelterin component in t-loop formation, and thus downregulation will lead to uncapping of telomeres and a persistent DDR (Doksani *et al.*, 2013). Telomere uncapping, as a consequence of steric constraints on the t-loop structure, seems unlikely in cardiomyocytes, so we therefore investigated if physical DSBs within telomere regions could induce senescence in these cells. By transfecting cells with an expression plasmid encoding a TRF1-FokI fusion protein, we were able to induce DSBs specifically in telomeric regions, which resulted in H9C2 cells displaying various characteristics of senescence, including elevated SA-β-Gal activity and p21 expression, increased cell size, and a decrease in the percentage of cells positive for the proliferation marker Ki-67. The physiological relevance of permanent cell cycle arrest in a cell which is unlikely to ever divide is questionable, however other aspects of the senescent-phenotype could potentially be detrimental to the surrounding tissue. Moreover, research has shown that senescent cells secrete a number of factors which can elicit a bystander effect, capable of inducing DNA damage and even senescence on neighbouring cells (Hubackova *et al.*, 2012a; Nelson *et al.*, 2012; Acosta *et al.*, 2013).

It will be important to understand the threshold of TAF required for inducing senescence, not only in cardiomyocytes, but in other cell types as well. Using the transient expression plasmid used for this investigation, one cannot control the number of cleavage events induced by the TRF1-FokI fusion protein. To address this, future research should focus on cloning the fusion protein into an inducible system in which expression can be turned on and off, thus being able to manipulate the length of time the fusion protein is expressed for. Our data also showed that the percentage of DDF in TRF1-FokI cells which co-localised with telomeres was not

100%, and therefore prevents assumptions to be made solely on the telomere-specific contribution to senescence, especially considering that both telomeric and non-telomeric DDF have been shown to contribute to cellular senescence (Nakamura *et al.*, 2008). Explanations for the lack of specificity could be due to the endonuclease cleaving genomic DNA prior to TRF1 binding to telomeres, or even once bound, cleaving genomic DNA which is spatially near. In the latter case, there would be no solution other than creating an endonuclease which only cleaved telomeric repeats, however, this could also be compromised because the telomere repeat sequence has been shown to appear in interstitial chromosomal locations in multiple vertebrate species, including humans (Meyne *et al.*, 1990; Weber *et al.*, 1990; Azzalin *et al.*, 1997; Ruiz-Herrera *et al.*, 2002). However, another explanation could be that the TRF1-FokI specifically cleaves telomeres, and the non-telomeric DDF arise due to elevated ROS, by a mechanism such as the aforementioned senescence-associated feedback loop (Passos *et al.*, 2010), in which case, studying the nature of telomere-specific dysfunction would require inhibition of the pathway to prevent non-specific ROS induced genomic damage, which would paradoxically effect the induction of cellular senescence.

Our data show that the TRF1-FokI fusion protein cleaves telomeres independently of telomere length. However interestingly, Q-FISH analysis of telomere length in H9C2 cells revealed that longer telomeres are more susceptible to IR-induced damage. If one assumes that ionising photons are striking the genome stochastically, probability suggests that longer telomeres are more likely to endure damage. As previously described, the mechanism of stress-induced telomere dysfunction has yet to be conclusively elucidated. It is possible that stress-induced DSBs occur and the repair is inhibited by the shelterin complex (Hewitt *et al.*, 2012), or alternatively, that stress destabilises the t-loop, leading to uncapping and a persistent DDR. Furthermore, both may occur independently, or the DDR signal from DSBs could even cause uncapping, by a yet unknown mechanism. To investigate this, we utilised the resolving power of STORM imaging, to visualise t-loop structures. Initially, we sought to couple the chromatin spread technique with immuno-staining for DDR proteins, such as  $\gamma$ H2AX, to discover whether t-loops could be maintained in the presence of a DDR. Alas, we could not couple these two techniques together, potentially due to the chromatin isolation procedure leading to the dissociation of DNA-bound proteins. If the technique had worked, I would have been able to investigate if a DDR can exist

in the presence of a t-loop. Although, if we were to have observed a DDR in the presence of t-loops, this would not have proven *ipso facto* that t-loops can be maintained in the presence of double-strand breaks, as DDR signals are known to spread up to several megabases (Rogakou *et al.*, 1999; Meier *et al.*, 2007; Iacovoni *et al.*, 2010), and thus the physical break could be occurring elsewhere in the genome. Contrary to this, if all observed telomeres co-localising with a DDR were uncapped, this would provide strong evidence that a DDR induces uncapping.

Our group have previously published that X-irradiation induces TAF in MEF cells (Hewitt *et al.*, 2012). To determine if X-irradiation leads to uncapping, we quantified the percentage of t-loops in 10Gy X-irradiated compared to untreated MEFs. Our data show that there is no significant difference in the percentage of t-loops after 10Gy irradiation, suggesting that X-irradiation induces persistent double strand breaks in telomeric regions independently of telomere uncapping. Unfortunately, the sensitivity of the technique is limited so that such conclusions cannot be asserted. Moreover, the procedure requires cross-linking of the DNA with psoralen, which has an efficiency of around 1 in 400 base pairs; considering the 3' overhang is on average 100 base pair (McElligott and Wellinger, 1997), this means that only 25% of capped telomeres would remain stabilised. Furthermore, previous data from our group shows that 10Gy X-irradiation only induces around 5 TAF per nuclei (Hewitt *et al.*, 2012), which accounts for just 6.3% of the total telomeres, assuming a total telomere count of 80. Therefore, even if all 5 were truly uncapped, the percentage of t-loops would be  $((80-5)*0.25)/80= 23.4375\%$ , which compared to 25% is still within the margin of standard error, and therefore inconclusive. It would be interesting to repeat these experiments in a model of significantly higher telomere dysfunction to conclusively elucidate if stress-induced telomere dysfunction is associated with destabilisation of the t-loop structure. The TRF1-FokI system could also be utilised to determine if t-loops remain stabilised in the presence of a telomeric DSB. This distinction could be important considering it has been shown that the downstream response pathway for telomere dysfunction is distinct from the genomic DNA damage response (Cesare *et al.*, 2013), and thus understanding the distinction between TIF and TAF may prove important in the event that the downstream DDR mechanisms vary. For example, it has been shown in human fibroblasts that as little as 5 TIF predicts the onset of senescence in human fibroblasts (Kaul *et al.*, 2012), however this may not be the case for TAF.

In summary, our data show that telomere dysfunction can be induced in cardiomyocyte cell models, and this damage can arise independently of DNA replication. Together, these observations suggest that telomere damage doesn't arise solely as a result of telomere-attrition driven uncapping of the t-loop, and that long telomeres are also susceptible to telomere dysfunction. Consequently, this suggests that telomere dysfunction can occur in post-mitotic and non-rapidly dividing cells which aren't subject to persistent end-replication associated shortening. Finally, we provide evidence that DSBs within telomere regions, regardless of telomere capping state, can drive senescence in cardiomyocyte cells *in vitro*.

## 4 Effect of Ageing on Telomere Dysfunction in Cardiomyocytes *in vivo*

In the previous chapter, we demonstrated that TAF can be generated in cardiomyocytes *in vitro*, and that this telomere dysfunction can occur independently of DNA replication. Our group have previously shown TAF accumulate with age in mouse hepatocytes and enterocytes *in vivo*, and that this damage occurs independently of telomere length (Hewitt *et al.*, 2012). These observations of TAF occurring independently of DNA replication and telomere shortening, made us question if a post-mitotic or non-rapidly dividing cell type could also be subject to telomere dysfunction *in vivo*. Hitherto, most studies which link telomeres to cardiac ageing analyse telomere shortening rates in circulating leucocytes (Haycock *et al.*, 2014; Masi *et al.*, 2014). Whilst this provides a good proxy for systemic organismal ageing, and often provides significant predictions to cardiac pathology, the method remains strictly correlative. We therefore investigated telomere dysfunction specifically in cardiomyocytes *in vivo*.

For years, it was thought that cardiomyocytes had no proliferation potential at all, and the entirety of a mammalian's cardiomyocyte life-time cell population would be present at birth, and thus, the physiological relevance of permanent cell cycle arrest would seem insubstantial. However, analysis of carbon-14 levels of cardiomyocyte DNA in people exposed to nuclear bomb tests during the Cold War revealed that cardiomyocyte renewal occurs in humans (Bergmann *et al.*, 2009). Furthermore, evidence shows that the cardiomyocytes themselves, as opposed to a stem-cell population, are capable of self-renewal during normal ageing; a process which is increased in areas adjacent to myocardial stress (Malliaras *et al.*, 2013; Senyo *et al.*, 2013). Besides proliferation cessation, senescent cells have also been shown to display a Senescence-Associated Secretory Phenotype (SASP), a secretory signalling response thought to attract immune cells to clear senescent cells (Coppé *et al.*, 2008; Rodier *et al.*, 2009). However, senescence clearance capability is thought to deteriorate with the age-associated decline in immune-system function, thus resulting in senescent cell persistence and a continuous SASP (Janko, 2008; Wang *et al.*, 2011). Furthermore, the SASP has been demonstrated to elicit a bystander effect, which can cause DNA damage and even induce cellular senescence in neighbouring cells (Kosar *et al.*, 2011; Nelson *et al.*, 2012; Acosta *et*

*al.*, 2013). This is of interest, as evidence now suggests that cellular senescence isn't a phenomenon confined only to proliferative cells. A significant percentage of purkinje, cortical, hippocampal and peripheral neurons from aged mice have been reported to elicit many features of cellular senescence, namely: high ROS production and oxidative damage, activated p38MAPkinase, high levels of DNA damage, heterochromatinisation, interleukin IL-6 production and SA- $\beta$ -Gal activity (Jurk *et al.*, 2012). Interestingly, these features were highly elevated in late-generation TERC<sup>-/-</sup> mice, suggesting that telomere dysfunction could be driving a senescent-like phenotype in these cells. These effects were rescued in TERC<sup>-/-</sup>CDKN1<sup>-/-</sup> mice, suggesting that telomere dysfunction leads to a senescent-like phenotype via p21 activation (Jurk *et al.*, 2012).

In the previous chapter we showed that cardiomyocytes can elicit a persistent DDR at telomeres which can drive senescence *in vitro*, however it is unknown if persistent telomere dysfunction occurs in cardiomyocytes *in vivo* and if they are associated with senescence.

To our knowledge, no studies have looked at telomere dysfunction occurring in cardiomyocytes specifically *in vivo*, and thus the aim was to investigate this, and if this is associated with cardiomyocyte cellular senescence.

#### **4.1 X-irradiation Induces TAF in Mouse Cardiomyocytes *in vivo***

In the previous chapter, we showed that X-irradiation induced TAF were persistent *in vitro* in mouse embryonic cardiomyocytes and H9C2 rat-derived cardiomyocytes. We then wanted to investigate if TAF could be induced in cardiomyocytes *in vivo* and if this damage was persistent. 1 month old mice were exposed to 2Gy whole body X-irradiation, followed by an 11 month recovery period, before culling at 12 months of age. We observed a significant increase in the mean number of cardiomyocyte TAF in X-irradiated mice compared to the untreated controls (Figure 4-1A-B).

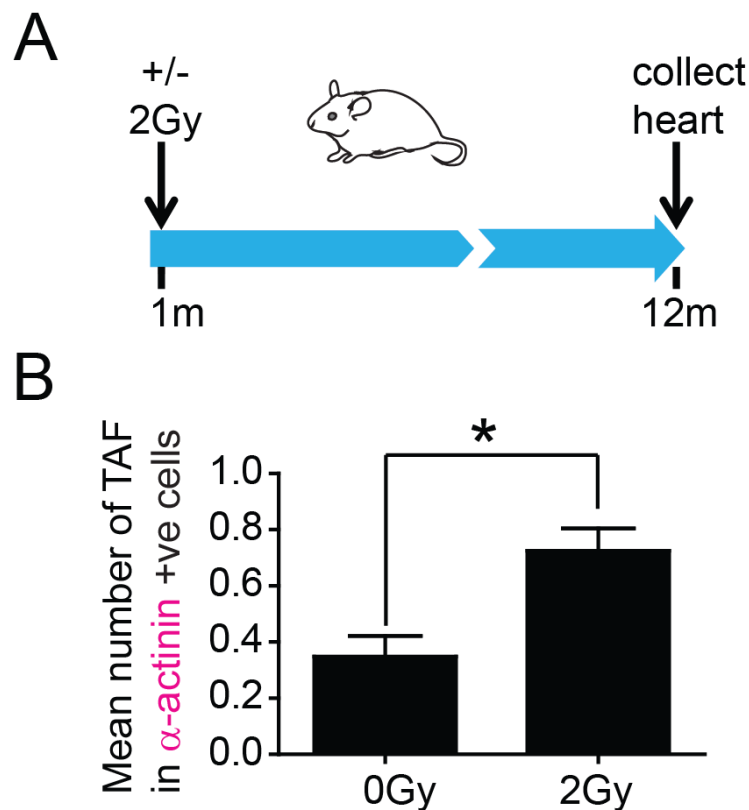


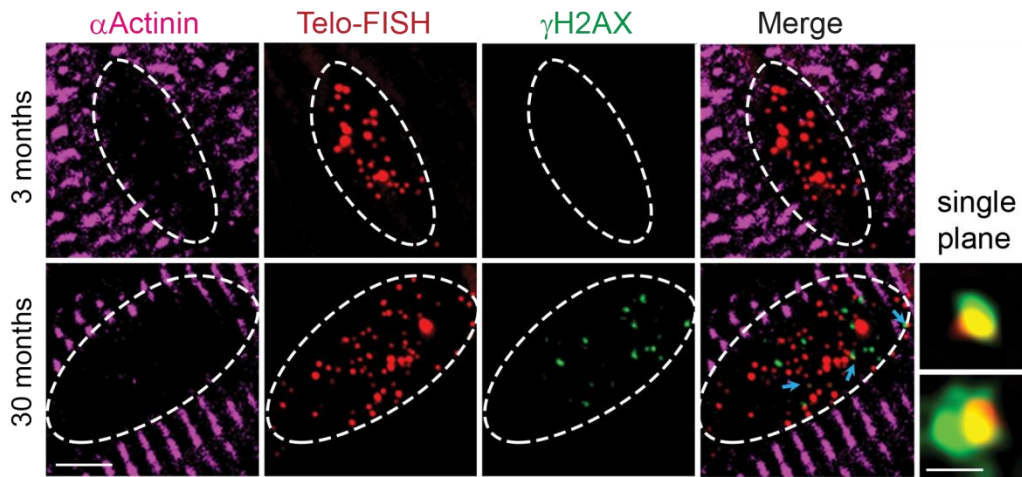
**Figure 4-1. Whole body X-irradiation Induces TAF in Mouse Cardiomyocytes.** (A) 1 Month old mice were treated with 2Gy whole body irradiation, followed by a recovery period of 11 months before culling at 12 months of age. (B) Mean number of TAF in  $\alpha$ -actinin positive cardiomyocytes. Data are mean  $\pm$  SEM of  $n=3$ . Statistical analysis performed using two tailed t test; \*  $P<0.05$ .

#### 4.2 TAF Increase in Mice Cardiomyocytes with Age Independently of Telomere Length

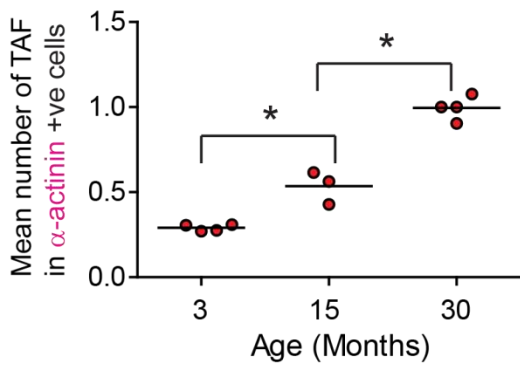
Telomere dysfunction is considered a biomarker for cellular senescence, and has been shown to accumulate with age in various tissues in a range of different organisms from mice to primates (Herbig *et al.*, 2006; Hewitt *et al.*, 2012). Having observed that TAF can be induced in mouse cardiomyocytes by X-irradiation, in collaboration with Clara Correia-Melo from ours and the von Zglinicki laboratory, we then investigated if TAF could occur in mouse cardiomyocytes *in vivo*, and if there was an age-dependent accumulation of telomere dysfunction. Quantifying only  $\alpha$ -actinin positive cardiomyocytes, we observed an age-dependent increase in both the mean number of TAF and the mean percentage of cardiomyocytes positive for TAF (Figure 4-2A-C). However, when we quantified the number of non-TAF, we found no significant changes with age (Figure 4-2D-E) To validate the observation that a DDR could occur at cardiomyocyte telomeres, in collaboration with Jelena Mann, we

performed chromatin-immuno precipitation for  $\gamma$ H2AX on whole ground frozen hearts, followed by quantitative real-time PCR for the detection of telomeric repeats. We observed a non-significant trend towards an enrichment of  $\gamma$ H2AX at telomeric regions from 3 to 30 months of age (Figure 4-2F).

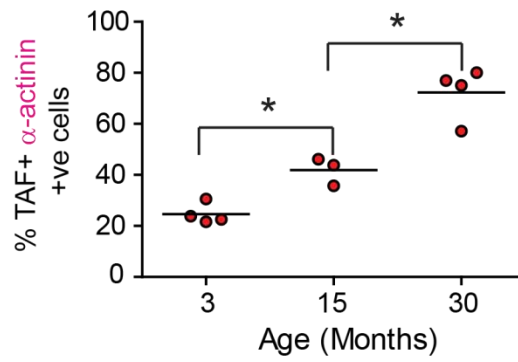
A



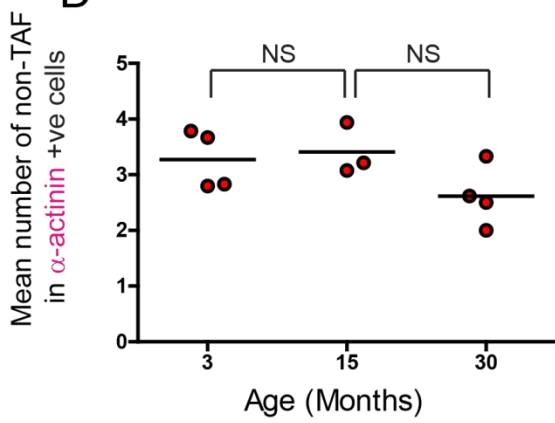
B



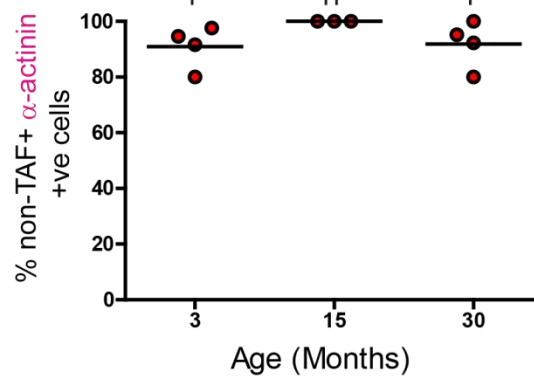
C



D



E



F

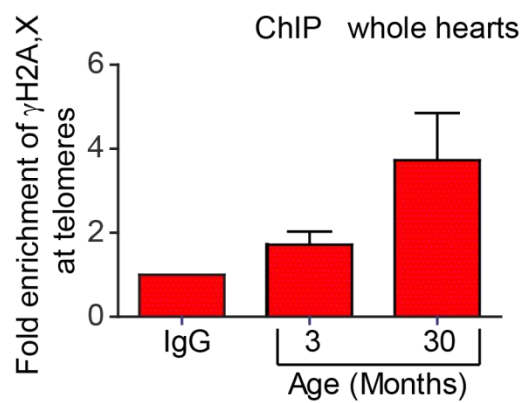


**Figure 4-2. TAF Accumulate with Age in Mouse Cardiomyocytes.** **(A)** Representative images of  $\gamma$ H2AX immuno-FISH in 3 and 30 month old  $\alpha$ -actinin positive mouse cardiomyocytes (magenta –  $\alpha$ -actinin; red – telo-FISH; green –  $\gamma$ H2AX). Images are z projections of 4.5 $\mu$ M stacks taken with 100X objective. Arrows indicate co-localisation between telomeres and  $\gamma$ H2AX, with co-localising foci amplified in the right panels (taken from single z planes where co-localisation was found). Scale bars: left panels: 2.5 $\mu$ M; right smaller panels 0.5 $\mu$ M **(B)** Mean number of TAF – **(C)** Mean percentage of TAF positive –  $\alpha$ -actinin positive cardiomyocytes in 3, 15 and 30 month old mice. Data are represented as the mean for individual animals, with the horizontal line representing group mean. **(D)** Mean number of non-TAF – **(E)** Mean percentage of non-TAF positive –  $\alpha$ -actinin positive cardiomyocytes in 3, 15 and 30 month old mice. Data are represented as the mean for individual animals, with the horizontal line representing group mean. **(F)** Fold enrichment of  $\gamma$ H2AX at telomere repeats by real-time PCR. Graph represents fold enrichment of  $\gamma$ H2AX at telomeric repeats between IgG control, 3 and 30 month whole mouse hearts, for 3 independent ChIP experiments. Statistical analysis performed using One Way ANOVA; \*  $P < 0.05$ , NS (Non-Significant)  $P > 0.05$

Having observed an age-dependent increase in TAF in mouse cardiomyocytes (Figure 4-2A-C), we wanted to determine if telomere length or telomerase activity were associated with this increase in telomere dysfunction. Using q-FISH analysis, we found that there was a slight, but significant, decrease in the mean telomere intensity per nucleus of cardiomyocytes from mice aged 3 compared to 30 months old (Figure 4-3A). Cardiac-specific adeno-associated virus activation of TERT has previously been shown to offer cardiac protection following myocardial infarction, and has been associated with longer telomeres and increased numbers of the proliferation markers Ki-67 and pH3 (Bär *et al.*, 2014). To assess TERT activity, we used liquid nitrogen-frozen, ground whole hearts, and performed TeloTAGGG Telomerase PCR ELISA (an extended TRAP assay). Our data show there is no significant difference in telomerase activity in whole mouse hearts between 3 and 30 months of age (Figure 4-3B). However, a caveat to consider is the lack of either a negative or positive control for telomerase activity, and thus one cannot rule out the possibility that the observed telomerase activity could be below the threshold for detection of a positive signal.

In proliferative tissue, telomere shortening occurs due to the end-replication problem coupled with oxidative stress associated attrition (von Zglinicki *et al.*, 1995; von Zglinicki *et al.*, 2000). Age-dependent telomere shortening has been reported in mouse enterocytes (Flores *et al.*, 2008; Wang *et al.*, 2009), however, another study observed an age-dependent increase in telomere dysfunction in enterocytes

independently of telomere shortening (Hewitt *et al.*, 2012). We sought to determine if the age-dependent increase in telomere dysfunction (Figure 4-2A-C) was associated with telomere length. We performed Q-FISH analysis, and quantified the intensity of telomeres co-localising with a DDR, compared to telomeres not co-localising with a DDR in 30 month old mice. Our data show that there is no significant difference between the lengths of telomeres which co-localise with a DDR, compared to those that do not (Figure 4-3C).

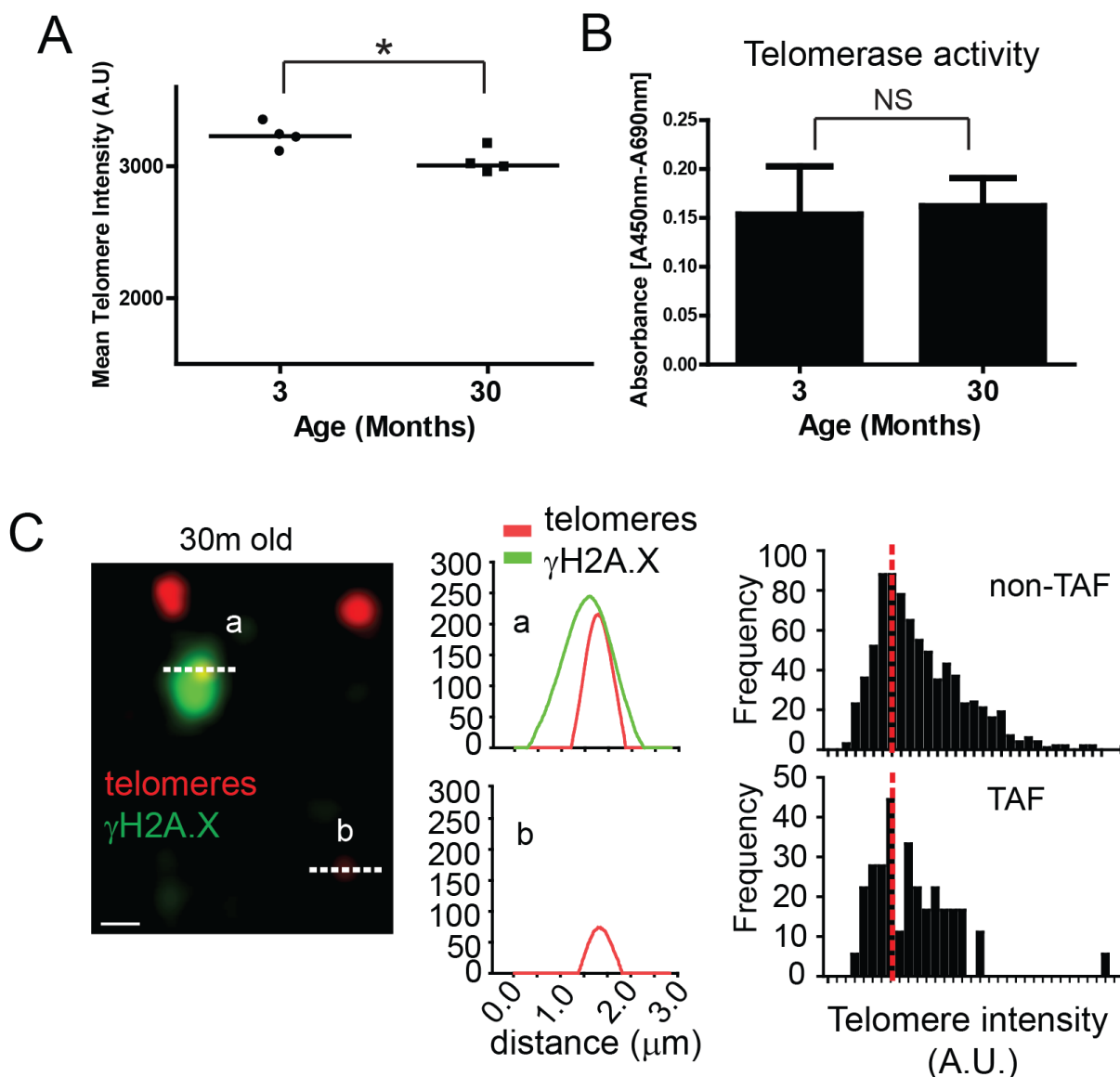


**Figure 4-3. TAF Accumulate in Mouse Cardiomyocytes Independently of Telomere Length.** **(A)** qFISH analysis comparing mean telomere intensity per nuclei of 3 and 30 month mouse cardiomyocytes. >100 nuclei were analysed per condition, and data are represented as the mean for individual animals, with the horizontal line representing group mean. **(B)** Quantitative PCR-ELISA TRAP assay comparing telomerase activity of 3 and 30 month mouse whole heart lysates. Data are mean  $\pm$

SEM of  $n=4$ . Scale bar:  $0.5\mu\text{M}$ . **(C)** Representative image of telomere co-localising (a) or not (b) with  $\gamma\text{H2AX}$  foci (red – telomere; green –  $\gamma\text{H2AX}$ ) taken from a single Z plane at 100X objective. Adjacent graphs represent quantification of telomere and  $\gamma\text{H2AX}$  signal intensity. Histograms displaying telomere intensity for telomeres co-localising (bottom) or not co-localising (top) with  $\gamma\text{H2AX}$  DDR foci. Red dotted lines represent median  $> 100$  telomeres per condition. Statistical analysis performed using two-tailed t test; \*  $P<0.05$ , NS (Non-Significant)  $P>0.05$ . Mann-Whitney tests show no significant difference in telomere intensity between TAF and non-TAF in 30 month old mouse cardiomyocytes ( $P>0.05$ ).

### 4.3 TAF Accumulate in Human Cardiomyocytes Independently of Telomere Length

Having shown an age-dependent accumulation of TAF in mouse cardiomyocytes, occurring independently of telomere shortening (Figure 4-2 & Figure 4-3), we then wanted to ascertain if human cardiomyocytes were also susceptible to telomere dysfunction. We acquired human right atrial appendage tissue from patients undergoing surgery for aortic stenosis, and thus the cardiomyocytes from this region should not be associated with any disease pathology. Immuno-FISH analysis revealed that there is an age-dependent increase in mean number of TAF and percentage of TAF positive cells, in pericentriolar material 1 (PCM-1) positive human cardiomyocytes (Figure 4-4A-C). We then performed Q-FISH analysis, and quantified the intensity of telomeres co-localising with a DDR, compared to telomeres not co-localising with a DDR in both the 46-65 and 74-82 year old age groups. Our data show that there is no significant difference between the lengths of telomeres which co-localise with a DDR, compared to those that do not in either of the two age groups (Figure 4-4D).

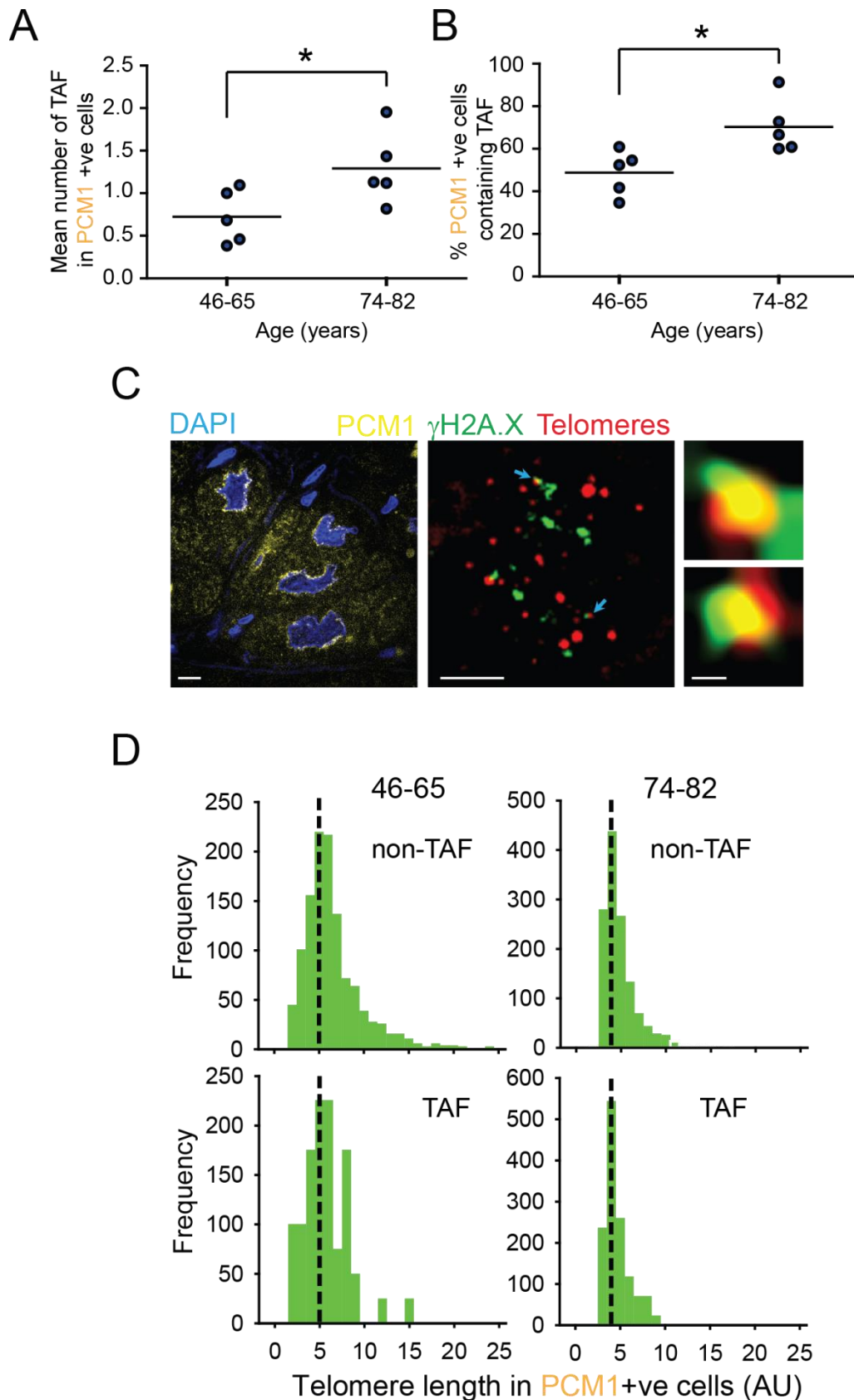


**Figure 4-4. TAF Accumulate with Age in Human Cardiomyocytes. (A)** Mean number of TAF – **(B)** Mean percentage of TAF positive – PCM1-positive human cardiomyocytes from 46-65 and 74-82 year old human heart tissue. Data are represented as the mean for individual patients, with the horizontal line representing group mean. **(C)** Representative images of  $\gamma$ H2AX immuno-FISH in PCM1-positive

human cardiomyocytes (blue – DAPI; yellow – PCM1; red – telo-FISH; green –  $\gamma$ H2AX). Images are z projections of 4.5 $\mu$ M stacks taken with 100X objective. Arrows indicate co-localisation between telomeres and  $\gamma$ H2AX, with co-localising foci amplified in the right panels (taken from single z planes where co-localisation was found). Scale bars: left panel - 5 $\mu$ M, middle panel – 2.5 $\mu$ M, right panels – 0.25 $\mu$ M **(D)** Histograms displaying telomere intensity for telomeres co-localising (bottom) or not co-localising (top) with  $\gamma$ H2AX DDR foci for cardiomyocytes taken from patients 46-65 (left) and (74-82) years old. Red dotted lines represent median intensity > 45 telomeres per condition. Mann-Whitney tests show no significant difference in telomere intensity between TAF and non-TAF in either, 46-65 or 74-82 year old patients ( $P>0.05$ ).

An intermediate state of telomeres has been proposed in which telomere uncapping could occur due to inhibition of TRF2 (Cesare *et al.*, 2009). Furthermore, *In vitro*, it has been shown by STORM imaging that knock down of the shelterin component TRF2 results in uncapping of the t-loop (Doksani *et al.*, 2013). We therefore investigated if TRF2 abundance varied at dysfunctional telomeres. Firstly, we observed that as expected, TRF2 co-localised with telomeres (Figure 4-5A). Next, Q-FISH analysis, of the mean abundance of TRF2 bound to telomeres co-localising with a DDR, compared to the abundance at telomeres not co-localising with a DDR revealed no significant differences; TRF2 abundance at human cardiomyocyte telomeres is independent of telomere dysfunction (Figure 4-5A-B).

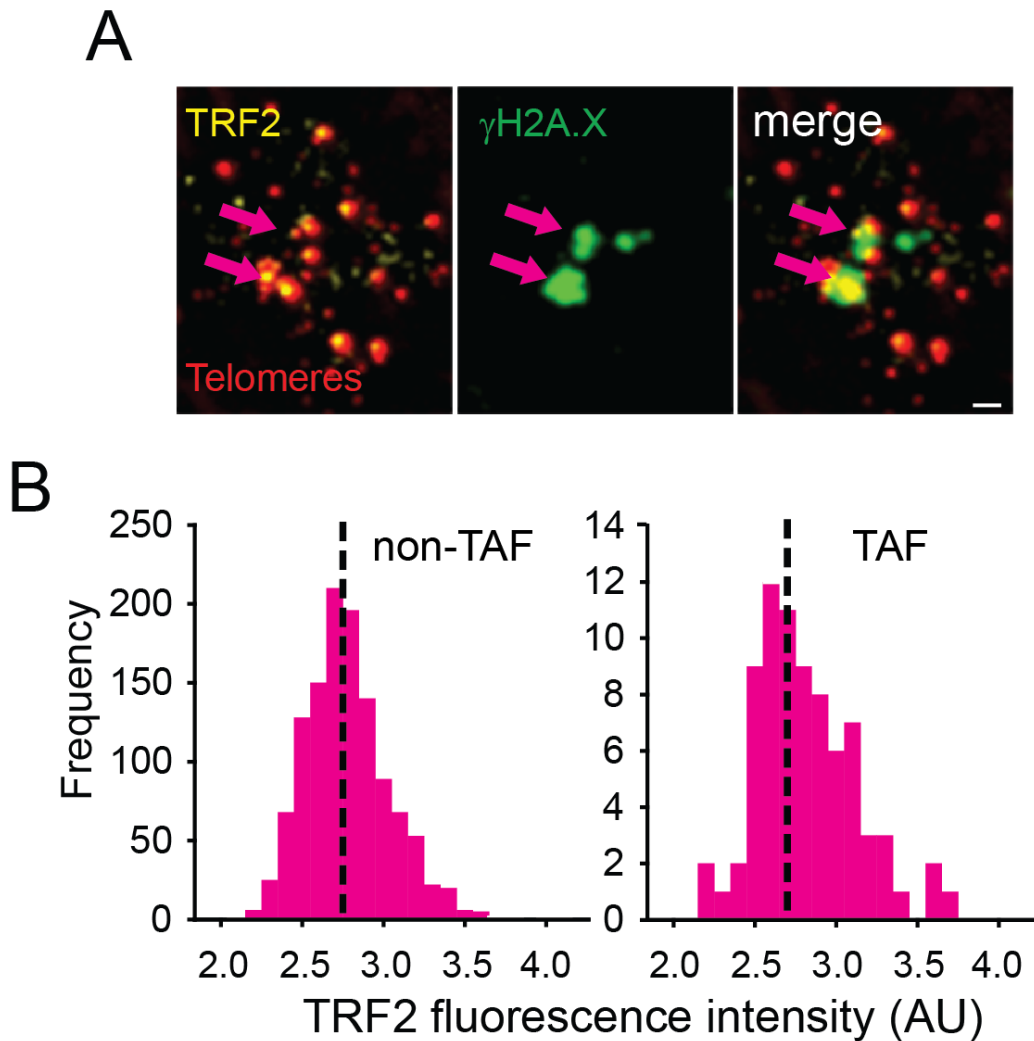


**Figure 4-5. TAF occur Independently of TRF2 Abundance in Human Cardiomyocytes.** **(A)** Representative images of TRF2 immuno-FISH in PCM1-positive human cardiomyocytes (blue – DAPI; yellow – TRF2; red – telo-FISH; green –  $\gamma$ H2AX). Images are z projections of 4.5 $\mu$ M stacks taken with 100X objective. Scale bar: 0.5 $\mu$ M. **(B)** Histograms displaying TRF2 fluorescence intensity for TRF2 foci co-localising with telomeres and either: not co-localising with  $\gamma$ H2AX (left) or co-localising with  $\gamma$ H2AX (right) in human cardiomyocytes. Red dotted lines represent median intensity > 75 telomeres per condition. Mann-Whitney tests show no significant difference in TRF2 intensity between TRF2 abundance at TAF and non-TAF ( $P > 0.05$ ).

#### 4.4 Cardiomyocytes are Associated with Senescent Markers.

Cellular senescence *in vivo* has been associated with numerous age-related diseases, as reviewed in (Muñoz-Espín and Serrano, 2014). Moreover, drug-induced clearance of p16(Ink4a) positive cells delayed age-related disorders in the BubR1 progeroid, *INK-ATTAC*, mouse model (Baker *et al.*, 2011). We sought to investigate if there is an age-dependent increase in senescent cells in cardiomyocytes. In

collaboration with Damien Maggiorani from the Mialet-Perez group, we isolated cardiomyocytes from 3 and 20 months old mice and performed qRT-PCR gene expression analysis and found that there is a significant age-dependent increase in p15, p16 and TGF- $\beta$  (Figure 4-6A)

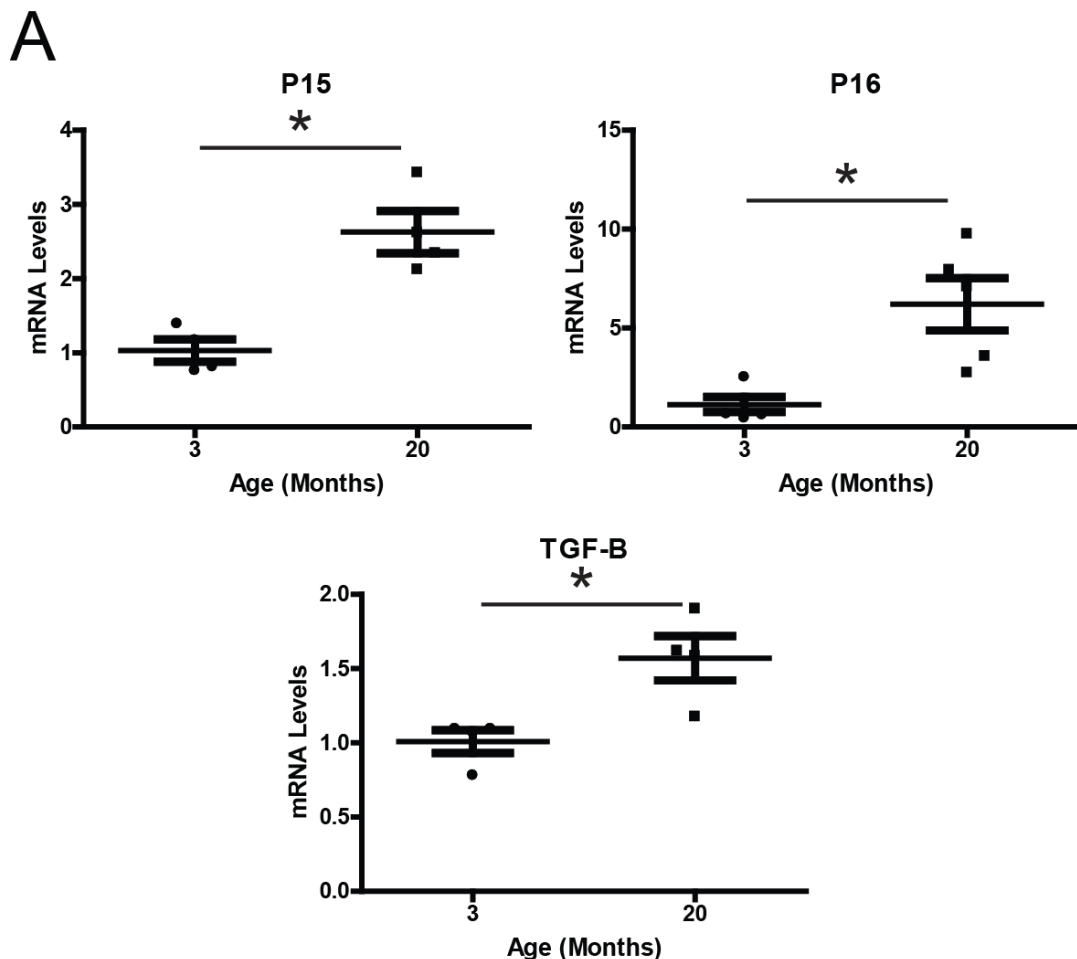


**Figure 4-6. Senescence-Associated Genes are Upregulated with Age in Mouse Cardiomyocytes. (A)** Gene expression analysis of senescence markers, by Real-Time PCR of isolated mouse cardiomyocytes from mice 3 and 20 months of age. Data are represented as the mean for individual mice, with the horizontal line representing group mean. Statistical analysis performed using two-tailed t test; \*  $P < 0.05$ .

Having observed an upregulation of senescent markers at the mRNA level, we wanted to investigate if any other markers of senescence were also up-regulated with age in cardiomyocytes. In collaboration with Jodie Birch from our laboratory, we observed an age dependent increase in p21 protein expression, as quantified by percentage of cardiomyocytes staining positive for p21 by IHC (Figure 4-7A-B).

Recent research has shown that centromeric satellite DNA becomes unravelled upon the induction of senescence in both mouse and human fibroblasts, a phenomenon coined senescence-associated distension of satellites (SADs) (Swanson *et al.*, 2013). In collaboration with Mikolaj Ogrodnik from both ours and the von Zglinicki laboratory, we investigated if SADs also occurred during cardiomyocyte ageing, and found an age-dependent increase in SADs events in mouse cardiomyocytes (Figure 4-7C-E). The lipid peroxidation marker has been shown to associate with various senescence markers in murine neurones (Jurk *et al.*, 2012), and we observed that there is also an age-dependent increase in 4-HNE positive cardiomyocytes (Figure 4-7F-G). Cardiac fibrosis has been observed to increase with age in numerous species from mice to humans (Burkauskiene *et al.*, 2006; Dai *et al.*, 2009), and thus we investigated fibrosis to confirm normal cardiac ageing in our mouse colony, and in collaboration with Gavin Richardson, we observed a significant increase in Sirius red staining with age (Figure 4-7H).

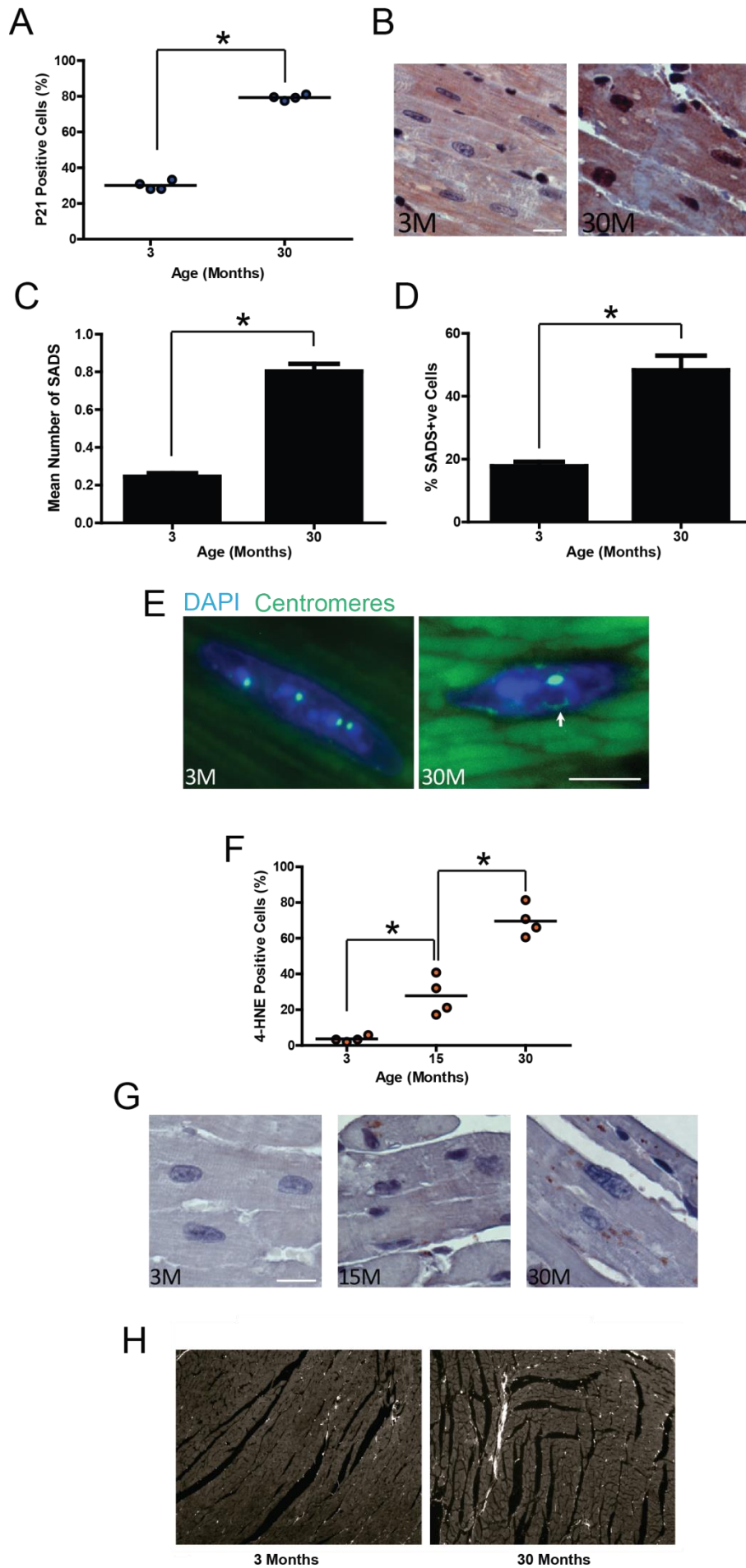


**Figure 4-7. Senescence Markers Increase with Age in Mouse Cardiomyocytes.** **(A)** Quantification of the percentage of cardiomyocytes staining positive for p21 by IHC. Data are represented as the mean for individual mice, with the horizontal line representing group mean. **(B)** Representative images of p21 IHC in cardiomyocytes from mice aged 3 and 30 months (nuclear counter stain – blue; p21 – brown). **(C)** Quantification of the average number of SADS events per cell in mouse cardiomyocytes aged 3 and 30 months. Data are mean  $\pm$  SEM of  $n=3$ . Scale bar: 15 $\mu$ M. **(D)** Quantification of the mean percentage of SADS positive mouse cardiomyocytes aged 3 and 30 months. Data are mean  $\pm$  SEM of  $n=3$ . **(E)** Representative images of SADS events in 3 and 30 month old mouse cardiomyocytes (blue – DAPI; green foci – centromeres). Arrow represents a SADS event. Scale bar: 10 $\mu$ M. **(F)** Mean percentage of 4-HNE positive cardiomyocytes in 3, 15 and 30 month old mice. Data are represented as the mean for individual animals, with the horizontal line representing group mean. **(G)** Representative images of 4-HNE IHC in 3, 15 and 30 month old mouse cardiomyocytes (blue – nuclear counter stain; brown cytoplasmic staining – 4-HNE). Scale bar: 15 $\mu$ M. **(H)** Representative image of fibrosis via Sirius red staining in mice aged 3 and 30 months (white; fibrosis). Scale bar: 50 $\mu$ M. Statistical analysis performed using One way ANOVA or two-tailed t test; \*  $P<0.05$ .

#### 4.5 An Age Dependent Bystander Effect from Mouse Cardiomyocytes

Having shown that there is an age-dependent increase in senescence markers in mouse cardiomyocytes *in vivo*, we wanted to determine if aged cardiomyocytes could have a detrimental effect on surrounding cells. Interestingly, we observed that TGF- $\beta$  is significantly upregulated with age in mouse cardiomyocytes (Figure 4-6), and this has been shown to be one of the key proteins associated with eliciting a detrimental bystander effect in fibroblasts (Acosta *et al.*, 2013). We wanted to determine if aged cardiomyocytes could elicit a detrimental bystander effect on neighbouring cells. We specifically isolated cardiomyocytes from 3 and 20 month age mice, from the same cohort showing an age-dependent increase in senescence markers. We then cultured the cardiomyocytes for 48 hours, before collecting conditioned medium from them. Following this, we cultured MAFs in conditioned medium from 3 and 20 month old mice for 4 days. On the last day, we cultured cells in the presence of the modified thymidine analogue EdU for 8 hours and then assessed proliferation levels in this time period as measured by EdU incorporation. Our data show that MAFs cultured in conditioned medium from cardiomyocytes from 20 month old mice had a significantly lower incorporation of EdU, compared to MAFs cultured in conditioned medium collected from cardiomyocytes from 3 months old mice (Figure 4-8A-C).

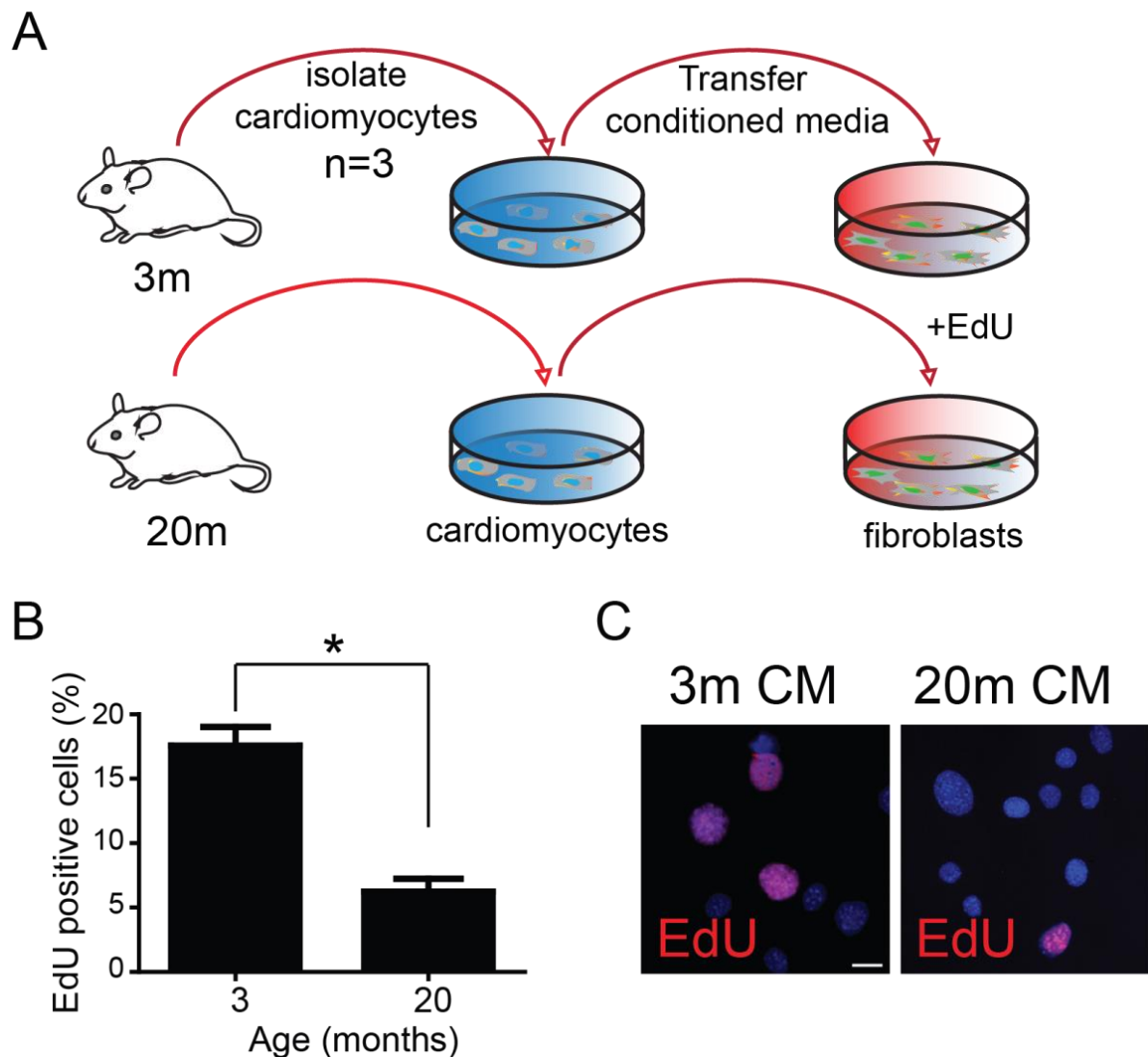


**Figure 4-8. Conditioned Medium from Old Mouse Cardiomyocytes Reduces Proliferation of Fibroblasts.** **(A)** Cardiomyocytes from 3 and 30 month old mice were isolated and cultured for 48 hours. Conditioned medium was then collected. MAFs were cultured in conditioned medium + normal growth medium (1:1), for 4 days, with medium replenished after 2 days. Following this, cells were incubated in the presence of 10 $\mu$ M EdU before fixation. **(B)** Quantification of the mean percentage of MAFs positive for EdU incorporation. Data are mean  $\pm$  SEM of  $n=3$ . **(C)** Representative images of EdU incorporation from MAFs cultured in conditioned medium from cardiomyocytes isolated from 3 or 20 months old mice (blue – DAPI; red – EdU). Statistical analysis performed using two-tailed t test; \*  $P<0.05$ .

#### 4.6 An Age-Dependent Increase in Quad Myocytes TAF

Having shown the phenomenon of telomere dysfunction occurring in cardiomyocytes *in vivo*, we wanted to determine if this could also occur in other non-rapidly dividing/post-mitotic cells. Immuno-FISH analysis revealed that there is an age-dependent increase in mean number of TAF and percentage of TAF positive cells, in quad muscle myocytes from 3 to 15 to 30 months of age (Figure 4-9A-B).

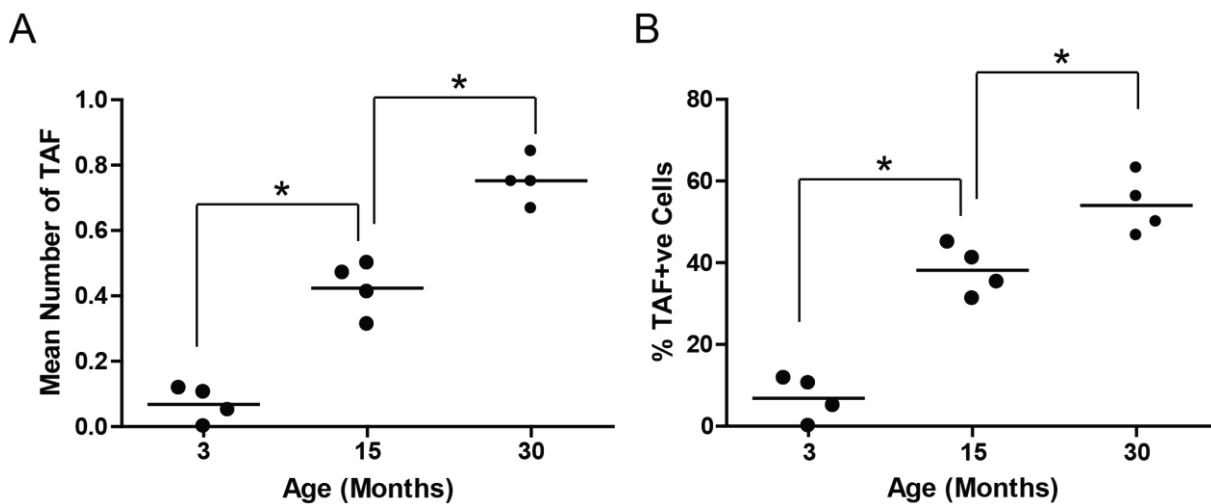


**Figure 4-9. TAF Accumulate with Age in Mouse Quad Muscle Myocytes. (A)** Mean number of TAF – **(B)** Mean percentage of TAF positive in quad muscle myocytes in 3, 15 and 30 month old mice. Data are represented as the mean for individual animals, with the horizontal line representing group mean. \* *P* value < 0.05.

## 4.7 Discussion

Following on from our observations that persistent TAF could be induced in cardiomyocytes independently of cell division *in vitro*, we wanted to ascertain if TAF could be induced in cardiomyocytes *in vivo*, and if there was an age-dependent association and increase in senescent markers. Cardiomyocytes provide a good model for assessing the persistence of damage, as due to negligible proliferation (Figure 4-3), damage can rarely be diluted via cell division. To begin, as a proof-of-principle we used whole body X-irradiation on 1 month old mice, and observed a significant increase in the number of TAF after an 11 month recovery period, suggesting that the damage is persistent. Unfortunately, we did not assess a group immediately after X-irradiation, to determine if TAF numbers had altered during the subsequent 11 month recovery period. Moreover, as discussed for our *in vitro* data for TAF persistence in the previous chapter, unless foci dynamics are constantly

monitored in real-time, one cannot conclusively confirm persistence. Furthermore, research has shown that persistent DDR results in activation of several downstream pathways, which results in mitochondrial dysfunction, and reactive oxygen species generation, which in turn causes further DNA damage, thus initialising a feedback loop (Passos *et al.*, 2010)(Correia-Melo *et al.*, 2016). However unlikely, it is therefore plausible that DDF could constantly be being turned over, whilst retaining a consistent number. However, considering our group and others have published that TAF are persistent in fibroblasts *in vitro* (Fumagalli *et al.*, 2012; Hewitt *et al.*, 2012), coupled with our observations that TAF are persistent in cardiomyocytes *in vitro*, an interpretation of the X-irradiation data is that TAF which are induced as a direct result of ionising radiation are irreparable and persisted for the following 11 months. However, live cell time-lapse microscopy *in vitro* experiments only tracked the persistence of TAF for a matter of several hours (Hewitt *et al.*, 2012), and fixed cell TAF time course experiments only for several weeks, and thus the long term persistence of TAF *in vivo*, cannot be conclusively deduced.

X-irradiation was only used as a proof-of-principle to induce TAF, however, patients who have been exposed to excessive ionising radiation have an increased risk of developing cardiovascular disease (Adams *et al.*, 2003; Mone *et al.*, 2004; Little, 2010; Shimizu *et al.*, 2010). This increased risk of heart disease in patients exposed to ionising radiation could be due to systemic effects rather than cardio-specific, however female patients who have had radiotherapy for left breast cancer, have a significantly higher risk of developing cardiovascular disease, compared to those patients treated for right breast cancer (Darby *et al.*, 2003; Taylor *et al.*, 2008; Taylor *et al.*, 2009). In this context, understanding the nature of ionising radiation induced cardiac damage therefore has therapeutic importance.

Next we showed that there is an age-dependent increase in TAF in both mouse and human cardiomyocytes. In addition, we also report an age-dependent increase in quad myocyte TAF, therefore confirming the existence of telomere dysfunction in another myocyte cell type. The potential mechanisms driving TAF generation in a non-rapidly dividing cell type will be discussed further in the next chapter. To confirm that we were observing DDR proteins in the telomeric regions, and not merely foci spatially close enough to provide false-positives from lack of microscopy resolving power, we performed CHIP for  $\gamma$ H2AX, followed by RT-PCR specifically for telomeric repeats in mouse heart tissue. The methodology used for this experiment used

ground whole hearts, and thus all cardiac cell types and not just cardiomyocytes were analysed. Nevertheless, this confirmed the presence of a DDR in telomeric repeats in cardiac cell types *in vivo*, however as discussed in the previous chapter, the possibility remains that physical damage could have occurred elsewhere in the genome, as the  $\gamma$ H2AX signal has been shown to be amplified, and can spread for several kilobases (Rogakou *et al.*, 1999; Meier *et al.*, 2007; Iacovoni *et al.*, 2010). Regardless, we observe a significant age-dependent increase in TAF, whereas non-TAF remain unaltered with age. This suggests that there is a significant distinction between what we observe to be TAF compared to non-TAF. If one were to hypothesise that all damage was occurring downstream and not at telomeres specifically, the only explanation for this would be that a DDR in telomeric regions is less readily resolved compared to the rest of the genome. Or if we assume the damage is occurring at telomeres, then there is evidence suggesting that telomere damage is irreparable (Fumagalli *et al.*, 2012; Hewitt *et al.*, 2012) and thus TAF would be significantly higher than non TAF. In addition, there is also evidence showing that guanine triplets, as found in telomeres, are more sensitive to oxidative stress-induced damage (Henle *et al.*, 1999; Oikawa *et al.*, 2001); these ideas are not mutually exclusive and could both contribute to the observation that TAF are significantly increased with age, whereas non-TAF are not. As discussed in the previous chapter, the nature of telomere dysfunction still remains elusive, whether the observed DDF are a result of uncapping, or a physical break in the DNA. There also remains the possibility that the observed telomere DDF are due to telomere uncapping, and evidence shows that the recognition of telomeres by TRF1 and TRF2 is disrupted following oxidative damage (Opresko *et al.*, 2005). However, our analysis of TRF2 abundance at telomeres co-localising with a DDR, compared to those which are not, would suggest that there is no association between TRF2 abundance and incidence of telomere dysfunction, suggesting that ROS-induced TRF2 inhibition-mediated uncapping is unlikely to be driving telomere dysfunction in human cardiomyocytes.

It has been proposed that an intermediate state of telomeres, which are uncapped and signal a DDR, but retain significant shelterin to inhibit NHEJ, are mainly due to steric constraints on short telomeres (Cesare *et al.*, 2009). Furthermore, research has shown that late generation *TERC*<sup>-/-</sup> mice, which have critically short telomeres, display decreased cardiomyocyte proliferation, and an increase in cardiac

hypertrophy and apoptosis (Leri *et al.*, 2003). Whilst we did not detect any variation in telomerase activity between young and old mice, we did observe a slight, but significant age-associated decrease in telomere length in cardiomyocytes from 3 compared to 30 month old mice. Mouse cardiomyocytes have been shown to turnover, albeit at rates of less than 4% annually (Malliaras *et al.*, 2013; Senyo *et al.*, 2013), however this may explain the slight decrease in telomere length we observed. Interestingly, telomere length has also been shown to decrease in the neurones of patients with Alzheimer's disease (Franco *et al.*, 2006), thus raising the possibility that telomere shortening may possibly occur due to a yet unknown mechanism, independent from DNA replication-induced end-replication problem and accompanying oxidative stress-accelerated attrition (von Zglinicki *et al.*, 1995; von Zglinicki *et al.*, 2000). Regardless of this, our data suggest that cardiomyocyte telomere shortening is not responsible for the age-dependent increase in telomere damage, as in both human and mouse cardiomyocytes we observed that telomere dysfunction was occurring independently of length, suggesting that uncapping due to steric constraints on the t-loop are unlikely to be driving age-associated telomere dysfunction.

As discussed in the previous chapter, the use of telomerase knock out mice, produces telomere shortening unlikely to be experienced under physiological conditions, and especially in cardiomyocytes, however if both TAF and TIF are shown to activate the same downstream signalling pathways, then it will provide a valuable tool for predicting the physiological impact of TAF on cells and tissue.

Research has shown that post-mitotic adipocytes and neurones can elicit a senescence-like phenotype (Minamino *et al.*, 2009; Jurk *et al.*, 2012), including a persistent DDR; which has been shown to trigger the SASP in fibroblasts (Rodier *et al.*, 2009). However, until now, there has been little evidence suggesting a senescent-like phenotype in cardiomyocytes *in vivo*. P21 has been shown to halt cell cycle following DNA damage, and if persistent can activate p38-MAPK upregulation which can lead to mitochondrial dysfunction and ROS production, followed by p16 activation in human fibroblasts (Passos *et al.*, 2010; Freund *et al.*, 2011). Our RT-PCR and IHC analysis revealed an age-dependent upregulation of p15, p16 and p21 all of which have been associated with an accumulation during senescence (Alcorta *et al.*, 1996; Serrano *et al.*, 1997; Robles and Adami, 1998; Hitomi *et al.*, 2007). TGF- $\beta$  is an important SASP component as it has been associated with driving paracrine

senescence is neighbouring cells (Acosta *et al.*, 2013). Furthermore, inhibition of TGF- $\beta$  in senescent cells has been shown to attenuate the increase in ROS production and DDR activation in bystander cells (Hubackova *et al.*, 2012a). We therefore investigated if cardiomyocytes elicited an age-associated bystander effect. Isolated cardiomyocytes from adult mice only survive for around 48 hours in cell culture, which wouldn't provide sufficient time to perform bystander experiments. We therefore collected conditioned medium from isolated cardiomyocytes within this time period and used this to culture MAFs for several days. Our data show that MAFs cultured in medium from aged cardiomyocytes have significantly decreased rates of proliferation, suggesting cardiomyocytes can also elicit a bystander effect. Due to sparsity of conditioned medium, we were unable to perform further experimentation into categorising the bystander effect for other markers of senescence. In addition, it will also be important to perform the bystander experiments in the presence of neutralising antibodies to ascertain which SASP factors are responsible for driving paracrine senescence in cardiomyocytes.

Epigenetic changes have also been shown to be a hallmark of cellular senescence in various cell types, for example senescence-associated heterochromatin foci (SAHF) appear following senescence and are associated with the stable repression of E2F target genes (Narita *et al.*, 2003). However, the use SAHF as a marker for cellular senescence is questionable as they appear to be absent from all senescent mouse cells and numerous senescent human cell types (Narita *et al.*, 2003; Kennedy *et al.*, 2010). Another epigenetic modification which has been observed is the unravelling of centromeres, known as senescence-associated distension of satellites (SADS) (Swanson *et al.*, 2013). Interestingly, SADS have been observed to occur in both mouse and human senescent cells, and by numerous senescence inducers, including both oxidative stress and oncogenic Ras overexpression (Swanson *et al.*, 2013). Another important finding is that SADS also appear during the induction of senescence in cells from patients with Hutchinson Gilford Progeria disease (Swanson *et al.*, 2013). Our data show an age-dependent increase in SADS in murine cardiomyocytes, and provide another marker to determine a senescent-like phenotype in cardiomyocytes *in vivo*.

Our analysis also revealed an age-dependent increase in the lipid peroxidation marker 4-HNE. Although 4-HNE is not generally considered to be a marker of cellular senescence *per se*, it's accumulation has been shown to associate with various other

senescence markers, including elevated SA- $\beta$ -Gal activity and increased  $\gamma$ H2AX foci (Wang *et al.*, 2009; Nelson *et al.*, 2012). 4-HNE can lead to stable 4-HNE protein adducts, by covalently modifying lysine, cysteine and histidine residues of proteins, which can lead to severe functional impairment of both soluble and membrane proteins (Crabb *et al.*, 2002; Negre-Salvayre *et al.*, 2003; Ferrington and Kappahn, 2004). Proliferative cells can dilute lipid peroxidation through cell division, however, considering the majority of cardiomyocytes present at birth are still present at 50 years of age (Bergmann *et al.*, 2009), cardiomyocytes can have to endure a lifetime of oxidative damage accumulation. For example, post-mitotic cells are prone to lipofuscin accumulation (Ulf and Alexei, 2002), therefore understanding the mechanisms driving this are of therapeutic importance.

Using a combination of different cellular senescence markers, we have shown, for the first time, that there is an age-dependent accumulation of a senescent phenotype specifically in cardiomyocytes *in vivo*. On a cell-autonomous level, senescence would act to prevent cardiomyocyte proliferation, which may seem inconsequential considering the low rate of cardiomyocyte proliferation (Bergmann *et al.*, 2009), however, cardiomyocyte replication has been shown to increase during times of myocardial stress (Senyo *et al.*, 2013), and thus senescence may attenuate the ability for cardiac repair after an infarction. Furthermore, our *in vitro* data show an increase in cardiomyocyte hypertrophy after senescence-initiation and cardiomyocyte hypertrophy is associated with various cardiomyopathies (Berenji *et al.*, 2005). It will be therefore be important to ascertain whether TAF are associated with cardiomyocyte hypertrophy *in vivo*. Although cardiomyocyte hypertrophy is a physiological response to exercise, pathological hypertrophy is detrimental, as it is not associated with increased pumping, however is associated with myocardial fibrosis, which we and others have shown accumulates with age in the heart (Lombardi *et al.*, 2003). On a non-cell autonomous level, senescence is associated with a SASP, which involves the secretion of pro-inflammatory cytokines, and chronic inflammation is a hallmark of pathological ageing, and has been observed in cardiomyopathies, such as atherosclerosis (Libby, 2002; Coppé *et al.*, 2008). In addition, senescent cells have been shown to elicit a bystander effect in neighbouring cells, which can induce DNA damage and further senescence (Hubackova *et al.*, 2012a; Nelson *et al.*, 2012; Acosta *et al.*, 2013).

To conclude, hitherto most studies investigating the role of telomeres in cardiac function have been correlative, by comparing telomere length in leucocytes and inferring (Masi *et al.*, 2014). We have shown for the first time that there is an age-dependent increase in telomere damage in both mouse and human cardiomyocytes, occurring independently of telomere length. We also observed an age-dependent increase in markers of senescence in cardiomyocyte *in vivo* and signs of aged cardiomyocytes being capable of eliciting a bystander effect. Our *in vitro* data using the TRF1-FokI fusion protein provides evidence that TAF trigger the development of senescence in cardiomyocyte *in vitro*, however, in order to truly ascertain if cardiomyocyte TAF drive cardiomyocyte senescence *in vivo*, a similar fusion protein would need to be targeted specifically to cardiomyocytes *in vivo*. Furthermore, to assess if cardiomyocyte senescence had an effect on cardiac function, it would then be important to couple the cardiomyocyte specific TRF1-FokI model, with a model such as the *INK-ATTACK* transgenic mouse (Baker *et al.*, 2011) , in which senescent cardiomyocytes could be specifically removed. However, despite evidence that cardiomyocyte proliferation is increased at sites adjacent to myocardial infarction (Malliaras *et al.*, 2013; Senyo *et al.*, 2013), it is unknown if replenishment of cardiomyocytes would occur following removal of senescent cardiomyocytes, and thus if the level of senescent cardiomyocytes were high, this could seriously alter tissue homeostasis.

## 5 Effects of Oxidative Stress/Rapamycin on Cardiomyocyte Telomere Dysfunction

In the previous chapter, we demonstrated an age-dependent increase in TAF in both mouse and human cardiomyocytes. In addition, we saw an age-dependent increase in various senescence markers. Interestingly, we observed an age-dependent increase in the lipid peroxidation marker 4-HNE, which provides a proxy for the levels of oxidative stress endured by the cell (Onorato *et al.*, 1998). Having previously shown that oxidative stress could induce telomere damage independently of cell division *in vitro*, and observing there is an age-dependent increase of TAF in non-rapidly dividing cardiomyocytes, we sought to ascertain if oxidative stress could drive telomere dysfunction *in vivo*. To investigate this, we used several mouse models for increased oxidative stress, namely, cardiac-specific overexpression of MAO-A, Catalase *-/-* and MnSOD*-/+*.

Finally, ROS levels have been shown to increase following replicative, oncogene- or stress-induced senescence (Gabriele *et al.*, 2003; Ramsey and Sharpless, 2006; Passos *et al.*, 2007; Lu and Finkel, 2008b). Furthermore, ROS have been implicated in contributing to the persistence of cellular senescence, for example, by replenishing short-lived DNA damage foci, thus maintaining an ongoing DDR, which activates p21, and is thought to activate a signalling cascade, which is thought to lead to mitochondrial dysfunction, which causes aberrant ROS production, which in turn causes further DNA damage, therefore instigating a feedback loop (Passos *et al.*, 2010). Interestingly, the mTOR inhibitory drug rapamycin has been shown to reduce ROS levels both *in vitro* and *in vivo* (Shin *et al.*, 2011) (Miwa *et al.*, 2014a), and can increase the lifespan of yeast (Powers *et al.*, 2006; Medvedik *et al.*, 2007), nematodes (Robida-Stubbs *et al.*, 2012), fruit flies (Bjedov *et al.*, 2010) and mice (Harrison *et al.*, 2009; Anisimov *et al.*, 2011; Miller *et al.*, 2011). mTOR has been shown to play important roles in senescence, for example, our group has recently published research showing that mTOR phosphorylation following a DDR, leads to PGC-1b dependent mitochondrial biogenesis, and that this increase in mitochondrial density is responsible for driving many features of the senescent phenotype (Correia-Melo *et al.*, 2016). Furthermore, inhibition of mTOR by rapamycin has been shown to attenuate the increase in the secretion of inflammatory cytokines such as IL1A and IL6 by senescent cells (Lalberge *et al.*, 2015). Moreover, mice fed with rapamycin

have been shown to release lower levels of hydrogen peroxide from mitochondria in both murine brain and liver tissues (Miwa *et al.*, 2014b).

We therefore investigated if rapamycin treatment could attenuate the senescent phenotype *in vitro* through reducing intra-cellular ROS levels and subsequent DNA damage, and finally if a rapamycin supplemented diet could reduce an accumulation of TAF with age in mice, and if this was associated with a decrease in a senescent-like phenotype in cardiomyocytes.

### 5.1 MAO-A Overexpression Drives TAF *in vivo*

We have previously shown *in vitro* that hydrogen peroxide can induce TAF independently of cell division. Our data showing accumulation of 4-HNE suggests that cardiomyocytes are exposed to high levels of oxidative stress, which compliments previous data showing an age-dependent increase in cardiac mitochondrial ROS production (Judge *et al.*, 2005). Interestingly, cardiac-specific over-expression of the pro-oxidant protein monoamine oxidase-A (MAO-A) results in increased oxidative stress in cardiomyocytes and leads to the development of cardiomyopathy (Villeneuve *et al.*, 2013). MAO-A is an enzyme which catalyses the oxidative deamination of monoamines; producing ammonia, aldehyde and H<sub>2</sub>O<sub>2</sub> as by-products (Villeneuve *et al.*, 2013), and MAO-A expression has been observed to increase during replicative senescence in human fibroblasts (Passos *et al.*, 2007). RT-PCR analysis revealed that there is an age-dependent increase in monoamine oxidase A (MAO-A) mRNA levels in mouse cardiomyocytes from 3 to 20 months (Figure 5-1A).

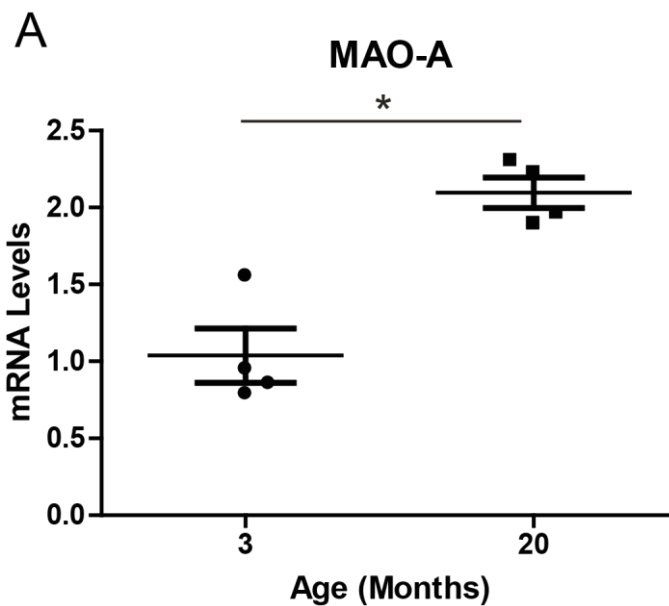


**Figure 5-1. An Age-Dependent Increase in MAO-A Expression in Mouse Cardiomyocytes. (A)** Gene expression analysis of MAO-A by Real-Time PCR of isolated mouse cardiomyocytes from 3 and 20 months of age. Data are represented as the mean for individual mice, with horizontal line representing group mean. Statistical analysis performed using two-tailed t test; \*  $P < 0.05$ .

We investigated if cardiac-specific over-expression of MAO-A could induce TAF in mouse cardiomyocytes. Immuno-FISH analysis revealed that cardiac-specific MAO-A overexpression can significantly increase the mean number of TAF and percentage of TAF positive cells, in mouse cardiomyocytes from mice aged 3 months (Figure 5-2A-B). This is also associated with a significant increase in the percentage of cells positive for 4-HNE, as shown by IHC (Figure 5-2C-D). As previously mentioned, MAO-A activity produces by products other than oxidants, for example ammonia and aldehyde (Villeneuve *et al.*, 2013), therefore to ascertain if TAF were induced as a result of oxidative stress, or by another mechanism, we supplemented the diet of MAO-A mice with the antioxidant *N*-acetylcysteine (NAC). Our subsequent immuno-FISH analysis revealed that a NAC-supplemented diet significantly reduced both the mean number of TAF, and the percentage of TAF positive cardiomyocytes (Figure 5-2E-F).

Fractional shortening is a commonly used cardiac functional readout (Villeneuve *et al.*, 2013), which represents the percentage of shortening of the left ventricular diameter at the end-diastole compared to end-systole. We performed fractional shortening analysis and discovered that wild-type mice have significantly higher

fractional shortening percentage than MAO-A transgenic mice at 3 months of age (Figure 5-2G). Furthermore, supplementing the diet of MAO-A transgenic mice was able to rescue the decline in fractional shortening (Figure 5-2H)

Finally, we performed correlation analysis, comparing both mean number of TAF and mean percentage of TAF positive cells, against fractional shortening, irrespective of genotype or diet supplementation. Our analysis revealed a significant inverse relationship between TAF (both mean and mean percentage of TAF positive cells) and heart function (as measured by fractional shortening) (Figure 5-2J).

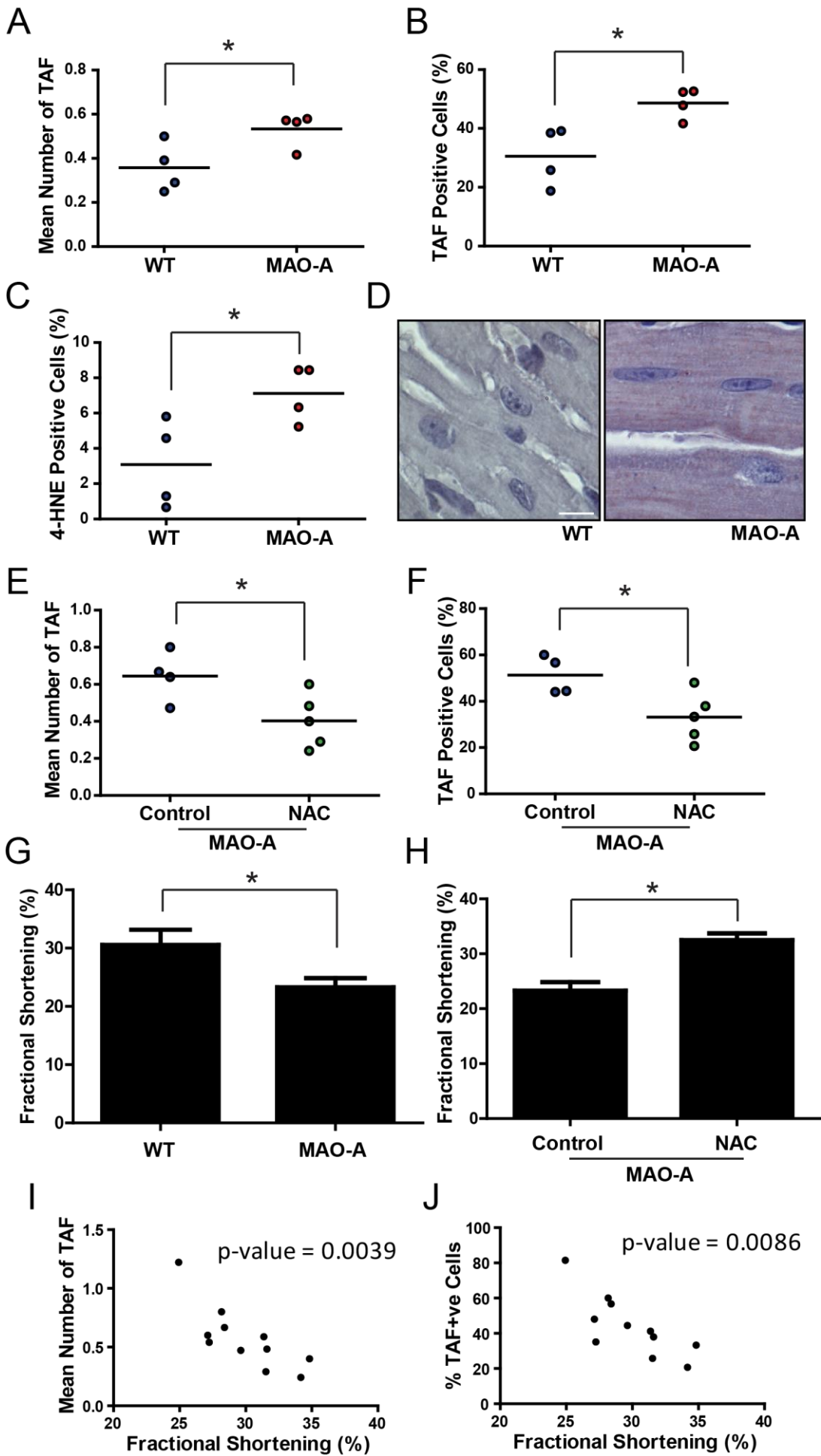


**Figure 5-2. MAO-A Overexpression drives TAF generation in mouse cardiomyocytes *in vivo*.** (A) Mean number of TAF – (B) Mean percentage of TAF positive – cardiomyocytes from 3 month old WT and MAO-A transgenic mice. Data are represented as the mean for individual animals, with the horizontal line representing group mean. (C) Mean percentage of 4-HNE positive cardiomyocytes in cardiomyocytes from WT and MAO-A transgenic mice. Data are represented as the mean for individual animals, with the horizontal line representing group mean (D) Representative images of 4-HNE IHC in WT and MAO-A transgenic mice (blue – nuclear counter stain; brown cytoplasmic staining – 4-HNE). (E) Mean number of TAF – (F) Mean percentage of TAF positive – cardiomyocytes from MAO-A transgenic mice supplemented with vehicle (Control) or antioxidant (NAC). Data are represented as the mean for individual animals, with the horizontal line representing group mean. (G-H) Fractional shortening analysis between (G) Wild-type compared to MAO-A transgenic at mice (H) MAO-A transgenic mice supplemented with vehicle (Control) or antioxidant (NAC). Data are mean  $\pm$  SEM of  $n=3$ . (I-J) Correlation analysis of the mean number of TAF (I) or percentage of TAF positive cells (J) versus fractional shortening (%) in both WT and MAO-A mice. Statistical analysis performed using two-tailed t test; \*  $P<0.05$ . Correlations were analysed using Pearson's correlation coefficient;  $P$  value  $<0.05$  considered significant.

## 5.2 A Reduction in MnSOD or Catalase Activity can Drive TAF Generation *in vivo*

Having shown that oxidative stress can drive TAF generation in cardiomyocytes via cardiac-specific MAO-A overexpression, we sought to investigate if other mouse models of elevated oxidative stress could also induce telomere dysfunction.

Catalase is an important antioxidant enzyme which catalyses the reaction of hydrogen peroxide into water and oxygen. Catalase expression has been shown to decrease with age in mouse brain and is associated with an increase in oxidative damage (Mo *et al.*, 1995). Interestingly, over-expression of mitochondrial catalase (mCAT) in mice attenuates of  $H_2O_2$  production, oxidative stress and mitochondrial deletions, as well as delaying the development of both cataracts and cardiac pathologies, and extending lifespan (Schriner *et al.*, 2005b). Overexpression of mCAT can also attenuate the age-dependent development of cardiomyopathies in mice which have mutations in mitochondrial DNA polymerase gamma, which are associated with elevated ROS, cardiac fibrosis, hypertrophy and dilatation (Dai *et al.*, 2010). We therefore wanted to ascertain if oxidative stress caused by aberrant catalase expression could also elevate TAF in cardiomyocytes and our immuno-FISH

analysis revealed that catalase<sup>-/-</sup> mice have both a significantly elevated mean number of TAF and mean percentage of TAF positive cells (Figure 5-3A-B).

Superoxide dismutases (SOD) are a family of antioxidant enzymes which catalyse the dismutation of superoxide to hydrogen peroxide and oxygen. Manganese superoxide (MnSOD) is a SOD which resides within mitochondria, and thus plays an important role in the detoxification of reactive oxygen species produced as a by-product of oxidative phosphorylation. Homozygous mutant mice for MnSOD die within a couple of weeks and present multiple pathologies including: metabolic acidosis, accumulation of lipid in liver and skeletal muscle, and dilated cardiomyopathy (Li *et al.*, 1995). Heterozygous mutants MnSOD<sup>-/+</sup> are viable, however are associated with an age-dependent elevation in vascular oxidative stress (Brown *et al.*, 2007). We used this model to investigate cardiomyocyte TAF generation and immuno-FISH analysis revealed that MnSOD<sup>-/+</sup> mice have both a significantly elevated mean number of TAF and mean percentage of TAF positive cells (Figure 5-3C-D).

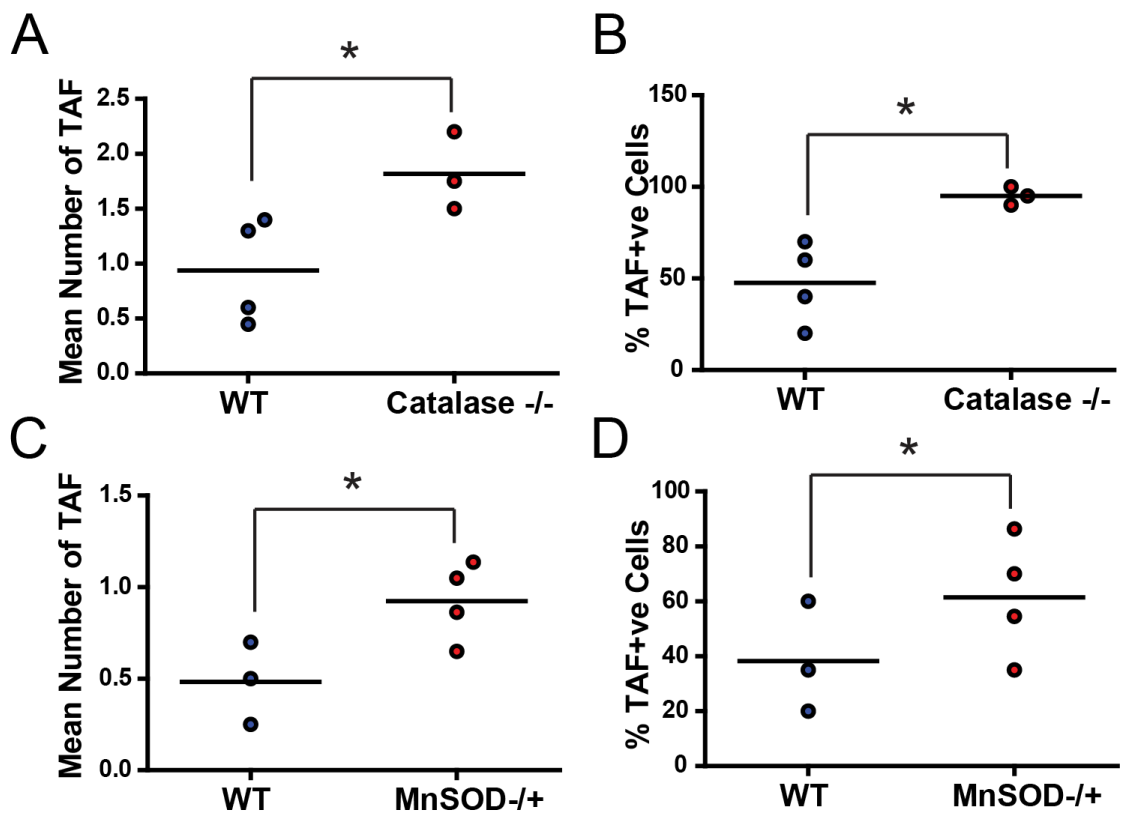


**Figure 5-3. Catalase<sup>-/-</sup> and MnSOD<sup>+/-</sup> models of Elevated Oxidative Stress also Drive TAF in Cardiomyocytes *in vivo*.** (A) Mean number of TAF – (B) Mean percentage of TAF positive – cardiomyocytes from WT and Catalase<sup>-/-</sup> transgenic

mice. Data are represented as the mean for individual animals, with the horizontal line representing group mean. **(C)** Mean number of TAF – **(D)** Mean percentage of TAF positive – cardiomyocytes from WT and MnSOD-/+ transgenic mice. Data are represented as the mean for individual animals, with the horizontal line representing group mean. Statistical analysis performed using two-tailed t test; \*  $P < 0.05$ .

### 5.3 mTOR Inhibition Impacts on ROS and Senescence in Human Fibroblasts

Mitochondria have long been implicated in oxidative stress-induced ageing phenotypes (Harman, 1972), and interestingly our group have recently published research which shows that many features of the senescent phenotype, including pro-inflammatory cytokine are dependent on increased mitochondrial density through a pathway involving mTORC1 phosphorylation (Correia-Melo *et al.*, 2016).

Furthermore, we show that during senescence, mitochondrial density is increased via mTOR activation, which leads to PGC-1b-dependent mitochondrial biogenesis. We therefore investigated if mTOR inhibition could attenuate this increase in mitochondrial biogenesis and subsequent increases in ROS and cellular senescence in cells which had undergone severe genotoxic stress. For this part of the study, we switched from using cardiomyocytes as our model, to human fibroblasts, as fibroblasts have a greater proliferation rate *in vitro*, which allows for an increase in experimental scope, as well as displaying a high resistance to apoptosis, thus making them ideal for investigating cellular senescence.

Flow cytometry analysis revealed a dose-dependent increase in mitochondrial mass following X-irradiation (Figure 5-4A). Furthermore, correlation analysis showed that this X-irradiation dose-dependent increase in mitochondrial mass also correlated with numerous senescence markers such as an increase in SA- $\beta$ -gal activity, an increase in p21 expression (by western blot), a decrease in percentage of cells positive for Ki-67 proliferation marker, and an increase in  $\gamma$ H2AX DNA damage foci (Figure 5-4B). Kinetic analysis revealed that both mitochondrial mass and ROS levels increase significantly until day 2 following X-irradiation with 20Gy, until they form a plateau which is continued until the final time point at day 10. When ROS is normalised to mitochondrial mass, there is no significant difference following exposure to 20Gy X-irradiation (Figure 5-4C).

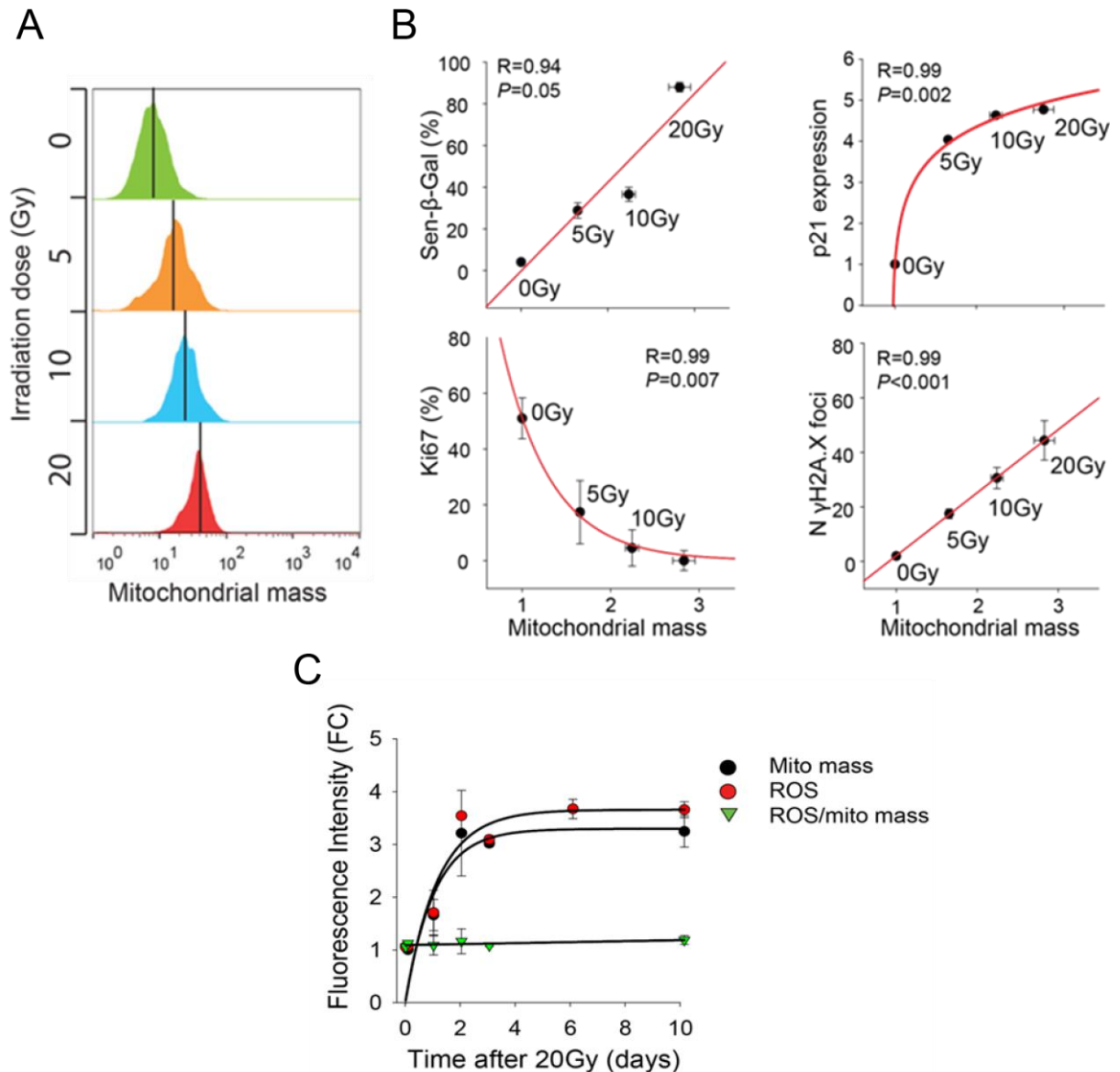


**Figure 5-4. Mitochondrial mass increases with X-irradiation and is associated with Cellular Senescence.** **(A)** Mitochondrial mass 3 days following X-irradiation with 0, 5, 10 or 20Gy, as measured by NAO fluorescence via flow cytometry. **(B)** Correlation analysis between mitochondrial mass and SA-β-Gal activity, p21 expression (measured by western blot), percentage of Ki-67 positive cells and mean number of γH2AX foci per cell, following varying doses of X-irradiation. Data are mean ± SEM of n=3. **(C)** Kinetic analysis of mitochondrial mass (as measured by NAO fluorescence via flow cytometry), ROS (as measured by DHR fluorescence via flow cytometry) and ROS/mitomass, following 20Gy X-irradiation in MRC5 fibroblasts. Data are mean ± SEM of n=3.

Next, we wanted to ascertain if the X-irradiation induced increase in mitochondrial mass was causative of observed ROS increases, by inhibiting the mitochondrial mass increase following X-irradiation. The mechanistic target of rapamycin (mTOR)

pathway has been widely associated with playing a key role in mitochondrial homeostasis, by affecting mitochondrial biogenesis and mitophagy, and mTORC1 has specifically been shown to control mitochondrial biogenesis (Morita *et al.*, 2013). To begin, we treated MRC5 fibroblasts with different genotoxic stresses, either in the presence of a vehicle control (DMSO) or rapamycin, and then quantified mitochondrial mass 3 days after. In young proliferating MRC5 cells, rapamycin has no effect on mitochondrial mass after treatment for 3 days. In MRC5 cells that have undergone genotoxic stress by either X-irradiation, etoposide, neocarzinostatin or hydrogen peroxide, the mitochondrial mass becomes significantly increased 3 days following treatment. However, if cells are cultured in the presence of rapamycin, there was no significant increase in mitochondrial mass, 3 days following treatment with any of the genotoxic stress treatments (Figure 5-5A).

Having shown that rapamycin treatment can abrogate a genotoxic-stress-induced increase in mitochondrial mass, we then wanted to ascertain if this had an effect on intracellular ROS levels. To detect ROS, we used flow cytometry with the superoxide indicator dihydroethidium (DHE), which exhibits blue fluorescence, until it becomes oxidised and then exhibits bright red fluorescence. In collaboration with Graeme Hewitt from ours and the Korolchuk laboratory, we found that ROS levels are significantly increased in MRC5 cells, 3 days following X-irradiation with 20Gy. Rapamycin treatment has no effect on ROS levels in untreated MRC5 cells, but significantly decreases ROS in X-irradiated cells compared to X-irradiated non-treated cells (Figure 5-5B).

To investigate if the decrease in ROS is due to inhibition of mTORC1 and not an off-target effect of rapamycin, we also performed siRNA to knock-down mTORC1 and observe ROS following X-irradiation. Using 2 different siRNAs targeted to mTORC1 and a scramble siRNA control, our data show that treatment with either mTORC1 siRNA has no effect on ROS on non-irradiated MRC5 cells, compared to treatment with scrambled siRNA. Confirming previous data (Figure 5-5B), we show that X-irradiation significantly increases ROS levels, however we also show that this increase in ROS can be significantly attenuated with both mTORC1 targeted siRNAs (Figure 5-5C).

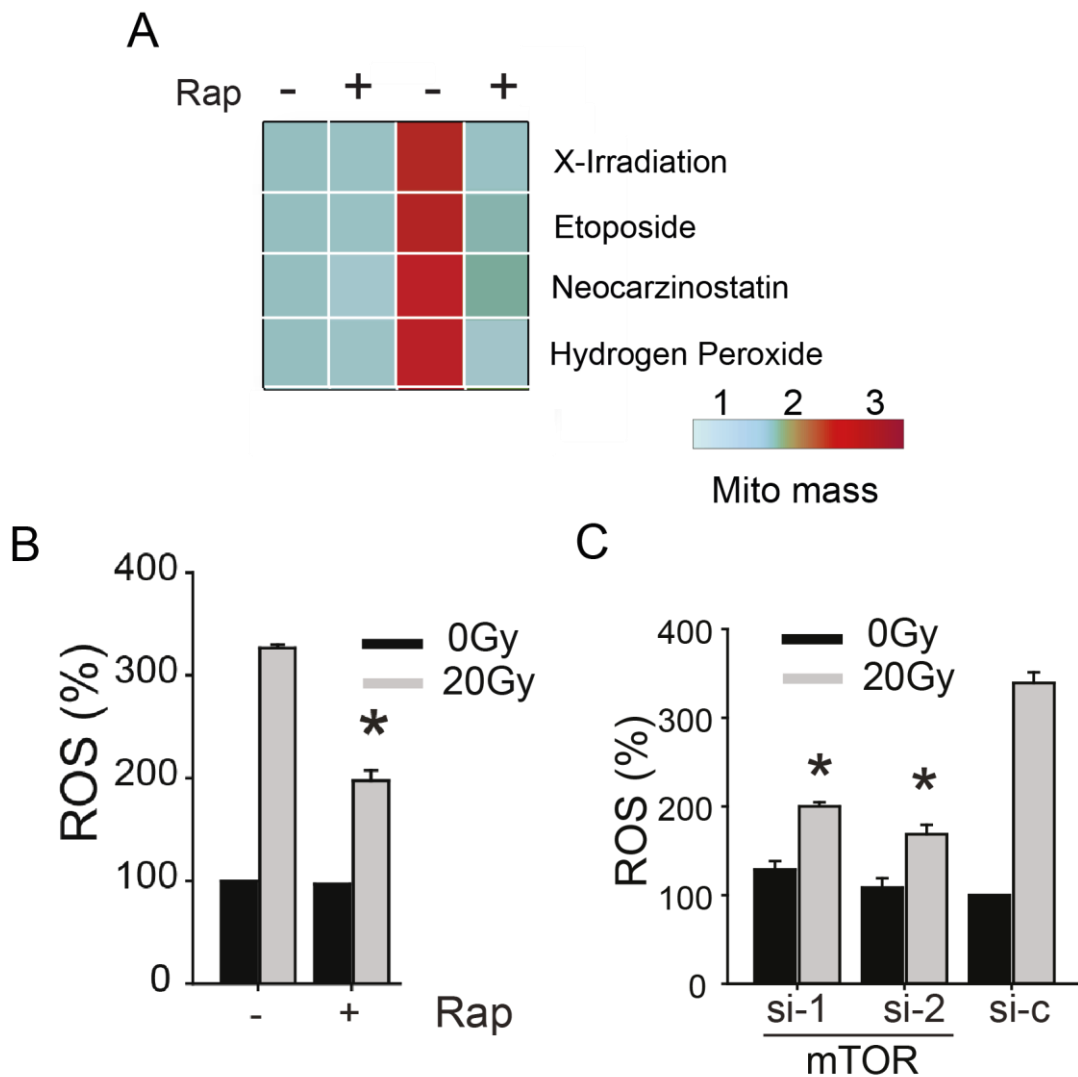
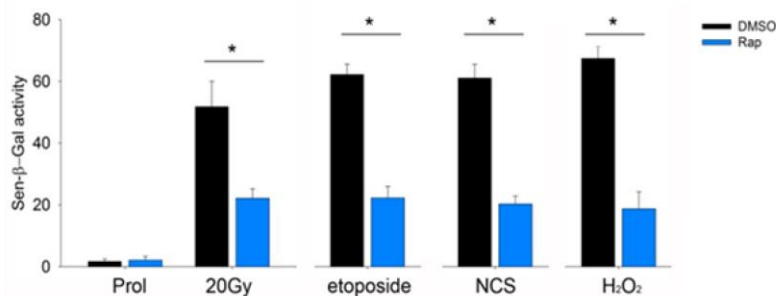


**Figure 5-5. X-irradiation- induced increases in mitochondrial mass can be attenuated with rapamycin treatment.** (A) Mitochondrial mass in MRC5 cells 3 days following genotoxic with either 20Gy X-irradiation, continual etoposide treatment (50 $\mu$ M), 1 hour treatment with neocarzinostatin (80ng ml<sup>-1</sup>), or 1 hour treatment with H<sub>2</sub>O<sub>2</sub> (400 $\mu$ M), in the presence of either vehicle control (DMSO) or rapamycin (100nM); as measured by NAO fluorescence via flow cytometry. Data are representative of 3 independent experiments per condition. (B) Intracellular ROS levels in MRC5 fibroblasts, as measured by DHE fluorescence, via flow cytometry, with or without rapamycin (100nm) and NAC (2.5mM), 3 days following 20Gy X-irradiation. Data are mean  $\pm$  SEM of  $n=3$ . (C) Effect of mTOR knock-down using siRNA on ROS measured by DHE fluorescence, 3 days following 20Gy X-irradiation. Data are mean  $\pm$  SEM of  $n=3$ . Statistical analysis performed using two-tailed t test; \*  $P<0.05$ .

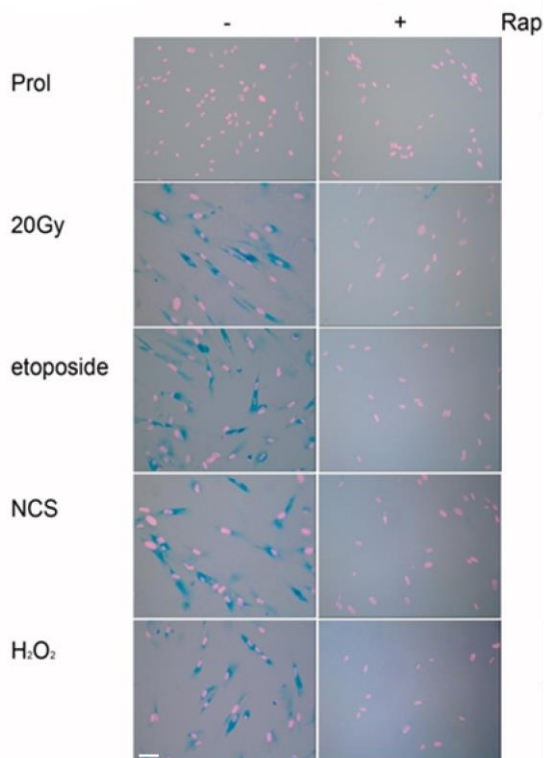
Having observed that mTOR inhibition, via rapamycin or siRNA treatment, could attenuate the appearance of ROS following numerous genotoxic stresses, we sought to ascertain if this would have any effect on the development of a senescent phenotype. MRC5 fibroblasts were treated with a range of genotoxic stresses, either

X-irradiation, etoposide, neocarzinostatin, or H<sub>2</sub>O<sub>2</sub>. After 10 days, SA-β-Gal activity was significantly elevated after each treatment compared to an untreated control. For each treatment, we also cultured cells in the presence of rapamycin, and observed a significant reduction in SA-β-Gal activity compared to the vehicle control for each condition. The level of SA-β-Gal was still significantly higher than non-treated controls for each of the rapamycin-treated genotoxic stress exposed cells (Figure 5-6A-B). After X-irradiation, p21 levels are significantly increased after 2 days, however this could be attenuated with rapamycin treatment (Figure 5-6C).

**A**



**B**



**C**

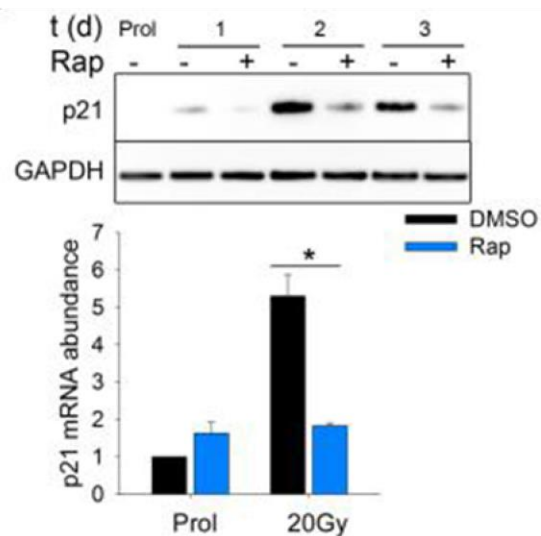


#### Figure 5-6. mTOR inhibition attenuates genotoxic stress induced senescence.

**(A)** Mean percentage of MRC5 cells staining positive for SA- $\beta$ -Gal activity 10 days following genotoxic stress with 20Gy X-irradiation, continual etoposide treatment (50 $\mu$ M), 1 hour treatment with neocarzinostatin (80ng ml<sup>-1</sup>), or 1 hour treatment with H<sub>2</sub>O<sub>2</sub> (400 $\mu$ M), in the presence of either vehicle control (DMSO) or rapamycin (100nM). Data are mean  $\pm$  SEM of  $n=3$ . **(B)** Representative SA- $\beta$ -Gal images (Cytoplasmic blue – SA- $\beta$ -Gal; pink – nucleus). Scale bar: 40 $\mu$ M. **(C)** p21 expression (measured by western blot) in MRC5 cells 1, 2 and 3 days following genotoxic stress with 20Gy X-irradiation, continual etoposide treatment (50 $\mu$ M), 1 hour treatment with neocarzinostatin (80ng ml<sup>-1</sup>), or 1 hour treatment with H<sub>2</sub>O<sub>2</sub> (400 $\mu$ M), in the presence of either vehicle control (DMSO) or rapamycin (100nM). Data are mean  $\pm$  SEM of  $n=3$ . Statistical analysis performed using two-tailed t test; \*  $P<0.05$ .

### 5.4 mTOR Inhibition Impacts on DDR During Senescence in Human Fibroblasts

Having observed that mTOR inhibition could attenuate ROS accumulation after senescence-inducing stimuli, we sought to ascertain if this was acting via a DDR. Research has shown that both telomeric and non-telomeric foci contribute to the initiation of cellular senescence (Nakamura *et al.*, 2008), and ROS have been implicated in replenishing short-lived DNA damage foci following senescence (Passos *et al.*, 2010). We investigated if rapamycin treatment could attenuate this increase in secondary DNA damage foci, and if this was ROS dependent.

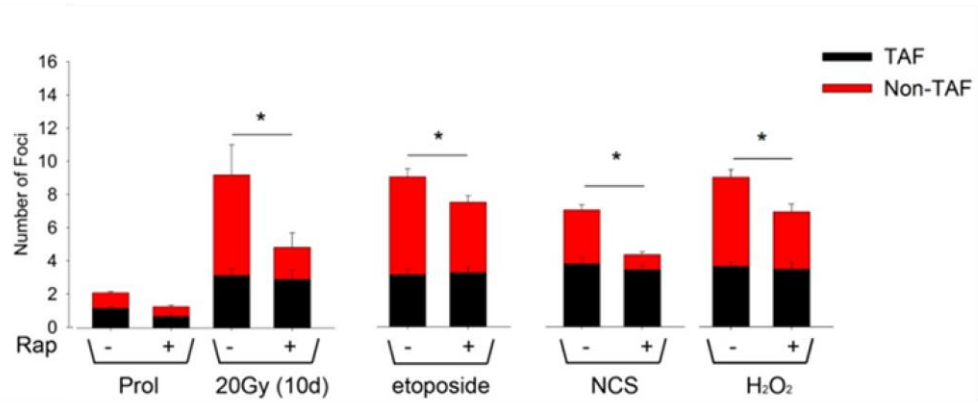
To begin, we treated MRC5 cells with various genotoxic stresses, and cultured them for 10 days either in the presence of a vehicle control (DMSO) or rapamycin, before performing immuno-FISH to quantify both TAF and non-TAF. Our analysis revealed there is a significant increase in both telomeric and non-telomeric DNA damage foci, 10 days following genotoxic stress with either: X-irradiation, etoposide, neocarzinostatin or H<sub>2</sub>O<sub>2</sub>, compared to untreated control cells. However, those cells cultured in the presence of rapamycin had a significantly reduced mean number of non-TAF for each genotoxic stress treatment, whereas the mean number of TAF was unaltered (Figure 5-7A-B).

To test whether the reduction in non-telomeric foci was due to rapamycin suppressing ROS generation, in collaboration with Graeme Hewitt from ours and the Korolchuk laboratory, we induced genotoxic stress in MRC5 cells with 20Gy X-

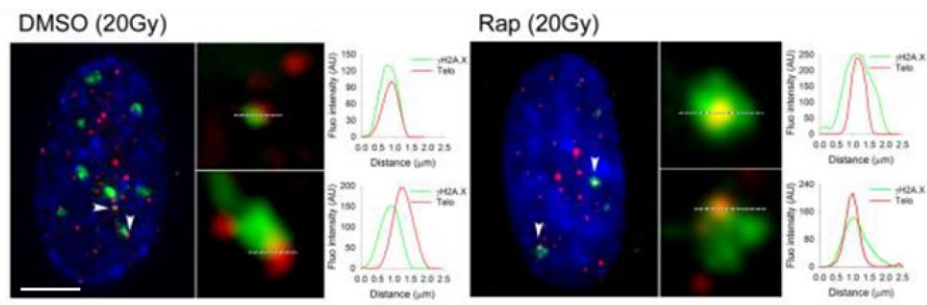
irradiation, and then cultured cells for a further 3 days in presence of rapamycin or NAC, or both together. Similar to before (Figure 5-7C), we observed an increase in both TAF and non-TAF after X-irradiation, but a decrease in only non-TAF following rapamycin treatment. Moreover, we found that NAC treatment alone also reduces the number of non-TAF to similar levels as to with rapamycin treatment alone, and likewise TAF remain unaffected. Furthermore, when we treat X-irradiated cells with both rapamycin and NAC, non-TAF are reduced to the same level as with either treatment separately i.e. there is no cumulative effect. To confirm that NAC treatment was reducing ROS levels in X-irradiated MRC5 cells; as before, we treated cells with 20Gy and cultured them for 3 days in the presence of rapamycin or NAC, or both together, and then quantified intra-cellular ROS levels using flow cytometry analysis of DHE fluorescence. Neither rapamycin, NAC or a combination of the two have any significant effect on ROS levels in non-irradiated control cells. Expanding on our data showing that rapamycin significantly reduces ROS levels in X-irradiated cells (Figure 5-5), we also observed that NAC treatment reduced ROS to a similar level (Figure 5-7D). Moreover, the combination of rapamycin and NAC reduced ROS levels to a similar level as with each treatment alone, once again signifying no cumulative effect (Figure 5-7E).

To test whether mTORC1 inhibition impacted on DDF stability, we transfected MRC5 fibroblasts with an AcGFP-53BP1c fusion protein, which allowed time resolved live-cell microscopy kinetic tracking of DDF after X-irradiation. In collaboration with Glyn Nelson from the von Zglinicki laboratory, we X-irradiated transfected MRC5 cells with 20Gy, and then cultured them in either a vehicle control (DMSO) or rapamycin, before conducting live-cell microscopy 3 days after IR. We observed that short-lived 53BP1 foci (<15 hours) were significantly reduced in irradiated cells treated with rapamycin treatment, but long-lived foci were unaffected (>15h) (Figure 5-7E).

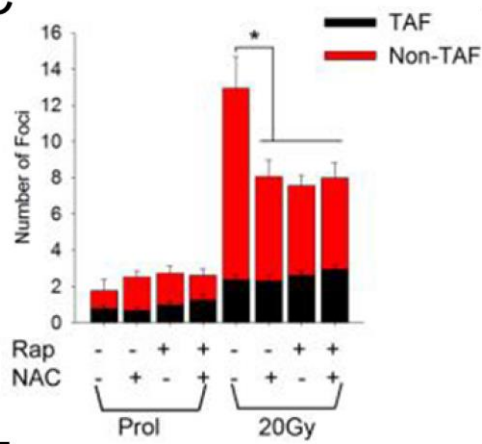
**A**



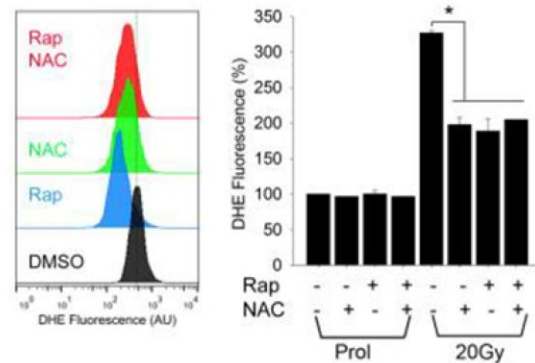
**B**



**C**



**D**



**E**

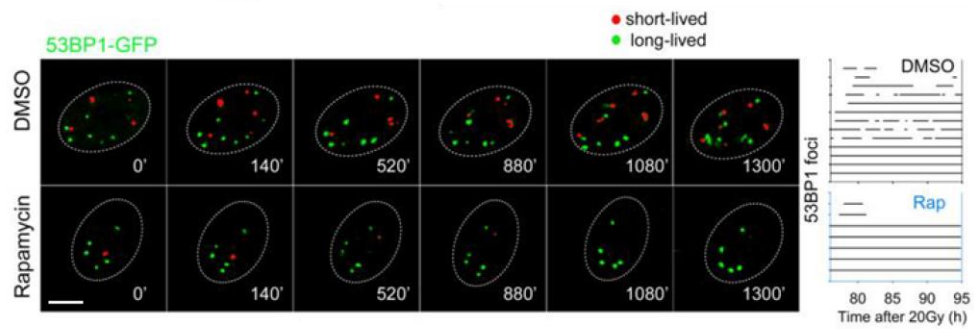


**Figure 5-7. mTOR Inhibition Reduces Replenishment of Short-lived foci following X-irradiation via ROS attenuation. (A)** Mean number of TAF and non-TAF in MRC5 cells, 10 days following genotoxic stress with 20Gy X-irradiation, continual etoposide treatment (50 $\mu$ M), 1 hour treatment with neocarzinostatin (80ng ml<sup>-1</sup>), or 1 hour treatment with H<sub>2</sub>O<sub>2</sub> (400 $\mu$ M), in the presence of either vehicle control (DMSO) or rapamycin (100nM), data are mean  $\pm$  SEM of  $n=3$ . **(B)** Representative images of  $\gamma$ H2AX immuno-FISH in MRC5 fibroblasts 3 days after x-irradiation with 20Gy, treated with either DMSO or rapamycin. Images are Huygens (SVI) deconvolved Z-projections of 3 $\mu$ M stacks taken with a 100X oil objective. White arrows indicate co-localisation between  $\gamma$ H2AX and telomeric signal, and co-localising foci are amplified in the right panel (amplified images are from single Z-planes where co-localisation was found). Graphs represent quantification of  $\gamma$ H2AX and telomere signals in selected regions of interest (dotted lines). Scale bar: 5 $\mu$ M. **(C)** Mean number of TAF and non-TAF in MRC5 cells, 3 days following X-irradiation with 20Gy, in the presence of either vehicle control (DMSO) or rapamycin (100nm) and NAC (2.5mM). Data are mean  $\pm$  SEM of  $n=3$ . Scale bar: 5 $\mu$ M. **(D)** Mean DHE fluorescence in MRC5 cells, 3 days following X-irradiation with 20Gy, in the presence of either vehicle control (DMSO) or rapamycin (100nm) and NAC (2.5mM). Data are mean  $\pm$  SEM of  $n=3$ . **(E)** Confocal time series of MRC5 expression AcGFP-53BP1c 3 days after 20Gy X-irradiation at the indicated times (min), with and without rapamycin treatment. Images are compressed stacks (maximum intensity projections) with a 4.5 $\mu$ m focal depth. 53BP1 foci with lifespans of less than 15 hours are labelled in red. Representative traces of AcGFP-53BP1c foci in one MRC5 nucleus with (rap) and without (DMSO) rapamycin are shown on the right. Each bar represents the track of one individual focus recorded for the indicated time interval. Scale bar: 5 $\mu$ M. Statistical analysis performed using One way ANOVA or two-tailed t test; \*  $P<0.05$ .

It has previously been published that a persistent DDR during senescence is involved in a feedback loop which drives mitochondrial dysfunction and increased ROS production (Passos *et al.*, 2010). Having shown that mTOR inhibition can attenuate this increase in ROS and markers of senescence following treatment with senescence-inducing stimuli, we wanted to ascertain if these effects were acting through this pathway, by inhibiting the DDR. In collaboration with Clara-Correia Melo from ours and the von Zglinicki laboratory, we treated MRC5 fibroblasts with 20Gy X-irradiation, supplemented them with either or both rapamycin and the ATM inhibitor Ku55933, 3 days following IR, and then analysed the cells at day 10 post-IR. Similarly to rapamycin treatment, ATM inhibition was also shown to inhibit senescence-associated increases in mitochondrial mass, however there was no cumulative effect when combined (Figure 5-8A-B). Furthermore, our data show that separately, both ATM inhibition and mTOR inhibition can attenuate the number of

$\gamma$ H2AX foci, decrease SA- $\beta$ -gal activity, and reduce p21 expression, however, again, there is no accumulative effect upon treatment with both (Figure 5-8C-E).

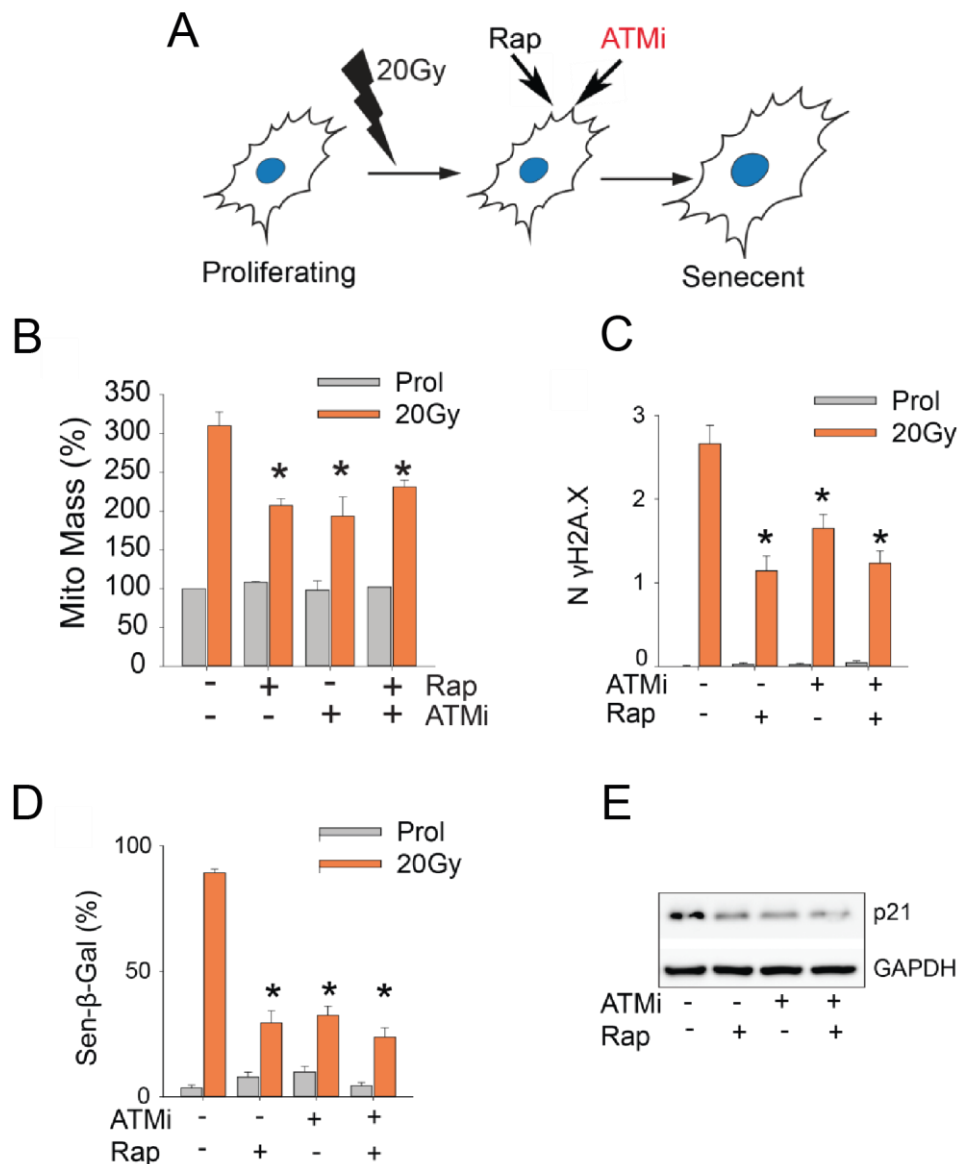


**Figure 5-8. An epistatic association between mTOR and ATM inhibition in attenuating the development of X-irradiation-induced senescence. (A)** A schematic illustration showing that proliferating MRC5 fibroblasts were treated with 20Gy X-irradiation, and treated with either an ATM inhibitor (Ku55933) or rapamycin or a combination of both 3 days following IR, and then fixed at day 10 post-IR for analysis. **(B)** Mean mitochondrial mass (NAO fluorescence. Data are mean  $\pm$  SEM of  $n=3$ . **(C)** Mean number of  $\gamma$ H2AX foci per cell. Data are mean  $\pm$  SEM of  $n=3$ . **(D)** Mean percentage of SA- $\beta$ -Gal positive cells. Data are mean  $\pm$  SEM of  $n=3$ . **(E)** Mean p21 expression via western blot. Data are mean  $\pm$  SEM of  $n=3$ . Statistical analysis performed using two-tailed t test; \*  $P<0.05$ .

## 5.5 mTOR Inhibition Impacts on TAF and ROS in Cardiomyocytes

Having shown that mTORC1 inhibition can reduce the accumulation of DNA damage which arises from an increase in ROS after exposure to genotoxic stress, we wanted to investigate what effect mTORC1 inhibition would have on DNA damage and senescence in cardiomyocytes *in vivo*. Rapamycin supplementation has been shown to delay a number of age-related changes in mice, including alterations in tendons, endometrium, adrenal glands, liver and heart (Wilkinson *et al.*, 2012), and can extend the lifespan of a number of different organisms (Bjedov *et al.*, 2010; Zhang *et al.*, 2014). We supplemented the diet of male *C57BL/6* mice with rapamycin from 3 months of age, and then culled one group at 6.5 months of age and other at 15 months. At 6.5 months, there is no difference in either mean number of TAF or the mean percentage of TAF positive cardiomyocytes for mice fed on either a control or rapamycin diet. We observed a significant increase in both the mean number of TAF and the mean percentage of TAF positive cardiomyocytes from 6.5 months to 15 months of age in the control-fed mice. Moreover, 15 months old mice fed on a rapamycin diet had a significantly less mean number of TAF and the mean percentage of TAF positive cardiomyocytes compared to their age-matched control-fed mice (Figure 5-9A-B). Furthermore the TAF levels in cardiomyocytes from 15 month rapamycin-fed mice were not significantly different to control-fed mice of only 6.5 months of age (Figure 5-9A-B). Our analysis revealed that there is no significant variation in the level of non-TAF in cardiomyocytes between control-fed mice of 6.5 months and 15 months of age, and a rapamycin diet had no effect on either group (Figure 5-9C). Finally, we show that rapamycin treatment attenuates the accumulation of the lipid peroxidation marker 4-HNE and the cyclin-dependent kinase inhibitor p21 (Figure 5-9D-E).

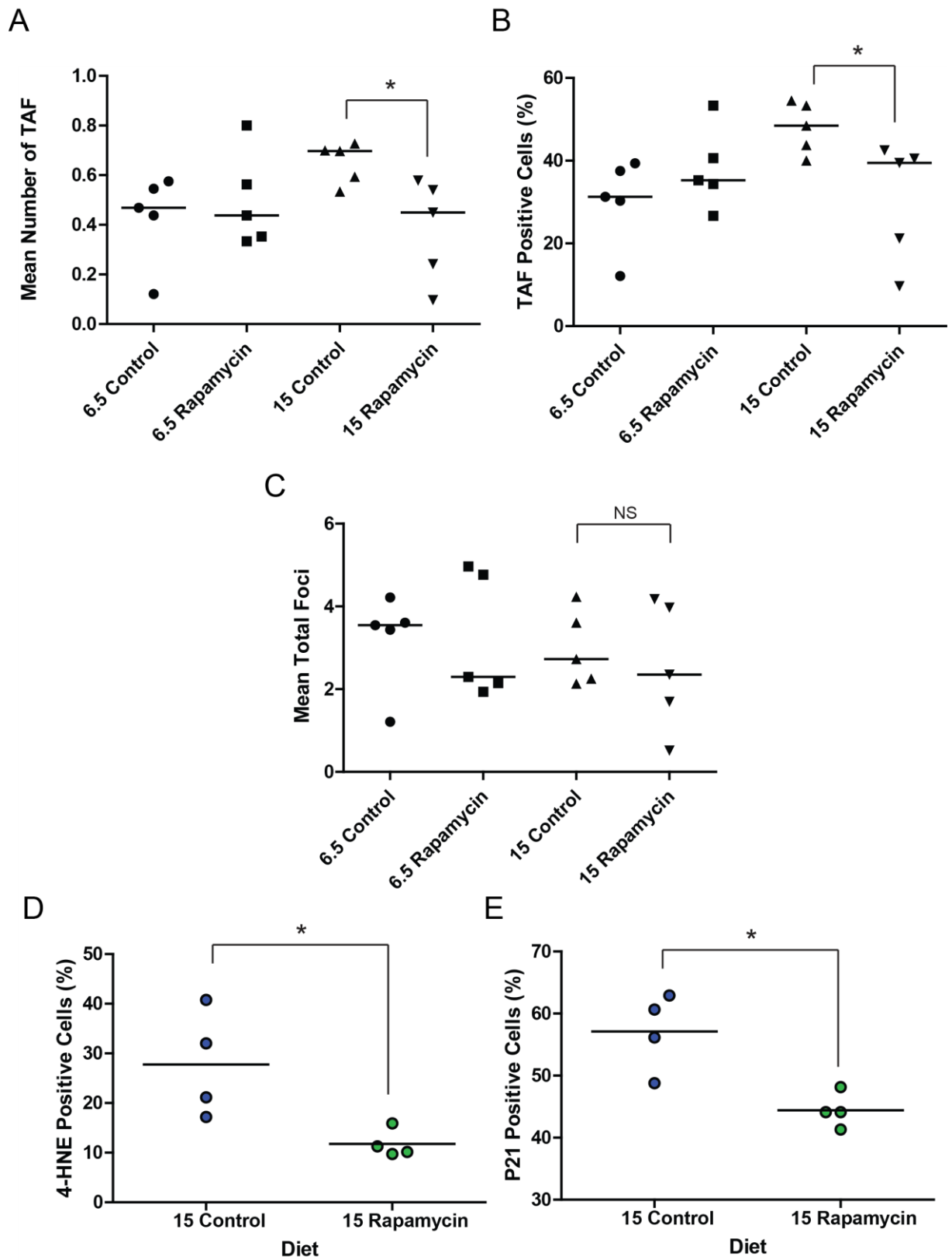


**Figure 5-9. Rapamycin supplemented diet reduces age-associated TAF accumulation, oxidative stress and senescence markers. (A)** Mean number of

TAF – **(B)** Mean percentage of TAF positive – cardiomyocytes in mice aged 6.5 and 15 months, on either a control or rapamycin supplemented diet. Data are represented as the mean for individual animals, with the horizontal line representing group mean. **(C)** Mean number of non-TAF in cardiomyocytes in mice aged 6.5 and 15 months, either on either a control or rapamycin supplemented diet. Data are represented as the mean for individual animals, with the horizontal line representing group mean. **(D-E)** Quantification of the percentage of cardiomyocytes staining positive for 4-HNE (D) or p21 (E) by IHC, 15 month old mice fed on either a control or rapamycin supplemented diet. Data are represented as the mean for individual patients, with the horizontal line representing group mean. Statistical analysis performed using One way ANOVA or two-tailed t test; \*  $P < 0.05$ .

## 5.6 Discussion

ROS are continuously formed in living cells, both via endogenous mechanisms, such as oxidative phosphorylation, as well as external sources such as ionising radiation. It is estimated that around 0.1%-1% of oxygen used during oxidative phosphorylation is converted to superoxide anion (Chance *et al.*, 1979). Moreover, cardiomyocytes contain an extremely high mitochondrial density, and thus produce considerable amounts of superoxide anion (Kaul *et al.*, 1993). Whilst superoxide is not a strong oxidant, and has limited reactivity, it is converted to  $H_2O_2$  by superoxide dismutase, which is a considerably more potent oxidant. ROS have been shown to oxidise bases, which can lead to mutation, as well as produce SSB, which if two are in close proximity on complementary DNA stands, are thought to generate DSB (Bont, 2004). Although ROS are involved in physiological processes, such as cell signalling (D'Autréaux and Toledano, 2007), and microbial defence (Dupre-Crochet *et al.*, 2013), if the level of ROS generation exceeds the rate in which natural antioxidant mechanisms can stabilise ROS, then oxidative stress ensues.

Previously, we have shown that TAF can be induced *in vitro* by exposing cells to oxidative stress, via  $H_2O_2$  treatment, and this can occur independently of DNA replication. Following on from this, we observed that TAF accumulate *in vivo*, and this correlated with an increase in the oxidative stress marker 4-HNE. Mitochondrial ROS production has also been shown to increase with age in both the heart (Judge *et al.*, 2005) and the vascular system of rats (Ungvari *et al.*, 2007). Interestingly,  $H_2O_2$  production has been shown to increase in rat hearts with age, which is dependent upon increases in MAO-A expression (Maurel *et al.*, 2003). MAO-A catalyses the oxidative deamination of monoamines, and produces  $H_2O_2$  as one of the by-products

of this reaction, and cardiac-specific over-expression of MAO-A results in elevated ROS leading to increases in DNA oxidation, with mitochondrial DNA especially sensitive (Villeneuve *et al.*, 2013). In particular, mitochondrial 8-oxoguanine (8-oxo-dG) was observed, which during replication can lead to the incorrect pairing of adenine with 8-oxo-dG, which upon further DNA replication drives a C to A and G to C mutation of the genetic code. Moreover, it has been hypothesised that increased mitochondrial mutations lead to an inefficient ETC, which is more prone to electron leakage, and ROS generation, which in turn leads to more genetic mutations, therefore instigating what has been coined a 'vicious cycle' positive feedback loop (Alexeyev *et al.*, 2004). Elevated ROS are known to increase lipid peroxidation, and our data from the previous chapter show a significant age-dependent increase in 4-HNE, which has also been shown to be associated with other senescence markers, such as  $\gamma$ H2AX and SA- $\beta$ -Gal (Wang *et al.*, 2009; Wang *et al.*, 2010; Nelson *et al.*, 2012), and is considered to be the most toxic aldehyde formed as a consequence of lipid peroxidation (Esterbauer *et al.*, 1991). Interestingly, our gene expression analysis in isolated mouse cardiomyocytes revealed an age-dependent up-regulation of MAO-A, and thus we wanted to further investigate if ROS could induce TAF *in vivo*. To specifically test the effect of elevated ROS on cardiomyocytes, we acquired cardiac tissue from a transgenic mouse model which over-expresses MAO-A specifically in cardiomyocytes and analysed TAF. Previous research has shown that the levels of MAO-A expression in the cardiomyocyte-specific MAO-A over-expressing mice are comparable to those found in aged mice, and thus can be considered a physiologically relevant model (Villeneuve *et al.*, 2013). Our data show that MAO-A overexpression can lead to a significant increase in TAF in mice, which as expected, is coupled with an increase in the oxidative stress marker 4-HNE. Furthermore, 4-HNE accumulation has previously been shown to be associated various senescent markers, including  $\gamma$ H2AX and SA- $\beta$ -Gal (Wang *et al.*, 2009; Wang *et al.*, 2010; Nelson *et al.*, 2012). MAO-A is involved in oxidative deamination of dietary amines and neurotransmitters, which produce, not only H<sub>2</sub>O<sub>2</sub> as a by-product, but also ammonia, as well as aldehyde from the corresponding amine (Kaludercic *et al.*, 2014). Moreover, to test if the observed TAF increases were ROS-dependent, we supplemented the drinking water of a MAO-A transgenic mouse group with the anti-oxidant *N*-acetyl-cysteine (NAC), and observed that the increases in TAF were attenuated. Unfortunately, we did not have corresponding control groups, which were fed on an antioxidant diet, and thus there still remains the

possibility the observed decreases were due to attenuation of the age-dependent oxidative damage that we have previously observed. It would have also been beneficial to have performed 4-HNE staining on the NAC treated mice to observe if the anti-oxidant was attenuating the accumulation of oxidative damage with time, although once again, the non-transgenic controls would have been beneficial to conclude that the changes were not attenuation of physiological age-dependent changes, as opposed to MAO-A-dependent effects. Finally, it would be interesting to investigate if MAO-A inhibition could attenuate the age-dependent increase in cardiomyocyte TAF.

To further investigate if oxidative stress could lead to telomere dysfunction, we analysed TAF in catalase *-/-* mice. Catalase is responsible for the conversion of H<sub>2</sub>O<sub>2</sub> into water and oxygen, and in mammalian cells it is mainly localised to the peroxisomes, where H<sub>2</sub>O<sub>2</sub> generation from various oxidases is high (van den Bosch *et al.*, 1992). Interestingly, catalase has also been discovered to be expressed in mouse and rat cardiac mitochondria (Radi *et al.*, 1991; Rindler *et al.*, 2013). In response to being fed a high fat diet, cardiac H<sub>2</sub>O<sub>2</sub> levels become elevated, due to the increase in fatty acid oxidation required for fat metabolism, and consequently, both cardiac mitochondrial catalase content and activity also become elevated (Rindler *et al.*, 2013). We observed an increase in telomere dysfunction in cardiomyocytes of catalase *-/-* mice, which compliments both our *in vitro* data providing evidence that H<sub>2</sub>O<sub>2</sub> treatment can induce TAF independently of cell division, as well as our *in vivo* data showing an increase in TAF in MAO-A over-expressing cardiac tissue. It would be interesting to investigate the relative effects of organelle-catalase modulation on TAF, for example mitochondrial-specific overexpression of catalase leads to an increase in lifespan and delayed development of cardiomyopathy in mice, whereas peroxisomal- or nuclear-specific over-expression of catalase had no effect (Schriner *et al.*, 2005a).

It is thought that an age-dependent reduction in the activity of electron transport complexes I and IV in cardiac mitochondria leads to elevated electron leakage and thus increased mitochondrial ROS generation (Navarro and Boveris, 2007). Interestingly, mice which have a decreased birth weight due to deprived *in utero* nutrition, show increased incidence of cardiovascular disease, which is thought to arise due to accelerated ageing caused by elevated oxidative stress. Moreover, by supplementing the diet of these mice with coenzyme Q<sub>10</sub>, an antioxidant and integral

ETC component, many of the accelerated ageing phenotypes such as DNA damage, telomere shortening, oxidative stress and cellular senescence, were reversed (Tarry-Adkins *et al.*, 2013), thus further implicating aberrant ROS production in cardiac ageing. To ascertain if mitochondrial ROS could be specifically contributing to TAF, we acquired hearts from MnSOD<sup>-/+</sup> mice and performed TAF analysis. MnSOD is the primary superoxide anion scavenger in mitochondria, and MnSOD activity is reduced by around 50% in MnSOD<sup>-/+</sup> mice, which is accompanied with elevated mitochondrial oxidative damage, and an increase in mitochondrial dysfunction, as quantified by a decrease in complex I respiration (Van Remmen *et al.*, 2001). Our data show that TAF are significantly decreased in MnSOD<sup>-/+</sup> mice, thus showing that mitochondrial ROS production can lead to telomere dysfunction if MnSOD activity is decreased. Furthermore, research has shown that there is an age-dependent decrease in cardiac MnSOD protein expression (Lu *et al.*, 2014), which may be a contributing factor to the age-dependent increase in TAF in cardiomyocytes.

Together, these data provide strong evidence that elevated ROS can lead to telomere dysfunction in cardiomyocytes *in vivo*, although the mechanism for this is not entirely understood. Cardiomyocyte proliferation is negligible and therefore the replication-induced conversion of a SSB to a DSB is unlikely, and thus one explanation for the observed increase in TAF is that ROS happens to cause two SSB in close proximity to one another so that a DSB is formed (Bont, 2004). The statistical likelihood of this would appear low, however data suggests that telomeres are more susceptible to oxidative stress-induced SSBs compared to the rest of the genome (Petersen *et al.*, 1998), and triple guanine repeats, as found in telomeric DNA, are particularly sensitive to oxidative damage (Henle *et al.*, 1999), and it is possible the telomere repeat code may have evolved specifically to be more susceptible to oxidative damage in order to protect genomic DNA from damage. Furthermore, budding yeast telomeres have been shown to often cluster at the nuclear periphery (Hediger *et al.*, 2002), and thus are spatially more susceptible to interacting with ROS diffusing across the nuclear membrane. However, contrary to this, lymphocyte telomeres have been shown to have a higher propensity for a central nuclear localisation (Amrichová *et al.*, 2003). Although, research has shown that during post-mitotic nuclear assembly, HeLa cells telomeres become enriched at the nuclear periphery, a process thought to be driven by an interaction between the shelterin component RAP1 and the nuclear envelope protein Sun1 (Crabbe *et al.*, 2012). It

would be interesting to assess the nuclear localisation of telomeres in cardiomyocytes *in vivo*, and to also investigate if those found near the peripheries are more prone to TAF. Moreover, the latter analysis may be flawed in fixed cells if cardiomyocyte telomeres have plasticity in their movement, for example in U2OS telomeres, live-cell imaging revealed that the majority of telomeres are physically constrained to a radius of around 0.5 $\mu$ M, however a significant minority were seen to move far greater distances (Molenaar *et al.*, 2003). To address this, it would be necessary to perform 3D live-cell imaging, using both a fluorescent DDR and telomere marker, with exogenous treatment of a membrane-permeable oxidative reagent, and analyse if there is an altered propensity for damage accumulation depending upon nuclear localisation.

It could also be surmised that the occurrence of DSB from the accumulation of SSB in times of elevated oxidative stress are not particularly rare occurrences, and are even more likely to occur at telomeres, considering it has been shown that UV-induced telomeric SSBs are less efficiently repaired when located at telomeres (Kruk *et al.*, 1995). Moreover, research has shown that X-irradiation-, oxidative stress- and genotoxic stress-induced telomere damage is persistent, and likely irreparable (Fumagalli *et al.*, 2012; Hewitt *et al.*, 2012). In this instance, telomeres would be more susceptible to accumulation of SSB than genomic DNA, due to decreased repair capability, resulting in an increased probability of DSBs forming, which once formed are irreparable (Fumagalli *et al.*, 2012; Hewitt *et al.*, 2012).

Finally, another scenario to consider is that ROS do not physically cause TAF, however as they are important signalling molecules (D'Autréaux and Toledano, 2007), their aberrant generation could lead to the activation of cellular pathways which cause telomere dysfunction by some unknown mechanism.

Interestingly, when we collated all of the data from the MAO-A study and performed correlation analysis, we found that there was a significant inverse relationship between TAF abundance in cardiomyocytes and cardiac function, as measured by fractional shortening. From these data, one cannot infer that TAF drive cardiac dysfunction, however it would appear that TAF can be used a marker for cardiac dysfunction. Considering that telomere damage is thought to be irreparable (Fumagalli *et al.*, 2012; Hewitt *et al.*, 2012), and a large number of cardiomyocytes present at birth survive until organismal death (Bergmann *et al.*, 2009),

cardiomyocyte telomere damage may represent a molecular diary of cardiac stress endured throughout the lifetime of an organism. As previously described, in order to truly ascertain the effects of TAF *in vivo*, a cardiomyocyte-specific mouse model such as the TRF1-FokI would have to be generated.

In this and previous chapters, we have provided evidence for ROS driving telomere dysfunction in cardiomyocytes both *in vitro* and *in vivo*. It has previously been shown that ROS levels become elevated as a consequence of cellular senescence, at around 2 days following either X-irradiation, or telomere-dependent senescence induction via TRF2 inhibition (Passos *et al.*, 2010). Furthermore, this elevation in ROS was shown to maintain a flux of short-lived DDF, thus instigating a persistent DDR (Passos *et al.*, 2010), one of the key hallmarks of cellular senescence. An increase in both mitochondrial mass and ROS have been observed in response to oncogenic RAS activation, and thus it is thought that mitochondria-derived ROS could be specifically driving this stabilisation of senescence (Passos *et al.*, 2007; Moiseeva *et al.*, 2009; Passos *et al.*, 2010). In agreement with these data, 2-4 days following either, oxidative- or genotoxic stress-induced senescence in human fibroblasts, we observed a dose-dependent increase in mitochondrial mass, which was accompanied with an increase in ROS. When mitochondrial mass was normalised to ROS, there was no change following IR, suggesting that the increase in mitochondrial mass could be responsible for increased ROS production. In addition to this, we observed a significant correlation between mitochondrial mass and various markers of senescence, including decreased Ki67, increased  $\gamma$ H2AX DDF, and an elevation of both SA- $\beta$ -Gal activity and p21 expression. The mechanistic target of rapamycin (mTOR) pathway, and specifically activation of mTORC1, has been shown to drive mitochondrial biogenesis (Morita *et al.*, 2013). We therefore investigated if mTOR was involved in this senescence-associated increase of mitochondria, by treating cells with the mTORC1 inhibitor rapamycin. Moreover, we found rapamycin treatment to prevent the senescence-associated increase in mitochondrial mass following either oxidative- or genotoxic stress. Furthermore, mTORC1 inhibition by either rapamycin treatment or siRNA also prevented ROS elevation, as measured by DHE, following X-irradiation. Considering this abrogation of the senescence-associated ROS increase, we investigated if levels of DNA damage and markers of senescence were also affected. We observed that continuous rapamycin treatment could decrease both SA- $\beta$ -Gal activity and p21

expression, 10 days following genotoxic or oxidative stress with either X-irradiation, etoposide, NCS or H<sub>2</sub>O<sub>2</sub>; and interestingly we observed a decrease in the levels of non-telomeric DDF, however TAF were insignificantly altered. One explanation for this observation could be that rapamycin treatment increases the rate of DNA damage repair, which considering that telomeric DDF have been shown to be irreparable (Fumagalli *et al.*, 2012; Hewitt *et al.*, 2012), would result in a decrease in only non-telomeric DDF, as observed, however evidence suggests that rapamycin treatment actually suppresses both homologous recombination and NHEJ by impairing the recruitment of Rad51 and BRCA1 to DNA repair foci (Chen *et al.*, 2011). Another possibility is that rapamycin treatment attenuates the ROS-dependent feedback loop shown to replenish short-lived DNA damage foci (Passos *et al.*, 2010), and it has previously been published that short-lived foci are non-telomeric (Hewitt *et al.*, 2012), thus fitting our data. To test this idea, we supplemented cells with NAC, and found a similar decrease in non-TAF following X-irradiation compared to rapamycin treatment, however, when both NAC and rapamycin were combined, we observed no additive effect, suggesting that rapamycin was reducing non-TAF through decreasing the senescence-associated increase in ROS. Additionally, NAC and rapamycin treatment had similar effects on ROS levels following X-irradiation, with no additive effect when combined. We performed live-cell imaging, using an AcGFP-53BP1c fusion protein, to assess the nature of the DDF foci decreased by rapamycin treatment following X-irradiation. We observed a decrease in the number of short-lived DNA damage foci, and although this experiment was not performed with a live-cell telomere marker, we have previously published that short-lived foci do not co-localise with telomeres, and considering our data in fixed cells shows only non-TAF decreasing, it seems plausible to conclude that rapamycin treatment attenuates the senescence-associated secondary ROS-driven short-lived DDF (Passos *et al.*, 2010). Furthermore, our data support mTORC1 inhibition to be attenuating the senescent phenotype through an abrogation of ROS-driven DDR, as when we inhibit the key DDR protein ATM following senescence induction, we observe similar effects to rapamycin treatment, such as a decrease in SA-β-Gal activity and reduction in DDR, however we observed no accumulative effect when both ATM and rapamycin inhibitors are combined.

It may appear contradictory, that we have previously shown that ROS can induce TAF *in vivo*, yet we only observe an increase in non-TAF as a consequence of

secondary ROS generation *in vitro*. We hypothesised that the DSB *in vivo* could be generated from the accumulation of SSB in close proximity on complementary strands. In our *in vitro* model, we quantified telomere dysfunction at a maximum of 10 days following senescence-inducing treatments, whereas in our *in vivo* models, the minimum observation period was 3 months, therefore providing significantly longer amounts of time for the generation of DSB to occur.

We have shown there is an age-dependent increase in TAF in cardiomyocytes *in vivo*, that TAF can be induced via oxidative stress *in vivo*, and that mTORC1 inhibition can attenuate the development of senescence via decreasing the level of ROS and subsequent DNA damage *in vitro*. We therefore wanted to ascertain if mTORC1 inhibition could have an effect on TAF *in vivo*. By supplementing the diet of mice with rapamycin, our data show that mTORC1 inhibition from 3 months of age, has no effect on TAF accumulation in mouse cardiomyocytes at 6.5 months of age, but can significantly prevent the age-dependent increase in TAF seen between 6.5 and 15 months of age. Our data also show that rapamycin treatment prevents the accumulation of a senescent-phenotype in cardiomyocytes, as quantified by an attenuation of the age-associated increase of lipid peroxidation marker 4-HNE, and expression of cyclin-dependent kinase inhibitor p21. ROS production has also been shown to increase with age in rat hearts (Judge *et al.*, 2005), and our group have shown that mice fed on a diet supplemented with rapamycin have decreased mitochondrial content, as quantified by mitochondrial volume fraction and mtDNA copy number (Correia-Melo *et al.*, 2016). One interpretation could therefore be that mTORC1 inhibition attenuates age-dependent mitochondrial mass increases, therefore lowering oxidative stress, resulting in less DNA damage, and thus delaying the development of senescence. It would therefore seem inconsistent that we did not see a decrease in non-TAF, however we always observe greater variation in non-TAF, likely due to the constant flux of generation and repair (Passos *et al.*, 2010), and thus we might not have had a large enough population size to detect any subtle differences. TAF, however, are thought to be irreparable (Fumagalli *et al.*, 2012; Hewitt *et al.*, 2012), therefore intrinsically having less variation at any given moment, making them a considerably more robust marker for genotoxic stress with time. It has been reported that mTORC1 inhibition can improve cardiac function and reduce cardiac hypertrophy (Shioi *et al.*, 2003; McMullen *et al.*, 2004). Moreover, hypertrophy is a common phenotype of senescent cells (Demidenko and

Blagosklonny, 2009), and we have shown that TAF can induce hypertrophy in cardiomyocyte *in vitro*. An interesting experiment would be to see if rapamycin treatment could attenuate TAF-induced hypertrophy *in vitro*.

To conclude, our data show as a proof-of-principle, that oxidative stress can increase telomere dysfunction in cardiomyocytes, and we have shown in the previous chapter that TAF are associated with numerous markers of senescence in cardiomyocytes. Furthermore, we show that mTORC1 inhibition, which reduces ROS production, can attenuate both increases in TAF and the development of a senescent-like phenotype in cardiomyocytes both *in vitro* and *in vivo*. It will be important for future research to specifically induce DSB at telomeres to determine if TAF are causative, or merely a consequence of cardiomyocyte senescence *in vivo*.

## 6 Conclusions

Since the initial discovery that somatic cells have only a finite replicative capacity (Hayflick and Moorhead, 1961; Hayflick, 1965), numerous discoveries have contributed to cellular senescence becoming a field of scientific research in its own right. Senescence has been shown to be involved in an eclectic mix of physiological processes, including embryonic development (Rajagopalan and Long, 2012; Muñoz-Espín *et al.*, 2013a; Storer *et al.*, 2013), wound healing (Jun and Lau, 2010) and tumour suppression (Serrano *et al.*, 1997). Contrary to these beneficial roles, senescent cells have been implicated in eliciting a bystander effect which can induce paracrine senescence (Hubackova *et al.*, 2012a; Nelson *et al.*, 2012; Acosta *et al.*, 2013), drive age-related diseases *in vivo* (Baker *et al.*, 2011) and even produce a pro-tumourigenic micro-environment (Alspach *et al.*, 2013). One of the main drivers of these detrimental effects is the SASP (Coppé *et al.*, 2008), which is thought to signal an immune response for clearance of senescent cells (Xue *et al.*, 2007; Kang *et al.*, 2011). However, an accumulation of senescent cells has been observed in several tissues across numerous mammalian species (Dimri *et al.*, 1995; Paradis *et al.*, 2001; Melk *et al.*, 2003; Erusalimsky and Kurz, 2005; Jeyapalan *et al.*, 2007), suggesting there is an age-dependent imbalance between the generation and clearance of senescent cells, and/or there are a subset of cellular cells which are resistant to clearance. Moreover, persistent senescent cells and thus a chronic SASP are what are thought to contribute to age-related pathologies. Interestingly, evidence is mounting which suggests that cellular senescence is not a phenomenon pertaining to proliferative cells alone, and that post-mitotic cells, including adipocytes and neurones, can also elicit a senescent-like phenotype (Minamino *et al.*, 2009; Jurk *et al.*, 2012). Although permanent proliferation cessation may seem inconsequential in a cell type which does not replicate, it will be important to determine if post-mitotic senescent cells are associated with a SASP which may contribute to the pathological effects described above.

Irreversible cell cycle arrest was first observed to occur once cells grown in culture reached a specific, and reproducible, number of population doublings, and this process was named 'replicative senescence' (Hayflick, 1965). The number of times a cell can divide before undergoing replication has been coined the 'Hayflick limit', and this number varies between cell types and species. Telomeres have been heavily

implicated in governing the Hayflick limit of a cell, as due to the end-replication problem (Olovnikov, 1971; Watson, 1972), telomeres get progressively shorter with each cell division, a process which is accelerated by oxidative stress-induced SSBs (von Zglinicki *et al.*, 1995; von Zglinicki *et al.*, 2000), until they reach a critical length, where the t-loop structure is thought to become 'uncapped' and elicit a DNA damage response which signals for cell cycle arrest (Griffith *et al.*, 1999). Our group observed there is an age-dependent increase in telomeres eliciting a DDR in murine enterocytes and hepatocytes *in vivo*, however remarkably, Q-FISH analysis revealed that a DDR was being elicited at telomeres independently of telomere length, and this observation was also made by another group in primate neurones (Fumagalli *et al.*, 2012; Hewitt *et al.*, 2012). These data confounded the dogma that telomere dysfunction occurs solely as a result of telomere shortening, and we proposed that double strand breaks within telomere regions could be driving this DDR, a phenomenon we coined telomere-associated DNA damage foci (TAF) (Hewitt *et al.*, 2012).

Considering the aforementioned observations, we questioned whether telomere damage could be driving a senescent-like phenotype in a non-rapidly dividing cell type, which should not be subject to excessive proliferation-associated telomere shortening, and thus would be unlikely to undergo canonical replicative senescence. We used cardiomyocytes as our model, as primary embryonic cardiomyocytes can be isolated and cultured, and the H9C2 rat cardiomyocyte line are susceptible to transfections.

Our group and another had previously published that telomere damage is irreparable in fibroblasts (Fumagalli *et al.*, 2012; Hewitt *et al.*, 2012), which is of interest in cardiomyocytes, considering that the majority of cardiomyocytes persist throughout the entirety of a human lifespan (Bergmann *et al.*, 2009). We confirmed in two separate cell lines that TAF are persistent in murine cardiomyocytes. DSBs can be generated at replication forks, due to replication errors when a SSB is encountered by the DNA replication machinery (Kuzminov, 1999). Furthermore, cardiomyocytes *in vivo* retain proliferative potential, however, the rates are extremely low (Bergmann *et al.*, 2009), and thus DSBs are likely to occur infrequently as a result of replication errors. One issue is that our cell lines still retained considerable rates of proliferation, and thus the formation of DSBs could have been occurring due to replication errors, therefore not providing a physiologically relevant model. To address this, we

analysed DSB formation in the presence of a detectable fluorescent nucleoside, therefore showing that DSBs could form independently of cell division via oxidative stress or X-irradiation. Having observed telomere damage could occur in cardiomyocytes *in vitro*, it was then important to ascertain if telomere damage had an effect on cardiomyocytes. Oxidative stress via H<sub>2</sub>O<sub>2</sub> treatment, and X-irradiation, although useful as a proof-of-principle for the induction and persistence of telomere damage, are not telomere specific, and thus inferences on the specific effect of telomere damage cannot be concluded. We therefore induced telomere-specific DSBs using a fusion protein of the FokI endonuclease, conjugated to the shelterin component TRF1. Our data showed that TAF could induce a senescent-like phenotype in cardiomyocytes, as shown by a decrease in proliferation marker Ki67, an increase in SA-β-Gal activity, and increased expression of p21. Previous evidence suggests, a minimum of 5 dysfunctional telomeres in human fibroblasts are required for the cell to enter cellular senescence (Kaul *et al.*, 2012). To address the exact threshold of TAF required to induce a senescent phenotype in cardiomyocytes *in vitro*, it will be important to develop an inducible TRF1-FokI fusion protein to create a spectra of telomere damage.

We next observed that there is an age-dependent increase in TAF in both mouse and human cardiomyocytes occurring independently of length *in vivo*. Furthermore, these increases in TAF correlated with various markers of senescence including cyclin-dependent kinase inhibitors and various SASP factors. Of note, IL-6 and TGF-β were shown to be upregulated, both of which have been implicated in driving a detrimental bystander effect (Hubackova *et al.*, 2012b; Acosta *et al.*, 2013). Furthermore, we showed that conditioned medium from isolated adult cardiomyocytes could attenuate cell division in mouse fibroblasts, suggesting that cardiomyocytes can also elicit a bystander effect. It will be important to follow up these experiments to see if cardiomyocytes can induce other characteristics of senescence, and what the key drivers of this process are. Although we showed that TAF could specifically induce senescence in cardiomyocyte *in vitro*, the *in vivo* data is only correlative. It would be important to develop a mouse model, such as a cardiomyocyte-specific TRF1-FokI fusion protein, to specifically damage cardiomyocytes telomeres.

Finally, we wanted to ascertain the mechanism in which telomere damage could be induced in cardiomyocytes *in vivo*. We had shown that TAF could be generated in cardiomyocytes *in vitro* via oxidative stress with H<sub>2</sub>O<sub>2</sub> treatment, and interestingly,

one of the genes we observed to be upregulated with age in mouse hearts encodes the protein MAO-A, which produces H<sub>2</sub>O<sub>2</sub> as a by-product, and has been shown to result in an age-dependent increase in H<sub>2</sub>O<sub>2</sub> in rat hearts (Maurel *et al.*, 2003). We observed that increased oxidative stress via cardiomyocyte specific MAO-A upregulation, or using catalase *-/-*, or MnSOD $\pm$  mouse models, led to an increase in TAF. ROS have previously been shown to contribute to the stability of cellular senescence through generation of DDF which maintain a persistent DDR (Passos *et al.*, 2010). We showed that the development of senescence, following genotoxic stress, could be attenuated by treating cells with rapamycin, which abrogated the senescence-associated increase in ROS. Moreover, supplementing the diet of mice with rapamycin resulted in an attenuation of age-related oxidative damage, TAF accumulation and p21 expression. Previous studies have shown rapamycin to extend the lifespan in numerous species (Bjedov *et al.*, 2010; Zhang *et al.*, 2014), and also to delay age-related cardiomyopathies, even when supplemented to aged mice for a period of just 3 months (Flynn *et al.*, 2013). RNAseq analysis revealed that these rapamycin fed mice showed decreases in hypertrophy and inflammation markers, both of which are associated with senescence, thus it is possible that rapamycin may act to abrogate any existing senescence phenotype through ROS attenuation, whilst decreasing the rate of further damage accumulation. Furthermore, rapamycin treatment has been shown to reduce hydrogen peroxide release in mouse brain and liver, thought to be a result of reducing the abundance of mitochondrial complex I matrix subunits (Miwa *et al.*, 2014b).

To conclude, evidence is mounting that telomere shortening isn't the only molecular phenomenon pertaining to telomere-related ageing (Fumagalli *et al.*, 2012; Hewitt *et al.*, 2012). Indeed, animal models exhibiting critically short telomere lengths are not physiologically comparable to the natural ageing process, and research across several mammalian species observed an inverse relationship between telomere length and lifespan (Gomes *et al.*, 2011), which would suggest that short telomeres are not an important driver in organismal ageing. We have provided evidence that TAF can induce senescence in cardiomyocytes *in vitro*, that there is an age-dependent increase in TAF in cardiomyocytes *in vivo*, which can be generated by oxidative stress, and cardiomyocytes display an age-related development of a senescent-like phenotype, which is associated with TAF. It will be important in the future to generate models which specifically induce telomere damage independently

of length *in vivo*, to truly ascertain if TAF are causative in driving cardiomyocyte senescence *in vivo*, and furthermore, to then develop models which specifically reverse the senescent phenotype or remove senescent cells, to assess the role of cardiomyocyte senescence in cardiac ageing.

Finally, our data provide evidence that cardiomyocytes are associated with a senescent-like phenotype that this is associated with telomere damage. Although it is difficult to deduce causation over correlation with regard to telomere damage and cardiomyocyte senescence, it is difficult to argue against TAF emerging as a robust biomarker for cardiomyocyte ageing.

## 7 References

- Acosta, J., Banito, A., Wuestefeld, T., Georgilis, A., Janich, P., Morton, J., Athineos, D., Kang, T.-W., Lasitschka, F., Andrulis, M., Pascual, G., Morris, K., Khan, S., Jin, H., Dharmalingam, G., Snijders, A., Carroll, T., Capper, D., Pritchard, C., Inman, G., Longerich, T., Sansom, O., Benitah, S., Zender, L. and Gil, J. (2013) 'A complex secretory program orchestrated by the inflammasome controls paracrine senescence', *Nature cell biology*, 15(8), pp. 978-990.
- Acosta, J., O'Loughlen, A., Banito, A., Guijarro, M., Augert, A., Raguz, S., Fumagalli, M., Da Costa, M., Brown, C., Popov, N., Takatsu, Y., Melamed, J., d'Adda di Fagagna, F., Bernard, D., Hernando, E. and Gil, J. (2008) 'Chemokine signaling via the CXCR2 receptor reinforces senescence', *Cell*, 133(6), pp. 1006-1018.
- Adams, M., Hardenbergh, P., Constone, L. and Lipshultz, S. (2003) 'Radiation-associated cardiovascular disease', *Critical reviews in oncology/hematology*, 45(1), pp. 55-75.
- Agarwal, P., Sandey, M., DeInnocentes, P. and Bird, R. (2013) 'Tumor suppressor gene p16/INK4A/CDKN2A-dependent regulation into and out of the cell cycle in a spontaneous canine model of breast cancer', *Journal of cellular biochemistry*, 114(6), pp. 1355-1363.
- Ahmed, S., Passos, J., Birket, M., Beckmann, T., Brings, S., Peters, H., Birch-Machin, M., von Zglinicki, T. and Saretzki, G. (2008) 'Telomerase does not counteract telomere shortening but protects mitochondrial function under oxidative stress', *Journal of cell science*, 121(Pt 7), pp. 1046-1053.
- Alcorta, D., Xiong, Y., Phelps, D., Hannon, G., Beach, D. and Barrett, J. (1996) 'Involvement of the cyclin-dependent kinase inhibitor p16 (INK4a) in replicative senescence of normal human fibroblasts', *Proceedings of the National Academy of Sciences of the United States of America*, 93(24), pp. 13742-13747.
- Alexeyev, M.F., Ledoux, S.P. and Wilson, G.L. (2004) 'Mitochondrial DNA and aging', *Clin Sci (Lond)*, 107(4), pp. 355-64.
- Alspach, E., Fu, Y. and Stewart, S. (2013) 'Senescence and the pro-tumorigenic stroma', *Critical reviews in oncogenesis*, 18(6), pp. 549-558.
- Amrichová, J., Lukášová, E., Kozubek, S. and Kozubek, M. (2003) 'Nuclear and territorial topography of chromosome telomeres in human lymphocytes', *Experimental cell research*, 289(1), pp. 11-26.

Ancrile, B., Lim, K.-H. and Counter, C. (2007) 'Oncogenic Ras-induced secretion of IL6 is required for tumorigenesis', *Genes & development*, 21(14), pp. 1714-1719.

Anisimov, V., Zabezhinski, M., Popovich, I., Piskunova, T., Semchenko, A., Tyndyk, M., Yurova, M., Rosenfeld, S. and Blagosklonny, M. (2011) 'Rapamycin increases lifespan and inhibits spontaneous tumorigenesis in inbred female mice', *Cell cycle (Georgetown, Tex.)*, 10(24), pp. 4230-4236.

Aoshiha, K., Tsuji, T., Kameyama, S., Itoh, M., Semba, S., Yamaguchi, K. and Nakamura, H. (2013) 'Senescence-associated secretory phenotype in a mouse model of bleomycin-induced lung injury', *Experimental and toxicologic pathology : official journal of the Gesellschaft für Toxikologische Pathologie*, 65(7-8), pp. 1053-1062.

Aoshiha, K., Tsuji, T. and Nagai, A. (2003) 'Bleomycin induces cellular senescence in alveolar epithelial cells', *The European respiratory journal*, 22(3), pp. 436-443.

Appella, E. and Anderson, C. (2001) 'Post-translational modifications and activation of p53 by genotoxic stresses', *European journal of biochemistry / FEBS*, 268(10), pp. 2764-2772.

Azzalin, C., Mucciolo, E., Bertoni, L. and Giulotto, E. (1997) 'Fluorescence in situ hybridization with a synthetic (T2AG3)<sub>n</sub> polynucleotide detects several intrachromosomal telomere-like repeats on human chromosomes', *Cytogenetics and cell genetics*, 78(2), pp. 112-115.

Bae, N. and Baumann, P. (2007) 'A RAP1/TRF2 complex inhibits nonhomologous end-joining at human telomeric DNA ends', *Molecular cell*, 26(3), pp. 323-334.

Baker, D., Jeganathan, K., Cameron, J., Thompson, M., Juneja, S., Kopecka, A., Kumar, R., Jenkins, R., de Groen, P., Roche, P. and van Deursen, J. (2004) 'BubR1 insufficiency causes early onset of aging-associated phenotypes and infertility in mice', *Nature genetics*, 36(7), pp. 744-749.

Baker, D., Perez-Terzic, C., Jin, F., Pitel, K., Niederländer, N., Jeganathan, K., Yamada, S., Reyes, S., Rowe, L., Hiddinga, H., Eberhardt, N., Terzic, A. and van Deursen, J. (2008) 'Opposing roles for p16Ink4a and p19Arf in senescence and ageing caused by BubR1 insufficiency', *Nature cell biology*, 10(7), pp. 825-836.

Baker, D., Wijshake, T., Tchkonja, T., LeBrasseur, N., Childs, B., van de Sluis, B., Kirkland, J. and van Deursen, J. (2011) 'Clearance of p16Ink4a-positive senescent cells delays ageing-associated disorders', *Nature*, 479(7372), pp. 232-236.

Bakkenist, C. and Kastan, M. (2003) 'DNA damage activates ATM through intermolecular autophosphorylation and dimer dissociation', *Nature*, 421(6922), pp. 499-506.

Bär, C., Bernardes de Jesus, B., Serrano, R., Tejera, A., Ayuso, E., Jimenez, V., Formentini, I., Bobadilla, M., Mizrahi, J., de Martino, A., Gomez, G., Pisano, D., Mulero, F., Wollert, K., Bosch, F. and Blasco, M. (2014) 'Telomerase expression confers cardioprotection in the adult mouse heart after acute myocardial infarction', *Nature communications*, 5, p. 5863.

Barnouin, K., Dubuisson, M.L., Child, E.S., Fernandez de Mattos, S., Glassford, J., Medema, R.H., Mann, D.J. and Lam, E.W. (2002) 'H<sub>2</sub>O<sub>2</sub> induces a transient multi-phase cell cycle arrest in mouse fibroblasts through modulating cyclin D and p21Cip1 expression', *J Biol Chem*, 277(16), pp. 13761-70.

Bartholomew, J., Volonte, D. and Galbiati, F. (2009) 'Caveolin-1 regulates the antagonistic pleiotropic properties of cellular senescence through a novel Mdm2/p53-mediated pathway', *Cancer research*, 69(7), pp. 2878-2886.

Bartkova, J., Horejsí, Z., Koed, K., Krämer, A., Tort, F., Zieger, K., Guldberg, P., Sehested, M., Nesland, J., Lukas, C., Ørntoft, T., Lukas, J. and Bartek, J. (2005) 'DNA damage response as a candidate anti-cancer barrier in early human tumorigenesis', *Nature*, 434(7035), pp. 864-870.

Bartkova, J., Rezaei, N., Liontos, M., Karakaidos, P., Kletsas, D., Issaeva, N., Vassiliou, L.-V.F., Kolettas, E., Niforou, K., Zoumpourlis, V., Takaoka, M., Nakagawa, H., Tort, F., Fugger, K., Johansson, F., Sehested, M., Andersen, C., Dyrskjot, L., Ørntoft, T., Lukas, J., Kittas, C., Helleday, T., Halazonetis, T., Bartek, J. and Gorgoulis, V. (2006) 'Oncogene-induced senescence is part of the tumorigenesis barrier imposed by DNA damage checkpoints', *Nature*, 444(7119), pp. 633-637.

Beauséjour, C., Krtolica, A., Galimi, F., Narita, M., Lowe, S., Yaswen, P. and Campisi, J. (2003) 'Reversal of human cellular senescence: roles of the p53 and p16 pathways', *The EMBO journal*, 22(16), pp. 4212-4222.

Bekker-Jensen, S., Lukas, C., Melander, F., Bartek, J. and Lukas, J. (2005) 'Dynamic assembly and sustained retention of 53BP1 at the sites of DNA damage are controlled by Mdc1/NFBD1', *The Journal of cell biology*, 170(2), pp. 201-211.

Berenji, K., Drazner, M.H., Rothermel, B.A. and Hill, J.A. (2005) 'Does load-induced ventricular hypertrophy progress to systolic heart failure?', *Am J Physiol Heart Circ Physiol*, 289(1), pp. H8-H16.

- Bergmann, O., Bhardwaj, R., Bernard, S., Zdunek, S., Barnabé-Heider, F., Walsh, S., Zupicich, J., Alkass, K., Buchholz, B., Druid, H., Jovinge, S. and Frisén, J. (2009) 'Evidence for cardiomyocyte renewal in humans', *Science (New York, N.Y.)*, 324(5923), pp. 98-102.
- Bernet, J., Doles, J., Hall, J., Kelly Tanaka, K., Carter, T. and Olwin, B. (2014) 'p38 MAPK signaling underlies a cell-autonomous loss of stem cell self-renewal in skeletal muscle of aged mice', *Nature medicine*, 20(3), pp. 265-271.
- Besancenot, R., Chaligné, R., Tonetti, C., Pasquier, F., Marty, C., Lécluse, Y., Vainchenker, W., Constantinescu, S. and Giraudier, S. (2010) 'A senescence-like cell-cycle arrest occurs during megakaryocytic maturation: implications for physiological and pathological megakaryocytic proliferation', *PLoS biology*, 8(9).
- Bevona, C., Goggins, W., Quinn, T., Fullerton, J. and Tsao, H. (2003) 'Cutaneous melanomas associated with nevi', *Archives of dermatology*, 139(12), p. 1620.
- Bhatia, B., Multani, A., Patrawala, L., Chen, X., Calhoun-Davis, T., Zhou, J., Schroeder, L., Schneider-Broussard, R., Shen, J., Pathak, S., Chang, S. and Tang, D. (2008) 'Evidence that senescent human prostate epithelial cells enhance tumorigenicity: cell fusion as a potential mechanism and inhibition by p16INK4a and hTERT', *International journal of cancer. Journal international du cancer*, 122(7), pp. 1483-1495.
- Bianchi, A., Stansel, R., Fairall, L., Griffith, J., Rhodes, D. and de Lange, T. (1999) 'TRF1 binds a bipartite telomeric site with extreme spatial flexibility', *The EMBO journal*, 18(20), pp. 5735-5744.
- Bjedov, I., Toivonen, J., Kerr, F., Slack, C., Jacobson, J., Foley, A. and Partridge, L. (2010) 'Mechanisms of life span extension by rapamycin in the fruit fly *Drosophila melanogaster*', *Cell metabolism*, 11(1), pp. 35-46.
- Blackburn, E. (1991) 'Structure and function of telomeres', *Nature*, 350(6319), pp. 569-573.
- Blasco, M. (2005) 'Telomeres and human disease: ageing, cancer and beyond', *Nature reviews. Genetics*, 6(8), pp. 611-622.
- Blasco, M.A., Lee, H.W., Hande, M.P., Samper, E., Lansdorp, P.M., DePinho, R.A. and Greider, C.W. (1997) 'Telomere shortening and tumor formation by mouse cells lacking telomerase RNA', *Cell*, 91(1), pp. 25-34.
- Bodnar, A., Ouellette, M., Frolkis, M., Holt, S., Chiu, C., Morin, G., Harley, C., Shay, J., Lichtsteiner, S. and Wright, W. (1998a) 'Extension of life-span by introduction of

telomerase into normal human cells', *Science (New York, N.Y.)*, 279(5349), pp. 349-352.

Bodnar, A.G., Ouellette, M., Frolkis, M., Holt, S.E., Chiu, C.P., Morin, G.B., Harley, C.B., Shay, J.W., Lichtsteiner, S. and Wright, W.E. (1998b) 'Extension of life-span by introduction of telomerase into normal human cells', *Science*, 279(5349), pp. 349-52.

Bont, R.D. (2004) 'Endogenous DNA damage in humans: a review of quantitative data', *Mutagenesis*, 19.

Bracken, A., Kleine-Kohlbrecher, D., Dietrich, N., Pasini, D., Gargiulo, G., Beekman, C., Theilgaard-Mönch, K., Minucci, S., Porse, B., Marine, J.-C., Hansen, K. and Helin, K. (2007) 'The Polycomb group proteins bind throughout the INK4A-ARF locus and are disassociated in senescent cells', *Genes & development*, 21(5), pp. 525-530.

Bradshaw, P., Stavropoulos, D. and Meyn, M. (2005) 'Human telomeric protein TRF2 associates with genomic double-strand breaks as an early response to DNA damage', *Nature genetics*, 37(2), pp. 193-197.

Braig, M., Lee, S., Loddenkemper, C., Rudolph, C., Peters, A., Schlegelberger, B., Stein, H., Dörken, B., Jenuwein, T. and Schmitt, C. (2005) 'Oncogene-induced senescence as an initial barrier in lymphoma development', *Nature*, 436(7051), pp. 660-665.

Braig, M. and Schmitt, C. (2006) 'Oncogene-induced senescence: putting the brakes on tumor development', *Cancer research*, 66(6), pp. 2881-2884.

Brinda, R., Coralie, V., Zdenek, B., Janet, E.D., Shouqing, L., Lourdes, G.O., Francesco, S., Douglas, F.E., Rainer, D., Cahir, J.O.K. and David, C.R. (2004) 'Inhibition of mTOR induces autophagy and reduces toxicity of polyglutamine expansions in fly and mouse models of Huntington disease', *Nature Genetics*, 36.

Brown, J., Wei, W. and Sedivy, J. (1997) 'Bypass of senescence after disruption of p21CIP1/WAF1 gene in normal diploid human fibroblasts', *Science (New York, N.Y.)*, 277(5327), pp. 831-834.

Brown, K.A., Didion, S.P., Andresen, J.J. and Faraci, F.M. (2007) 'Effect of aging, MnSOD deficiency, and genetic background on endothelial function: evidence for MnSOD haploinsufficiency', *Arterioscler Thromb Vasc Biol*, 27(9), pp. 1941-6.

Burkauskiene, A., Mackiewicz, Z., Virtanen, I. and Konttinen, Y.T. (2006) 'Age-related changes in myocardial nerve and collagen networks of the auricle of the right atrium', *Acta Cardiol*, 61(5), pp. 513-8.

- Cameron, K., Golightly, A., Miwa, S., Speakman, J., Boys, R. and von Zglinicki, T. (2011) 'Gross energy metabolism in mice under late onset, short term caloric restriction', *Mechanisms of ageing and development*, 132(4), pp. 202-209.
- Campisi, J. (2001) 'Cellular senescence as a tumor-suppressor mechanism', *Trends in cell biology*, 11(11), p. 31.
- Campisi, J. (2005) 'Senescent cells, tumor suppression, and organismal aging: good citizens, bad neighbors', *Cell*, 120(4), pp. 513-522.
- Campisi, J. (2011) 'Cellular senescence: putting the paradoxes in perspective', *Current opinion in genetics & development*, 21(1), pp. 107-112.
- Campisi, J. (2013) 'Aging, cellular senescence, and cancer', *Annual review of physiology*, 75, pp. 685-705.
- Campisi, J. and d'Adda di Fagagna, F. (2007) 'Cellular senescence: when bad things happen to good cells', *Nature reviews. Molecular cell biology*, 8(9), pp. 729-740.
- Carson, C., Schwartz, R., Stracker, T., Lilley, C., Lee, D. and Weitzman, M. (2003) 'The Mre11 complex is required for ATM activation and the G2/M checkpoint', *The EMBO journal*, 22(24), pp. 6610-6620.
- Cawthon, R. (2002) 'Telomere measurement by quantitative PCR', *Nucleic acids research*, 30(10).
- Celli, G. and de Lange, T. (2005) 'DNA processing is not required for ATM-mediated telomere damage response after TRF2 deletion', *Nature cell biology*, 7(7), pp. 712-718.
- Cesare, A., Hayashi, M., Crabbe, L. and Karlseder, J. (2013) 'The telomere deprotection response is functionally distinct from the genomic DNA damage response', *Molecular cell*, 51(2), pp. 141-155.
- Cesare, A., Kaul, Z., Cohen, S., Napier, C., Pickett, H., Neumann, A. and Reddel, R. (2009) 'Spontaneous occurrence of telomeric DNA damage response in the absence of chromosome fusions', *Nature structural & molecular biology*, 16(12), pp. 1244-1251.
- Chance, B., Sies, H. and Boveris, A. (1979) 'Hydroperoxide metabolism in mammalian organs', *Physiological reviews*, 59(3), pp. 527-605.
- Chen, H., Ma, Z., Vanderwaal, R.P., Feng, Z., Gonzalez-Suarez, I., Wang, S., Zhang, J., Roti Roti, J.L. and Gonzalo, S. (2011) 'The mTOR inhibitor rapamycin suppresses DNA double-strand break repair', *Radiat Res*, 175(2), pp. 214-24.
- Chen, Q., Fischer, A., Reagan, J., Yan, L. and Ames, B. (1995) 'Oxidative DNA damage and senescence of human diploid fibroblast cells', *Proceedings of the*

*National Academy of Sciences of the United States of America*, 92(10), pp. 4337-4341.

Chen, Q., Prowse, K., Tu, V., Purdom, S. and Linskens, M. (2001) 'Uncoupling the senescent phenotype from telomere shortening in hydrogen peroxide-treated fibroblasts', *Experimental cell research*, 265(2), pp. 294-303.

Chen, Q.M., Bartholomew, J.C., Campisi, J., Acosta, M., Reagan, J.D. and Ames, B.N. (1998) 'Molecular analysis of H<sub>2</sub>O<sub>2</sub>-induced senescent-like growth arrest in normal human fibroblasts: p53 and Rb control G1 arrest but not cell replication', *Biochem J*, 332 ( Pt 1), pp. 43-50.

Chen, Z., Trotman, L., Shaffer, D., Lin, H.-K., Dotan, Z., Niki, M., Koutcher, J., Scher, H., Ludwig, T., Gerald, W., Cordon-Cardo, C. and Pandolfi, P. (2005) 'Crucial role of p53-dependent cellular senescence in suppression of Pten-deficient tumorigenesis', *Nature*, 436(7051), pp. 725-730.

Chien, Y., Scuoppo, C., Wang, X., Fang, X., Balgley, B., Bolden, J., Premsrirut, P., Luo, W., Chicas, A., Lee, C., Kogan, S. and Lowe, S. (2011) 'Control of the senescence-associated secretory phenotype by NF- $\kappa$ B promotes senescence and enhances chemosensitivity', *Genes & development*, 25(20), pp. 2125-2136.

Chuprin, A., Gal, H., Biron-Shental, T., Biran, A., Amiel, A., Rozenblatt, S. and Krizhanovsky, V. (2013) 'Cell fusion induced by ERVWE1 or measles virus causes cellular senescence', *Genes & development*, 27(21), pp. 2356-2366.

Collado, M., Gil, J., Efeyan, A., Guerra, C., Schuhmacher, A., Barradas, M., Benguría, A., Zaballos, A., Flores, J., Barbacid, M., Beach, D. and Serrano, M. (2005) 'Tumour biology: senescence in premalignant tumours', *Nature*, 436(7051), p. 642.

Coppé, J.-P., Desprez, P.-Y., Krtolica, A. and Campisi, J. (2010a) 'The senescence-associated secretory phenotype: the dark side of tumor suppression', *Annual review of pathology*, 5, pp. 99-118.

Coppé, J.-P., Kauser, K., Campisi, J. and Beauséjour, C. (2006) 'Secretion of vascular endothelial growth factor by primary human fibroblasts at senescence', *The Journal of biological chemistry*, 281(40), pp. 29568-29574.

Coppé, J.-P., Patil, C., Rodier, F., Krtolica, A., Beauséjour, C., Parrinello, S., Hodgson, J., Chin, K., Desprez, P.-Y. and Campisi, J. (2010b) 'A human-like senescence-associated secretory phenotype is conserved in mouse cells dependent on physiological oxygen', *PLoS ONE*, 5(2).

Coppé, J.-P., Patil, C., Rodier, F., Sun, Y., Muñoz, D., Goldstein, J., Nelson, P., Desprez, P.-Y. and Campisi, J. (2008) 'Senescence-associated secretory phenotypes

reveal cell-nonautonomous functions of oncogenic RAS and the p53 tumor suppressor', *PLoS biology*, 6(12), pp. 2853-2868.

Cortez, D., Guntuku, S., Qin, J. and Elledge, S. (2001) 'ATR and ATRIP: partners in checkpoint signaling', *Science (New York, N.Y.)*, 294(5547), pp. 1713-1716.

Cosgrove, B., Gilbert, P., Porpiglia, E., Mourkioti, F., Lee, S., Corbel, S., Llewellyn, M., Delp, S. and Blau, H. (2014) 'Rejuvenation of the muscle stem cell population restores strength to injured aged muscles', *Nature medicine*, 20(3), pp. 255-264.

Counter, C., Ailion, A., LeFeuvre, C., Stewart, N., Greider, C., Harley, C. and Bacchetti, S. (1992) 'Telomere shortening associated with chromosome instability is arrested in immortal cells which express telomerase activity', *The EMBO journal*, 11(5), pp. 1921-1929.

Court, R., Chapman, L., Fairall, L. and Rhodes, D. (2005) 'How the human telomeric proteins TRF1 and TRF2 recognize telomeric DNA: a view from high-resolution crystal structures', *EMBO reports*, 6(1), pp. 39-45.

Courtois-Cox, S., Genter Williams, S., Reczek, E., Johnson, B., McGillicuddy, L., Johannessen, C., Hollstein, P., MacCollin, M. and Cichowski, K. (2006) 'A negative feedback signaling network underlies oncogene-induced senescence', *Cancer cell*, 10(6), pp. 459-472.

Crabb, J.W., O'Neil, J., Miyagi, M., West, K. and Hoff, H.F. (2002) 'Hydroxynonenal inactivates cathepsin B by forming Michael adducts with active site residues', *Protein Sci*, 11(4), pp. 831-40.

Crabbe, L., Cesare, A., Kasuboski, J., Fitzpatrick, J. and Karlseder, J. (2012) 'Human telomeres are tethered to the nuclear envelope during postmitotic nuclear assembly', *Cell reports*, 2(6), pp. 1521-1529.

Cui, H., Kong, Y. and Zhang, H. (2012) 'Oxidative stress, mitochondrial dysfunction, and aging', *J Signal Transduct*, 2012, p. 646354.

d'Adda di Fagagna, F., Reaper, P., Clay-Farrace, L., Fiegler, H., Carr, P., Von Zglinicki, T., Saretzki, G., Carter, N. and Jackson, S. (2003) 'A DNA damage checkpoint response in telomere-initiated senescence', *Nature*, 426(6963), pp. 194-198.

D'Autr aux, B. and Toledano, M. (2007) 'ROS as signalling molecules: mechanisms that generate specificity in ROS homeostasis', *Nature reviews. Molecular cell biology*, 8(10), pp. 813-824.

Dai, D.F., Chen, T., Wanagat, J., Laflamme, M., Marcinek, D.J., Emond, M.J., Ngo, C.P., Prolla, T.A. and Rabinovitch, P.S. (2010) 'Age-dependent cardiomyopathy in

mitochondrial mutator mice is attenuated by overexpression of catalase targeted to mitochondria', *Aging Cell*, 9(4), pp. 536-44.

Dai, D.F., Santana, L.F., Vermulst, M., Tomazela, D.M., Emond, M.J., MacCoss, M.J., Gollahon, K., Martin, G.M., Loeb, L.A., Ladiges, W.C. and Rabinovitch, P.S. (2009) 'Overexpression of catalase targeted to mitochondria attenuates murine cardiac aging', *Circulation*, 119(21), pp. 2789-97.

Dankort, D., Filenova, E., Collado, M., Serrano, M., Jones, K. and McMahon, M. (2007) 'A new mouse model to explore the initiation, progression, and therapy of BRAFV600E-induced lung tumors', *Genes & development*, 21(4), pp. 379-384.

Darby, S., McGale, P., Peto, R., Granath, F., Hall, P. and Ekblom, A. (2003) 'Mortality from cardiovascular disease more than 10 years after radiotherapy for breast cancer: nationwide cohort study of 90 000 Swedish women', *BMJ (Clinical research ed.)*, 326(7383), pp. 256-257.

de Lange, T. (2005) 'Shelterin: the protein complex that shapes and safeguards human telomeres', *Genes & development*, 19(18), pp. 2100-2110.

Demaria, M., Ohtani, N., Youssef, S., Rodier, F., Toussaint, W., Mitchell, J., Laberge, R.-M., Vijg, J., Van Steeg, H., Dollé, M., Hoeijmakers, J., de Bruin, A., Hara, E. and Campisi, J. (2014) 'An essential role for senescent cells in optimal wound healing through secretion of PDGF-AA', *Developmental cell*, 31(6), pp. 722-733.

Demidenko, Z. and Blagosklonny, M. (2009) 'Quantifying pharmacologic suppression of cellular senescence: prevention of cellular hypertrophy versus preservation of proliferative potential', *Aging*, 1(12), pp. 1008-1016.

Deng, C., Zhang, P., Harper, J., Elledge, S. and Leder, P. (1995) 'Mice lacking p21CIP1/WAF1 undergo normal development, but are defective in G1 checkpoint control', *Cell*, 82(4), pp. 675-684.

Der, C., Krontiris, T. and Cooper, G. (1982) 'Transforming genes of human bladder and lung carcinoma cell lines are homologous to the ras genes of Harvey and Kirsten sarcoma viruses', *Proceedings of the National Academy of Sciences of the United States of America*, 79(11), pp. 3637-3640.

Di Leonardo, A., Linke, S., Clarkin, K. and Wahl, G. (1994) 'DNA damage triggers a prolonged p53-dependent G1 arrest and long-term induction of Cip1 in normal human fibroblasts', *Genes & development*, 8(21), pp. 2540-2551.

Di Micco, R., Fumagalli, M., Cicalese, A., Piccinin, S., Gasparini, P., Luise, C., Schurra, C., Garre, M., Nuciforo, P., Bensimon, A., Maestro, R., Pelicci, P. and

d'Adda di Fagagna, F. (2006) 'Oncogene-induced senescence is a DNA damage response triggered by DNA hyper-replication', *Nature*, 444(7119), pp. 638-642.

Dimri, G., Lee, X., Basile, G., Acosta, M., Scott, G., Roskelley, C., Medrano, E., Linskens, M., Rubelj, I. and Pereira-Smith, O. (1995) 'A biomarker that identifies senescent human cells in culture and in aging skin in vivo', *Proceedings of the National Academy of Sciences of the United States of America*, 92(20), pp. 9363-9367.

Doksani, Y., Wu, J., de Lange, T. and Zhuang, X. (2013) 'Super-Resolution Fluorescence Imaging of Telomeres Reveals TRF2-Dependent T-loop Formation', *Cell*, 155(2), pp. 345-356.

Donath, M., Dalmas, É., Sauter, N. and Böni-Schnetzler, M. (2013) 'Inflammation in obesity and diabetes: islet dysfunction and therapeutic opportunity', *Cell metabolism*, 17(6), pp. 860-872.

Dong, R., Xu, X., Li, G., Feng, W., Zhao, G., Zhao, J., Wang, D. and Tu, L. (2013) 'Bradykinin inhibits oxidative stress-induced cardiomyocytes senescence via regulating redox state', *PLoS ONE*, 8(10).

Duan, J., Duan, J., Zhang, Z. and Tong, T. (2005) 'Irreversible cellular senescence induced by prolonged exposure to H<sub>2</sub>O<sub>2</sub> involves DNA-damage-and-repair genes and telomere shortening', *The International Journal of Biochemistry & Cell Biology*, 37(7), pp. 1407-1420.

Dunham, M., Neumann, A., Fasching, C. and Reddel, R. (2000) 'Telomere maintenance by recombination in human cells', *Nature genetics*, 26(4), pp. 447-450.

Dupre-Crochet, S., Erard, M. and Nubetae, O. (2013) 'ROS production in phagocytes: why, when, and where?', *J Leukoc Biol*, 94(4), pp. 657-70.

Dyson, N. (1998) 'The regulation of E2F by pRB-family proteins', *Genes Dev*, 12(15), pp. 2245-62.

el-Deiry, W., Tokino, T., Velculescu, V., Levy, D., Parsons, R., Trent, J., Lin, D., Mercer, W., Kinzler, K. and Vogelstein, B. (1993) 'WAF1, a potential mediator of p53 tumor suppression', *Cell*, 75(4), pp. 817-825.

Elizabeth, H.B. (2001) 'Switching and Signaling at the Telomere'.

Ellis, R., Yuan, J. and Horvitz, H. (1991) 'Mechanisms and functions of cell death', *Annual review of cell biology*, 7, pp. 663-698.

Erusalimsky, J. and Kurz, D. (2005) 'Cellular senescence in vivo: its relevance in ageing and cardiovascular disease', *Experimental gerontology*, 40(8-9), pp. 634-642.

Esterbauer, H., Schaur, R.J. and Zollner, H. (1991) 'Chemistry and biochemistry of 4-hydroxynonenal, malonaldehyde and related aldehydes', *Free Radic Biol Med*, 11(1), pp. 81-128.

Falck, J., Coates, J. and Jackson, S. (2005) 'Conserved modes of recruitment of ATM, ATR and DNA-PKcs to sites of DNA damage', *Nature*, 434(7033), pp. 605-611.

Ferrington, D.A. and Kapphahn, R.J. (2004) 'Catalytic site-specific inhibition of the 20S proteasome by 4-hydroxynonenal', *FEBS Lett*, 578(3), pp. 217-23.

Fingar, D. and Blenis, J. (2004) 'Target of rapamycin (TOR): an integrator of nutrient and growth factor signals and coordinator of cell growth and cell cycle progression', *Oncogene*, 23(18), pp. 3151-3171.

Flores, I., Canela, A., Vera, E., Tejera, A., Cotsarelis, G. and Blasco, M. (2008) 'The longest telomeres: a general signature of adult stem cell compartments', *Genes & development*, 22(5), pp. 654-667.

Flynn, J., O'Leary, M., Zambataro, C., Academia, E., Presley, M., Garrett, B., Zykovich, A., Mooney, S., Strong, R., Rosen, C., Kapahi, P., Nelson, M., Kennedy, B. and Melov, S. (2013) 'Late-life rapamycin treatment reverses age-related heart dysfunction', *Aging cell*, 12(5), pp. 851-862.

Franco, S., Blasco, M., Siedlak, S., Harris, P., Moreira, P., Perry, G. and Smith, M. (2006) 'Telomeres and telomerase in Alzheimer's disease: epiphenomena or a new focus for therapeutic strategy?', *Alzheimer's & dementia : the journal of the Alzheimer's Association*, 2(3), pp. 164-168.

Freund, A., Orjalo, A., Desprez, P.-Y. and Campisi, J. (2010) 'Inflammatory networks during cellular senescence: causes and consequences', *Trends in molecular medicine*, 16(5), pp. 238-246.

Freund, A., Patil, C. and Campisi, J. (2011) 'p38MAPK is a novel DNA damage response-independent regulator of the senescence-associated secretory phenotype', *The EMBO journal*, 30(8), pp. 1536-1548.

Fridovich, I. (1995) 'Superoxide radical and superoxide dismutases', *Annu Rev Biochem*, 64, pp. 97-112.

Fujita, K., Mondal, A., Horikawa, I., Nguyen, G., Kumamoto, K., Sohn, J., Bowman, E., Mathe, E., Schetter, A., Pine, S., Ji, H., Vojtesek, B., Bourdon, J.-C., Lane, D. and Harris, C. (2009) 'p53 isoforms Delta133p53 and p53beta are endogenous regulators of replicative cellular senescence', *Nature cell biology*, 11(9), pp. 1135-1142.

Fumagalli, M., Rossiello, F., Clerici, M., Barozzi, S., Cittaro, D., Kaplunov, J., Bucci, G., Dobрева, M., Matti, V., Beausejour, C., Herbig, U., Longhese, M. and d'Adda di

- Fagagna, F. (2012) 'Telomeric DNA damage is irreparable and causes persistent DNA-damage-response activation', *Nature cell biology*, 14(4), pp. 355-365.
- Furumoto, K., Inoue, E., Nagao, N., Hiyama, E. and Miwa, N. (1998) 'Age-dependent telomere shortening is slowed down by enrichment of intracellular vitamin C via suppression of oxidative stress', *Life sciences*, 63(11), pp. 935-948.
- Gabriele, S., Michael, P.M. and Thomas von, Z. (2003) 'MitoQ counteracts telomere shortening and elongates lifespan of fibroblasts under mild oxidative stress', *Aging Cell*, 2.
- George, C.W. (1957) 'Pleiotropy, Natural Selection, and the Evolution of Senescence', *Evolution*, 11.
- Gil, J., Bernard, D., Martínez, D. and Beach, D. (2004) 'Polycomb CBX7 has a unifying role in cellular lifespan', *Nature cell biology*, 6(1), pp. 67-72.
- Gire, V., Roux, P., Wynford-Thomas, D., Brondello, J.-M. and Dulic, V. (2004) 'DNA damage checkpoint kinase Chk2 triggers replicative senescence', *The EMBO journal*, 23(13), pp. 2554-2563.
- Goel, V., Ibrahim, N., Jiang, G., Singhal, M., Fee, S., Flotte, T., Westmoreland, S., Haluska, F. and Hinds, P. (2009) 'Melanocytic nevus-like hyperplasia and melanoma in transgenic BRAFV600E mice', *Oncogene*, 28(23), pp. 2289-2298.
- Gomes, N., Ryder, O., Houck, M., Charter, S., Walker, W., Forsyth, N., Austad, S., Venditti, C., Pagel, M., Shay, J. and Wright, W. (2011) 'Comparative biology of mammalian telomeres: hypotheses on ancestral states and the roles of telomeres in longevity determination', *Aging cell*, 10(5), pp. 761-768.
- Gorgoulis, V., Vassiliou, L.-V.F., Karakaidos, P., Zacharatos, P., Kotsinas, A., Liloglou, T., Venere, M., Dittullo, R., Kastrinakis, N., Levy, B., Kletsas, D., Yoneta, A., Herlyn, M., Kittas, C. and Halazonetis, T. (2005) 'Activation of the DNA damage checkpoint and genomic instability in human precancerous lesions', *Nature*, 434(7035), pp. 907-913.
- Green, D. and Chipuk, J. (2006) 'p53 and metabolism: Inside the TIGAR', *Cell*, 126(1), pp. 30-32.
- Green, D. and Evan, G. (2002) 'A matter of life and death', *Cancer cell*, 1(1), pp. 19-30.
- Gregor, M. and Hotamisligil, G. (2011) 'Inflammatory mechanisms in obesity', *Annual review of immunology*, 29, pp. 415-445.

- Griffith, J., Comeau, L., Rosenfield, S., Stansel, R., Bianchi, A., Moss, H. and de Lange, T. (1999) 'Mammalian telomeres end in a large duplex loop', *Cell*, 97(4), pp. 503-514.
- Guo, X., Deng, Y., Lin, Y., Cosme-Blanco, W., Chan, S., He, H., Yuan, G., Brown, E. and Chang, S. (2007) 'Dysfunctional telomeres activate an ATM-ATR-dependent DNA damage response to suppress tumorigenesis', *The EMBO journal*, 26(22), pp. 4709-4719.
- Guo, Z., Kozlov, S., Lavin, M., Person, M. and Paull, T. (2010) 'ATM activation by oxidative stress', *Science (New York, N.Y.)*, 330(6003), pp. 517-521.
- Hanahan, D. and Weinberg, R. (2000) 'The hallmarks of cancer', *Cell*, 100(1), pp. 57-70.
- Hanaoka, S., Nagadoi, A. and Nishimura, Y. (2005) 'Comparison between TRF2 and TRF1 of their telomeric DNA-bound structures and DNA-binding activities', *Protein science : a publication of the Protein Society*, 14(1), pp. 119-130.
- Hande, M.P., Samper, E., Lansdorp, P. and Blasco, M.A. (1999) 'Telomere length dynamics and chromosomal instability in cells derived from telomerase null mice', *J Cell Biol*, 144(4), pp. 589-601.
- Hansen, M., Chandra, A., Mitic, L., Onken, B., Driscoll, M. and Kenyon, C. (2008) 'A role for autophagy in the extension of lifespan by dietary restriction in *C. elegans*', *PLoS genetics*, 4(2).
- Hara, K., Maruki, Y., Long, X., Yoshino, K., Oshiro, N., Hidayat, S., Tokunaga, C., Avruch, J. and Yonezawa, K. (2002) 'Raptor, a binding partner of target of rapamycin (TOR), mediates TOR action', *Cell*, 110(2), pp. 177-89.
- Harley, C., Futcher, A. and Greider, C. (1990) 'Telomeres shorten during ageing of human fibroblasts', *Nature*, 345(6274), pp. 458-460.
- Harley, C.B., Vaziri, H., Counter, C.M. and Allsopp, R.C. (1992) 'The telomere hypothesis of cellular aging', *Exp Gerontol*, 27(4), pp. 375-82.
- Harman, D. (1956) 'Aging: a theory based on free radical and radiation chemistry', *Journal of gerontology*, 11(3), pp. 298-300.
- Harman, D. (1972) 'The biologic clock: the mitochondria?', *J Am Geriatr Soc*, 20(4), pp. 145-7.
- Harms, K., Nozell, S. and Chen, X. (2004) 'The common and distinct target genes of the p53 family transcription factors', *Cellular and molecular life sciences : CMLS*, 61(7-8), pp. 822-842.

Harrison, D., Strong, R., Sharp, Z., Nelson, J., Astle, C., Flurkey, K., Nadon, N., Wilkinson, J., Frenkel, K., Carter, C., Pahor, M., Javors, M., Fernandez, E. and Miller, R. (2009) 'Rapamycin fed late in life extends lifespan in genetically heterogeneous mice', *Nature*, 460(7253), pp. 392-395.

Hartman, T., Wengenack, T., Poduslo, J. and van Deursen, J. (2007) 'Mutant mice with small amounts of BubR1 display accelerated age-related gliosis', *Neurobiology of aging*, 28(6), pp. 921-927.

Haupt, Y., Maya, R., Kazaz, A. and Oren, M. (1997) 'Mdm2 promotes the rapid degradation of p53', *Nature*, 387(6630), pp. 296-299.

Haycock, P., Heydon, E., Kaptoge, S., Butterworth, A., Thompson, A. and Willeit, P. (2014) 'Leucocyte telomere length and risk of cardiovascular disease: systematic review and meta-analysis', *BMJ (Clinical research ed.)*, 349.

Hayflick, L. (1965) 'THE LIMITED IN VITRO LIFETIME OF HUMAN DIPLOID CELL STRAINS', *Experimental cell research*, 37, pp. 614-636.

Hayflick, L. and Moorhead, P. (1961) 'The serial cultivation of human diploid cell strains', *Experimental cell research*, 25, pp. 585-621.

Heaphy, C.M., Subhawong, A.P., Hong, S.M., Goggins, M.G., Montgomery, E.A., Gabrielson, E., Netto, G.J., Epstein, J.I., Lotan, T.L., Westra, W.H., Shih Ie, M., Iacobuzio-Donahue, C.A., Maitra, A., Li, Q.K., Eberhart, C.G., Taube, J.M., Rakheja, D., Kurman, R.J., Wu, T.C., Roden, R.B., Argani, P., De Marzo, A.M., Terracciano, L., Torbenson, M. and Meeker, A.K. (2011) 'Prevalence of the alternative lengthening of telomeres telomere maintenance mechanism in human cancer subtypes', *Am J Pathol*, 179(4), pp. 1608-15.

Hecker, L., Logsdon, N., Kurundkar, D., Kurundkar, A., Bernard, K., Hock, T., Meldrum, E., Sanders, Y. and Thannickal, V. (2014) 'Reversal of persistent fibrosis in aging by targeting Nox4-Nrf2 redox imbalance', *Science translational medicine*, 6(231).

Hediger, F., Neumann, F., Van Houwe, G., Dubrana, K. and Gasser, S. (2002) 'Live imaging of telomeres: yKu and Sir proteins define redundant telomere-anchoring pathways in yeast', *Current biology : CB*, 12(24), pp. 2076-2089.

Henderson, E. and Blackburn, E. (1989) 'An overhanging 3' terminus is a conserved feature of telomeres', *Molecular and cellular biology*, 9(1), pp. 345-348.

Henle, E., Han, Z., Tang, N., Rai, P., Luo, Y. and Linn, S. (1999) 'Sequence-specific DNA cleavage by Fe<sup>2+</sup>-mediated fenton reactions has possible biological implications', *The Journal of biological chemistry*, 274(2), pp. 962-971.

Hensel, M., Goetzenich, A., Lutz, T., Stoehr, A., Moll, A., Rockstroh, J., Hanhoff, N., Jäger, H. and Mosthaf, F. (2011) 'HIV and cancer in Germany', *Deutsches Ärzteblatt international*, 108(8), pp. 117-122.

Herbig, U., Ferreira, M., Condel, L., Carey, D. and Sedivy, J. (2006) 'Cellular senescence in aging primates', *Science (New York, N.Y.)*, 311(5765), p. 1257.

Herbig, U., Jobling, W., Chen, B., Chen, D. and Sedivy, J. (2004) 'Telomere shortening triggers senescence of human cells through a pathway involving ATM, p53, and p21(CIP1), but not p16(INK4a)', *Molecular cell*, 14(4), pp. 501-513.

Hewitt, G., Jurk, D., Marques, F., Correia-Melo, C., Hardy, T., Gackowska, A., Anderson, R., Taschuk, M., Mann, J. and Passos, J. (2012) 'Telomeres are favoured targets of a persistent DNA damage response in ageing and stress-induced senescence', *Nature communications*, 3, p. 708.

Hitomi, T., Matsuzaki, Y., Yasuda, S., Kawanaka, M., Yogosawa, S., Koyama, M., Tantin, D. and Sakai, T. (2007) 'Oct-1 is involved in the transcriptional repression of the p15(INK4b) gene', *FEBS letters*, 581(6), pp. 1087-1092.

Hockemeyer, D., Daniels, J.-P., Takai, H. and de Lange, T. (2006) 'Recent expansion of the telomeric complex in rodents: Two distinct POT1 proteins protect mouse telomeres', *Cell*, 126(1), pp. 63-77.

Hoenicke, L. and Zender, L. (2012) 'Immune surveillance of senescent cells-- biological significance in cancer- and non-cancer pathologies', *Carcinogenesis*, 33(6), pp. 1123-1126.

Holmstrom, K.M. and Finkel, T. (2014) 'Cellular mechanisms and physiological consequences of redox-dependent signalling', *Nat Rev Mol Cell Biol*, 15(6), pp. 411-21.

Huang, T. and Rivera-Pérez, J. (2014) 'Senescence-associated  $\beta$ -galactosidase activity marks the visceral endoderm of mouse embryos but is not indicative of senescence', *Genesis (New York, N.Y. : 2000)*, 52(4), pp. 300-308.

Hubackova, S., Krejcikova, K., Bartek, J. and Hodny, Z. (2012a) 'IL1- and TGF $\beta$ -Nox4 signaling, oxidative stress and DNA damage response are shared features of replicative, oncogene-induced, and drug-induced paracrine 'bystander senescence'', *Aging*, 4(12), pp. 932-951.

Hubackova, S., Krejcikova, K., Bartek, J. and Hodny, Z. (2012b) 'IL1-and TGF $\beta$ -Nox4 signaling, oxidative stress and DNA damage response are shared features of replicative, oncogene-induced, and drug-induced paracrine ...', *Aging (Albany NY)*.

Iacovoni, J., Caron, P., Lassadi, I., Nicolas, E., Massip, L., Trouche, D. and Legube, G. (2010) 'High-resolution profiling of gammaH2AX around DNA double strand breaks in the mammalian genome', *The EMBO journal*, 29(8), pp. 1446-1457.

Itahana, K., Zou, Y., Itahana, Y., Martinez, J.-L., Beausejour, C., Jacobs, J., Van Lohuizen, M., Band, V., Campisi, J. and Dimri, G. (2003) 'Control of the replicative life span of human fibroblasts by p16 and the polycomb protein Bmi-1', *Molecular and cellular biology*, 23(1), pp. 389-401.

Jackson, J. and Pereira-Smith, O. (2006) 'p53 is preferentially recruited to the promoters of growth arrest genes p21 and GADD45 during replicative senescence of normal human fibroblasts', *Cancer research*, 66(17), pp. 8356-8360.

Jackson, S. and Bartek, J. (2009) 'The DNA-damage response in human biology and disease', *Nature*, 461(7267), pp. 1071-1078.

Jacobs, J. and de Lange, T. (2004) 'Significant role for p16INK4a in p53-independent telomere-directed senescence', *Current biology : CB*, 14(24), pp. 2302-2308.

Janko, N.-Ž. (2008) 'Ageing and life-long maintenance of T-cell subsets in the face of latent persistent infections', *Nature Reviews Immunology*, 8.

Jazayeri, A., Falck, J., Lukas, C., Bartek, J., Smith, G., Lukas, J. and Jackson, S. (2006) 'ATM- and cell cycle-dependent regulation of ATR in response to DNA double-strand breaks', *Nature cell biology*, 8(1), pp. 37-45.

Jean-Philippe, C., Christopher, K.P., Francis, R., Yu, S., Denise, P.M., Joshua, G., Peter, S.N., Pierre-Yves, D., Judith, C. and Julian, D. (2008) 'Senescence-Associated Secretory Phenotypes Reveal Cell-Nonautonomous Functions of Oncogenic RAS and the p53 Tumor Suppressor', *PLoS Biology*, 6.

Jeyapalan, J., Ferreira, M., Sedivy, J. and Herbig, U. (2007) 'Accumulation of senescent cells in mitotic tissue of aging primates', *Mechanisms of ageing and development*, 128(1), pp. 36-44.

Judge, S., Jang, Y., Smith, A., Hagen, T. and Leeuwenburgh, C. (2005) 'Age-associated increases in oxidative stress and antioxidant enzyme activities in cardiac interfibrillar mitochondria: implications for the mitochondrial theory of aging', *FASEB journal : official publication of the Federation of American Societies for Experimental Biology*, 19(3), pp. 419-421.

Jun, J.-I. and Lau, L. (2010) 'The matricellular protein CCN1 induces fibroblast senescence and restricts fibrosis in cutaneous wound healing', *Nature cell biology*, 12(7), pp. 676-685.

Jurk, D., Wang, C., Miwa, S., Maddick, M., Korolchuk, V., Tsolou, A., Gonos, E., Thrasivoulou, C., Saffrey, M., Cameron, K. and von Zglinicki, T. (2012) 'Postmitotic neurons develop a p21-dependent senescence-like phenotype driven by a DNA damage response', *Aging cell*, 11(6), pp. 996-1004.

Kaeberlein, M., Powers, R., Steffen, K., Westman, E., Hu, D., Dang, N., Kerr, E., Kirkland, K., Fields, S. and Kennedy, B. (2005) 'Regulation of yeast replicative life span by TOR and Sch9 in response to nutrients', *Science (New York, N.Y.)*, 310(5751), pp. 1193-1196.

Kaludercic, N., Mialet-Perez, J., Paolocci, N., Parini, A. and Di Lisa, F. (2014) 'Monoamine oxidases as sources of oxidants in the heart', *Journal of molecular and cellular cardiology*, 73, pp. 34-42.

Kang, M., Kameta, A., Shin, K.-H., Baluda, M., Kim, H.-R. and Park, N.-H. (2003) 'Senescence-associated genes in normal human oral keratinocytes', *Experimental cell research*, 287(2), pp. 272-281.

Kang, T.-W., Yevsa, T., Woller, N., Hoenicke, L., Wuestefeld, T., Dauch, D., Hohmeyer, A., Gereke, M., Rudalska, R., Potapova, A., Iken, M., Vucur, M., Weiss, S., Heikenwalder, M., Khan, S., Gil, J., Bruder, D., Manns, M., Schirmacher, P., Tacke, F., Ott, M., Luedde, T., Longerich, T., Kubicka, S. and Zender, L. (2011) 'Senescence surveillance of pre-malignant hepatocytes limits liver cancer development', *Nature*, 479(7374), pp. 547-551.

Karl Lenhard, R., Sandy, C., Han-Woong, L., Maria, B., Geoffrey, J.G., Carol, G. and Ronald, A.D. (1999) 'Longevity, Stress Response, and Cancer in Aging Telomerase-Deficient Mice', *Cell*, 96.

Karlseder, J., Broccoli, D., Dai, Y., Hardy, S. and de Lange, T. (1999) 'p53- and ATM-dependent apoptosis induced by telomeres lacking TRF2', *Science (New York, N.Y.)*, 283(5406), pp. 1321-1325.

Kastan, M. (2008) 'DNA damage responses: mechanisms and roles in human disease: 2007 G.H.A. Clowes Memorial Award Lecture', *Molecular cancer research : MCR*, 6(4), pp. 517-524.

Kaul, N., Siveski-Iliskovic, N., Hill, M., Slezak, J. and Singal, P.K. (1993) 'Free radicals and the heart', *J Pharmacol Toxicol Methods*, 30(2), pp. 55-67.

Kaul, Z., Cesare, A., Huschtscha, L., Neumann, A. and Reddel, R. (2012) 'Five dysfunctional telomeres predict onset of senescence in human cells', *EMBO reports*, 13(1), pp. 52-59.

Kendellen, M., Barrientos, K. and Counter, C. (2009) 'POT1 association with TRF2 regulates telomere length', *Molecular and cellular biology*, 29(20), pp. 5611-5619.

Kennedy, A., McBryan, T., Enders, G., Johnson, F., Zhang, R. and Adams, P. (2010) 'Senescent mouse cells fail to overtly regulate the HIRA histone chaperone and do not form robust Senescence Associated Heterochromatin Foci', *Cell division*, 5, p. 16.

Khwaja, A., Rodriguez-Viciana, P., Wennström, S., Warne, P. and Downward, J. (1997) 'Matrix adhesion and Ras transformation both activate a phosphoinositide 3-OH kinase and protein kinase B/Akt cellular survival pathway', *The EMBO journal*, 16(10), pp. 2783-2793.

Kipling, D. and Cooke, H.J. (1990) 'Hypervariable ultra-long telomeres in mice', *Nature*, 347(6291), pp. 400-2.

Klobutcher, L., Swanton, M., Donini, P. and Prescott, D. (1981) 'All gene-sized DNA molecules in four species of hypotrichs have the same terminal sequence and an unusual 3' terminus', *Proceedings of the National Academy of Sciences of the United States of America*, 78(5), pp. 3015-3019.

Kolesnichenko, M., Hong, L., Liao, R., Vogt, P. and Sun, P. (2012) 'Attenuation of TORC1 signaling delays replicative and oncogenic RAS-induced senescence', *Cell cycle (Georgetown, Tex.)*, 11(12), pp. 2391-2401.

Kosar, M., Bartkova, J., Hubackova, S., Hodny, Z., Lukas, J. and Bartek, J. (2011) 'Senescence-associated heterochromatin foci are dispensable for cellular senescence, occur in a cell type- and insult-dependent manner and follow expression of p16(ink4a)', *Cell cycle (Georgetown, Tex.)*, 10(3), pp. 457-468.

Krishnamurthy, J., Torrice, C., Ramsey, M., Kovalev, G., Al-Regaiey, K., Su, L. and Sharpless, N. (2004) 'Ink4a/Arf expression is a biomarker of aging', *The Journal of clinical investigation*, 114(9), pp. 1299-1307.

Krizhanovsky, V., Yon, M., Dickins, R., Hearn, S., Simon, J., Miething, C., Yee, H., Zender, L. and Lowe, S. (2008) 'Senescence of activated stellate cells limits liver fibrosis', *Cell*, 134(4), pp. 657-667.

Krtolica, A., Parrinello, S., Lockett, S., Desprez, P. and Campisi, J. (2001) 'Senescent fibroblasts promote epithelial cell growth and tumorigenesis: a link between cancer and aging', *Proceedings of the National Academy of Sciences of the United States of America*, 98(21), pp. 12072-12077.

Kruk, P., Rampino, N. and Bohr, V. (1995) 'DNA damage and repair in telomeres: relation to aging', *Proceedings of the National Academy of Sciences of the United States of America*, 92(1), pp. 258-262.

Kruse, J.-P. and Gu, W. (2009) 'Modes of p53 regulation', *Cell*, 137(4), pp. 609-622.

Ksiazek, K., Jörres, A. and Witowski, J. (2008) 'Senescence induces a proangiogenic switch in human peritoneal mesothelial cells', *Rejuvenation research*, 11(3), pp. 681-683.

Kubbutat, M., Jones, S. and Vousden, K. (1997) 'Regulation of p53 stability by Mdm2', *Nature*, 387(6630), pp. 299-303.

Kuilman, T., Michaloglou, C., Vredeveld, L., Douma, S., van Doorn, R., Desmet, C., Aarden, L., Mooi, W. and Peeper, D. (2008) 'Oncogene-induced senescence relayed by an interleukin-dependent inflammatory network', *Cell*, 133(6), pp. 1019-1031.

Kuilman, T. and Peeper, D. (2009) 'Senescence-messaging secretome: SMS-ing cellular stress', *Nature reviews. Cancer*, 9(2), pp. 81-94.

Kuzminov, A. (1999) 'Recombinational repair of DNA damage in Escherichia coli and bacteriophage lambda', *Microbiology and molecular biology reviews : MMBR*, 63(4), p. 751.

Laberge, R.-M., Awad, P., Campisi, J. and Desprez, P.-Y. (2012) 'Epithelial-mesenchymal transition induced by senescent fibroblasts', *Cancer microenvironment : official journal of the International Cancer Microenvironment Society*, 5(1), pp. 39-44.

Laberge, R.-M., Sun, Y., Orjalo, A., Patil, C., Freund, A., Zhou, L., Curran, S., Davalos, A., Wilson-Edell, K., Liu, S., Limbad, C., Demaria, M., Li, P., Hubbard, G., Ikeno, Y., Javors, M., Desprez, P.-Y., Benz, C., Kapahi, P., Nelson, P. and Campisi, J. (2015) 'MTOR regulates the pro-tumorigenic senescence-associated secretory phenotype by promoting IL1A translation', *Nature cell biology*, 17(8), pp. 1049-1061.

Land, H., Parada, L. and Weinberg, R. (1983) 'Tumorigenic conversion of primary embryo fibroblasts requires at least two cooperating oncogenes', *Nature*, 304(5927), pp. 596-602.

Lawless, C., Wang, C., Jurk, D., Merz, A., Zglinicki, T. and Passos, J. (2010) 'Quantitative assessment of markers for cell senescence', *Experimental gerontology*, 45(10), pp. 772-778.

Lee, A., Fenster, B., Ito, H., Takeda, K., Bae, N., Hirai, T., Yu, Z., Ferrans, V., Howard, B. and Finkel, T. (1999a) 'Ras proteins induce senescence by altering the intracellular levels of reactive oxygen species', *The Journal of biological chemistry*, 274(12), pp. 7936-7940.

- Lee, A., Fenster, B., Ito, H., Takeda, K. and Bae... , N. (1999b) 'Ras proteins induce senescence by altering the intracellular levels of reactive oxygen species', *Journal of Biological ...*
- Lee, B., Han, J., Im, J., Morrone, A., Johung, K., Goodwin, E., Kleijer, W., DiMaio, D. and Hwang, E. (2006) 'Senescence-associated beta-galactosidase is lysosomal beta-galactosidase', *Aging cell*, 5(2), pp. 187-195.
- Lee, H.W., Blasco, M.A., Gottlieb, G.J., Horner, J.W., 2nd, Greider, C.W. and DePinho, R.A. (1998) 'Essential role of mouse telomerase in highly proliferative organs', *Nature*, 392(6676), pp. 569-74.
- Lei, M., Podell, E. and Cech, T. (2004) 'Structure of human POT1 bound to telomeric single-stranded DNA provides a model for chromosome end-protection', *Nature structural & molecular biology*, 11(12), pp. 1223-1229.
- Leri, A., Franco, S., Zacheo, A., Barlucchi, L., Chimenti, S., Limana, F., Nadal-Ginard, B., Kajstura, J., Anversa, P. and Blasco, M. (2003) 'Ablation of telomerase and telomere loss leads to cardiac dilatation and heart failure associated with p53 upregulation', *The EMBO journal*, 22(1), pp. 131-139.
- Levine, A. (1997) 'p53, the cellular gatekeeper for growth and division', *Cell*, 88(3), pp. 323-331.
- Li, F., Wang, X., Bungler, P. and Gerdes, A. (1997) 'Formation of binucleated cardiac myocytes in rat heart: I. Role of actin-myosin contractile ring', *Journal of molecular and cellular cardiology*, 29(6), pp. 1541-1551.
- Li, Y., Huang, T., Carlson, E., Melov, S., Ursell, P., Olson, J., Noble, L., Yoshimura, M., Berger, C., Chan, P., Wallace, D. and Epstein, C. (1995) 'Dilated cardiomyopathy and neonatal lethality in mutant mice lacking manganese superoxide dismutase', *Nature genetics*, 11(4), pp. 376-381.
- Libby, P. (2002) 'Inflammation and Atherosclerosis', *Circulation*, 105.
- Lieber, M. (2010) 'The mechanism of double-strand DNA break repair by the nonhomologous DNA end-joining pathway', *Annual review of biochemistry*, 79, pp. 181-211.
- Lindsten, T., Ross, A.J., King, A., Zong, W.X., Rathmell, J.C., Shiels, H.A., Ulrich, E., Waymire, K.G., Mahar, P., Frauwirth, K., Chen, Y., Wei, M., Eng, V.M., Adelman, D.M., Simon, M.C., Ma, A., Golden, J.A., Evan, G., Korsmeyer, S.J., MacGregor, G.R. and Thompson, C.B. (2000) 'The combined functions of proapoptotic Bcl-2 family members bak and bax are essential for normal development of multiple tissues', *Mol Cell*, 6(6), pp. 1389-99.

Little, M. (2010) 'Exposure to radiation and higher risk of circulatory disease', *BMJ (Clinical research ed.)*, 340.

Liu, D. and Hornsby, P. (2007) 'Senescent human fibroblasts increase the early growth of xenograft tumors via matrix metalloproteinase secretion', *Cancer research*, 67(7), pp. 3117-3126.

Lombardi, R., Betocchi, S., Losi, M., Tocchetti, C., Aversa, M., Miranda, M., D'Alessandro, G., Cacace, A., Ciampi, Q. and Chiariello, M. (2003) 'Myocardial collagen turnover in hypertrophic cardiomyopathy', *Circulation*, 108(12), pp. 1455-1460.

Lou, Z., Minter-Dykhouse, K., Franco, S., Gostissa, M., Rivera, M., Celeste, A., Manis, J., van Deursen, J., Nussenzweig, A., Paull, T., Alt, F. and Chen, J. (2006) 'MDC1 maintains genomic stability by participating in the amplification of ATM-dependent DNA damage signals', *Molecular cell*, 21(2), pp. 187-200.

Lowe, S. and Sherr, C. (2003) 'Tumor suppression by Ink4a-Arf: progress and puzzles', *Current opinion in genetics & development*, 13(1), pp. 77-83.

Lu, T. and Finkel, T. (2008a) 'Free radicals and senescence', *Experimental cell research*, 314(9), pp. 1918-1922.

Lu, T. and Finkel, T. (2008b) 'Free radicals and senescence', *Exp Cell Res*, 314(9), pp. 1918-22.

Lu, T.M., Tsai, J.Y., Chen, Y.C., Huang, C.Y., Hsu, H.L., Weng, C.F., Shih, C.C. and Hsu, C.P. (2014) 'Downregulation of Sirt1 as aging change in advanced heart failure', *J Biomed Sci*, 21, p. 57.

Lv, X.-x., Wang, X.-x., Li, K., Wang, Z.-y., Li, Z., Lv, Q., Fu, X.-m. and Hu, Z.-w. (2013) 'Rupatadine protects against pulmonary fibrosis by attenuating PAF-mediated senescence in rodents', *PLoS ONE*, 8(7).

Ma, L., Wagner, J., Rice, J.J., Hu, W., Levine, A.J. and Stolovitzky, G.A. (2005) 'A plausible model for the digital response of p53 to DNA damage', *Proc Natl Acad Sci U S A*, 102(40), pp. 14266-71.

Macip, S., Igarashi, M., Berggren, P., Yu, J., Lee, S. and Aaronson, S. (2003) 'Influence of induced reactive oxygen species in p53-mediated cell fate decisions', *Molecular and cellular biology*, 23(23), pp. 8576-8585.

Macip, S., Igarashi, M., Fang, L., Chen, A., Pan, Z.-Q., Lee, S. and Aaronson, S. (2002) 'Inhibition of p21-mediated ROS accumulation can rescue p21-induced senescence', *The EMBO journal*, 21(9), pp. 2180-2188.

- Mailand, N., Falck, J., Lukas, C., Syljuâsen, R., Welcker, M., Bartek, J. and Lukas, J. (2000) 'Rapid destruction of human Cdc25A in response to DNA damage', *Science (New York, N.Y.)*, 288(5470), pp. 1425-1429.
- Mair, W., Goymer, P., Pletcher, S. and Partridge, L. (2003) 'Demography of dietary restriction and death in *Drosophila*', *Science (New York, N.Y.)*, 301(5640), pp. 1731-1733.
- Malliaras, K., Zhang, Y., Seinfeld, J., Galang, G., Tseliou, E., Cheng, K., Sun, B., Aminzadeh, M. and Marbán, E. (2013) 'Cardiomyocyte proliferation and progenitor cell recruitment underlie therapeutic regeneration after myocardial infarction in the adult mouse heart', *EMBO molecular medicine*, 5(2), pp. 191-209.
- Mann, J., Chu, D., Maxwell, A., Oakley, F., Zhu, N.-L., Tsukamoto, H. and Mann, D. (2010) 'MeCP2 controls an epigenetic pathway that promotes myofibroblast transdifferentiation and fibrosis', *Gastroenterology*, 138(2), p. 705.
- Markowski, D., Thies, H., Gottlieb, A., Wenk, H., Wischnewsky, M. and Bullerdiek, J. (2013) 'HMGA2 expression in white adipose tissue linking cellular senescence with diabetes', *Genes & nutrition*, 8(5), pp. 449-456.
- Marks, R., Dorevitch, A. and Mason, G. (1990) 'Do all melanomas come from "moles"? A study of the histological association between melanocytic naevi and melanoma', *The Australasian journal of dermatology*, 31(2), pp. 77-80.
- Martin, J. and Buckwalter, J. (2003) 'The role of chondrocyte senescence in the pathogenesis of osteoarthritis and in limiting cartilage repair', *The Journal of bone and joint surgery. American volume*, 85-A Suppl 2, pp. 106-110.
- Masi, S., D'Aiuto, F., Martin-Ruiz, C., Kahn, T., Wong, A., Ghosh, A., Whincup, P., Kuh, D., Hughes, A., von Zglinicki, T., Hardy, R., Deanfield, J., scientific, N. and data collection, t. (2014) 'Rate of telomere shortening and cardiovascular damage: a longitudinal study in the 1946 British Birth Cohort', *European heart journal*, 35(46), pp. 3296-3303.
- Mason, D., Jackson, T. and Lin, A. (2004) 'Molecular signature of oncogenic ras-induced senescence', *Oncogene*, 23(57), pp. 9238-9246.
- Matsumoto, T., Baker, D., d'Uscio, L., Mozammel, G., Katusic, Z. and van Deursen, J. (2007) 'Aging-associated vascular phenotype in mutant mice with low levels of BubR1', *Stroke; a journal of cerebral circulation*, 38(3), pp. 1050-1056.
- Maurel, A., Hernandez, C., Kunduzova, O., Bompert, G., Cambon, C., Parini, A. and Francés, B. (2003) 'Age-dependent increase in hydrogen peroxide production by

cardiac monoamine oxidase A in rats', *American journal of physiology. Heart and circulatory physiology*, 284(4), p. 7.

McClintock, B. (1938) 'fusion of broken ends of sister half-chromatids following chromatid breakage at meiotic anaphases', *University of Missouri, College of Agriculture, Agricultural Experiment Station*.

McClintock, B. (1941) 'The Stability of Broken Ends of Chromosomes in Zea Mays', *Genetics*, 26(2), pp. 234-282.

McElligott, R. and Wellinger, R. (1997) 'The terminal DNA structure of mammalian chromosomes', *The EMBO journal*, 16(12), pp. 3705-3714.

McMullen, J.R., Sherwood, M.C., Tarnavski, O., Zhang, L., Dorfman, A.L., Shioi, T. and Izumo, S. (2004) 'Inhibition of mTOR signaling with rapamycin regresses established cardiac hypertrophy induced by pressure overload', *Circulation*, 109(24), pp. 3050-5.

Medvedik, O., Lamming, D., Kim, K. and Sinclair, D. (2007) 'MSN2 and MSN4 link calorie restriction and TOR to sirtuin-mediated lifespan extension in *Saccharomyces cerevisiae*', *PLoS biology*, 5(10).

Meier, A., Fiegler, H., Muñoz, P., Ellis, P., Rigler, D., Langford, C., Blasco, M., Carter, N. and Jackson, S. (2007) 'Spreading of mammalian DNA-damage response factors studied by ChIP-chip at damaged telomeres', *The EMBO journal*, 26(11), pp. 2707-2718.

Melk, A., Kittikowit, W., Sandhu, I., Halloran, K., Grimm, P., Schmidt, B. and Halloran, P. (2003) 'Cell senescence in rat kidneys in vivo increases with growth and age despite lack of telomere shortening', *Kidney international*, 63(6), pp. 2134-2143.

Meyne, J., Baker, R., Hobart, H., Hsu, Ryder, O., Ward, O., Wiley, J., Wurster-Hill, D., Yates, T. and Moyzis, R. (1990) 'Distribution of non-telomeric sites of the (TTAGGG)<sub>n</sub> telomeric sequence in vertebrate chromosomes', *Chromosoma*, 99(1), pp. 3-10.

Michaloglou, C., Vredeveld, L., Soengas, M., Denoyelle, C., Kuilman, T., van der Horst, C.M.A., Majoor, D., Shay, J., Mooi, W. and Peeper, D. (2005) 'BRAFE600-associated senescence-like cell cycle arrest of human naevi', *Nature*, 436(7051), pp. 720-724.

Midwood, K., Williams, L. and Schwarzbauer, J. (2004) 'Tissue repair and the dynamics of the extracellular matrix', *The international journal of biochemistry & cell biology*, 36(6), pp. 1031-1037.

Miller, R., Harrison, D., Astle, C., Baur, J., Boyd, A., de Cabo, R., Fernandez, E., Flurkey, K., Javors, M., Nelson, J., Orihuela, C., Pletcher, S., Sharp, Z., Sinclair, D., Starnes, J., Wilkinson, J., Nadon, N. and Strong, R. (2011) 'Rapamycin, but not resveratrol or simvastatin, extends life span of genetically heterogeneous mice', *The journals of gerontology. Series A, Biological sciences and medical sciences*, 66(2), pp. 191-201.

Millis, A., Hoyle, M., McCue, H. and Martini, H. (1992) 'Differential expression of metalloproteinase and tissue inhibitor of metalloproteinase genes in aged human fibroblasts', *Experimental cell research*, 201(2), pp. 373-379.

Minamino, T., Orimo, M., Shimizu, I., Kunieda, T., Yokoyama, M., Ito, T., Nojima, A., Nabetani, A., Oike, Y., Matsubara, H., Ishikawa, F. and Komuro, I. (2009) 'A crucial role for adipose tissue p53 in the regulation of insulin resistance', *Nature medicine*, 15(9), pp. 1082-1087.

Mitchell, J.R., Wood, E. and Collins, K. (1999) 'A telomerase component is defective in the human disease dyskeratosis congenita', *Nature*, 402(6761), pp. 551-5.

Miwa, S., Jow, H., Baty, K., Johnson, A., Czapiewski, R., Saretzki, G., Treumann, A. and von Zglinicki, T. (2014a) 'Low abundance of the matrix arm of complex I in mitochondria predicts longevity in mice', *Nature communications*, 5, p. 3837.

Miwa, S., Jow, H., Baty, K., Johnson, A., Czapiewski, R., Saretzki, G., Treumann, A. and von Zglinicki, T. (2014b) 'Low abundance of the matrix arm of complex I in mitochondria predicts longevity in mice', *Nat Commun*, 5, p. 3837.

Mo, J.Q., Hom, D.G. and Andersen, J.K. (1995) 'Decreases in protective enzymes correlates with increased oxidative damage in the aging mouse brain', *Mech Ageing Dev*, 81(2-3), pp. 73-82.

Moiseeva, O., Bourdeau, V., Roux, A., Deschênes-Simard, X. and Ferbeyre, G. (2009) 'Mitochondrial dysfunction contributes to oncogene-induced senescence', *Molecular and cellular biology*, 29(16), pp. 4495-4507.

Moldovan, G.-L., Pfander, B. and Jentsch, S. (2007) 'PCNA, the maestro of the replication fork', *Cell*, 129(4), pp. 665-679.

Molenaar, C., Wiesmeijer, K., Verwoerd, N., Khazen, S., Eils, R., Tanke, H. and Dirks, R. (2003) 'Visualizing telomere dynamics in living mammalian cells using PNA probes', *The EMBO journal*, 22(24), pp. 6631-6641.

Momand, J., Jung, D., Wilczynski, S. and Niland, J. (1998) 'The MDM2 gene amplification database', *Nucleic acids research*, 26(15), pp. 3453-3459.

Momand, J., Zambetti, G., Olson, D., George, D. and Levine, A. (1992) 'The mdm-2 oncogene product forms a complex with the p53 protein and inhibits p53-mediated transactivation', *Cell*, 69(7), pp. 1237-1245.

Mone, S., Gillman, M., Miller, T., Herman, E. and Lipshultz, S. (2004) 'Effects of environmental exposures on the cardiovascular system: prenatal period through adolescence', *Pediatrics*, 113(4 Suppl), pp. 1058-1069.

Morita, M., Gravel, S.-P., Chénard, V., Sikström, K., Zheng, L., Alain, T., Gandin, V., Avizonis, D., Arguello, M., Zakaria, C., McLaughlan, S., Nouet, Y., Pause, A., Pollak, M., Gottlieb, E., Larsson, O., St-Pierre, J., Topisirovic, I. and Sonenberg, N. (2013) 'mTORC1 controls mitochondrial activity and biogenesis through 4E-BP-dependent translational regulation', *Cell metabolism*, 18(5), pp. 698-711.

Muñoz-Espín, D., Cañamero, M., Maraver, A., Gómez-López, G., Contreras, J., Murillo-Cuesta, S., Rodríguez-Baeza, A., Varela-Nieto, I., Ruberte, J., Collado, M. and Serrano, M. (2013a) 'Programmed cell senescence during mammalian embryonic development', *Cell*, 155(5), pp. 1104-1118.

Muñoz-Espín, D., Cañamero, M., Maraver, A., Gómez-López, G., Contreras, J., Murillo-Cuesta, S., Rodríguez-Baeza, A., Varela-Nieto, I., Ruberte, J., Collado, M. and Serrano, M. (2013b) 'Programmed Cell Senescence during Mammalian Embryonic Development', *Cell*.

Muñoz-Espín, D. and Serrano, M. (2014) 'Cellular senescence: from physiology to pathology', *Nature reviews. Molecular cell biology*, 15(7), pp. 482-496.

Nacher, V., Carretero, A., Navarro, M., Armengol, C., Llombart, C., Rodríguez, A., Herrero-Fresneda, I., Ayuso, E. and Ruberte, J. (2006) 'The quail mesonephros: a new model for renal senescence?', *Journal of vascular research*, 43(6), pp. 581-586.

Nakamura, A., Chiang, Y., Hathcock, K., Horikawa, I., Sedelnikova, O., Hodes, R. and Bonner, W. (2008) 'Both telomeric and non-telomeric DNA damage are determinants of mammalian cellular senescence', *Epigenetics & chromatin*, 1(1), p. 6.

Narita, M., Nunez, S., Heard, E., Narita, M., Lin, A., Hearn, S., Spector, D., Hannon, G. and Lowe, S. (2003) 'Rb-mediated heterochromatin formation and silencing of E2F target genes during cellular senescence', *Cell*, 113(6), pp. 703-716.

Navarro, A. and Boveris, A. (2007) 'The mitochondrial energy transduction system and the aging process', *American journal of physiology. Cell physiology*, 292(2), p. 86.

Negre-Salvayre, A., Vieira, O., Escargueil-Blanc, I. and Salvayre, R. (2003) 'Oxidized LDL and 4-hydroxynonenal modulate tyrosine kinase receptor activity', *Mol Aspects Med*, 24(4-5), pp. 251-61.

Nelson, G., Wordsworth, J., Wang, C., Jurk, D., Lawless, C., Martin-Ruiz, C. and von Zglinicki, T. (2012) 'A senescent cell bystander effect: senescence-induced senescence', *Aging cell*, 11(2), pp. 345-349.

Nickoloff, B., Lingen, M., Chang, B.-D., Shen, M., Swift, M., Curry, J., Bacon, P., Bodner, B. and Roninson, I. (2004) 'Tumor suppressor maspin is up-regulated during keratinocyte senescence, exerting a paracrine antiangiogenic activity', *Cancer research*, 64(9), pp. 2956-2961.

Nouredine, H., Gary-Bobo, G., Alifano, M., Marcos, E., Saker, M., Vienney, N., Amsellem, V., Maitre, B., Chaouat, A., Chouaid, C., Dubois-Rande, J.-L., Damotte, D. and Adnot, S. (2011) 'Pulmonary artery smooth muscle cell senescence is a pathogenic mechanism for pulmonary hypertension in chronic lung disease', *Circulation research*, 109(5), pp. 543-553.

Oikawa, S., Tada-Oikawa, S. and Kawanishi, S. (2001) 'Site-specific DNA damage at the GGG sequence by UVA involves acceleration of telomere shortening', *Biochemistry*, 40(15), pp. 4763-4768.

Olovnikov, A. (1971) '[Principle of marginotomy in template synthesis of polynucleotides]', *Doklady Akademii nauk SSSR*, 201(6), pp. 1496-1499.

Olsen, C., Gardie, B., Yaswen, P. and Stampfer, M. (2002) 'Raf-1-induced growth arrest in human mammary epithelial cells is p16-independent and is overcome in immortal cells during conversion', *Oncogene*, 21(41), pp. 6328-6339.

Onorato, J.M., Thorpe, S.R. and Baynes, J.W. (1998) 'Immunohistochemical and ELISA assays for biomarkers of oxidative stress in aging and disease', *Ann N Y Acad Sci*, 854, pp. 277-90.

Opresko, P., Fan, J., Danzy, S., Wilson, D. and Bohr, V. (2005) 'Oxidative damage in telomeric DNA disrupts recognition by TRF1 and TRF2', *Nucleic acids research*, 33(4), pp. 1230-1239.

Orr-Weaver, T., Szostak, J. and Rothstein, R. (1981) 'Yeast transformation: a model system for the study of recombination', *Proceedings of the National Academy of Sciences of the United States of America*, 78(10), pp. 6354-6358.

Pang, J. and Chen, K. (1994) 'Global change of gene expression at late G1/S boundary may occur in human IMR-90 diploid fibroblasts during senescence', *Journal of cellular physiology*, 160(3), pp. 531-538.

Parada, L., Tabin, C., Shih, C. and Weinberg, R. (1982) 'Human EJ bladder carcinoma oncogene is homologue of Harvey sarcoma virus ras gene', *Nature*, 297(5866), pp. 474-478.

Paradis, V., Youssef, N., Dargère, D., Bâ, N., Bonvoust, F., Deschatrette, J. and Bedossa, P. (2001) 'Replicative senescence in normal liver, chronic hepatitis C, and hepatocellular carcinomas', *Human pathology*, 32(3), pp. 327-332.

Parrinello, S., Coppe, J.-P., Krtolica, A. and Campisi, J. (2005) 'Stromal-epithelial interactions in aging and cancer: senescent fibroblasts alter epithelial cell differentiation', *Journal of cell science*, 118(Pt 3), pp. 485-496.

Parrinello, S., Samper, E., Krtolica, A., Goldstein, J., Melov, S. and Campisi, J. (2003) 'Oxygen sensitivity severely limits the replicative lifespan of murine fibroblasts', *Nature cell biology*, 5(8), pp. 741-747.

Passos, J., Nelson, G., Wang, C., Richter, T., Simillion, C., Proctor, C., Miwa, S., Olijslagers, S., Hallinan, J., Wipat, A., Saretzki, G., Rudolph, K., Kirkwood, T. and von Zglinicki, T. (2010) 'Feedback between p21 and reactive oxygen production is necessary for cell senescence', *Molecular systems biology*, 6, p. 347.

Passos, J., Saretzki, G., Ahmed, S., Nelson, G., Richter, T., Peters, H., Wappler, I., Birket, M., Harold, G., Schaeuble, K., Birch-Machin, M., Kirkwood, T. and von Zglinicki, T. (2007) 'Mitochondrial dysfunction accounts for the stochastic heterogeneity in telomere-dependent senescence', *PLoS biology*, 5(5).

Perry, J. and Tainer, J. (2011) 'All stressed out without ATM kinase', *Science signaling*, 4(167).

Petersen, S., Saretzki, G. and von Zglinicki, T. (1998) 'Preferential accumulation of single-stranded regions in telomeres of human fibroblasts', *Experimental cell research*, 239(1), pp. 152-160.

Pollock, P., Harper, U., Hansen, K., Yudt, L., Stark, M., Robbins, C., Moses, T., Hostetter, G., Wagner, U., Kakareka, J., Salem, G., Pohida, T., Heenan, P., Duray, P., Kallioniemi, O., Hayward, N., Trent, J. and Meltzer, P. (2003) 'High frequency of BRAF mutations in nevi', *Nature genetics*, 33(1), pp. 19-20.

Polyak, K., Xia, Y., Zweier, J., Kinzler, K. and Vogelstein, B. (1997) 'A model for p53-induced apoptosis', *Nature*, 389(6648), pp. 300-305.

Pospelova, T., Leontieva, O., Bykova, T., Zubova, S., Pospelov, V. and Blagosklonny, M. (2012) 'Suppression of replicative senescence by rapamycin in rodent embryonic cells', *Cell cycle (Georgetown, Tex.)*, 11(12), pp. 2402-2407.

- Powers, R., Kaeberlein, M., Caldwell, S., Kennedy, B. and Fields, S. (2006) 'Extension of chronological life span in yeast by decreased TOR pathway signaling', *Genes & development*, 20(2), pp. 174-184.
- Pribluda, A., Elyada, E., Wiener, Z., Hamza, H., Goldstein, R.E., Biton, M., Burstain, I., Morgenstern, Y., Brachya, G., Billauer, H., Biton, S., Snir-Alkalay, I., Vucic, D., Schlereth, K., Mernberger, M., Stiewe, T., Oren, M., Alitalo, K., Pikarsky, E. and Ben-Neriah, Y. (2013) 'A senescence-inflammatory switch from cancer-inhibitory to cancer-promoting mechanism', *Cancer Cell*, 24(2), pp. 242-56.
- Quinlan, C., Perevoshchikova, I., Hey-Mogensen, M., Orr, A. and Brand, M. (2013) 'Sites of reactive oxygen species generation by mitochondria oxidizing different substrates', *Redox biology*, 1, pp. 304-312.
- Radi, R., Turrens, J.F., Chang, L.Y., Bush, K.M., Crapo, J.D. and Freeman, B.A. (1991) 'Detection of catalase in rat heart mitochondria', *J Biol Chem*, 266(32), pp. 22028-34.
- Rajagopalan, S. and Long, E. (2012) 'Cellular senescence induced by CD158d reprograms natural killer cells to promote vascular remodeling', *Proceedings of the National Academy of Sciences of the United States of America*, 109(50), pp. 20596-20601.
- Ramsey, M. and Sharpless, N. (2006) 'ROS as a tumour suppressor?', *Nature cell biology*, 8(11), pp. 1213-1215.
- Rausser, C., Mueller, L. and Rose, M. (2006) 'The evolution of late life', *Ageing research reviews*, 5(1), pp. 14-32.
- Rebbaa, A., Zheng, X., Chou, P. and Mirkin, B. (2003) 'Caspase inhibition switches doxorubicin-induced apoptosis to senescence', *Oncogene*, 22(18), pp. 2805-2811.
- Riballo, E., Kühne, M., Rief, N., Doherty, A., Smith, G., Recio, M.-J., Reis, C., Dahm, K., Fricke, A., Krempler, A., Parker, A., Jackson, S., Gennery, A., Jeggo, P. and Löbrich, M. (2004) 'A pathway of double-strand break rejoining dependent upon ATM, Artemis, and proteins locating to gamma-H2AX foci', *Molecular cell*, 16(5), pp. 715-724.
- Richter, T., Saretzki, G., Nelson, G., Melcher, M., Olijslagers, S. and von Zglinicki, T. (2007) 'TRF2 overexpression diminishes repair of telomeric single-strand breaks and accelerates telomere shortening in human fibroblasts', *Mechanisms of ageing and development*, 128(4), pp. 340-345.

Rindler, P., Plafker, S., Szweda, L. and Kinter, M. (2013) 'High dietary fat selectively increases catalase expression within cardiac mitochondria', *The Journal of biological chemistry*, 288(3), pp. 1979-1990.

Robida-Stubbs, S., Glover-Cutter, K., Lamming, D., Mizunuma, M., Narasimhan, S., Neumann-Haefelin, E., Sabatini, D. and Blackwell, T. (2012) 'TOR signaling and rapamycin influence longevity by regulating SKN-1/Nrf and DAF-16/FoxO', *Cell metabolism*, 15(5), pp. 713-724.

Robinson, W., Lemon, M., Elefanty, A., Harrison-Smith, M., Markham, N. and Norris, D. (1998) 'Human acquired naevi are clonal', *Melanoma research*, 8(6), pp. 499-503.

Robles, S. and Adami, G. (1998) 'Agents that cause DNA double strand breaks lead to p16INK4a enrichment and the premature senescence of normal fibroblasts', *Oncogene*, 16(9), pp. 1113-1123.

Rodier, F. and Campisi, J. (2011) 'Four faces of cellular senescence', *The Journal of cell biology*, 192(4), pp. 547-556.

Rodier, F., Coppé, J.-P., Patil, C., Hoeijmakers, W., Muñoz, D., Raza, S., Freund, A., Campeau, E., Davalos, A. and Campisi, J. (2009) 'Persistent DNA damage signalling triggers senescence-associated inflammatory cytokine secretion', *Nature cell biology*, 11(8), pp. 973-979.

Rogakou, E., Boon, C., Redon, C. and Bonner, W. (1999) 'Megabase chromatin domains involved in DNA double-strand breaks in vivo', *The Journal of cell biology*, 146(5), pp. 905-916.

Rouse, J. (2002) 'Interfaces Between the Detection, Signaling, and Repair of DNA Damage', *Science*, 297.

Rudolph, K.L., Chang, S., Lee, H.W., Blasco, M., Gottlieb, G.J., Greider, C. and DePinho, R.A. (1999) 'Longevity, stress response, and cancer in aging telomerase-deficient mice', *Cell*, 96(5), pp. 701-12.

Ruiz-Herrera, A., García, F., Azzalin, C., Giulotto, E., Egozcue, J., Ponsà, M. and Garcia, M. (2002) 'Distribution of intrachromosomal telomeric sequences (ITS) on *Macaca fascicularis* (Primates) chromosomes and their implication for chromosome evolution', *Human genetics*, 110(6), pp. 578-586.

Saleh-Gohari, N., Bryant, H.E., Schultz, N., Parker, K.M., Cassel, T.N. and Helleday, T. (2005) 'Spontaneous homologous recombination is induced by collapsed replication forks that are caused by endogenous DNA single-strand breaks', *Mol Cell Biol*, 25(16), pp. 7158-69.

Sarbassov, D.D., Ali, S.M., Kim, D.H., Guertin, D.A., Latek, R.R., Erdjument-Bromage, H., Tempst, P. and Sabatini, D.M. (2004) 'Rictor, a novel binding partner of mTOR, defines a rapamycin-insensitive and raptor-independent pathway that regulates the cytoskeleton', *Curr Biol*, 14(14), pp. 1296-302.

Saretzki, G., Murphy, M.P. and von Zglinicki, T. (2003) 'MitoQ counteracts telomere shortening and elongates lifespan of fibroblasts under mild oxidative stress', *Aging Cell*, 2(2), pp. 141-3.

Sarkisian, C., Keister, B., Stairs, D., Boxer, R., Moody, S. and Chodosh, L. (2007) 'Dose-dependent oncogene-induced senescence in vivo and its evasion during mammary tumorigenesis', *Nature cell biology*, 9(5), pp. 493-505.

Schmitt, C., Fridman, J., Yang, M., Lee, S., Baranov, E., Hoffman, R. and Lowe, S. (2002) 'A senescence program controlled by p53 and p16INK4a contributes to the outcome of cancer therapy', *Cell*, 109(3), pp. 335-346.

Schriner, S., Linford, N., Martin, G., Treuting, P., Ogburn, C., Emond, M., Coskun, P., Ladiges, W., Wolf, N., Van Remmen, H., Wallace, D. and Rabinovitch, P. (2005a) 'Extension of murine life span by overexpression of catalase targeted to mitochondria', *Science (New York, N.Y.)*, 308(5730), pp. 1909-1911.

Schriner, S.E., Linford, N.J., Martin, G.M., Treuting, P., Ogburn, C.E., Emond, M., Coskun, P.E., Ladiges, W., Wolf, N., Van Remmen, H., Wallace, D.C. and Rabinovitch, P.S. (2005b) 'Extension of murine life span by overexpression of catalase targeted to mitochondria', *Science*, 308(5730), pp. 1909-11.

Seluanov, A., Gorbunova, V., Falcovitz, A., Sigal, A., Milyavsky, M., Zurer, I., Shohat, G., Goldfinger, N. and Rotter, V. (2001) 'Change of the death pathway in senescent human fibroblasts in response to DNA damage is caused by an inability to stabilize p53', *Molecular and cellular biology*, 21(5), pp. 1552-1564.

Senyo, S., Steinhauser, M., Pizzimenti, C., Yang, V., Cai, L., Wang, M., Wu, T.-D., Guerquin-Kern, J.-L., Lechene, C. and Lee, R. (2013) 'Mammalian heart renewal by pre-existing cardiomyocytes', *Nature*, 493(7432), pp. 433-436.

Serrano, M., Lin, A., McCurrach, M., Beach, D. and Lowe, S. (1997) 'Oncogenic ras provokes premature cell senescence associated with accumulation of p53 and p16INK4a', *Cell*, 88(5), pp. 593-602.

Seshadri, T. and Campisi, J. (1990) 'Repression of c-fos transcription and an altered genetic program in senescent human fibroblasts', *Science (New York, N.Y.)*, 247(4939), pp. 205-209.

Severino, J., Allen, R., Balin, S., Balin, A. and Cristofalo, V. (2000) 'Is beta-galactosidase staining a marker of senescence in vitro and in vivo?', *Experimental cell research*, 257(1), pp. 162-171.

Shampay, J., Szostak, J.W. and Blackburn, E.H. (1984) 'DNA sequences of telomeres maintained in yeast', *Nature*, 310(5973), pp. 154-7.

Sharpless, N. and DePinho, R. (2007) 'How stem cells age and why this makes us grow old', *Nature reviews. Molecular cell biology*, 8(9), pp. 703-713.

Shay, J. and Bacchetti, S. (1997) 'A survey of telomerase activity in human cancer', *European journal of cancer (Oxford, England : 1990)*, 33(5), pp. 787-791.

Shay, J. and Roninson, I. (2004) 'Hallmarks of senescence in carcinogenesis and cancer therapy', *Oncogene*, 23(16), pp. 2919-2933.

Shay, J. and Wright, W. (2005) 'Senescence and immortalization: role of telomeres and telomerase', *Carcinogenesis*, 26(5), pp. 867-874.

Shelton, D., Chang, E., Whittier, P., Choi, D. and Funk, W. (1999) 'Microarray analysis of replicative senescence', *Current biology : CB*, 9(17), pp. 939-945.

Sherr, C. (2000) 'The Pezcoller lecture: cancer cell cycles revisited', *Cancer research*, 60(14), pp. 3689-3695.

Sherr, C. and McCormick, F. (2002) 'The RB and p53 pathways in cancer', *Cancer cell*, 2(2), pp. 103-112.

Shibata, A., Conrad, S., Birraux, J., Geuting, V., Barton, O., Ismail, A., Kakarougkas, A., Meek, K., Taucher-Scholz, G., Lobrich, M. and Jeggo, P.A. (2011) 'Factors determining DNA double-strand break repair pathway choice in G2 phase', *EMBO J*, 30(6), pp. 1079-92.

Shieh, S.-Y., Ahn, J., Tamai, K., Taya, Y. and Prives, C. (2000) 'The human homologs of checkpoint kinases Chk1 and Cds1 (Chk2) phosphorylate p53 at multiple DNA damage-inducible sites', *Genes & development*, 14(3), pp. 289-300.

Shieh, S., Ikeda, M., Taya, Y. and Prives, C. (1997) 'DNA damage-induced phosphorylation of p53 alleviates inhibition by MDM2', *Cell*, 91(3), pp. 325-334.

Shimizu, Y., Kodama, K., Nishi, N., Kasagi, F., Suyama, A., Soda, M., Grant, E., Sugiyama, H., Sakata, R., Moriwaki, H., Hayashi, M., Konda, M. and Shore, R. (2010) 'Radiation exposure and circulatory disease risk: Hiroshima and Nagasaki atomic bomb survivor data, 1950-2003', *BMJ (Clinical research ed.)*, 340.

Shin, Y.J., Cho, D.Y., Chung, T.Y., Han, S.B., Hyon, J.Y. and Wee, W.R. (2011) 'Rapamycin reduces reactive oxygen species in cultured human corneal endothelial cells', *Curr Eye Res*, 36(12), pp. 1116-22.

Shioi, T., McMullen, J.R., Tarnavski, O., Converso, K., Sherwood, M.C., Manning, W.J. and Izumo, S. (2003) 'Rapamycin attenuates load-induced cardiac hypertrophy in mice', *Circulation*, 107(12), pp. 1664-70.

Singhapol, C., Pal, D., Czapiewski, R., Porika, M., Nelson, G. and Saretzki, G. (2013) 'Mitochondrial telomerase protects cancer cells from nuclear DNA damage and apoptosis', *PLoS ONE*, 8(1).

Smogorzewska, A. and de Lange, T. (2002) 'Different telomere damage signaling pathways in human and mouse cells', *The EMBO journal*, 21(16), pp. 4338-4348.

Smogorzewska, A., Karlseder, J., Holtgreve-Grez, H., Jauch, A. and de Lange, T. (2002) 'DNA ligase IV-dependent NHEJ of deprotected mammalian telomeres in G1 and G2', *Current biology : CB*, 12(19), pp. 1635-1644.

Smogorzewska, A. and van, B. (2000) 'Control of human telomere length by TRF1 and TRF2', ... *and cellular biology*.

Sone, H. and Kagawa, Y. (2005) 'Pancreatic beta cell senescence contributes to the pathogenesis of type 2 diabetes in high-fat diet-induced diabetic mice', *Diabetologia*, 48(1), pp. 58-67.

Sousa-Victor, P., Gutarra, S., García-Prat, L., Rodriguez-Ubreva, J., Ortet, L., Ruiz-Bonilla, V., Jardí, M., Ballestar, E., González, S., Serrano, A., Perdiguero, E. and Muñoz-Cánoves, P. (2014) 'Geriatric muscle stem cells switch reversible quiescence into senescence', *Nature*, 506(7488), pp. 316-321.

Spallarossa, P., Altieri, P., Aloï, C., Garibaldi, S., Barisione, C., Ghigliotti, G., Fugazza, G., Barsotti, A. and Brunelli, C. (2009) 'Doxorubicin induces senescence or apoptosis in rat neonatal cardiomyocytes by regulating the expression levels of the telomere binding factors 1 and 2', *American journal of physiology. Heart and circulatory physiology*, 297(6), p. 81.

Stein, G., Drullinger, L., Robetorye, R., Pereira-Smith, O. and Smith, J. (1991) 'Senescent cells fail to express cdc2, cycA, and cycB in response to mitogen stimulation', *Proceedings of the National Academy of Sciences of the United States of America*, 88(24), pp. 11012-11016.

Stein, G., Drullinger, L., Soulard, A. and Dulić, V. (1999) 'Differential roles for cyclin-dependent kinase inhibitors p21 and p16 in the mechanisms of senescence and differentiation in human fibroblasts', *Molecular and cellular biology*, 19(3), pp. 2109-2117.

Stewart, R.D. (2001) 'Two-lesion kinetic model of double-strand break rejoining and cell killing', *Radiat Res*, 156(4), pp. 365-78.

Storer, M., Mas, A., Robert-Moreno, A., Pecoraro, M., Ortells, M., Di Giacomo, V., Yosef, R., Pilpel, N., Krizhanovsky, V., Sharpe, J. and Keyes, W. (2013) 'Senescence is a developmental mechanism that contributes to embryonic growth and patterning', *Cell*, 155(5), pp. 1119-1130.

Sugisaki, H. and Kanazawa, S. (1981) 'New restriction endonucleases from *Flavobacterium okeanoikoites* (FokI) and *Micrococcus luteus* (MluI)', *Gene*, 16.

Swanson, E., Manning, B., Zhang, H. and Lawrence, J. (2013) 'Higher-order unfolding of satellite heterochromatin is a consistent and early event in cell senescence', *The Journal of cell biology*, 203(6), pp. 929-942.

Szostak, J.W. and Blackburn, E.H. (1982) 'Cloning yeast telomeres on linear plasmid vectors', *Cell*, 29(1), pp. 245-55.

Takai, H., Smogorzewska, A. and de Lange, T. (2003) 'DNA damage foci at dysfunctional telomeres', *Current biology : CB*, 13(17), pp. 1549-1556.

Tanya, M.G. and Stephen, P.J. (1993) 'The DNA-dependent protein kinase: Requirement for DNA ends and association with Ku antigen', *Cell*, 72.

Tao, W. and Levine, A. (1999) 'Nucleocytoplasmic shuttling of oncoprotein Hdm2 is required for Hdm2-mediated degradation of p53', *Proceedings of the National Academy of Sciences of the United States of America*, 96(6), pp. 3077-3080.

Tarry-Adkins, J., Blackmore, H., Martin-Gronert, M., Fernandez-Twinn, D., McConnell, J., Hargreaves, I., Giussani, D. and Ozanne, S. (2013) 'Coenzyme Q10 prevents accelerated cardiac aging in a rat model of poor maternal nutrition and accelerated postnatal growth', *Molecular metabolism*, 2(4), pp. 480-490.

Taylor, C., Nisbet, A., McGale, P., Goldman, U., Darby, S., Hall, P. and Gagliardi, G. (2009) 'Cardiac doses from Swedish breast cancer radiotherapy since the 1950s', *Radiotherapy and oncology : journal of the European Society for Therapeutic Radiology and Oncology*, 90(1), pp. 127-135.

Taylor, C., Povall, J., McGale, P., Nisbet, A., Dodwell, D., Smith, J. and Darby, S. (2008) 'Cardiac dose from tangential breast cancer radiotherapy in the year 2006', *International journal of radiation oncology, biology, physics*, 72(2), pp. 501-507.

Tchkonia, T., Morbeck, D., Von Zglinicki, T., Van Deursen, J., Lustgarten, J., Scrable, H., Khosla, S., Jensen, M. and Kirkland, J. (2010) 'Fat tissue, aging, and cellular senescence', *Aging cell*, 9(5), pp. 667-684.

Tomasek, J., Gabbiani, G., Hinz, B., Chaponnier, C. and Brown, R. (2002) 'Myofibroblasts and mechano-regulation of connective tissue remodelling', *Nature reviews. Molecular cell biology*, 3(5), pp. 349-363.

- Tran, S.L., Haferkamp, S., Scurr, L.L., Gowrishankar, K., Becker, T.M., Desilva, C., Thompson, J.F., Scolyer, R.A., Kefford, R.F. and Rizos, H. (2012) 'Absence of distinguishing senescence traits in human melanocytic nevi', *J Invest Dermatol*, 132(9), pp. 2226-34.
- Trougakos, I., Saridaki, A., Panayotou, G. and Gonos, E. (2006) 'Identification of differentially expressed proteins in senescent human embryonic fibroblasts', *Mechanisms of ageing and development*, 127(1), pp. 88-92.
- Tsao, H., Bevona, C., Goggins, W. and Quinn, T. (2003) 'The transformation rate of moles (melanocytic nevi) into cutaneous melanoma: a population-based estimate', *Archives of dermatology*, 139(3), pp. 282-288.
- Ulf, T.B. and Alexei, T. (2002) 'Lipofuscin: mechanisms of age-related accumulation and influence on cell function' 12 1Guest Editor: Rajindar S. Sohal 2This article is part of a series of reviews on "Oxidative Stress and Aging." The full list of papers may be found on the homepage of the journal', *Free Radical Biology and Medicine*, 33.
- Ungvari, Z., Orosz, Z., Labinsky, N., Rivera, A., Xiangmin, Z., Smith, K. and Csiszar, A. (2007) 'Increased mitochondrial H<sub>2</sub>O<sub>2</sub> production promotes endothelial NF- $\kappa$ B activation in aged rat arteries', *American journal of physiology. Heart and circulatory physiology*, 293(1), p. 47.
- Valavanidis, A., Vlachogianni, T. and Fiotakis, K. (2009) 'Tobacco Smoke: Involvement of Reactive Oxygen Species and Stable Free Radicals in Mechanisms of Oxidative Damage, Carcinogenesis and Synergistic Effects with Other Respirable Particles', *Int J Environ Res Public Health*, 6(2), pp. 445-62.
- van den Bosch, H., Schutgens, R., Wanders, R. and Tager, J. (1992) 'Biochemistry of peroxisomes', *Annual review of biochemistry*, 61, pp. 157-197.
- van Deursen, J. (2014) 'The role of senescent cells in ageing', *Nature*, 509(7501), pp. 439-446.
- Van Remmen, H., Williams, M.D., Guo, Z., Estlack, L., Yang, H., Carlson, E.J., Epstein, C.J., Huang, T.T. and Richardson, A. (2001) 'Knockout mice heterozygous for Sod2 show alterations in cardiac mitochondrial function and apoptosis', *Am J Physiol Heart Circ Physiol*, 281(3), pp. H1422-32.
- van Steensel, B. and de Lange, T. (1997) 'Control of telomere length by the human telomeric protein TRF1', *Nature*, 385(6618), pp. 740-743.
- van Steensel, B., Smogorzewska, A. and de Lange, T. (1998) 'TRF2 protects human telomeres from end-to-end fusions', *Cell*, 92(3), pp. 401-413.

Ventura, A., Kirsch, D., McLaughlin, M., Tuveson, D., Grimm, J., Lintault, L., Newman, J., Reczek, E., Weissleder, R. and Jacks, T. (2007) 'Restoration of p53 function leads to tumour regression in vivo', *Nature*, 445(7128), pp. 661-665.

Vera, E., Bernardes de Jesus, B., Foronda, M., Flores, J. and Blasco, M. (2012) 'The rate of increase of short telomeres predicts longevity in mammals', *Cell reports*, 2(4), pp. 732-737.

Vidal, A. and Koff, A. (2000) 'Cell-cycle inhibitors: three families united by a common cause', *Gene*, 247(1-2), pp. 1-15.

Villeneuve, C., Guilbeau-Frugier, C., Sicard, P., Lairez, O., Ordener, C., Duparc, T., De Paulis, D., Couderc, B., Spreux-Varoquaux, O., Tortosa, F., Garnier, A., Knauf, C., Valet, P., Borch, E., Nediani, C., Gharib, A., Ovize, M., Delisle, M.-B., Parini, A. and Mialet-Perez, J. (2013) 'p53-PGC-1 $\alpha$  pathway mediates oxidative mitochondrial damage and cardiomyocyte necrosis induced by monoamine oxidase-A upregulation: role in chronic left ventricular dysfunction in mice', *Antioxidants & redox signaling*, 18(1), pp. 5-18.

von Zglinicki, T. (2002) 'Oxidative stress shortens telomeres', *Trends in biochemical sciences*, 27(7), pp. 339-344.

von Zglinicki, T., Pilger, R. and Sitte, N. (2000) 'Accumulation of single-strand breaks is the major cause of telomere shortening in human fibroblasts', *Free radical biology & medicine*, 28(1), pp. 64-74.

von Zglinicki, T., Saretzki, G., Döcke, W. and Lotze, C. (1995) 'Mild hyperoxia shortens telomeres and inhibits proliferation of fibroblasts: a model for senescence?', *Experimental cell research*, 220(1), pp. 186-193.

Vousden, K. and Lu, X. (2002) 'Live or let die: the cell's response to p53', *Nature reviews. Cancer*, 2(8), pp. 594-604.

Wada, T., Joza, N., Cheng, H.-y.M., Sasaki, T., Kozieradzki, I., Bachmaier, K., Katada, T., Schreiber, M., Wagner, E., Nishina, H. and Penninger, J. (2004) 'MKK7 couples stress signalling to G2/M cell-cycle progression and cellular senescence', *Nature cell biology*, 6(3), pp. 215-226.

Wang, C., Jurk, D., Maddick, M., Nelson, G., Martin-Ruiz, C. and von Zglinicki, T. (2009) 'DNA damage response and cellular senescence in tissues of aging mice', *Aging cell*, 8(3), pp. 311-323.

Wang, C., Maddick, M., Miwa, S., Jurk, D., Czapiewski, R., Saretzki, G., Langie, S., Godschalk, R., Cameron, K. and von Zglinicki, T. (2010) 'Adult-onset, short-term dietary restriction reduces cell senescence in mice', *Aging*, 2(9), pp. 555-566.

- Wang, J., Geiger, H. and Rudolph, K. (2011) 'Immunoaging induced by hematopoietic stem cell aging', *Current opinion in immunology*, 23(4), pp. 532-536.
- Watson, J. (1972) 'Origin of concatemeric T7 DNA', *Nature: New biology*, 239(94), pp. 197-201.
- Weber, B., Collins, C., Robbins, C., Magenis, R., Delaney, A., Gray, J. and Hayden, M. (1990) 'Characterization and organization of DNA sequences adjacent to the human telomere associated repeat (TTAGGG)<sub>n</sub>', *Nucleic acids research*, 18(11), pp. 3353-3361.
- Wilkinson, J.E., Burmeister, L., Brooks, S.V., Chan, C.C., Friedline, S., Harrison, D.E., Hejtmancik, J.F., Nadon, N., Strong, R., Wood, L.K., Woodward, M.A. and Miller, R.A. (2012) 'Rapamycin slows aging in mice', *Aging Cell*, 11(4), pp. 675-82.
- Wright, W., Piatyszek, M., Rainey, W., Byrd, W. and Shay, J. (1996) 'Telomerase activity in human germline and embryonic tissues and cells', *Developmental genetics*, 18(2), pp. 173-179.
- Wu, L. and Levine, A.J. (1997) 'Differential regulation of the p21/WAF-1 and mdm2 genes after high-dose UV irradiation: p53-dependent and p53-independent regulation of the mdm2 gene', *Mol Med*, 3(7), pp. 441-51.
- Xue, W., Zender, L., Miething, C., Dickins, R., Hernando, E., Krizhanovsky, V., Cordon-Cardo, C. and Lowe, S. (2007) 'Senescence and tumour clearance is triggered by p53 restoration in murine liver carcinomas', *Nature*, 445(7128), pp. 656-660.
- Ye, J., Hockemeyer, D., Krutchinsky, A., Loayza, D., Hooper, S., Chait, B. and de Lange, T. (2004) 'POT1-interacting protein PIP1: a telomere length regulator that recruits POT1 to the TIN2/TRF1 complex', *Genes & development*, 18(14), pp. 1649-1654.
- Yip, C.K., Murata, K., Walz, T., Sabatini, D.M. and Kang, S.A. (2010) 'Structure of the human mTOR complex I and its implications for rapamycin inhibition', *Mol Cell*, 38(5), pp. 768-74.
- Yoon, I., Kim, H., Kim, Y., Song, I.-H., Kim, W., Kim, S., Baek, S.-H., Kim, J. and Kim, J.-R. (2004) 'Exploration of replicative senescence-associated genes in human dermal fibroblasts by cDNA microarray technology', *Experimental gerontology*, 39(9), pp. 1369-1378.
- Youdim, M., Edmondson, D. and Tipton, K. (2006) 'The therapeutic potential of monoamine oxidase inhibitors', *Nature reviews. Neuroscience*, 7(4), pp. 295-309.

Yui, J., Chiu, C. and Lansdorp, P. (1998) 'Telomerase activity in candidate stem cells from fetal liver and adult bone marrow', *Blood*, 91(9), pp. 3255-3262.

Zhang, J., Pickering, C.R., Holst, C.R., Gauthier, M.L. and Tlsty, T.D. (2006) 'p16INK4a modulates p53 in primary human mammary epithelial cells', *Cancer Res*, 66(21), pp. 10325-31.

Zhang, Y., Bokov, A., Gelfond, J., Soto, V., Ikeno, Y., Hubbard, G., Diaz, V., Sloane, L., Maslin, K., Treaster, S., Réndon, S., van Remmen, H., Ward, W., Javors, M., Richardson, A., Austad, S. and Fischer, K. (2014) 'Rapamycin extends life and health in C57BL/6 mice', *The journals of gerontology. Series A, Biological sciences and medical sciences*, 69(2), pp. 119-130.

Zhu, J., Woods, D., McMahon, M. and Bishop, J. (1998) 'Senescence of human fibroblasts induced by oncogenic Raf', *Genes & development*, 12(19), pp. 2997-3007.

Zoncu, R., Efeyan, A. and Sabatini, D. (2011) 'mTOR: from growth signal integration to cancer, diabetes and ageing', *Nature reviews. Molecular cell biology*, 12(1), pp. 21-35.

Zou, L. (2003) 'Sensing DNA Damage Through ATRIP Recognition of RPA-ssDNA Complexes', *Science*, 300.